LEABHARLANN CHOLÁISTE NA TRÍONÓIDE, BAILE ÁTHA CLIATH
Ollscoil Átha Cliath
TRINITY COLLEGE LIBRARY DUBLIN
The University of Dublin

Terms and Conditions of Use of Digitised Theses from Trinity College Library Dublin

Copyright statement

All material supplied by Trinity College Library is protected by copyright (under the Copyright and Related Rights Act, 2000 as amended) and other relevant Intellectual Property Rights. By accessing and using a Digitised Thesis from Trinity College Library you acknowledge that all Intellectual Property Rights in any Works supplied are the sole and exclusive property of the copyright and/or other IPR holder. Specific copyright holders may not be explicitly identified. Use of materials from other sources within a thesis should not be construed as a claim over them.

A non-exclusive, non-transferable licence is hereby granted to those using or reproducing, in whole or in part, the material for valid purposes, providing the copyright owners are acknowledged using the normal conventions. Where specific permission to use material is required, this is identified and such permission must be sought from the copyright holder or agency cited.

Liability statement

By using a Digitised Thesis, I accept that Trinity College Dublin bears no legal responsibility for the accuracy, legality or comprehensiveness of materials contained within the thesis, and that Trinity College Dublin accepts no liability for indirect, consequential, or incidental, damages or losses arising from use of the thesis for whatever reason. Information located in a thesis may be subject to specific use constraints, details of which may not be explicitly described. It is the responsibility of potential and actual users to be aware of such constraints and to abide by them. By making use of material from a digitised thesis, you accept these copyright and disclaimer provisions. Where it is brought to the attention of Trinity College Library that there may be a breach of copyright or other restraint, it is the policy to withdraw or take down access to a thesis while the issue is being resolved.

Access Agreement

By using a Digitised Thesis from Trinity College Library you are bound by the following Terms & Conditions. Please read them carefully.

I have read and I understand the following statement: All material supplied via a Digitised Thesis from Trinity College Library is protected by copyright and other intellectual property rights, and duplication or sale of all or part of any of a thesis is not permitted, except that material may be duplicated by you for your research use or for educational purposes in electronic or print form providing the copyright owners are acknowledged using the normal conventions. You must obtain permission for any other use. Electronic or print copies may not be offered, whether for sale or otherwise to anyone. This copy has been supplied on the understanding that it is copyright material and that no quotation from the thesis may be published without proper acknowledgement.

The Geological Evolution of the Southern Tanzanian Continental Margin

The Geological Evolution of the Southern Tanzanian Continental Margin

Ph.D. Thesis

University of Dublin (Trinity College)

2013

Volume 1

Niamh O'Sullivan

TRINITY COLLEGE
2 4 MAY 2013
LIBRARY DUBLIN

Thesis 10058.1

Declaration

This thesis has not previously been submitted as an exercise for a degree at this or any other university. It is entirely my own work, except where I have consulted the work of others and this has always been clearly attributed with the source given. I agree that the Library may lend or copy this thesis on request.

Niamh O'Sullivan

February 2013

Summary

The southern Tanzanian continental margin is a regionally significant geological and geomorphological feature, which originated in the breakup of Gondwana in the Permian and is presently undergoing active extension a part of the South Eastern Branch of the East African Rift. Despite this long and varied history of activation and reactivation, there has been no academic, publicly available study of the margin. This study is the first complete structural, sedimentological and stratigraphic study of the evolution of this complex margin since the Cretaceous.

Based on the acquisition, processing and interpretation of over 2,000km of multichannel reflection seismic data, a robust seismic stratigraphic scheme was erected for the margin, extending from the shoreline to the Davie Ridge. Several structural 'zones' were identified in the margin and individual stratigraphic schemes erected based on seismic markers, facies and sedimentological interpretations. As there were no exploration wells available to calibrate the ages of key seismic markers, previous work, newly acquired box cores and sequence stratigraphic principles were incorporated to establish four key seismic markers traceable through the entire margin; (1) Top Cretaceous, (2) Eocene – Oligocene (3) intra Mid-Miocene and (4) Base Pliocene.

The regionally significant Oligocene to Recent 'Tipuli Unit' is recognisable as a chronostratigraphic unit separate from the underlying Upper Cretacecous to Lower Oligocene 'Kilwa Group'. Unconformities within this unit extend to the transition zone and correlate with the sequence stratigraphic scheme erected there.

The margin may be considered a partitioned transpressional strike slip zone as tectonic features identified in this study include relatively straight fault traces, positive flower structures, regionally extensive en-echelon folds and faults, abrupt changes in seismic facies across faults and varying normal to reverse separations along single faults. The southern Tanzanian margin is undergoing active extension and compressional phases in response to the clockwise rotation of the Rovuma microplate, which is part of the East African Rift System.

The Tanzanian margin forms a part of the youngest and only offshore arm of the East African Rift. As a result of the uplift of the hinterland, there has been a marked increase in sediment flux to the margin. A broad network of V-shaped canyons incising the shelf has developed since the late Miocene, exploiting the SW-NE structural trend, providing a sediment pathway for material from the African continent to the Somali Abyssal Plain.

Acknowledgements

This project was supervised by Dr Chris Nicholas, and I must thank him for his advice, encouragement and guidance, particularly in the field. I will always appreciate this time and opportunity afforded me. The European Science Foundation (ESF) and the Irish Research Council for Science and Engineering Technology (IRCSET) kindly funded this project, and I would especially like to thank the' GLOW' team for their constant support and enthusiasm.

My research has benefited from numerous fruitful discussions in the field with many experienced geologists, and I must particularly mention Stuart Bennett, Wellington Hudson, Sophia Gold, Laura Cotton and our kind Tanzanian colleagues at TPDC.

The technicians from the Geology Department, Trinity College, Dublin, namely Neil, Declan, Frank, Maura and Noel, also deserve a special mention for their understanding and patience throughout my time in Trinity.

Many thanks to the following who provided support during this study: Dominion Petroleum who provided logistical support in the field; T.P.D.C. who provided assistance with logistics, samples and data; NIOZ and particularly Henk de Haas for support and guidance with seismic data processing in Texel; Robin Edwards and Schlumberger for arranging a university license of the Kingdom suite which was used to interpret seismic data in this study.

Lucie, Lara, Aoife, Jo, Eloise, Kieran, Ben, Nick and Daniel; the occupants of the URL, deserve particular thanks for their unending love of a good prank. I must thank the friends who have put up with me while undertaking this study, Kate, Jason, Dooley, Alan, Keith, Fowley, Paul, Peter, John, Caoimhe, Sarah, John, Darci, Cees, Lesley, Aine, Jonny, Niall, Aoife; thank you all. The staff and postgrads in the Geology department could never have been more supportive or encouraging in all my years in Trinity.

I must offer a special thanks to Dr Stuart Bennett, Dr Dave Chew, Dr. Sophia Gold and Dr. Wellington Hudson, without whom this study would certainly not have reached its current conclusion. It has been a pleasure working with them. I'd like to thanks my printing team for their efficiency and goodwill!

I would like to show my gratitude for Dr. Lisa McNeill and Dr. Ian Sanders for their discussion and great advice on corrections for this thesis.

To Kieran, I owe so much and am indebted to him for always being there. My inspirational aunt and uncle; Helen and Noel; this could definitely not have been done without them. The final thank you must go to my parents for their unwavering support, kindness, and belief in me.

Table of Contents

1. INTRODUCTION *1*

2. REGIONAL GEOLOGICAL CONTEXT AND RESEARCH AIMS *7*

2.1. GEOGRAPHY OF SOUTHERN COASTAL TANZANIA *8*

2.2. REGIONAL TECTONIC SETTING *8*

2.2.1. Gondwana Breakup *9*

2.2.2. West Somali Basin Seafloor Creation – Dextral Strike Slip Movement *11*

2.2.3. Stabilisation/ Passive Margin *13*

2.2.4. Neo-rifting/Reactivation due to the East African Rift Development *14*

2.2.5. Seismicity and Geodetics of the Rovuma-Somalia Microplate boundary *18*

2.2.6. Onshore evidence of compression and transpression *22*

2.2.7. Theme 1 Research Questions; Tectonics *24*

2.3. STRATIGRAPHIC FRAMEWORK OF ONSHORE AND OFFSHORE TANZANIA 24

2.3.1. Theme 2 Research questions; Stratigraphy Onshore and Offshore *25*

2.4. OFFSHORE AGE CONTROL 25

2.4.1. Theme 3 Research questions; Age control *25*

2.5. SEDIMENTARY TRANSPORT ON THE MARGIN 26

2.5.1. Theme 4 Research questions; Oceanography and sedimentary response *27*

2.6. AIMS AND OBJECTIVES FOR THE PRESENT STUDY 27

2.6.1. Primary objectives *27*

3. METHODS ***29***

3.1. THE MULTIDISCIPLINARY APPROACH *30*

3.2. DESK STUDY *30*

3.3. PRIMARY OFFSHORE DATA *32*

3.3.1. Survey Planning *32*

3.3.2. 'GLOW' Survey 2009; Acquisition. *34*

3.4. MULTICHANNEL REFLECTION SEISMIC PROCESSING *40*

3.4.1. Theory *40*

3.5. MULTICHANNEL SEISMIC INTERPRETATION *44*

3.5.1. The seismic stratigraphic methodology *44*

3.6. MULTIBEAM BATHYMETRY ACQUISITION AND INTERPRETATION *51*

3.7. BOX AND PISTON CORING *51*

3.8. ONSHORE GEOLOGICAL MAPPING *53*

3.9. VELOCITY MODEL AND DEPTH CONVERSION *54*

3.10. AGE CORRELATIONS *55*

4. SEISMIC STRATIGRAPHY OF THE DAVIE RIDGE (DR) AND DAVIE RIDGE INNER EXTENSIONAL ZONE (DRIEZ); THE GLOW SEISMIC SURVEY 2009. *57*

4.1. INTRODUCTION *58*

4.2. DAVIE RIDGE (DR) *65*

4.2.1. DR Unit I *68*

4.2.2. DR SM 01 *68*

4.2.3. DR Unit II *72*

4.2.4. DR SM 02 *79*

4.2.5. DR Unit III *80*

4.2.6. Davie Ridge Summary Seismic Stratigraphy *83*

4.2.7. Sedimentological Interpretation of the Davie Ridge Seismic Facies. *86*

4.3. DAVIE RIDGE INNER EXTENSIONAL ZONE (DRIEZ) *90*

4.3.1. DRIEZ Unit I *92*

4.3.2. DZ SM 01 *92*

4.3.3. DRIEZ Unit II *96*

4.3.4. DRIEZ Summary Seismic Stratigraphy *98*

4.3.5. Sedimentological Interpretation of Davie Ridge Inner Extensional Zone Seismic *99*

4.4. SEDIMENTOLOGICAL CORRELATIONS BETWEEN THE DAVIE RIDGE AREA (DR) AND THE DAVIE RIDGE INNER EXTENSIONAL ZONE (DRIEZ). *100*

4.5. SUMMARY *103*

5. SEISMIC STRATIGRAPHY OF THE KERIMBAS BASIN (KB) AND THE SEAGAP FRACTURE ZONE (SGFZ); THE GLOW SEISMIC SURVEY 2009. ***105***

5.1. INTRODUCTION *106*

5.2. KERIMBAS BASIN (KB) *107*

5.2.1. KB Unit I *113*

5.2.2. KB SM 01 *117*

5.2.3. KB Unit II *118*

5.2.4. Kerimbas Basin Summary Seismic Stratigraphy *119*

5.2.5. Sedimentological Interpretation of the Kerimbas Basin Seismic Facies. *120*

5.3. THE SEAGAP FRACTURE ZONE (SG) *123*

5.3.1. SG Unit I *127*

5.3.2. SG SM 01 *129*

5.3.3. SG Unit II *130*

5.3.4. SG SM 02 *132*

5.3.5. SG Unit III *133*

5.3.6. SeaGap Summary Seismic Stratigraphy *133*

5.3.7. Sedimentological Interpretation of the SeaGap Seismic Facies. *136*

5.4. CORRELATING BETWEEN THE SEDIMENTOLOGY OF THE KERIMBAS BASIN AND THE SEAGAP FRACTURE ZONE. *137*

5.5. SUMMARY *138*

6. THE STRATIGRAPHY OF OFFSHORE SOUTHERN COASTAL TANZANIA- INCORPORATING PRE-EXISTING DATA AND NEW BIOSTRATIGRAPHIC CONTROLS. ***141***

6.1. INTRODUCTION *142*

6.2. THE DEEP OFFSHORE GLOW SEISMIC STRATIGRAPHIC SCHEME *143*

6.2.1. Coastal Wells *147*

6.2.2. Offshore Wells *149*

6.3. PRE-EXISTING SEISMIC SURVEYS *154*

6.3.1. Lamont-Doherty Survey (1980) Coffin et al. (1988) *154*

6.3.2. TZ-AGIP Phillips Survey (1976) *155*

6.3.3. MACAMO-MD40 Survey (1983) Mougenot et al. (1986) *156*

6.4. CORRELATING COASTAL WELLS TO THE GLOW, LD AND TZ-AGIP SURVEYS. *157*

6.4.1. Mnazi Bay-1 to GLOW 7 and 8. *157*

6.4.2. Songo-Songo 1 to TZ and LD *160*

6.5. UNINTERPRETED AND INTERPRETED PRE-EXISTING DATA *161*

6.5.1. DSDP 241 – Lamont Doherty (& Songo Songo-1) *161*

6.5.2. DSDP 242 – Mougenot et al. (1986) *167*

6.5.3. The TZ AGIP 1975 Survey (Kidson et al. 1997) *171*

6.6. GLOW PISTON AND BOX CORE AGE DATA. *175*

6.7. ASSIGNING AGES TO THE SEISMIC STRATIGRAPHY OF THE STRUCTURAL 'ZONES' *176*

6.7.1. The Davie Ridge Area *176*

6.7.2. The Davie Ridge Inner Extensional Zone (DRIEZ) *188*

6.7.3. Kerimbas Basin *192*

6.7.4. SeaGap Area (SG) *195*

6.8. ESTIMATED AGES OF GLOW SEISMIC MARKERS FOR THE DR, DRIEZ, KB AND SG AREAS. *201*

6.9. PREVIOUS STRATIGRAPHIC NOMENCLATURE *203*

6.9.1. Mafia Deep Offshore Basin (MDOB) Seismostratigraphy; Cope (2000) *203*

6.10. SUMMARY *205*

7. THE ONSHORE GEOLOGY OF SOUTHERN COASTAL TANZANIA; ASSESSING REGIONAL UNCONFORMITIES AND INTRODUCING THE UPPER OLIGOCENE-QUATERNARY TIPULI UNIT. ***207***

7.1. INTRODUCTION *208*

7.2. PREVIOUS STRATIGRAPHIC NOMENCLATURE *210*

7.2.1. Geological Maps *210*

7.2.2. Onshore Stratigraphy (and Existing Stratigraphic Information) *216*
7.3. FIELD GEOLOGY OF THE KISWERE AREA *225*
7.3.1. Nangurukuru Formation and Kivinje Formation (Kiswere Hillock 1) *231*
7.3.2. Masoko Formation (Kiswere Hillock 2) *233*
7.3.3. Pande Formation (Kiswere Hillocks 2-3) *235*
7.3.4. Depositional Environment of the Kiswere Area *238*
7.4. FIELD GEOLOGY OF THE MCHINGA/NORTH MCHINGA AREA *239*
7.4.1. Lake Mkoe Area; Eocene-Oligocene reef knolls *241*
7.4.2. Ngomba Quarry; A Pleistocene (?) Fossil Mangrove Deposit *244*
7.4.3. Mchinga Bay Area –Early to Mid Miocene Facies *247*
7.4.4. Summary of interpreted depositional environments of the North Mchinga Area. *259*
7.5. FIELD GEOLOGY OF THE LINDI AREA *262*
7.5.1. North Lindi (Likonga-Mitonga-Mbanja) *262*
7.5.2. Lindi Bay Area *271*
7.6. THE COASTAL RUVUMA AREA *285*
7.6.1. Lake Kitere *285*
7.6.2. Mtwara –Mikindani –Ntegu. *287*
7.7. THE UPPER OLIGOCENE-PLEISTOCENE TIPULI UNIT (TU) AND THE PLEISTOCENE (?) MBANJA SUBUNIT (MSU) *290*
7.7.1. Upper Oligocene-Lower Miocene occurrences and facies *294*
7.7.2. Lower -Mid Miocene occurrences and facies *294*
7.7.3. Upper Miocene occurrences and facies *295*
7.7.4. Mid and Upper Miocene in the Ruvuma Basin *295*
7.7.5. The Mbanja subunit *296*
7.8. THE TIPULI UNIT AND GLOBAL CLIMATIC INTERVALS. *299*
7.9. PALAEOGEOGRAPHIC MAPS *302*
7.10. SUMMARY *308*

8. SEISMIC STRATIGRAPHY OF THE TANZANIAN TRANSITION ZONE; INCORPORATING ONSHORE-OFFSHORE CORRELATIONS AND PREVIOUSLY PUBLISHED DATA. ***309***

8.1. INTRODUCTION *310*
8.2. THE COASTAL BASIN (CB) *312*
8.2.1. Coastal Basin Seismic Stratigraphy *312*
8.2.2. Sedimentological Interpretation of the Coastal Basin Seismic Facies. *318*
8.3. THE KITUNDA BLOCK (KTB) *319*
8.3.1. KTB Unit I *319*
8.3.2. KTB SM 01 *322*
8.3.3. KTB Unit II *323*

8.3.4. KTB SM 02 327
8.3.5. KTB Unit III 327
8.3.6. Kitunda Block Summary Seismic Stratigraphy 331
8.3.7. Sedimentological Interpretation of the Kitunda Block seismic facies. 332
8.4. THE SHELF AND SLOPE (SS) 333
8.5. CORRELATING THE ONSHORE FIELD GEOLOGY TO THE TRANSITION ZONE GLOW SEISMICS. 333
THE PRINCIPAL BOUNDING SURFACES AND SYSTEMS TRACTS 337
8.6. INCORPORATING PREVIOUSLY PUBLISHED DATA AND NEW BOX-CORE DATA. 345
8.6.1. Coastal Basin (CB) 346
8.6.2. The Shelf and Slope Area 346
8.6.3. Kitunda Block (KTB) 351
8.7. THE AGES OF THE KITUNDA BLOCK SEISMIC MARKERS 358
8.8. THE GLOW SEISMIC STRATIGRAPHIC SCHEME 359
8.9. SUMMARY 364

9. OFFSHORE STRUCTURAL REGIME; A PARTITIONED TRANSPRESSIONAL STRIKE-SLIP SYSTEM IN AN EXTENSIONAL RIFT SETTING. ***365***

9.1. INTRODUCTION 366
9.1.1. Previous work and aims 366
9.1.2. Structural Features 367
9.2. BASEMENT CONFIGURATION 368
9.2.1. Interpretation of Gravity Datasets 373
9.2.2. 'Old' inherited structures 379
9.3. FAULT ARCHITECTURE AND STRUCTURAL SETTING OFFSHORE SOUTHERN COASTAL TANZANIA. 379
9.3.1. The Davie Ridge Inner Extensional Zone 389
9.3.2. The SeaGap Fault Zone 393
9.4. THE STRIKE-SLIP PARTITIONED SYSTEM OF THE SOUTHERN TANZANIAN MARGIN. 409
9.4.1. Pre-Oligocene Inherited structural elements 409
9.4.2. The post-Oligocene structural evolution of the south Tanzanian margin 411

10. THE SOUTHERN TANZANIAN CONTINENTAL MARGIN: OCEANOGRAPHIC REGIME AND SEDIMENTARY RESPONSE. ***415***

10.1. INTRODUCTION 416
10.2. MORPHOLOGY AND PHYSIOLOGY OF THE STUDY AREA 417
10.3. OCEANOGRAPHIC REGIME OF THE STUDY AREA 419
10.3.1. Stratification of bottom and surface water 420
10.3.2. Interaction between bathymetry and current activity in the Mozambique Channel 423

10.3.3. Transport in the water column above the Davie Ridge. *423*

10.4. SEDIMENTARY PROCESSES ON THE TANZANIAN CONTINENTAL MARGIN *425*

10.4.1. Pelagic/Hemipelagic Sedimentation *425*

10.4.2. Downslope Processes *426*

10.4.3. Alongslope processes (bottom currents) *427*

10.5. TURBIDITY CURRENT PATHWAYS (TCPS) *435*

10.5.1. Terminology *436*

10.5.2. Canyons on the shelf/slope *437*

10.5.3. Deep Sea Channels *449*

10.6. DISCUSSION AND CONCLUSIONS *457*

11. THE GEOLOGICAL EVOLUTION OF THE SOUTHERN TANZANIAN MARGIN SINCE THE CRETACEOUS ***461***

11.1 INTRODUCTION *462*

11.2 END LOWER CRETACEOUS *463*

11.3 MID CRETACEOUS TO END EOCENE *464*

11.4 UPPER OLIGOCENE TO LOWER MIOCENE *465*

11.5. LOWER TO MID MIOCENE *466*

11.6 MID TO UPPER MIOCENE *466*

11.7. BASE PLIOCENE TO PRESENT *467*

APPENDICES

I GLOW CRUISE NAVIGATION INFORMATION *477*

II GLOW SAMPLING STATIONS 1-20 ('GLOW CRUISE REPORT, 2009 (SHIPBOARD PARTY) *485*

II FIELD DATA *517*

ENCLOSURES (A0 INSERTS)

ENCLOSURE A: GEOLOGICAL MAP OF THE SOUTHERN TANZANIAN COASTAL REGION

ENCLOSURE B: GEOLOGICAL MAP INDEX (ACCOMPANIES CHAPTER 7)

ENCLOSURE C: ONSHORE STRATIGRAPHIC CORRELATION PANEL

ENCLOSURE D: UNINTERPRETED AND INTERPRETED GLOW SEISMIC LINES 5-19 (CHAPTERS 4-11)

ENCLOSURE E: UNINTERPRETED AND INTERPRETED GLOW SEISMIC LINES 20-31(CHAPTERS 4-11)

ENCLOSURE F: GEOLOGICAL EVOLUTION OF THE SOUTHERN TANZANIAN MARGIN (ACCOMPANIES CHAPTER11)

1. Introduction

Tanzania is located in East Africa (Figs. 1.1 and Fig 1.2), bordered by Kenya, Uganda, Malawi and Mozambique. The Tanzanian coastal belt is located between the coast on the east and the basement outcrop on the west. The coastline and islands are fringed with coral reef development and the offshore shelf (200m isobath) is very narrow (several km) in the south. Offshore the southern coastal region exhibits present day fault scarps on the seafloor and a highly incised near shore slope.

The southern coastal area of Tanzania is of significance for regional geological studies for several reasons; it is a relatively unstudied margin with outstanding questions with regard to its stratigraphy, sedimentology, structure and potential hydrocarbon prospectivity.

This thesis aims to give a broad synthesis of a range of new and legacy datasets to give an overview of the sedimentological, structural and stratigraphic evolution of the southern Tanzanian margin. A number of enclosures (A0) are included at the rear of the thesis for your ease of navigation and it is recommended that the reader uses them in conjunction with reading the text. They comprise a geological map, uninterpreted and interpreted seismic lines and the final synthesis series of diagrams.

To begin with, the reader is advised to consult Fig. 1.2 for a wide overview of the datasets used in this thesis in relation to the study area. Furthermore, Fig. 1.1 should be a key guide to placenames, locations and survey line numbers to accompany reading. An introduction to the geological context and the research questions is given in Chapter 2, and the methods utilised to answer these outstanding questions are described in Chapter 3. Interpretation of a new offshore 2D seismic survey (GLOW) begins in Chapters 4 to 6. Beginning from first principles, seismic markers, units and facies are identified. Given that major faults transect the area and the depth of resolution of the seismic data is not enough to confidently correlate across the faults, a range of seismic stratigraphic schemes are created for key areas. In Chapter 7, nearby wells, published data that intersects with the GLOW seismic data and new biostratigraphic ages from targeted box cores are incorporated. As a result of this

analysis, a robust chronostratigraphic scheme is erected and applied, ranging from the Eocene-Oligocene to Recent.

Furthermore, in Chapter 7, the onshore geology is defined for the Oligocene and younger on the coastal belt of Tanzania; the 'Tipuli Unit' is introduced for the first time here. Key unconformities onshore are correlated to the shallow water/nearshore (transition zone) seismic data via sequence stratigraphic principles in Chapter 8.

The structural geology of the area is discussed in Chapter 10, and by analysing the faults in seismic data, outcrop and multibeam bathymetric data, it is proposed that the study area is a strike slip partitioned system. The oceanography, seabed morphology and sediment response on the margin are described and discussed in relation particularly to timing of fault movement. A concluding synthesis is included in Chapter 11, which compiles the results acquired in previous chapters and discusses the evolution of the margin in a series of key time slices.

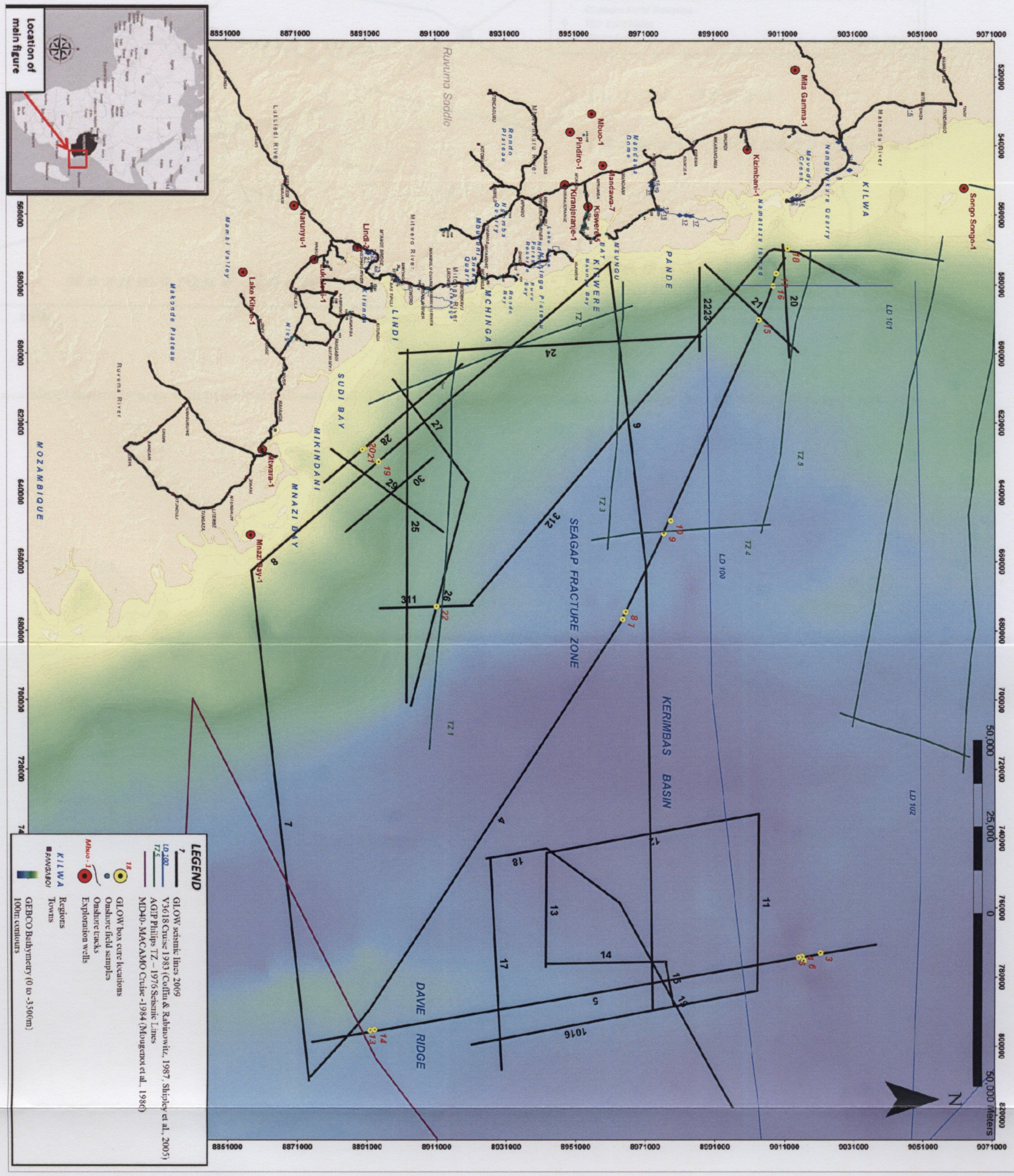

Figure 1.1: Reference basemap of the study area. The acquisition and processing of the GLOW seismic survey (2009) is described in Chapter 3. Interpretation of the Davie Ridge Area, Kerimbas Basin and SeaGap Fracture Zone seismic facies are provided in Chapters 4 and 5. Chapter 6 incorporates results from published data (published seismic surveys and wells shown) to assign ages to the defined seismic architecture and correlate between zones of interest. In Chapter 7, the onshore Cretaceous and younger geology is established in the area adjacent to the GLOW seismic survey. The survey tracks, samples and key regions are shown. The results of Chapter 7 are extrapolated to assign ages to the shelf seismic stratigraphy and transition zone via sequence stratigraphic principles. Chapter 9 examines the structural regime of the area and the post-Cretaceous reactivation history of the margin. Chapter 10 describes the oceanographic regime and sedimentary response of the margin evolution. Finally Chapter 11 summarises the geological evolution of the margin in a series of time slices.

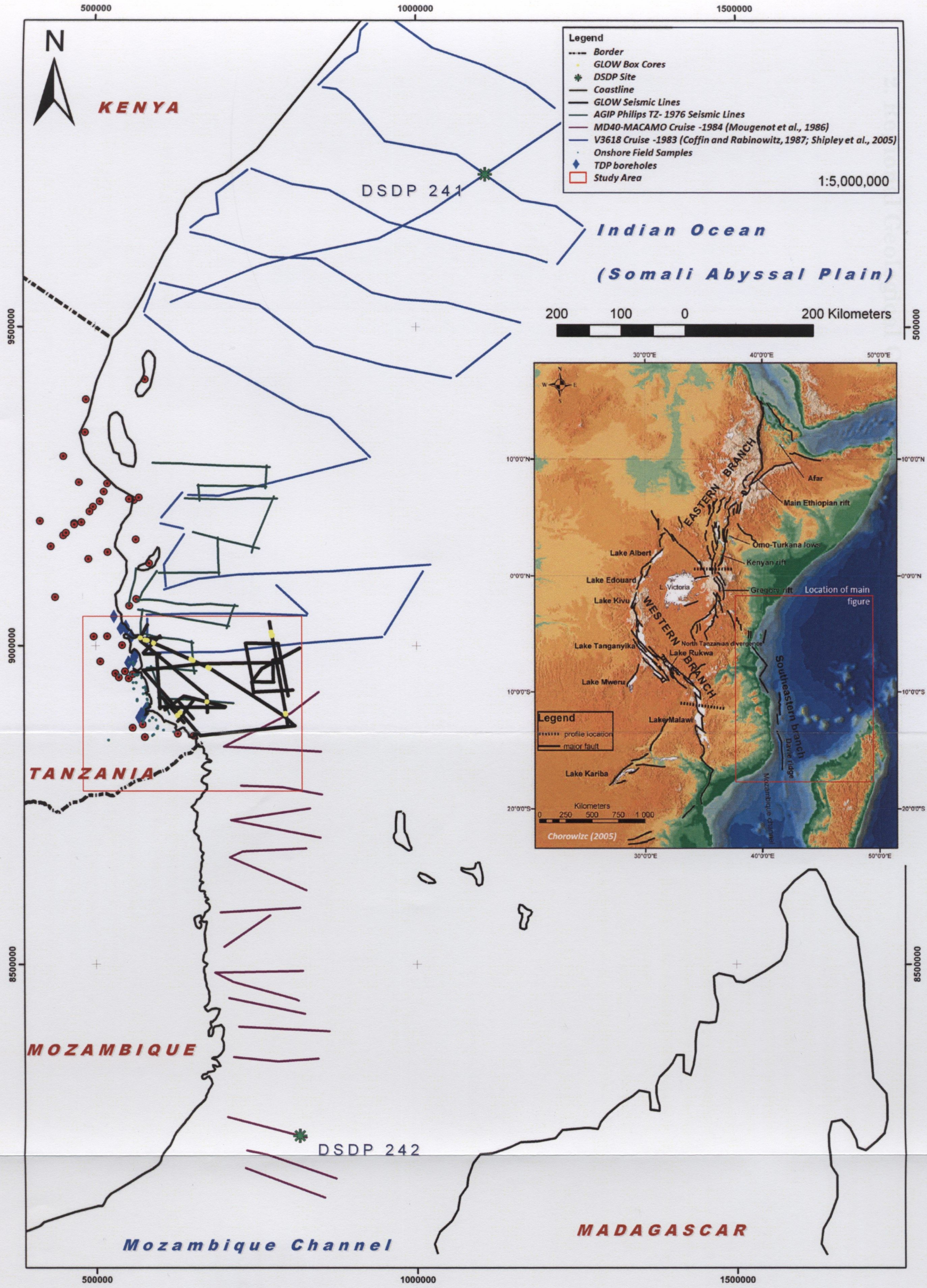

Figure 1.2: Location of the study area with principal datasets used. The location of the study area (Fig. 1.1) within the East African Rift system is shown.

2. Regional Geological Context and Research Aims

2.1. *Geography of southern coastal Tanzania*

Tanzania is located in East Africa (Figs. 1.2 and 1.2), bordered by Kenya, Uganda, Malawi and Mozambique. The Tanzanian coastal belt is located between the coast on the east and the basement outcrop on the west. The two major rivers are the Ruvuma and the Rufiji with associated deltas. Lesser but still important are the Mbwemburu, Ruvu, and smaller rivers all draining into the Indian Ocean in an approximate ESE-WNW orientation, perpendicular to the strike of the geological outcrop. The coastline and islands are fringed with coral reef development which degrades the quality of onshore to offshore seismic ties because of logistics and the poor energy coupling of geophones on a porous carbonate outcrop. The offshore shelf (200m isobath) is very narrow (several km) in the south, swings out to include Mafia and Zanzibar islands and then shifts landward off Pemba Island. Offshore the southern coastal region exhibits present day fault scarps on the seafloor and a highly incised near shore slope.

2.2. *Regional tectonic setting*

The present day Tanzanian margin began to evolve during the Permian, when Madagascar began drifting away from Africa as a result of Gondwana breakup (Reeves & de Wit 2000) and the East African coastal basins (Mandawa, Ruvuma and Selous of Tanzania and the Morondava Basin of Madagascar) were developed (Fig. 2.1). There has been a substantial amount of research conducted to support this hypothesis (Schandelmeier & Bremer 2004; Salman & Abdula 1995; Montenat *et al.* 1996; Geiger 2004). After the breakup of Gondwana, ocean seafloor spreading began in the West Somali Basin during the Late Jurassic (Eagles *et al.* 2008) and led to the dextral strike slip motion of Madagascar along a prominent fault zone; the Davie Fracture Zone (DFZ). After > 600km of displacement along the DFZ, the structural fabric of the Tanzanian margin was well established. A period of margin stability and

thermal sag took place during the Cretaceous and Paleogene before 'reactivation' or 'neo-rifting' took place (Salman & Abdula 1995). This is hypothesised as being related to the impact of a superplume beneath the African craton and the subsequent evolution of the East African Rift in the Oligocene. Recent geodetic data onshore indicates that the Tanzanian margin is the locus for a compressive regime as the African continent essentially unzips and east African moves away from west Africa (Calais *et al.* 2006; Stamps *et al.* 2008). Both the 'neo-rifting' and 'reactivation' hypotheses are poorly understood in relation to Tanzanian geology.

2.2.1. Gondwana Breakup

The African continent was largely established in the Early Palaeozoic. A stable African plate was bound by weak structural zones along which adjacent plates moved away from the main plate. In the Late Palaeozoic, the breakup of Gondwana began. From the Late Carboniferous/Early Permian to Late Triassic a series of pull apart basins formed along zones of weakness within the Gondwanan landmass (Schandelmeier & Bremer 2004; Salman & Abdula 1995; Montenat *et al.* 1996; Geiger 2004).

Rifting in the Late Triassic/Early Jurassic led to the disintegration of Gondwana into separate blocks. Rifting towards the southwest in the Selous area of Tanzania from the Permian to earliest Jurassic (Nilsen *et al.* 1999) eventually failed and jumped eastwards to the present day coastal zone. Approximate W-E extensional faulting during the latter stage of Gondwana breakup (303– 150Ma; Late Carboniferous to Mid Jurassic), led to the development of horsts and grabens which the basement structure reflects. 'Horsts' during this phase include the Masasi spur (Salman & Abdula 1995) and grabens Mandawa, Ruvuma in Tanzania and Morondava Basins in Madagascar (Morondava). The deposits of these intercontinental rifts are thick Permo-Triassic 'Karoo' deposits. The dominant structural fabric from that time is dominated by approximately N-S oriented normal faults extending in a West-East direction.

A number of plate reconstructions are available, drawing on coastal outlines, bathymetry, gravity, magnetic and palaeomagnetic data (Du Toit 1937; Smith & Hallam 1970; Heirtzler *et al.* 1980; Rabinowitz 1971; Rabinowitz *et al.* 1983; Scrutton 1978; Bunce *et al.* 1977; Mougenot *et al.* 1986; Reeves *et al.* 2002; Geiger *et al.* 2004; Eagles *et al.* 2008). The understanding of the tectonics of the Gondwana breakup in the literature for the purposes of studying the Tanzanian margin are quite clear. There are questions raised in the literature however, about the influence of older, inherited structures located along zones of weakness as sites of reactivation along the East African margin. The identification of these potential zones is critical in understanding this role.

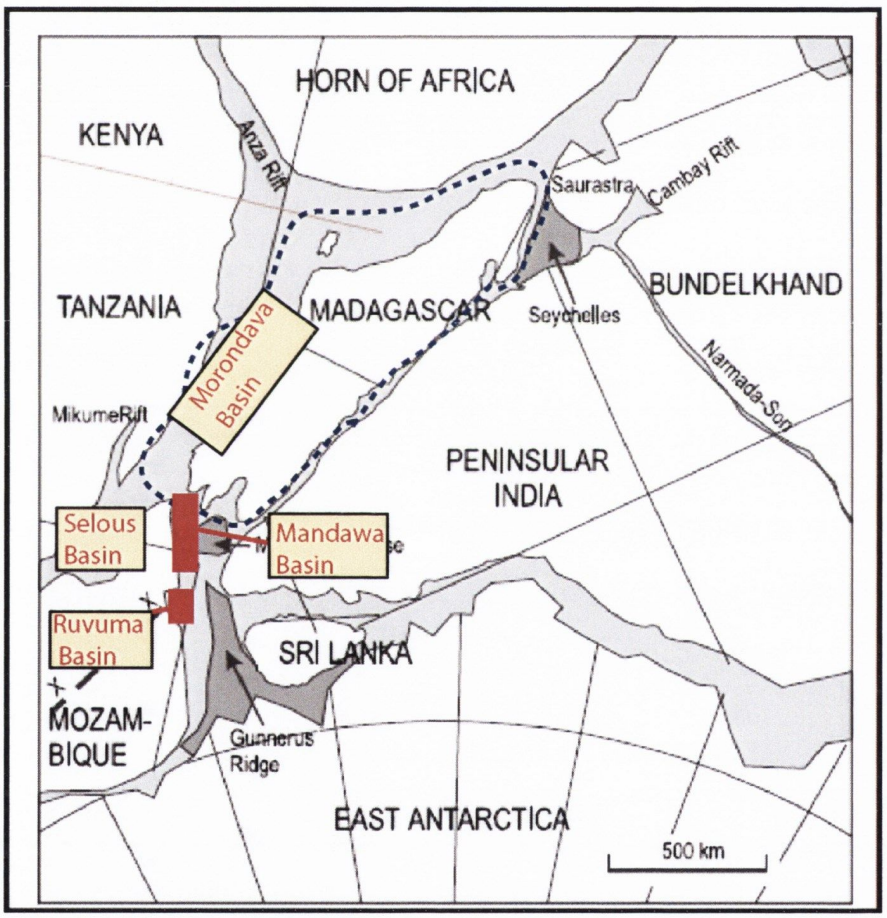

Figure 2.1: An adaptation of a reconstruction of Gondwana fragments at 200Ma by Reeves *et al.* (2002) based on ocean floor topography and fracture zone orientations. Sedimentary basins in Tanzania and Madagascar are indicated. Areas in white indicate continental crust while areas in grey are zones of weakness and continental rifting. Present day outline of Madagascar is shown in blue dashed outline (Geiger *et al.* 2004)

2.2.2. West Somali Basin Seafloor Creation – Dextral Strike Slip Movement

Seafloor spreading was initiated in the West Somali Basin (WSB) at magnetic chron M22 (150.21Ma – Upper Jurassic) and ceased at M10n during the Lower Cretaceous at approximately 188Ma (Segoufin & Patriat 1980). The spreading axis, located at 45E, 8S is placed approximately 300km directly east of Mafia Island by Eagles *et al.* 2008, following a review of the published plate reconstructions (Fig. 2.2). The initial azimuth of movement was in an approximate NNW-SSE direction, with linear gravity spurs off the Davie Ridge interpreted as fracture zones formed at transform faults. The azimuth later shifted to a N-S direction and by M10n (138.85Ma mid Lower Cretaceous) seafloor spreading had ceased.

Thus, from the Upper Jurassic to Lower Cretaceous, the Davie Fracture Zone (DFZ) was composed of a series of en-echelon ridge segments with medium offset transforms traversing in a NW-SE orientation. Coffin & Rabinowitz 1983 proposed a spreading rate of 24-26km/Myr which did not decrease prior to cessation and exhibited no prominent axial gravity anomaly. Thus the DFZ experienced >600km of dextral offset as an Upper Jurassic – Lower Cretaceous strike slip transform margin, with stretched continental crust to the west and newly formed oceanic crust to the east. Thus it is often termed a 'fossil-' or 'relic- transform zone' (Bruce & Molnar 1977; Rabinowitz 1971; Scrutton 1978; Scrutton *et al.* 1981; Coffin & Rabinowitz 1987; and Mascle & Blarez 1987).

The change in extensional direction from approximate W-E during the breakup of Gondwana to N-S during seafloor spreading led to an almost 90 degree rotation in the direction of extension in the margin (Salman & Abdula 1995). Thus, the principal structures on the margin at this time on the Tanzanian margin are the older N-S oriented normal faults reactivated as strike slip faults with W-E normal faults enabling the stretching of the continental lithosphere. The reactivation of these faults has not been studied in detail. The tectonic chronology and kinematics of faulting may be mapped using the identification of major faults and fault intersections. The location of

the continent-ocean boundary is traditionally placed along the Davie Fracture Zone, however, the kinematics of the geodynamic and structural relationship along this margin are poorly understood.

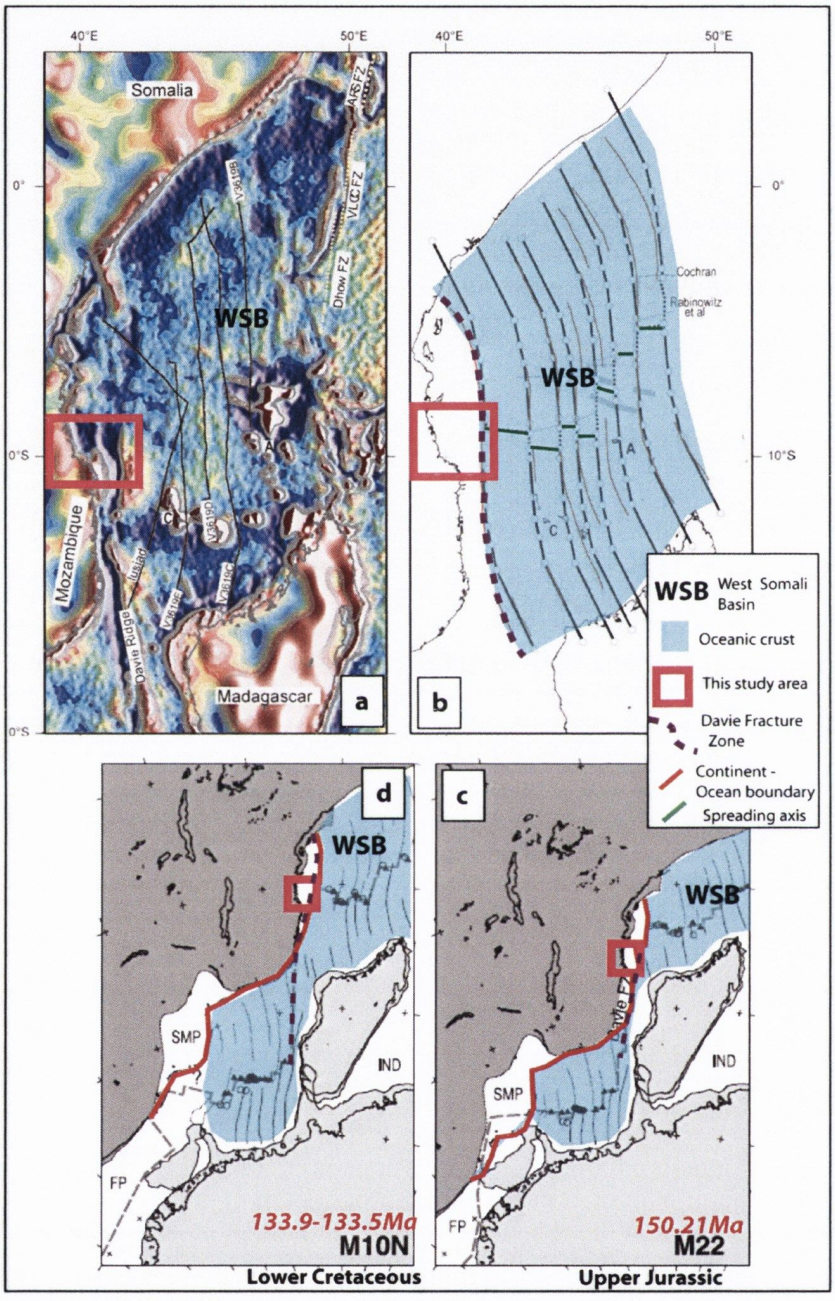

Figure 2.2: (a) Free air gravity anomaly map of the West Somali Basin (WSB) located north of Madagascar and east of Tanzania and b) interpreted map. The newly created oceanic crust is highlighted in blue and the continent-ocean boundary is highlighted in red; (c) and (d) are reconstructions of the strike slip motion along the DFZ at 150.2 and 133.5 Ma. (Adapted from Eagles *et al.* 2008)

2.2.3. Stabilisation/ Passive Margin

Following the cessation of seafloor spreading in the WSB in the Lower Cretaceous, strike slip movement on the DFZ was terminated. A period of stabilisation occurred across the East African Margin from 118Ma-35Ma during which the entire East African margin experienced remarkable margin stability and steady, uniform subsidence across the shelf (Salman & Abdula 1995; Nicholas *et al.* 2006). This phase of development is often referred to as a 'passive margin' which persisted until the Mid Oligocene (Salman & Abdula 1995) (Fig. 2.3). There is no evidence of any fault activity offshore Tanzania at this time.

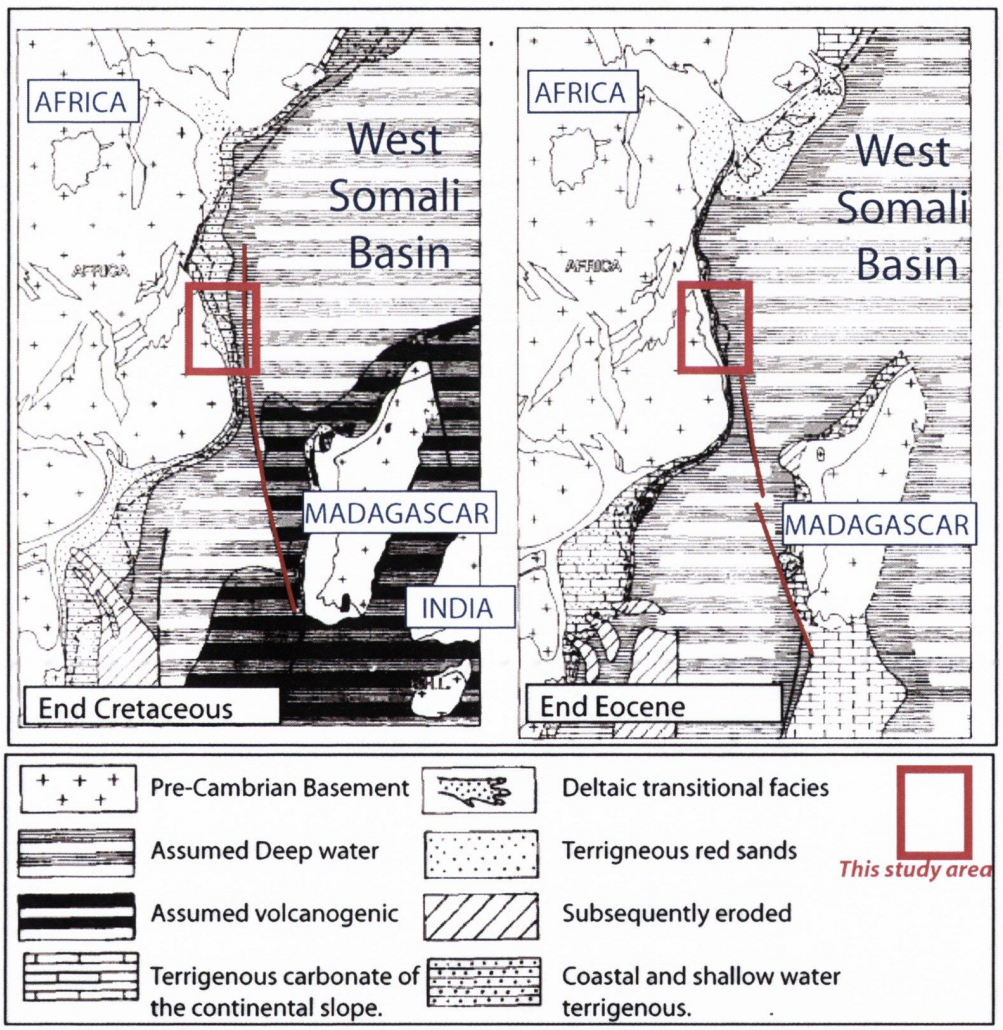

Figure 2.3: Palaeogeographic reconstruction of the East African margin at the End Cretaceous (left) and End Eocene (right) with the location of the Davie Fracture Zone shown in red. There is no evidence of fault activity offshore southern coastal Tanzania during this time period and widespread stability takes place.

2.2.4. Neo-rifting/Reactivation due to the East African Rift Development

A phase of neo-rifting or reactivation was initiated 35 million years ago on the East African margin that was related to the inception and development of the East African Rift System (EARS) (Salman & Abdula 1995). The African craton rose in the Oligocene due to the impact of a plume, dubbed 'the African superswell' (Ritsema *et al.* 1999; Nyblade & Robinson 1994; Nyblade 2011). Tomographic studies (Fig. 2.4) have shown there is a broad (>300km) and deep (>400km) low-velocity zone beneath East Africa at the 410km discontinuity indicating higher than normal temperatures leading to doming, Cenozoic rifting and volcanism (Huerta *et al.* 2009; Nyblade 2011). During the late Miocene, active rifting of the continental margin led to the development of the various topographic highs and lows of the East African coast. The topographic highs of Zanzibar, Pemba, Mafia Islands and the horsts of the Davie Ridge (Schluter 1997; Mougenot *et al.* 1986) were progressively developed by relative uplift, mostly interrupted by slower subsidence associated with closely spaced faulting in the Neogene. Similarly, the Kerimbas and Coastal Basins were initiated as grabens at this time. East African Rift fracturing and subsidence nucleated at different locations during the Late Miocene and is presently still propagating southern offshore Tanzania along the Davie Ridge area, as shown by the distribution of seismic activity (Grimison & Chen 1988). Unroofing of the inland basement Masasi Spur to the west seems to have been constant for ~55Ma and seismic reflection evidence indicates the presence of large palaeo-fluvial systems where the present day Ruvuma and Rufiji are situated (Nicholas *et al.* 2006).

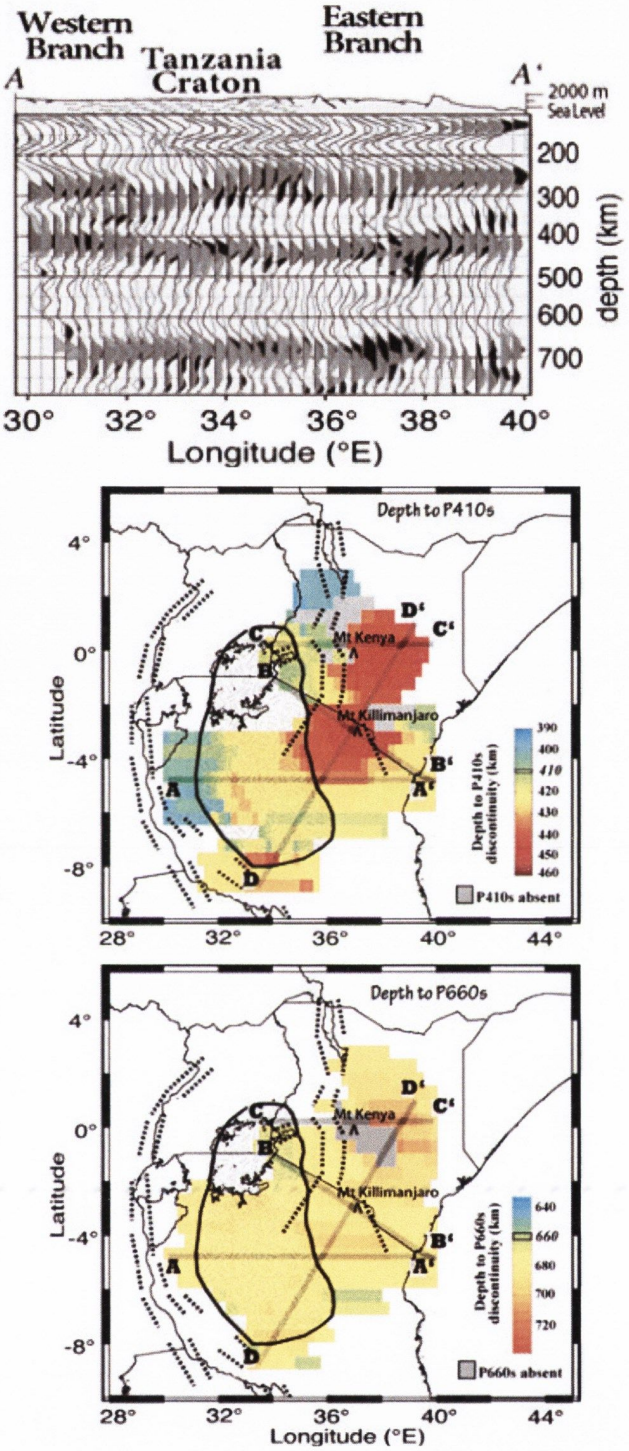

Figure 2.4: Stacks of P-wave receiver functions image Ps conversions from the 410 and 660km discontinuities beneath the eastern branch of the rift system in Kenya and Tanzania (Huerta *et al.* 2009) and a cross section along the Kenya-Tanzania border showing the 410km discontinuity. The doming beneath the Tanzanian craton and accompanying rifting in the EARS arms (dashed) is clearly shown.

The Tanzanian margin was first hypothesised as the youngest and only offshore segment of the Eastern Branch of the EARS by Mougenot *et al.* (1986) who imaged Miocene extension offshore Mozambique and Tanzania. It has since been referred to as the southeastern branch of the EAR by Chorowicz (2005) in his review of the EARS (Fig. 2.5). Less developed than others, it is suggested by these researchers that this may be due to hotter, thinner lithosphere. The Pemba, Mafia, Kerimbas and Lacerda Basins are >20km wide half graben zones of normal faulting mostly parallel to the main trend of the margin. The fault motion may have been favoured by the tendency of margin sediments to sag due to gravity forces. Chorowicz (2005) proposed the Kerimbas and Lacerda basins are probably due to the extensional reactivation of ancient strike slip faults of the Davie Ridge.

The nature of this reactivation is unclear however and our understanding of the margin in terms of classification is quite poor. The Davie Ridge area in Tanzania has been relatively poorly studied in relation to the main tectonic features, evidence of volcanism, fault kinematics, transfer and accommodation zones and the temporal and spatial evolution of the SE branch of the EARS.

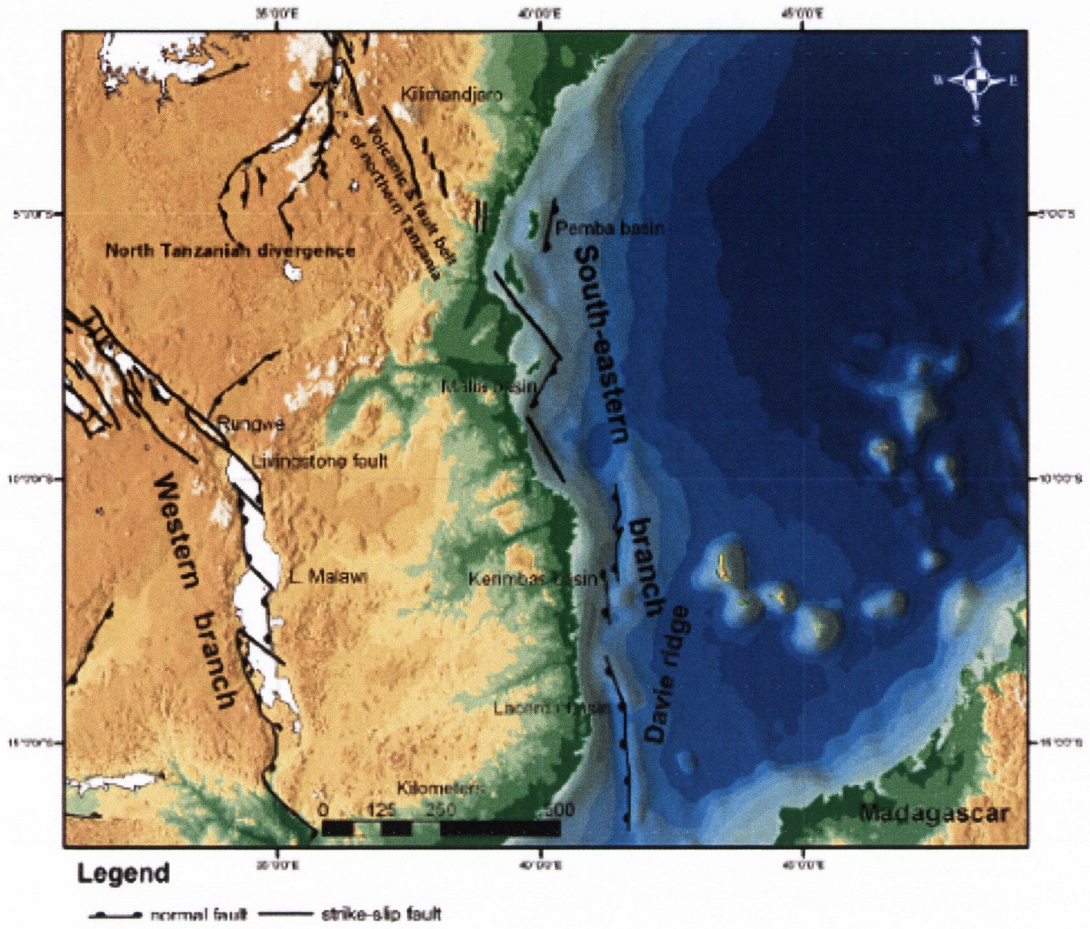

Figure 2.5: The southeastern branch of the EARS located in a N-S direction parallel to the Tanzanian margin. It has been suggested that the Davie Ridge faults have been reactivated in extension leading to the formation of the newest rift arm (Chorowicz 2005).

2.2.5. Seismicity and Geodetics of the Rovuma-Somalia Microplate boundary

Earthquake slip vectors, located on the Tanzanian and Mozambican margins follow a well defined belt of seismicity contiguous with active structures of the Davie Ridge (Mougenot *et al.* 1986; Grimison & Chen 1988; Stamps *et al.* 2008). Pointing predominantly towards the southeast quadrant, they indicate the direction of maximum displacement at this location.

The African continent is split into several blocks, on the basis of seismological and structural grounds. The EARS is essentially splitting the continent into western and eastern tectonic blocks (Nubia and Somalia respectively) around a triple junction between the Red Sea and the Gulf of Aden. More complex structure in East Africa has led to further identification of three microplates (Victoria, Rovuma and Lwandle) between Nubia and Somalia (Fig. 2.6). The large relatively aseismic lithospheric blocks are bordered by narrower belts of neotectonic rifting, volcanism and concentrated earthquake activity. The Rovuma microplate encompasses the Tanzanian craton and its eastern boundary with the Somalia plate is located along the Tanzanian continental margin and ostensibly the Davie Ridge and the southeastern extension of the EARS. The placing of the Rovuma-Somalia boundary at this location is based on limited GPS data and earthquake magnitudes measured by the thirty year global NEIC catalogue. Along the Davie Ridge, the earthquake slip vector directions are primarily pointing southeast (Calais *et al.* 2008), thus describing the motion of the hanging wall with respect to the footwall.

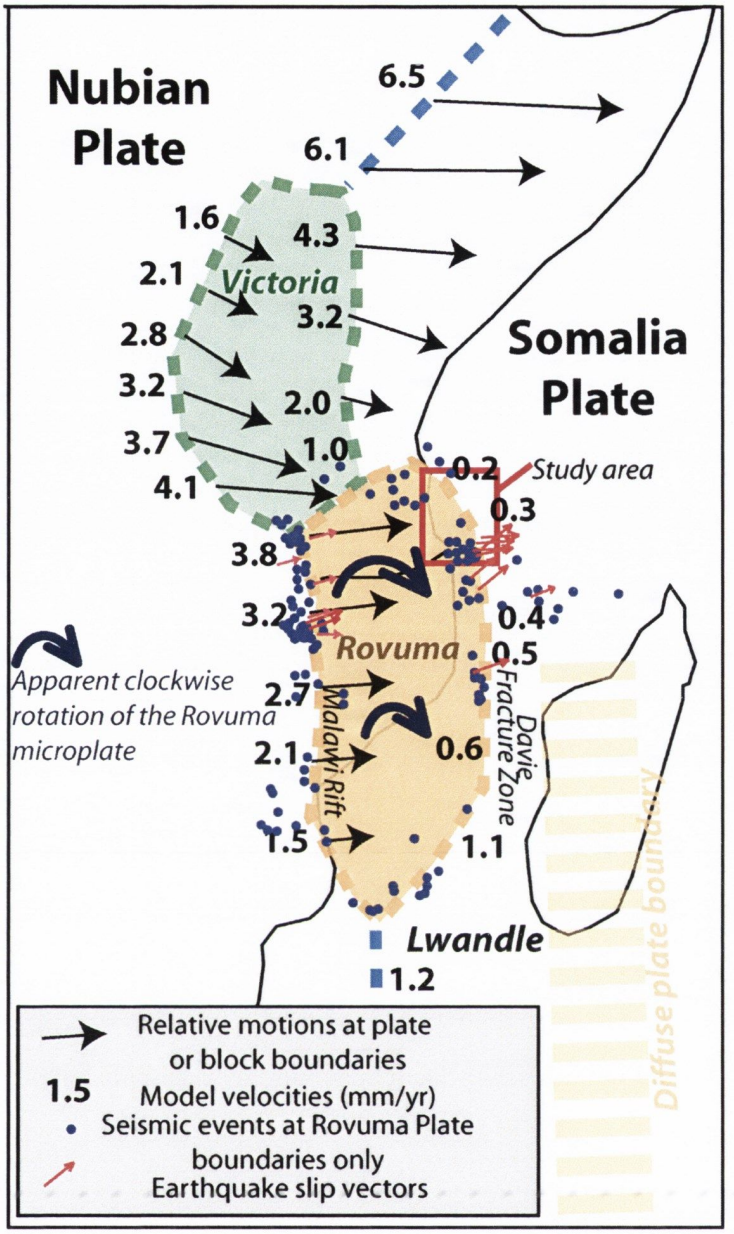

Figure 2.6: Relative motions at plate boundaries in East Africa, particularly around the Rovuma microplate (adapted from Stamps *et al.* 2008 and Calais *et al.* 2006). The East African plate comprises three microplates; Rovuma, Victoria and Lwandle. The Rovuma Plate in the north is moving eastwards away from Nubia at 3.2-3.8mm/yr whereas at the eastern boundary of the Rovuma it is moving east at 0.2-0.3mm/yr. It is inferred from this data that the Davie Fracture Zone area is accommodating a large portion of this compression and taking up the strain with a vertical component of uplift. The calculation of the clockwise Rovuma microplate motion with respect to Nubia (Calais *et al.* 2006) is primarily based on the seismicity data (NEIC) on the Davie Ridge (red arrows). Circles represent locations of seismic events at the Rovuma boundaries and arrows indicate earthquake slip vectors. In Tanzania, they are heavily concentrated in one area close to the Tanzanian-Mozambican border, to the south of the study area.

The Nubian-Somalian plate boundary consists of two distinct portions; one accommodating convergence and one accommodating divergence. The Tanzanian portion of the plate is identified as accommodating convergence as the Rovuma plate is rotating clockwise with respect to the Somalia plate (Fig. 2.6). Stamps *et al.* (2008) synthesised the existing data for plate motions along plate or block boundaries and show that in southern Tanzania the Rovuma plate is moving eastwards away from Nubia at 3.7-3.8 mm/year (Fig. 2.6, 2.7). However, on the eastern side of the Rovuma plate the relative motion is only 0.2-0.3mm/year (Fig. 2.7). Thus between the Malawi Rift and the Davie Fracture Zone, approximately 3.4-3.6mm/yr of convergence (or 90% of microplate motion) is accommodated at the Davie Fracture Zone, probably with a vertical component of motion or uplift. Thus, the Tanzanian margin is one of the most southerly expressions of deformation or seismicity of the EARS due to the relative motion of these two distinct plates.

Grimison & Chen (1988) modelled a series of seismic events that occurred along the Davie Ridge in 1985. Events 850514a and 850514b were modelled using body-waveform inversion. Both events had epicentres very close together on the Davie Ridge, between Mozambique and Madagascar, and yielded identical source parameters, showing pure normal faulting with nodal planes striking north-northwest and no significant component of strike slip motion. The centroid depth for both events was difficult to constrain; Grimison & Chen (1988) proposed double ruptures at 40 km and 20 km. Honda & Yomogida (1991) proposed that the 850514a event consisted of a normal-faulting subevent followed by an isotropic source, and they fixed the depths of both subevents to be 7.5 km. Grimison & Chen (1988) noted that the scattered nature of seismicity indicated that extensional deformation was taking place along different parts of the ridge along much of its length. However, the limited extent of the source region of the 1985 sequence meant that continuous or large scale normal faulting has not occurred along the length of the ridge. Delvaux & Barth (2010) show a similar ENE–WSW (N063/067°E) extension in the Davie Ridge with normal faulting (Fig. 2.9). These authors correlated this clearly extensional regime offshore with evidence of a transpressional regime onshore as evidence of unstable interactions

between the Rovuma and Somalia plates since the Pliocene with episodic compression and extension periods.

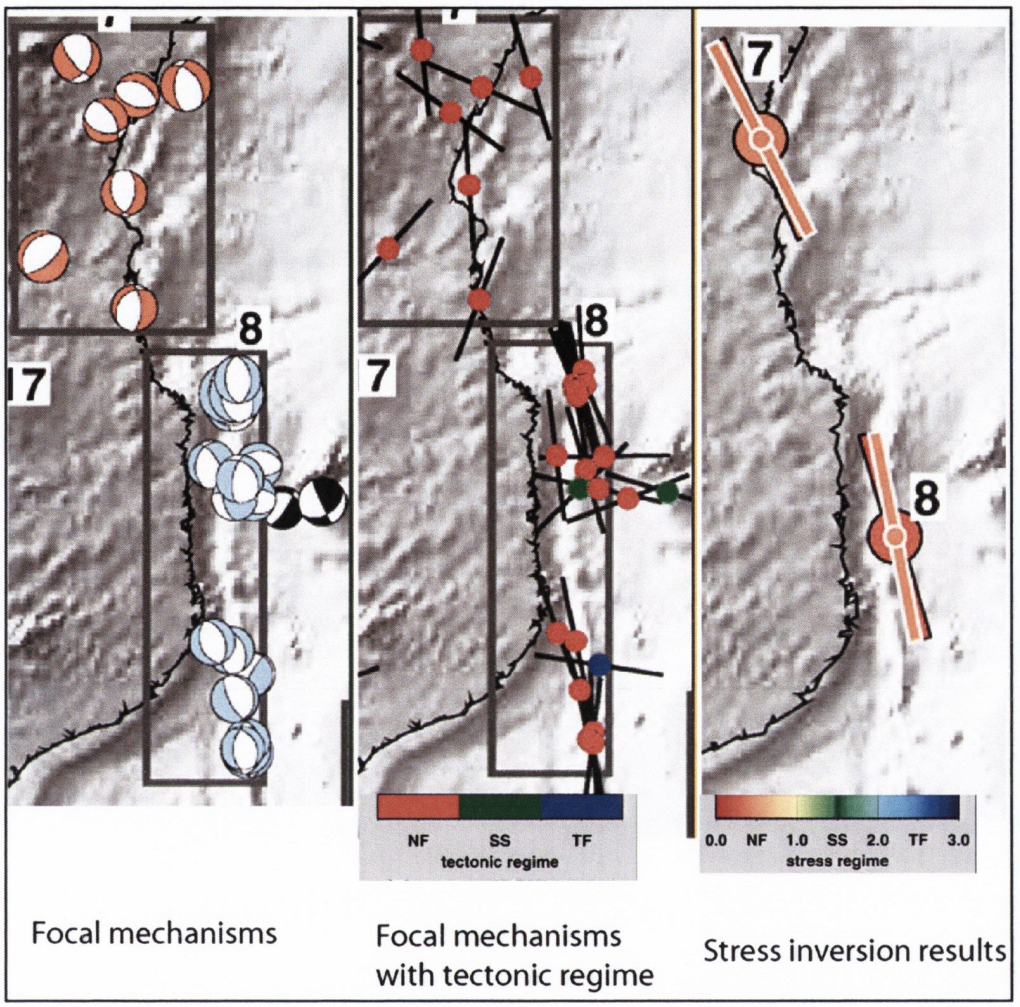

Figure 2.7: Focal mechanisms, superimposed with tectonic regime and stress inversion results for the Mozambique Channel area (Delvaux & Barth 2010). They indicate a dominant NNW-SSE trending normal fault plane along the length of the Davie Ridge. However, this faulting is concentrated in two pockets primarily, the north and south of the bathymetric expression of the Davie Ridge. Some strike slip motion is observed in northern Mozambique that probably indicates a WSW-ENE transfer fault.

2.2.6. Onshore evidence of compression and transpression

Post-Miocene tectonism has been identified onshore southern Tanzania by a number of authors. Nicholas *et al.* (2007) and Reuter *et al.* (2009) observed post-Miocene inversion, strike slip motion and periodic uplift of marine terraces. Nicholas *et al.* (2007) suggest that gravity data indicates the Davie Ridge is thickened continental crust, bound by Jurassic-Cretaceous strike-slip faults. Onshore evidence linking field exposures and seismic reflection data indicates that southern coastal Tanzania is experiencing inversion and reactivation of older faults. A regional scale mechanism proposed by Nicholas *et al.* (2007) is that clockwise rotation of the Rovuma microplate (Fig. 2.8) is leading to transpressional strike slip motion along the Davie Ridge, thus reactivating the Jurassic-Cretaceous faults and leading to uplift. Reuter *et al.* (2009) proposed an uplift rate of 2.5mm/year of the coastal belt as a result of transpressional inversion. The SeaGap Fracture Zone/SeaGap Ridge (Fig. 2.10) has been termed an 'inverted strike slip structure' in Nicholas *et al.* (2007) and Kidson *et al.* (1997) and various unpublished industry reports. However, the structural and tectonic history and evolution of this enigmatic bathymetric feature have not been studied.

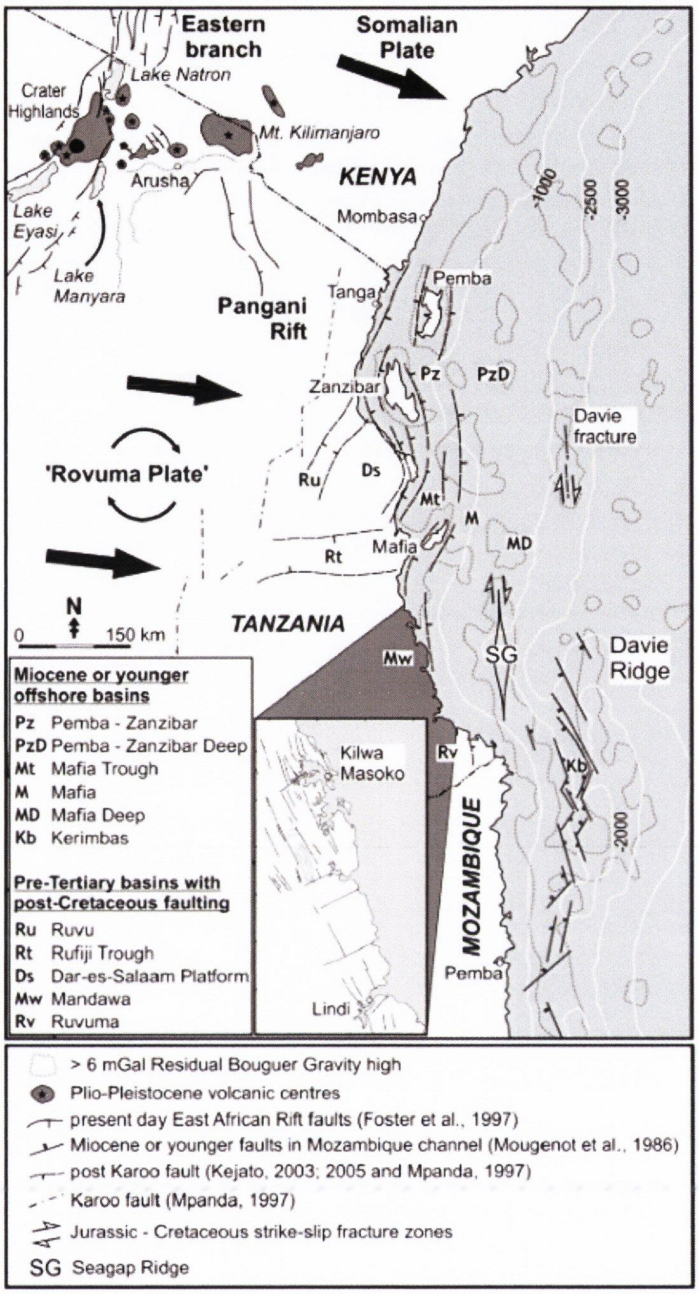

Figure 2.8: Synthesis of the main structural elements active in the Cenozoic, superimposed on a simplified topographic and bathymetric map (Nicholas *et al.* 2007).

2.2.7. Theme 1 Research Questions; Tectonics

1) Can the tectonic chronology and fault kinematics of the Tanzanian margin from Gondwana breakup to present be mapped?
2) What is the nature of the transform continent-ocean boundary located along the Tanzanian margin?
3) Is there any geological evidence either onshore or offshore of the (a) tectonically stable period hypothesised from Lower Cretaceous to Oligocene, (b) the Miocene extensional event and (c) the present day compressional/transpressional hypothesis based on the geodetic, seismic and onshore field data?
4) Can the southeastern branch of the EAR be described in terms of main tectonic features, evidence of volcanism, fault kinematics, transfer and accommodation zones and the temporal and spatial evolution?
5) Can the geological evolution of the 'SeaGap Fracture Zone' be described?

2.3. Stratigraphic framework of onshore and offshore Tanzania

The stratigraphic framework of the Tanzanian margin does not appear to be fully understood in the literature. In Chapter 7, a synthesis of the previous studies and stratigraphic nomenclature is given. What is clear arising from the pre-existing body of work is that the post Oligocene stratigraphy onshore has not been well defined. It is of critical importance when resolving tectonic and sedimentological evolution that the stratigraphy is established. As can be seen from the previous sections, the post-Oligocene geological evolution refers to a period of reactivation of the Tanzanian margin. Offshore, there is one published seismostratigraphic scheme (Cope 2000). However, this is a general scheme that applies to the offshore area from Mafia south to Ruvuma and offshore towards the Davie Ridge. As there are clear structural features offsetting the offshore stratigraphy, ensuring good stratigraphic control was very important.

2.3.1. Theme 2 Research questions; Stratigraphy Onshore and Offshore

6) Can the stratigraphy of offshore southern coastal Tanzania be defined and correlated on the basis of seismic data?
7) Is there a geological lithological/sedimentological or chronostratigraphic unit identifiable onshore southern Tanzania that can be distinguished from the well-defined pre-Oligocene geology?

2.4. Offshore Age control

Due to a recent burst in hydrocarbon exploration activity in East Africa there are currently a number of exploration wells drilled offshore Tanzania (2010-2012). However, for the purposes of this study, no access to existing industry offshore wells was obtained. As well ties and control are the primary and most important methods of assigning ages to marine seismic stratigraphy it has rendered the chronostratigraphic control of the marine portion of the margin very poor. Previous surveys have correlated marine seismic surveys to DSDP Wells 241 and 242 located offshore Kenya and Mozambique respectively, to coastal wells Songo-Songo- 1 and Mnazi Bay-1 and to onshore wells via seismic data.

2.4.1. Theme 3 Research questions; Age control

8) By synthesising previous published and unpublished surveys, can accurate age constraints be placed on the seismic stratigraphy erected for the offshore realm?
9) Can identification of unconformities and bounding surfaces in the onshore stratigraphy be extended into the shallow marine seismic stratigraphy?
10) Can a regional chronostratigraphic framework for both onshore and offshore Tanzania be erected?

2.5. *Sedimentary transport on the margin*

The nature of the oceanographic regime, sedimentary processes on and morphology of the Tanzania margin is poorly understood. Although the oceanographic regime and the interaction between currents and seafloor topography is well established for the Mozambique Channel (Ridderinkhof & Ruijter 2003) the area offshore Tanzania has been poorly studied, except for Swallow (1991) who gave an appraisal of the surface currents along the East African coast. The interaction of bottom currents and bathymetric features and their influence over sedimentation on the Tanzanian margin however, has not been studied. A sedimentary seismic facies termed 'contourites' were observed offshore Tanzania and named locally as the 'Davie Drift' by Virlogeux *et al.* (1988) and published in Faugeres *et al.* (1999). Further investigation of the origin of these climbing sediment waves and the timing of slope (and possibly fault movement) initiation was identified as a potential for further study.

There has been no comprehensive survey of the seabed topography, architecture and sediment pathways on the Tanzanian margin. Although significant erosion and sediment redistribution has been proposed due to the thermal doming of the African craton, there has been no study of the offshore sedimentary response. Bourget *et al.*, 2008 described the presence of a 10km wide, 70m deep giant submarine channel at 4,000m water depth over 800km from the coast into the Somali Abyssal plain; 'the Tanzania Channel'. Sediment core data proved the presence of remains of reworked and transported terrestrial fauna on the canyon floor. Based on the GEBCO bathymetric maps of the Tanzanian margin, Bourget *et al.* 2008 proposed a distributary network of canyons across the Tanzanian shelf transporting terrigenous sediment from the thermally up-domed hinterland to the Somali Abyssal Plain. The authors proposed that some structural control of the sediment pathway probably exists. However, also present on the bathymetric maps are the structurally complex SeaGap Fracture Zone and the Davie Ridge. Thus seafloor bathymetric profiling and analysis of the hypothesised 'distributary network' was proposed.

2.5.1. Theme 4 Research questions; Oceanography and sedimentary response

11) Can the morphology and sedimentation of the Tanzanian continental margin be classified?
12) Is there any evidence on the margin of the downslope tributary channels converging into the Tanzania Channel as proposed by Bourget *et al.* (2008)?
13) Can the contouritic facies identified by Virlogeux *et al.* (1988) be identified on the Tanzanian margin and can its development be linked with timing of fault activity in the area?
14) Are present day processes relevant to past sedimentary processes?

2.6.Aims and Objectives for the present study

Previous research on the Tanzanian margin has been briefly described above and a number of research question arising from this body of work identified. Many of these research questions form the framework in which this study was carried out to contribute to the existing body of knowledge. The overall aim of the present study is to construct a regional overview of the sedimentological, structural and stratigraphical evolution of the Tanzanian margin. This aim will be using the methods described in Chapter 3.

2.6.1. Primary objectives

1) To collate the existing but disparate published and unpublished data (reflection seismic, wells, maps) relevant to the study.
2) To identify key regional, yet poorly understood bathymetric and structurally controlled features offshore Tanzania.
3) To plan, acquire and process a 30day high frequency seismic survey offshore Tanzania as part of the GLOW multidisciplinary team.
4) To acquire box-core data targeting outcropping reflectors imaged in the seismic survey to assign biostratigraphic control to those reflectors.

5) To construct a seismic stratigraphic framework for offshore southern Tanzania.
6) To integrate previously existing data to assign ages to the offshore seismic stratigraphy, thus creating a chronostratigraphic framework.
7) To identify and define the 'Oligocene/Miocene and younger' geology onshore.
8) To extend the unconformities and sequence boundaries identified by detailed field mapping into the transition zone and shallow water seismic data.
9) Using the newly constructed age constrained seismic stratigraphy; assess the structural regime on the Tanzanian margin.
10) To identify the Post-Oligocene tectonics of the East African Rift in its proposed southeastern branch.

To construct detailed palaeogeographic models of the Tanzanian margin at key geological times and to construct 3D diagrams of the geological evolution of the Tanzanian margin.

3. Methods

3.1. The Multidisciplinary Approach

The thesis objectives (Chapters 1 and 2) were sought using a highly multi-disciplinary approach, combining a desk study of unpublished industry and publicly available data, newly acquired primary offshore data and onshore geological mapping. In this chapter these methods are introduced.

Table 3.1 depicts the range of primary and secondary data sources used and the range of methods employed. A description of the methods used will be discussed in the following sections of this chapter.

3.2. Desk Study

In this study, newly acquired primary data (Table 3.1) have been combined with older, unpublished or partially published industry data (Figs. 1.1 and 1.2). Primary data were obtained during the course of this PhD study and includes multichannel seismic data, offshore sediment samples, multibeam bathymetric data and onshore field data. Secondary data refers to data that pre-dated this study and has been made available for incorporation into the study, primarily from the archives of the Tanzania Petroleum Development Corporation (T.P.D.C.).

Table 3.1: A compilation of the datasets used in this study; their nature, location, source and section referring to methods discussion.

Data Type	Data Nature	Location	Name	Secondary Data Source	Methods	Section
Seismic	*Primary*	Offshore	GLOW Lines 1-31 MCS		Cruise Planning	3.3.1
					Acquisition	3.3.2
					Processing	3.4
					Interpretation	3.5
	Secondary	Offshore	V3618 Cruise (1983)	Shipley et al., 2005	Interpretation	3.5
			MD40-MACAMO Cruise (1984)	Mougenot et al., 1986	Interpretation	3.5
			MD40-MACAMO Cruise (1984)	Mascle & Blarez, 1987	Interpretation	3.5
			Phillips - AGIP Survey (1976)	TPDC	Interpretation	3.5
			DSDP 241 MCS (1974)	DSDP Leg 25 Shipboard Scientific Party, 1974	Interpretation	3.5
			DSDP 242 SCS	DSDP Leg 25 Shipboard Scientific Party, 1974	Interpretation	3.5
		Onshore	Prefix MDW/TNZ/LND	TPDC	Interpretation	3.5
Multibeam	*Primary*	Offshore	GLOW Lines 1-31		Cruise Planning	3.3.1
					Acquisition	3.6
					Processing	3.6
					Interpretation	3.6
Sediment Samples	*Primary*	Offshore	Box and Piston Cores - GLOW		Biostratigraphic analysis	3.7
Geophysical	*Secondary*	Onshore	ARK Gravity East Africa	ARK	Interpretation	
			Combined Aero and Marine Total Intensity Magnetics	Kidson et al. 1997	Interpretation	
			Combined mag data set	Kidson et al. 1997	Interpretation	
			7.5-32.5km Band Pass Filter Bouguer Gravity	Kidson et al. 1997	Interpretation	
			75-150km Band Pass Filter Bouguer Gravity	Kidson et al. 1997	Interpretation	
			Free air gravity anomlaies of the West Somali Basin	Eagles et al., 2008	Interpretation	
Remote Sensing	*Secondary*		Surface elevation data tiles (SRTM).	Nasa, 2010	Interpretation	
			Seismic hazard map.	IRIS, 2011	Interpretation	
			Seismic hazard map.	Grimison & Chen, 1988	Interpretation	
			Seismic hazard map.	Stamps et al., 2010	Interpretation	
Wells	*Secondary*	Offshore	DSDP 241	DSDP Leg 25 Shipboard Scientific Party, 1974	Interpretation	
			DSDP 242	DSDP Leg 25 Shipboard Scientific Party, 1975	Interpretation	
		Onshore	Suite	TPDC/Corelabs	Interpretation	
Geological Mapping	*Primary*	Onshore			Mapping	3.8
					Sample collection	3.8
					Thin section interpretation	3.8
					Biostratigraphic analysis	3.8
	Secondary	Onshore	TDP Maps	Nicholas et al. 2006, 2007	Interpretation	
			TDP Wells	Nicholas et al. 2006, 2008; Berrocoso et al. 2010	Interpretation	
			Geology of Southern Coastal Tanzania	Kent et al 1971	Interpretation	
			Geology of the Kilwa Peninsula	Terris and Stoneley 1955	Interpretation	
			Ruvuma Basin Field Study	Texaco 1991	Interpretation	
			Mandawa Thesis	Hudson 2011	Interpretation	
			Topographic Maps	Governement of Tanzania	Interpretation	
			Satellite Imagery	Google Earth, Landsat, Virtual Earth	Interpretation	

3.3.Primary Offshore Data

The primary, new data examined in this thesis are a suite of high resolution multichannel seismic (MCS) reflection profiles, swath bathymetry and bottom-sediment samples from offshore Tanzania collected by the scientific team and crew of the R.V. Pelagia in February and March 2009 under the direction of the Universities of Edinburgh, Cardiff, Kiel, Dublin and Vrijie Universitat Amsterdam. This international collaboration, known as the acronym 'GLOW' (**GLO**bal **W**arming Events) aimed to record data that may shed light on tropical global warming events at low latitudes, particularly during the Cenozoic. The relevant data are located in Appendices I-IV.

3.3.1. Survey Planning

Two key areas were considered in survey layout design; a) defining the scientific aims and b) project planning.

The desk study prior to establishing the survey layout involved assessing the available data, which included 2D seismic reflection data, wells, maps, geophysical and well log information. The scientific aims of the cruise were confirmed amongst the scientists of the GLOW team in a pre-cruise meeting and subsequently the ideal acquisition parameters established. The principal scientific aims of the GLOW Survey were to a) complete a regional scale seismic survey, b) sail as close as possible to areas with good age constraint, i.e. wells and coastal areas with good field control c) to record seismic data of potential future IODP sites for Cenozoic recovery (referred to as 'Tanzania to Offshore Paleogene Survey' or TOPS) and d) take sediment cores and seismic reflection data along the continental shelf for Plio-Pleistocene and Holocene studies.

Once the scientific aims were established, practical matters such as time constraints, ship paths and jurisdiction were considered. A pre-cruise meeting held at NIOZ (Royal Dutch Oceanographic Institute) in November 2008 involved all scientists' input and further consultation took place via email. A working consensus of scientific aims incorporating those of all participants was agreed upon. An order of priority was set and subsequently, a preliminary cruise path was established (Fig. 3.1). Previous

industry surveys completed in the area were consulted to avoid duplication. The relevant government authorities (COSTECH – Commission for Science and Technology) awarded research permits to the Chief Scientist.

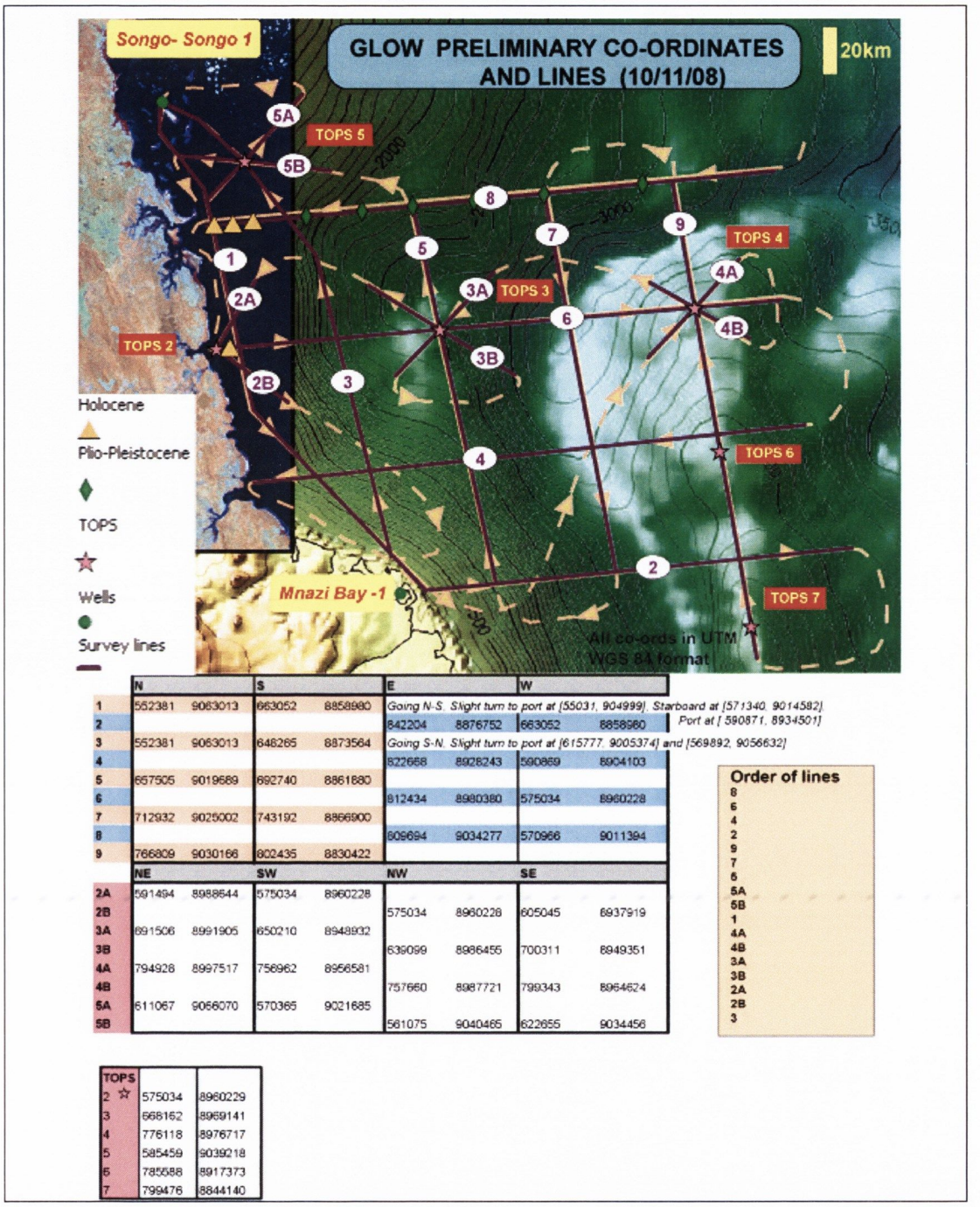

	N		S		E		W	
1	562381	9063013	663052	8858980	Going N-S. Slight turn to port at [55031, 904999]. Starboard at [571340, 9014582]			
2					842204	8876752	663052	8858980
3	562381	9063013	648265	8873564	Going S-N. Slight turn to port at [615777, 9005374] and [569892, 9056632]			
4					822668	8928243	590869	8904103
5	667505	9019689	692740	8861880				
6					812434	8980380	575034	8960228
7	712932	9025002	743192	8866900				
8					809694	9034277	570966	9011394
9	766809	9030166	802435	8830422				

	NE		SW		NW		SE	
2A	591494	8988644	575034	8960228				
2B					575034	8960228	605045	8937919
3A	691506	8991905	650210	8948932				
3B					639099	8986455	700311	8949351
4A	794928	8997517	756962	8956581				
4B					757660	8987721	799343	8964624
5A	611067	9066070	570365	9021685				
5B					561075	9040486	622655	9034456

TOPS		
2	575034	8960229
3	668162	8969141
4	776118	8976717
5	585459	9039218
6	785588	8917373
7	799476	8844140

Figure 3.1: GLOW cruise survey layout design including line nos., co-ordinates, wells, potential cross points for IODP (TOPS) survey, planned sites for box cores and the order of shooting.

3.3.2. 'GLOW' Survey 2009; Acquisition.

This section describes the seismic data acquisition specific to the GLOW seismic survey, carried out in February-March 2009 offshore southern Tanzania.

The GLOW survey was shot during February-March 2009 and covers a square area of approximately 400km^2. The vessel R.V. Pelagia, operated by the Dutch Royal Institute for Oceanographic Research (NIOZ) conducted the 2-D seismic survey and associated sampling on behalf of the GLOW/ESF consortium. A total of approximately 2,000km of seismic reflection profiles were collected in various directions. The most extended lines are 250km long while the shortest are 15km long. As described in the introduction, the seismic data collected in this survey was to be utilised primarily as a regional survey and as a site survey for an IODP proposal. For the latter, two crossing points at right angles were required. The potential sites were chosen during the cruise. This explains why the survey is not a typical seismic grid layout.

Seismic operations began with a Sercel 210 in^3 GI gun (Fig. 3.2). A pneumatic source, it contains two independent airguns within the same casing. The first air gun is called the 'generator', as it generates the primary pulse. The second air gun is called the 'injector' as it injects air inside the bubble produced by the 'generator'. It is used to control and to reduce the oscillation of the bubble created by the generator.

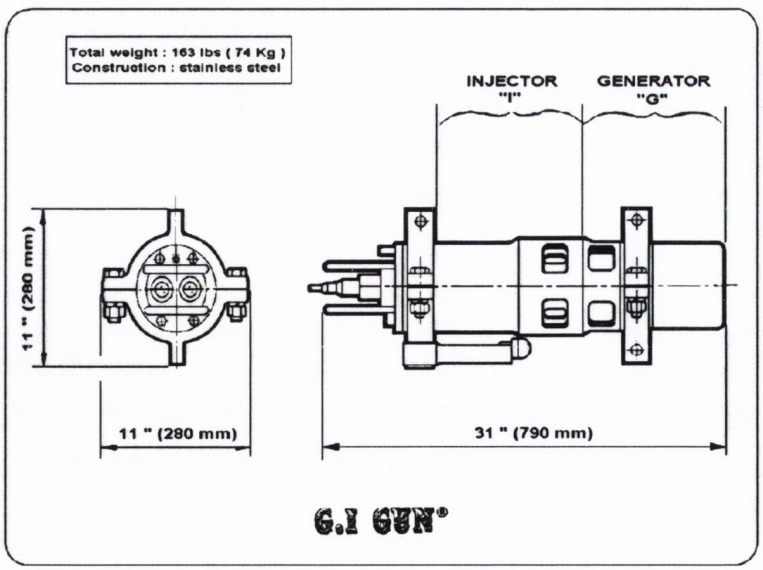

Figure 3.2: GI gun interior schematics. (www.sercel.com)

The generator and injector chamber were reduced to 45 in^3 each, because the compressors used were unable to supply sufficient air at the required pressure. However, after the returning signal of the GI gun on Line 1 and 2 was considered to be too weak, an array of 4 sleeve guns was deployed instead. After Lines 3 and 4 were adequately recorded, the Line 1 was re-recorded (and labelled Line 5), albeit with a small lateral offset so an additional strip if multibeam echosounder data could be recorded.

From Line 3 onwards four sleeve guns with a volume of 10, 20 and 2x40 in^3 were used. While traditional air guns use multiple ports and the resulting discharge becomes rapidly disorganised, the sleeve guns use a single 360 degree port resulting in a predictable, spherical bubble with a reliable and repeatable interaction with adjacent guns. However, the sleeve gun does not produce an exact impulse but is tuned to produce a broadband spectrum in the typical seismic frequencies. The peak frequency of the combined signal of the guns was within the range of 50-150 Hz with lower amplitude frequencies up to 400 Hz. The guns were towed in a frame at a depth of 1.7m while 42 metres behind the stern of the ship and fired every 10 seconds at a pressure of 115 bars (Fig. 3.3).

The average sailing speed was 4.2 knots which resulted in an average distance between the shots of 21m, twice the receiver group interval of the 24 channel streamer. The streamer consisted of four 63m long active sections with 6 channels each. Each channel consists of 10 Teledyne T2 hydrophones with a hydrophone interval of 1m. The streamer is ended by a 0.5 m tail-end, which contains the last terminating end connector. The receiver was attached to the ship by a tow leader of 60 m and a stretch member of 25m. The streamer was towed at a depth of 1 metre below the surface. Three (front, mid, end) 5010 DigiBIRDS were used to keep the streamer at depth. During the recording of line 2 one bird failed. From line 3 onwards only 2 birds (front, end) were used with no noticeable effect on the streamer position. The acquisition layout is depicted in Fig. (3.4).

Figure 3.3: Submerged sleeve guns immediately after shooting and streamer cables from stern of the Pelagia., GLOW Survey 2009.

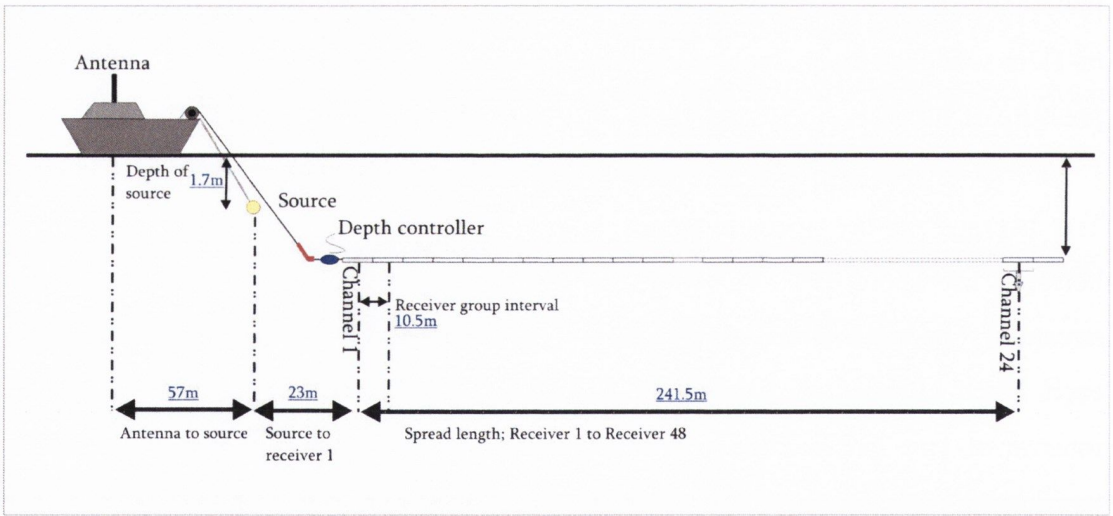

Figure 3.4: GLOW Survey acquisition layout.

Data recording was performed using the Geo-Resources Geo-Trace 24 hard- and software (lines 1 and 2 software version 9.0, after a software crash lines 3 and onwards version 8.4). The system has a 24 channel digital pre-amplification system and 24 channel band pass filter already integrated. The record length was 7500 ms, the sampling rate was 2 kHz for 1-4 and 1 kHz for lines 5 onwards. The data was

recorded with a 10 Hz high pass filter. In order to keep the file size within workable limits, the data was stored in separate files with a length of 2 hours.

For quality control and onboard use an online raw image (channel 1, 30 Hz high pass filter only) of the data was plotted on a CodaOctopus high resolution thermal printer. The time sweep on the paper was 2 seconds, the paper speed 0.05 mm/s. This resulted in good quality images suitable to help in planning cross lines and coring stations.

During the recording of all lines channel 1 was slightly noisy while channel 2 was very noisy. The signal of channel 23 was amplified more than all other channels due to the presence of a different type of amplifier for this channel (old type no longer available). Channels 7, 14 and 24 were not working at all, although channel 7 sometimes did give data.

The recording and acquisition details for each line within the GLOW survey were described in the observer logs (Fig. 3.5). These paper reports are the only records made in the field which may record deviations from the acquisition specifications, such as missed shots, bad traces, noise files, levels of interference, operator error, data recording.

Seismics GLOW, Pelagia			**Line no.:**		
Start of line	Date Time (GMT)	Latitude Longitude	**End of line**	Date Time (GMT)	Latitude Longitude
			GeoTrace (24 Channels):		Sampling rate (ms): Record length (ms):
			Total no. of shotpoints:		**Shot interval (ms):** **Recording delay (ms):**
Every half hour:					
Date Time (GMT) Shotpoint 6 ch: Shotpoint 24 ch:		Latitude Longitude Speed (knts) Gun pressure (bar):		Remarks	
Date Time (GMT) Shotpoint 6 ch: Shotpoint 24 ch:		Latitude Longitude Speed (knts) Gun pressure (bar):		Remarks	
Date Time (GMT) Shotpoint 6 ch: Shotpoint 24 ch:		Latitude Longitude Speed (knts) Gun pressure (bar):		Remarks	

Figure 3.5: Typical observer log as used in seismic acquisition, GLOW survey.

Instrumentation and Recording Parameters, GLOW 2009 Survey	
Parameter	**Value**
Total distance shot	
Source	Dual tuned airgun array
Airguns	Sercel 210 cubic inches GI gun (Lines1-3) Sleeve gun array (Lines 5-31)
Array	4 parallel sub array per source 10, 20 and 2x40 cubic inches.
Volume	Total 110 cubic inches.
Pressure	115 bars
Operating Depth	1.7m
Array Separation	42m
Average near group offset	
Recording system	Geo-Resources Geo-Trace Version 9.0 for lines1-3 Version 8.4 for lines 4-31
Tape/Cartridge decks	
Tape format	SEG, 8 byte
Tape polarity	A positive pressure at the hydrophone produces a negative number on tape and a downward deflection on the field tape monitor.
Number of channels	24
Recording length	7500 ms
Sample rate	2 kHz for Lines 1-4 and 1 kHz for lines 5-31.
Recording filters	10 Hz high pass filter
Shotpoint interval	21m
Group interval	10.5m
Hydrophones per group	60
Hydrophone interval	1m
Hydrophone type	Teledyne T2
Streamer length	241.5m
Navigation system	Differential GPS

Figure 3.6: Summary of instrumentation and recording parameters, GLOW Survey 2009.

3.4.Multichannel Reflection Seismic Processing

The aim of seismic processing is to manipulate the acquired data into the best possible image from which to infer sub-surface structure. If the seismic acquisition system were perfect, only minimal processing would be required.

Seismic reflection data can be thought of as containing two types of information about the earth structure: traveltime and amplitude. A two-way traveltime is the total time for the seismic energy to travel from the source to the reflector and finally to the receiver. It can be used to deduce the location of reflectors. Secondly, amplitude information yields knowledge about the relative impedance changes across reflector boundaries, and can be used to infer material properties of the earth structure.

Seismic processing is the alteration of seismic data to suppress noise, enhance signal and migrate seismic events to the appropriate location in space. However, it is important to note that there is no single 'correct' processing sequence for a given volume of data. At several stages judgements and interpretations are required. Processing flows, steps or routines often fall into one of the following categories: enhancing signal to noise ratio, providing velocity information, collapsing diffractions, increasing resolution. As this study is mainly concerned with the enhancing signal and extracting velocity information, they will be discussed here in more detail.

The following section will follow each step pursued in the processing flow applied to the GLOW 2009 Survey (Fig. 3.9), with a brief description of the theory behind major processing steps such as velocity analysis, deconvolution, normal moveout, stacking and migration. Seismic processing leads to better interpretation because the signal to noise ration is increased and subsurface structures and reflection geometries are more apparent.

3.4.1. Theory

There are many steps the processor can take in order to enhance the seismic data. However, only the steps taken in this project shall be described as shown in the

GLOW 2009 seismic survey processing flow in Fig.3.14. Pre-stack processing, stacking and migration are the principal steps described here. The stack process typically reduces the data volume by 30-60 times so that post-stack processes are often much quicker to apply. Amplitude correction, bandpass filtering and predictive deconvolution were applied before velocity analysis, stacking and finally, migration.

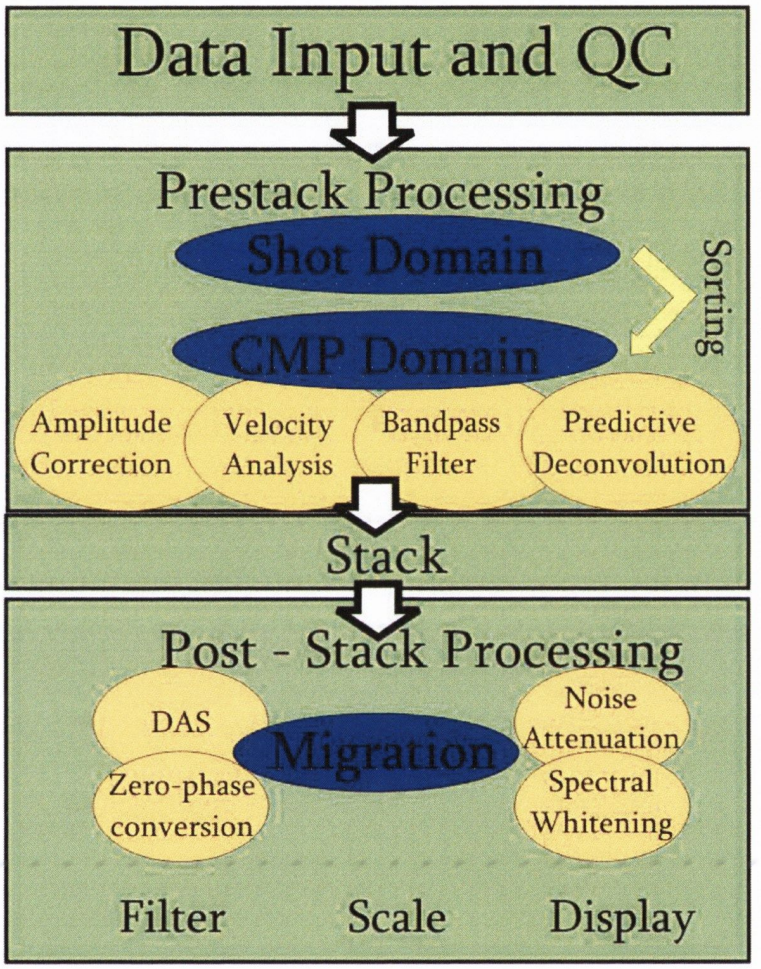

Figure 3.7: Typical 2D marine processing flow

Scaling or correction is often applied during prestack processing to compensate for spherical spreading. It is critical that both the processor and interpreter understand the scaling corrections that have been applied to the data, particularly if stratigraphic interpretation or other amplitude related work is to be conducted on the data. Scaling corrections are often specified in terms of decibels per second. The decibel is a unit of scale defined in acoustics as 20log (A/B) where A and B are the amplitudes in

question. If A is twice the amplitude of B this translates to 6dB, a factor of 10 to 20dB and a factor of 100 to 40dB.

Processing of the raw seg-y (seismic reflection data format) acquired on the GLOW seismic survey took place by this researcher at NIOZ in April – July 2009. The following section outlines the steps taken in processing the raw seg-y data to give the final migrated output. Most parameters within these routines are tested for best results. Initial establishment of these parameters was decided by using lines which best represented the geology in certain areas. Broadly, the applications performed can be subdivided into (a) Data Input, (b) Prestack Processing (c) Stack (d) Poststack Processing.

The **RadexPro** (Deco Geophysical Moscow) software operates like a tree with each step separate from the previous. However it is not linked, thus if the output of one step forms the input of the next step the processor must manually repeat all subsequent steps. The project 'GLOW_Tanzania' was defined and each subsequent line assigned a different data flow. These flows are the most important part of the processing procedure; intended to perform a certain operation on the data before outputting a new file that can then be incorporated into the next file. At each stage a menu of operations was available (Fig. 3.8).

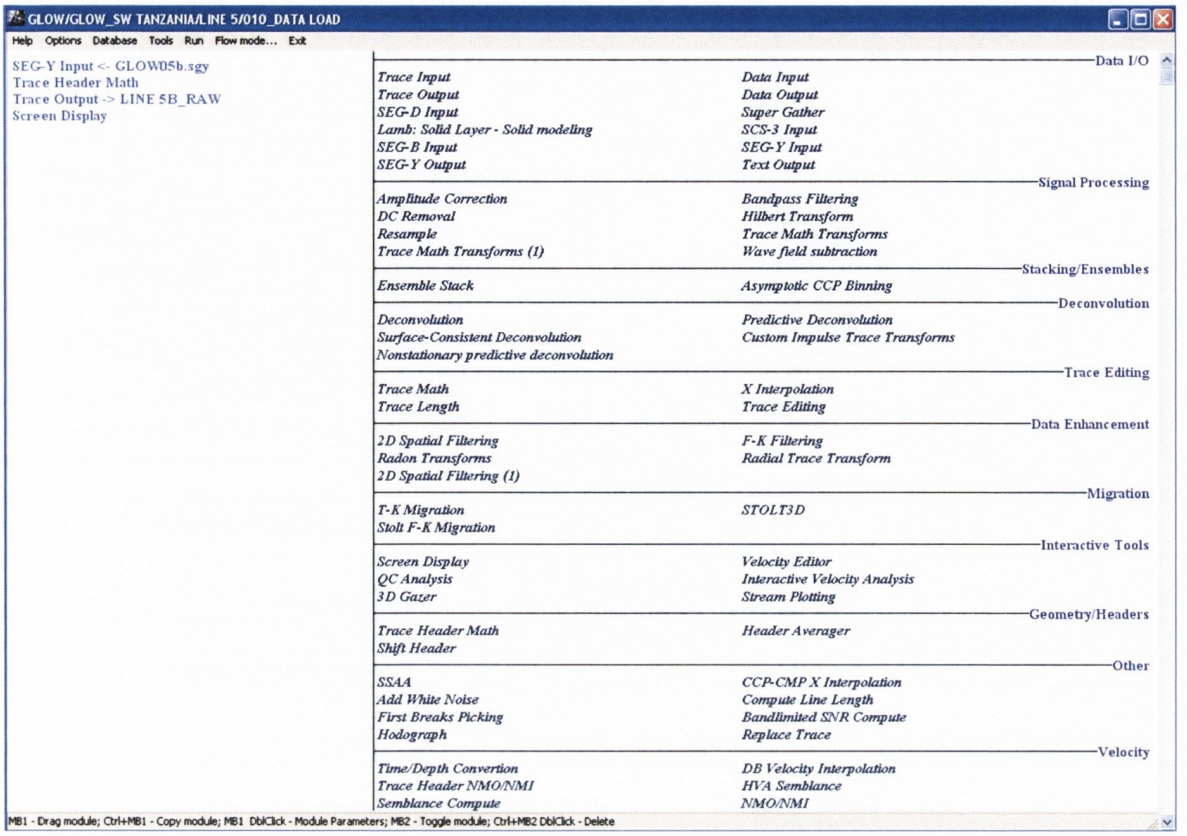

Figure 3.8: The RadexPro base screen with commands to the left and the choice of operations displayed on the right.

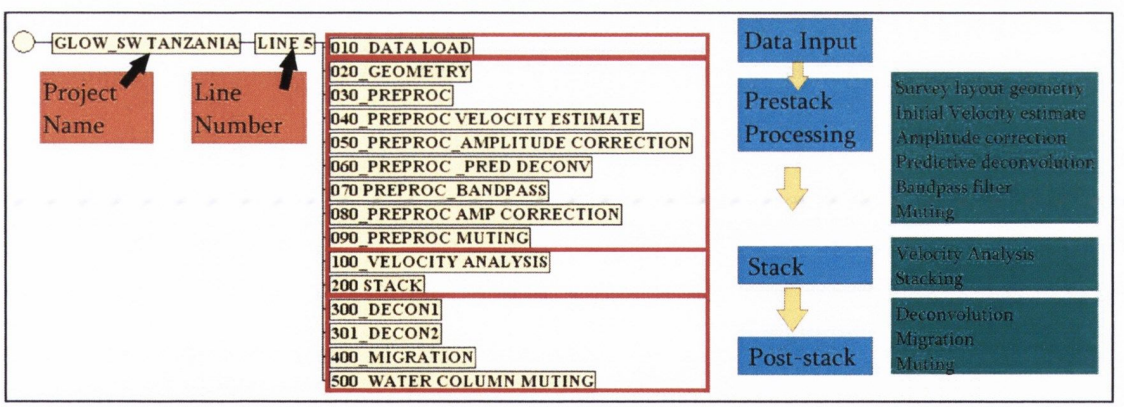

Figure 3.9: GLOW 2009 Survey Processing flow and schematic of the flow.

3.5.Multichannel Seismic Interpretation

In order to establish the stratigraphic, tectonic and sedimentological framework of the Cenozoic sediments of southern Tanzania, seismic facies, interpretation and sequence stratigraphic principles described by Vail *et al.* (1977) and Catuneau (2002) were employed. Seismic interpretation of digital SEGY data has been performed using the Seismic Micro-Technologies Kingdom Software 2d/3d PAK. Paper-copy only seismic profiles have been interpreted by hand on paper and interpretations digitised to be combined with digital data in a Fledermaus 3D visualisation environment. 3D horizon surfaces and sediment isopachs have been interpolated from 2D seismic data through a combination of gridding algorithms and hand contouring. Sediment surfaces and multibeam bathymetry have been visualised using ArcGIS and Fledermaus.

3.5.1. The seismic stratigraphic methodology

Seismic stratigraphy is the study of stratigraphic units that are defined on the basis of their seismic characteristics. In this section, some of the techniques and guidelines for conducting a seismic stratigraphic investigation are discussed. There is no definitive methodical approach to seismic stratigraphic analysis and these steps come as a working approach which must always by adjusted to fit the data for a given area It is important to note it is not the same as sequence stratigraphy though it can be used for sequence stratigraphic analyses. Seismic stratigraphic interpretation is based on an analysis of amplitude data and its representative geology. A number of assumptions are made in seismic stratigraphic analysis. Primarily, it is assumed that the seismic reflection layering represents the surfaces of sedimentary layers of a stratigraphic section. Whereas layers in a stratigraphic succession may be differentiated using a number of characteristics, including lithology, grain size, colour, structure seismic reflection layering is based upon the acoustic impedance contrast between layers with different acoustic properties (Paynton 1977).

Resolution is a key concern in interpreting the type of contrast seen. Seismic reflection observations are subject to the limitations of the vertical and horizontal resolution. Generally, the thinnest resolvable rock layer/reflector in the vertical scale

on seismic reflection data is one quarter of the dominant wavelength (λ), which is equal to the velocity of the p wave within the rock divided by the frequency of the seismic pulse (Henry 1997). Using an average frequency of 150Hz and an average velocity of 1740m/s, the vertical resolution is approximately 3m. Since the process of wave-equation migration reduces the Fresnel zone, the interval between common midpoints is the absolute limit of the lateral resolution of the migrated seismic data (Berkhout & van Wufften Palthe 1979; Safar 1985). In this study, this interval is 10.5m, thus the vertical and horizontal resolution is 8m and 10.5m respectively.

The processing seismic stratigraphic methodology is shown as a flow in Fig. 3.10. After the seismic processing flow, vertical and horizon scales are understood and reflector terminations are identified. A sequence boundary can be drawn defined by the reflector terminations. Between the sequence boundaries are seismic packages of stratified packages of sediment. The internal characteristics of these seismic packages can be described in terms of geometry, continuity, amplitude, frequency and internal velocity. Megasequences bound smaller scale sequences. Sequences can be interpreted in terms of where sediment was being deposited at a certain time, the type of depositional process and the control on development. Megasequences represent the sedimentary response to a major phase of basin evolution, generally bound by regional unconformities. Interpretation of megasequence development can be shown in chronostratigraphic diagrams, depositional sequences and cyclicity and correlation to the global sea level charts. Due to varying factors such as velocity and density of certain lithologies and accumulation rates in both space and time, seismic packages have a heterogeneous thickness.

The surfaces (reflections) that bound a sedimentary sequence (marked as a seismic package) transgress time and the sub-sequences of a sedimentary sequence (internal reflections of the seismic package) also transgress time while being continually reworked though a series of geological events (Payton 1977; Sarg 1988; Galloway 1989; Embry 2002). In other words, the surfaces that bound sequences and sub-sequences are diachronous. In this study the seismic interpretations simplify this situation and the surfaces (reflections) that bound sedimentary sequences (a seismic package) are taken to represent instances locally in time (synchronous) between which sediments continuously accumulated.

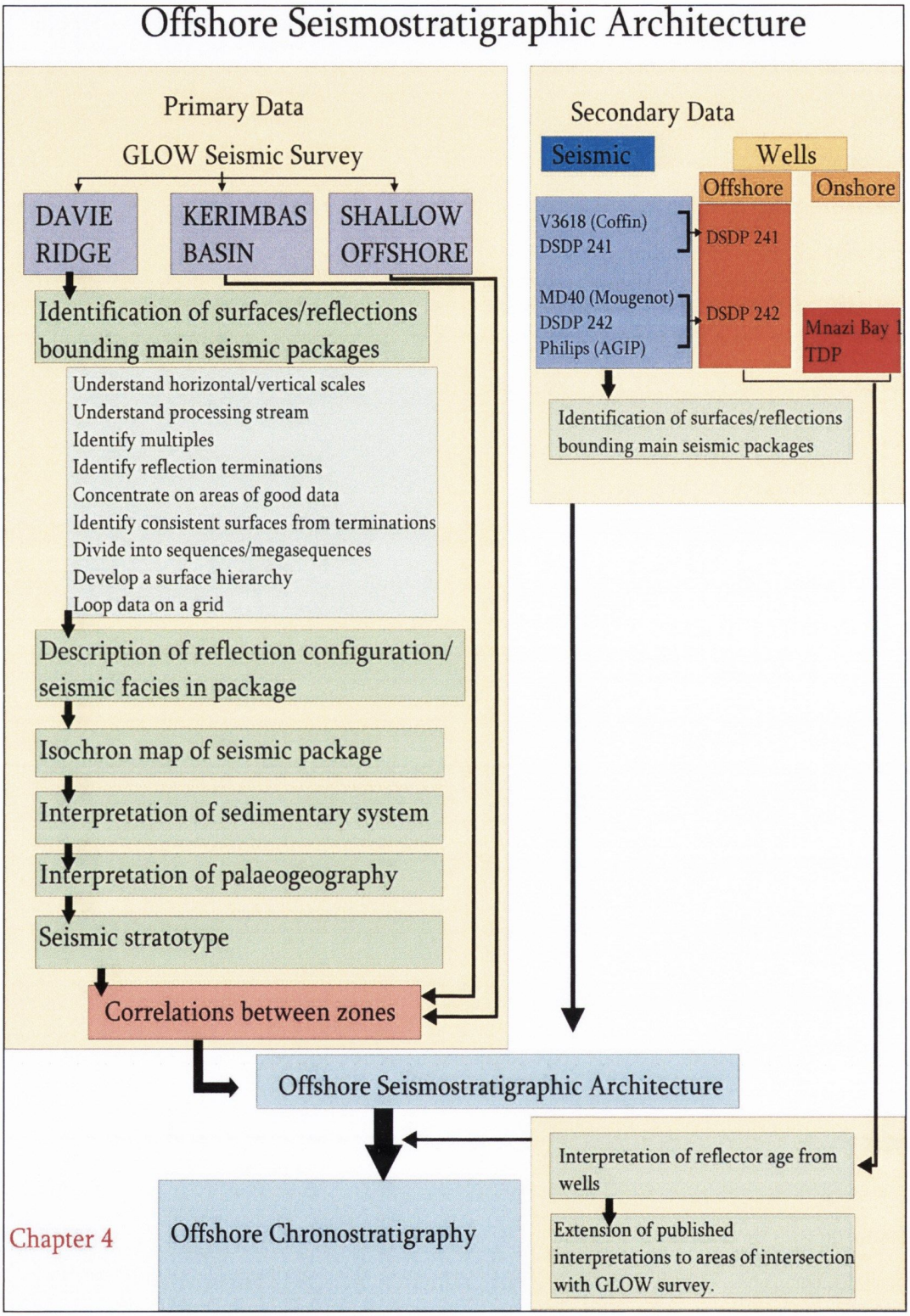

Figure 3.10: Flow chart of the seismic stratigraphic methods employed in this study.

Data Preparation

Preparing data for analysis usually requires the following six steps:

a) Plot regional base map showing shot points and wells with bathymetry. Base maps serve several functions, including places to mark seismic facies notations, areas of interest and anomalies to further investigate and checking line ties.

b) From the base map select key lines emphasizing regional features with good coverage. Choose lines of good data, as close as possible to important well-ties. Select lines to allow loop ties in a progressively widening grid, avoiding severe tectonic deformation zones, if possible. Identify possible key lines which show clear stratigraphic trends and tie key wells.

c) Plot paper copies of selected regional seismic lines at a reduced scale. Use wiggle trace paper sections at this stage which best display complex stratal relationships and terminations over long distances. On the seismic workstation, such stratal observations are often obscured or masked by a high degree of vertical exaggeration. Long regional lines often require panning back and forth on a workstation, whereas paper sections allow uninterrupted visual scanning for key terminations.

d) Avoid areas of bad data or coverage.

e) Prepare well-ties.

f) Construct a well tie template for illustrating the relationship between seismically defined surfaces, time based well log, biostratigraphic calibration and global chronostratigraphy.

Seismic Stratigraphy Interpretation

After the data has been prepared for seismic stratigraphic interpretation, areas of major structural deformation and data artefacts (sideswipe and diffraction) on the seismic sections are identified. In structurally complex terrains, it can be useful to do an initial correlation of a few surfaces across faults to see key tectonic relationships. An initial review of key lines to become familiar with seismic sequences (1st, 2nd, 3rd order) and pre-, syn and post-orogenic sequences is useful. The next major step is

to identify major angular truncations (Fig. 3.11) and connect the onlap and angular truncation terminations as a candidate sequence boundary. Downlaps may be connected as a candidate maximum flooding surface (MFS) while toplaps remain unconnected temporarily. Care is needed when interpreting onlaps and downlaps in strike sections or in tectonically rotated and growth fault sections. Sequence boundary (SB) correlations are continued through a complete loop in a progressively widening set of line ties.

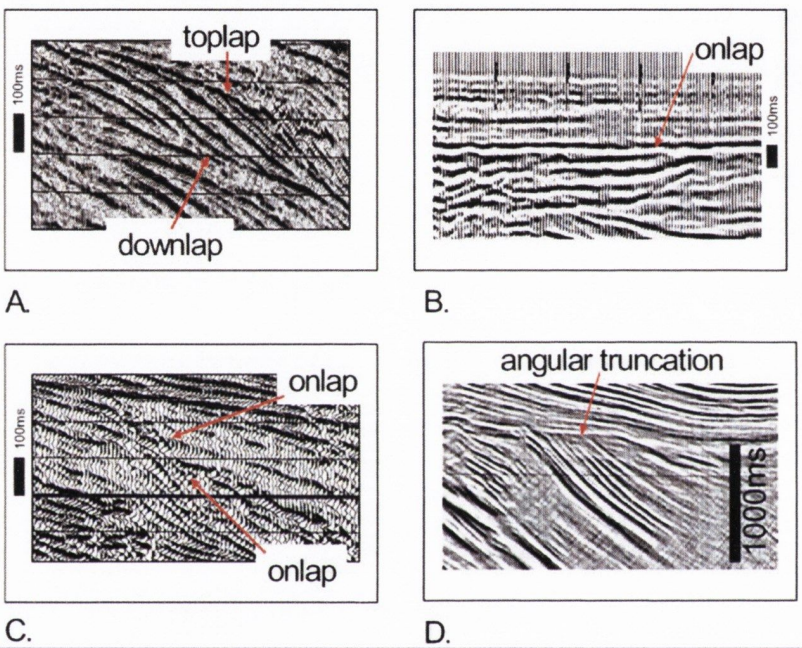

Stratal terminations
-angular truncation obvious erosional termination of dipping reflections up against a reflection of lesser dip)
-onlap (stratal termination up against a reflection of greater dip)
-downlap (stratal termination down against a reflection of lesser dip)
-toplap (termination of successively younger reflections against a reflection,passing downdip to prograding clinoforms (in some cases))

Figure 3.11: Stratal terminations (adapted from Bally 1982)

Seismic Facies Analysis

Seismic facies mapping involves qualitative to quantitative analysis of seismic character to infer areal trends in lithology, palaeoenvironment or both. Generally, seismic characteristics analyzed from two standpoints: external form (geometry) and internal character. Internal form includes the continuity, frequency and amplitude of seismic reflections. Many of these parameters relate to lithology or the processes responsible for deposition. Others relate to the acoustic impedance contrast, tuning,

etc., and thus seismic resolution plays a role in their discernible patterns of occurrence. Bed or stratal continuity is assumed to exceed the Fresnel zone width for a given seismic frequency.

Seismic facies mapping was definitively explained by Ramsayer (1979), called the 'A-B-C' mapping approach. Observations are made upon the upper boundary (A), the lower boundary (B) and internal reflection character (C); illustrated in Figure 3.12.
The morphology of the boundaries of stratigraphic cycles can be used to interpret depositional environments. Facies (lithology) predictions require a wider geological and geophysical understanding. However, the lithology encountered in onlapping and progradational seismic intervals varies according to (i) the water-depth, (ii) the balance between rate of sedimentary supply, (iii) the rate of relative change of sea level, which, in turn, is controlled by the subsidence and the global eustatic variations and (iv) uplift due to tectonic or isostatic vertical motions.

Sequence Stratigraphy

The aim of applying the seismic stratigraphic method to the seismic data was to divide the data into seismic sequences, each of which are interpreted as depositional systems. Sequence Stratigraphy is the study of rock relationships within a chronostratigraphic framework of repetitive and genetically related strata bounded by surfaces of erosion or their correlative conformities.
The sequence stratigraphic method is described in detail by Catuneau (2002) and is outlined briefly in the following steps:

1) Recognition of unconformities using onlap and truncation reflection terminations.
2) Identification of stratigraphic cycles. For sequence-cycles, identify type I and II unconformities.
3) Location of shelf breaks for each sequence cycle using sedimentary dip changes.
4) Construction of coastal onlap and Relative Sea Level (R.S.L.) Curves.
5) Recognition of Systems Tracts inside each sequence cycle.
6) Facies (lithology) prediction for each depositional system composing the different systems tracts.

7) Calibration of sequence cycles and systems tracts using exploration wells.

8) Calibration of sequence cycles and systems tracts with sea level curves.

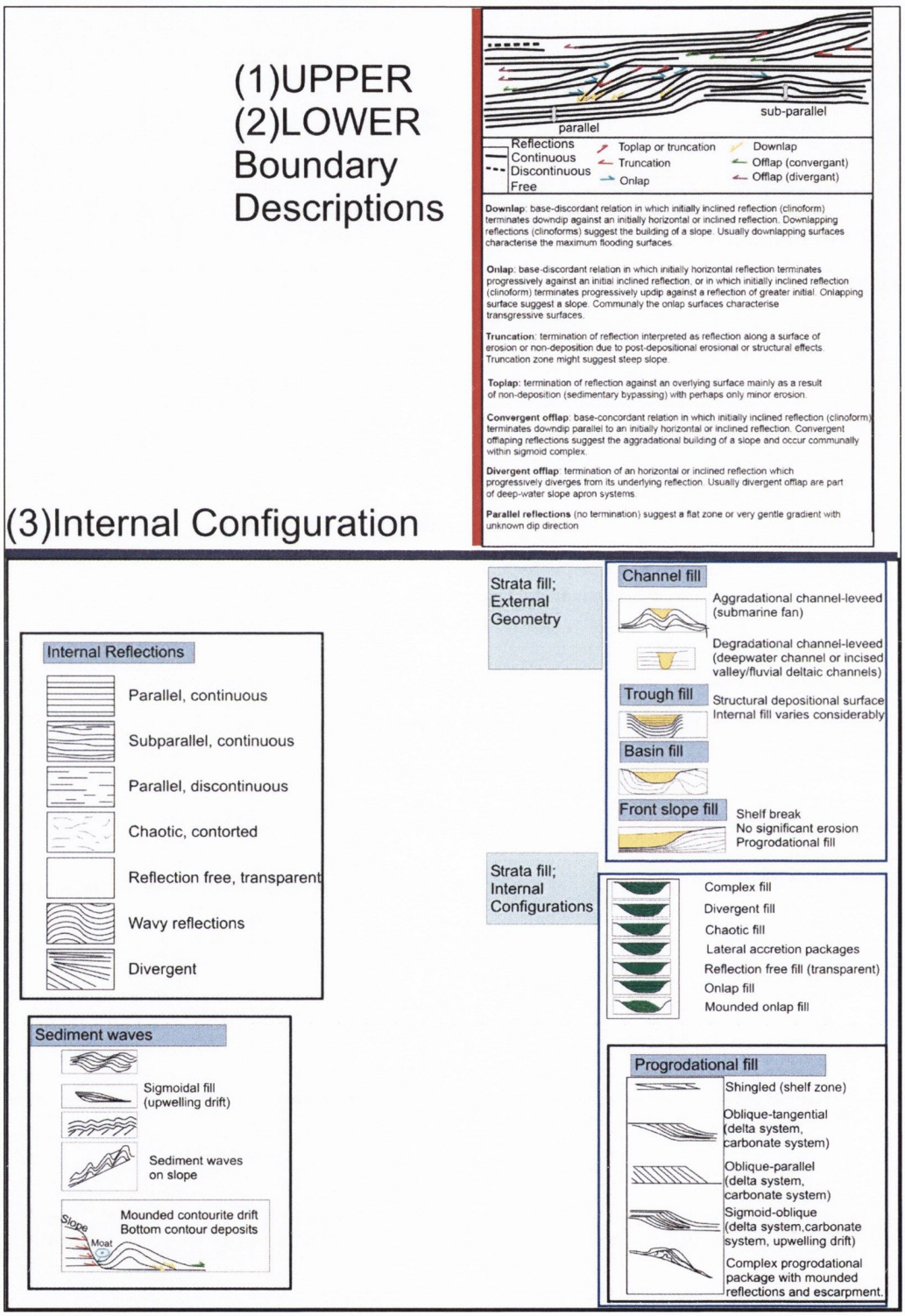

Figure 3.12: Descriptive terms and illustrations of the boundaries and internal configurations of seismic packages, modeifed from Tremblay, (2005). .

3.6. *Multibeam Bathymetry Acquisition and Interpretation*

Bathymetric surveys were performed simultaneously with recording of the GLOW seismic lines using the Kongsberg EM302 multibeam echosounder permanently installed on board the R.V. Pelagia. The EM302 is a deep water (>7000 m) echosounder with a maximum swath opening angle of 150 degrees. The transmit and receive transducer arrays are installed in a Mills cross configuration in a gondola located on the port side of the vessel at a distance of about one third of the vessel length from the bow of the ship. The transmitter array has a beam opening angle of 2 degrees while the receiver array has a beam opening angle of 1 degree. These arrays are connected to a transceiver unit (TRU) which receives the ships attitude (heave, roll, pitch and heading) from a Kongsberg MRU5 motion sensor. A Seapath200 serves as positioning system and also sends its data to the TRU. The sound velocity in the water column is determined from a salinity/temperature CTD deployment and calculated using the Chen-Millero formula. Data regarding water depth and backscatter intensity are sent from the TRU to a recording PC running the SIS (Kongsberg, Seafloor Information System) software. The recording PC can be operated from the bridge through an ethernet connection to the measuring lab. On board processing of selected sampling areas was performed using the Neptune software (Kongsberg). Imaging and printing of processed data was done by means of the CFloor software package, supplied CFloor AS.

3.7. *Box and Piston Coring*

Seabed samples were taken using a NIOZ designed box corer. The box core has a barrel with a diameter of 30 cm and a height of 55 cm (Fig. 3.13). The corer is supplied with a lid that closes the box from the top as soon as it has penetrated the sediment. In this way sloshing of the water above the sediment surface is avoided when the core is retrieved and hoisted on deck, resulting in an undisturbed sample of the seabed sediments.

Figure 3.13: Box corers used in GLOW Box coring and sediment retrieved via plastic liners with way-up indicators (arrows) marked on the tubes (GLOW Survey Team).

On deck the bottom water was siphoned off and the surface sediments were described photographed. Four plastic liners with diameters of 90 and 63 mm (2 of each diameter) were inserted and retrieved from the core. These sub-samples were stored upright at a temperature of 4° Celsius.

Long cores were retrieved by means of the NIOZ designed piston corer system. The system consists of a weight (bomb) with a mass of 1.5 metric tons attached to a core barrel of variable length. The core barrel is build up of 6 m long sections. During this cruise the total length of the barrel was 12 m during every deployment. The piston contains a valve that allows water to flow into the core barrel if the pressure difference with the ambient water becomes too high and could result in implosion of the liner. The pressure difference at which the valves opens can be adjusted by the operator. After retrieval the cores were cut into 1.10 m long sections and stored at 4°Celsius.

Core data were compiled for each box core including navigation data, bathymetric and seismic data, penetration, colour, surface description, sediment and layer descriptions, key forams and biostratigraphic age (Fig. 3.14).

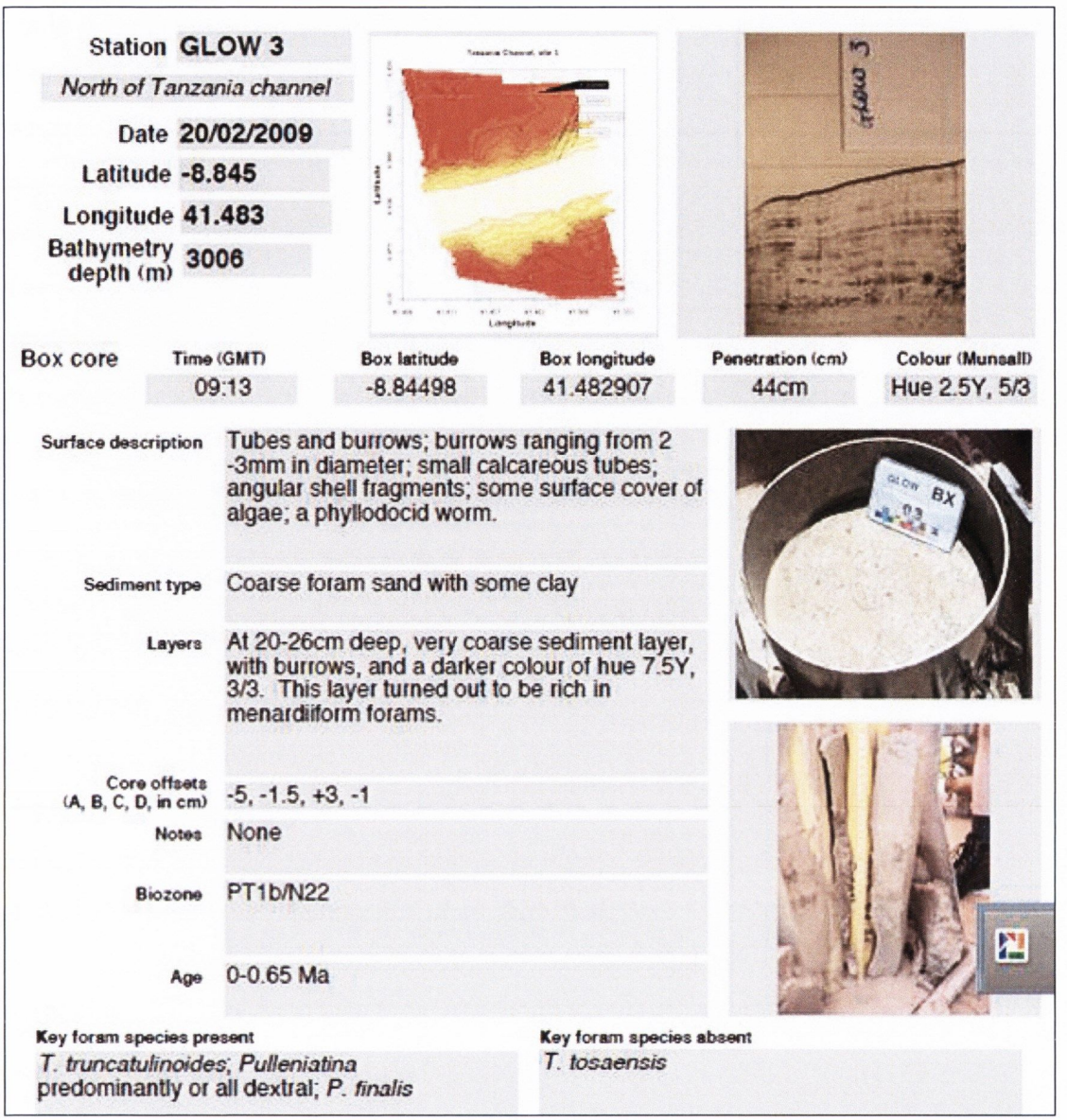

Figure 3.14: Example of the compilation of box core data. (This is for GLOW Box core 3).(GLOW Survey Team)

3.8. Onshore Geological Mapping

Onshore, a thorough investigation of the Cenozoic tectonics, stratigraphy and sedimentology of the southern coastal region, from Kilwa in the north through to Mtwara in the south, has been conducted (Chapter 7).

A series of published maps, unpublished industry report and satellite imagery were used in mapping onshore. Topographic maps on a scale of 1:50,000 were purchased

directly from the Ministry Of Lands And Human Settlements (Ardhi House, Kivukoni Front, P.O. Box 9132, Dar es Salaam). These base maps were further complemented by a collection of 1:10,000 Google Earth images and false coloured Landsat images. A 10km Universal Trans-Mercator (UTM) Grid using the WGS 84 datum was overlain. Major settlements and villages were recorded as many of these have changed location/ name since the base topographic maps were published (1966). Altitudes were obtained using a combination of GPS and Sunnto digital altimeter, calibrated to barometric pressure variations and accurate to within one metre. The altimeter was reset before each survey at the mean high water mark by Kilwa Masoko Jetty/Lindi Shoreline/Mikindani Shoreline.

Outcrop locations were noted, described and placed directly onto field sheets. Structural measurements, lithofacies and biofacies information was recorded. The field data were used to review the geological structures, boundaries and stratigraphy. Samples were collected and shipped from Dar es Salaam to Dublin. Unfortunately it was not possible to erect a regional stratigraphy according to the 'ICS' guidelines. However a chronostratigraphic 'time-equivalent' unit was established. Digital Elevation Models (DEMs) were generated and interpreted to identify possible lineaments and fault traces, and to resolve fault orientation. A key element of this work was the identification of benthic and planktonic foraminiferal species by a team of palaeontologists from Cardiff University; Paul Pearson and Laura Cotton (who accompanied this survey in August 2009).

3.9. Velocity model and depth conversion

The multichannel seismic reflection profiles recorded by the GLOW cruise in 2009 can be broadly divided into three areas with respect to their prevailing sedimentation regime. These areas are governed by inner continental shelf, turbiditic channel and distal, deepwater pelagic regimes. For this study we considered data of existing DSDP Sites 241 and 242, existing drill sites depending on the availability of data, shelf geometry, location on the shelf and seismic characteristics. Incorporating various data resources the best possible depth control of the proximal shelf to distal offshore

sequences is attained to enable regional stratigraphic correlations across the site survey area.

Of all recorded velocity values in the Davie Ridge area the average over the depth interval 1-700 mbsf is 1.74km/s TWTT. There is good agreement between the seismic profiles available across Site 242 and the area in the northern Davie. Principal seismic markers were identified and traced northwards with confidence. Even though the degree of compaction may differ between the sediments, there is remarkable agreement between the seismic facies of Site 242. In addition to geological reasons the decision to take Site 242 velocity values is based on the availability of logged data. The seismic profiles in this area were processed therefore based upon the seismic velocity data produced in the shipboard report of DSDP 242. In calculating the depths, we have used the average velocity of 1.74km/s, as per the most recent published data.

The Tanzanian continental shelf, consists of shelf deposits and well stratified, horizontally bedded, laterally continuous sediments (Kitunda Block). The sedimentary facies on the shelf north and south of the Kitunda Block are much more chaotic, sandy and less well stratified. The lithology of the Kitunda Block is inferred to be proximal shelf clays with minor turbiditic sands and carbonate. Box and piston cores (GLOW 19-22) indicate a clay rich facies with abundant marine microfossils, very consistent with onshore sediments drilled by the Tanzania Drilling Project. The average velocity for this area is interpreted as 1.7km/s to 1.65km/s TWTT.

The velocities inferred here were applied in the processing of the MCS data and also in the depth and sediment thickness calculations performed throughout the thesis.

3.10. Age Correlations

As described in Chapter 2, one of the key research aims of this study was to assign age control to the stratigraphic schemes erected. As there are no wells in the area by which direct well-ties could be made, a range of pre-existing and new data was incorporated as no single line of evidence was deemed robust enough. The methods

employed involved a) studying the major sequence boundaries of nearby coastal and offshore wells, b) inferring correlations from these wells to the GLOW seismic data, c) interpreting pre-existing surveys that have good well ties and subsequently intercept with the GLOW survey and d) extending the onshore field control to the transition zone and offshore area via sequence stratigraphic principles.

4. Seismic Stratigraphy of the Davie Ridge (DR) and Davie Ridge Inner Extensional Zone (DRIEZ); The GLOW Seismic Survey 2009.

4.1.Introduction

The aim of this chapter is to define the general stratigraphy of part of the offshore study area (Fig.4.1) by studying the available seismic data (Appendix II, IV) using the methods described in Chapter 3. The entire offshore seismic survey area lies on the continental rise of the southern Tanzanian coastline containing approximately 2,000km of original 2D seismic data (Fig. 4.2).

The study area is quite structurally complex and the depth of imaged seismic data is often not deep enough to correlate confidently across significant faults, therefore the stratigraphy of individual 'structural zones' or areas are described in separate chapters (Fig. 4.3) relating to seven zones:

1) **Davie Ridge (DR), [Chapter 4]**
2) **Davie Ridge Inner Extensional Zone (DRIEZ), [Chapter 4]**
3) Kerimbas Basin (KB), [Chapter 5]
4) SeaGap Zone (SG), [Chapter 5]
5) Coastal Basin (CB), [Chapter 8]
6) Shelf and Slope (SS), [Chapter 8]
7) Kitunda Block (KTB), [Chapter 8]

This chapter shall establish the seismic stratigraphy for the Davie Ridge and the Davie Ridge Inner Extensional Zone (DRIEZ). By establishing the correct stratigraphy and estimating the age of horizons, tectonic and sedimentological information is extracted in subsequent chapters.

Seismic reflection configuration, seismic features and distinct surfaces were used to divide the stratigraphy of each zone into distinct seismic units. Sedimentary processes, sedimentological evolution and palaeogeographic maps for each seismic unit are described and produced. In Chapter 6, an array of data is incorporated to assign ages to

the stratigraphy produced in this chapter and hence to create a chronostratigraphic evolution of the Davie Ridge and DRIEZ areas.

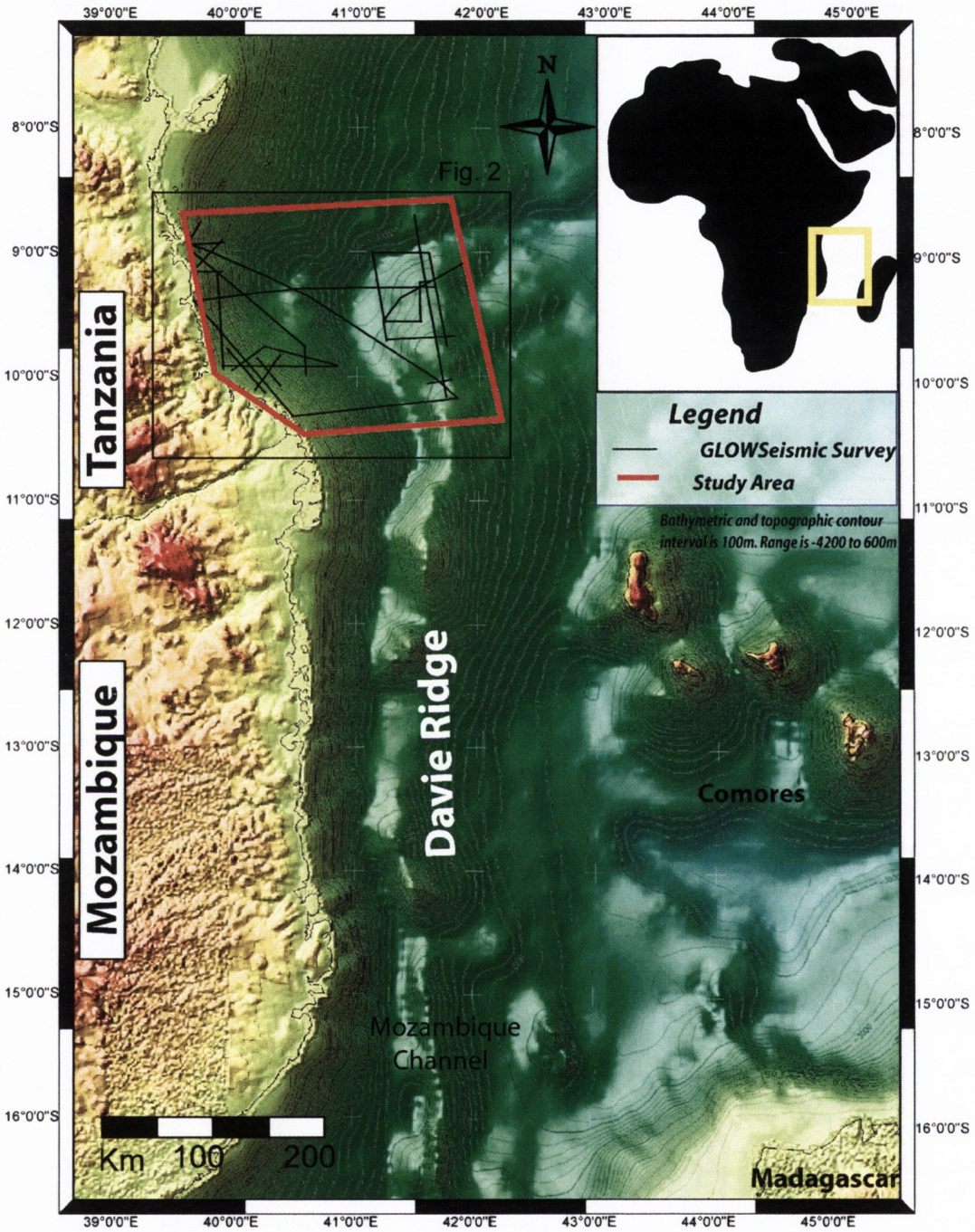

Figure 4.1: A bathymetric and topographic map of the East African coastline. Principal features and the overall study area are highlighted.

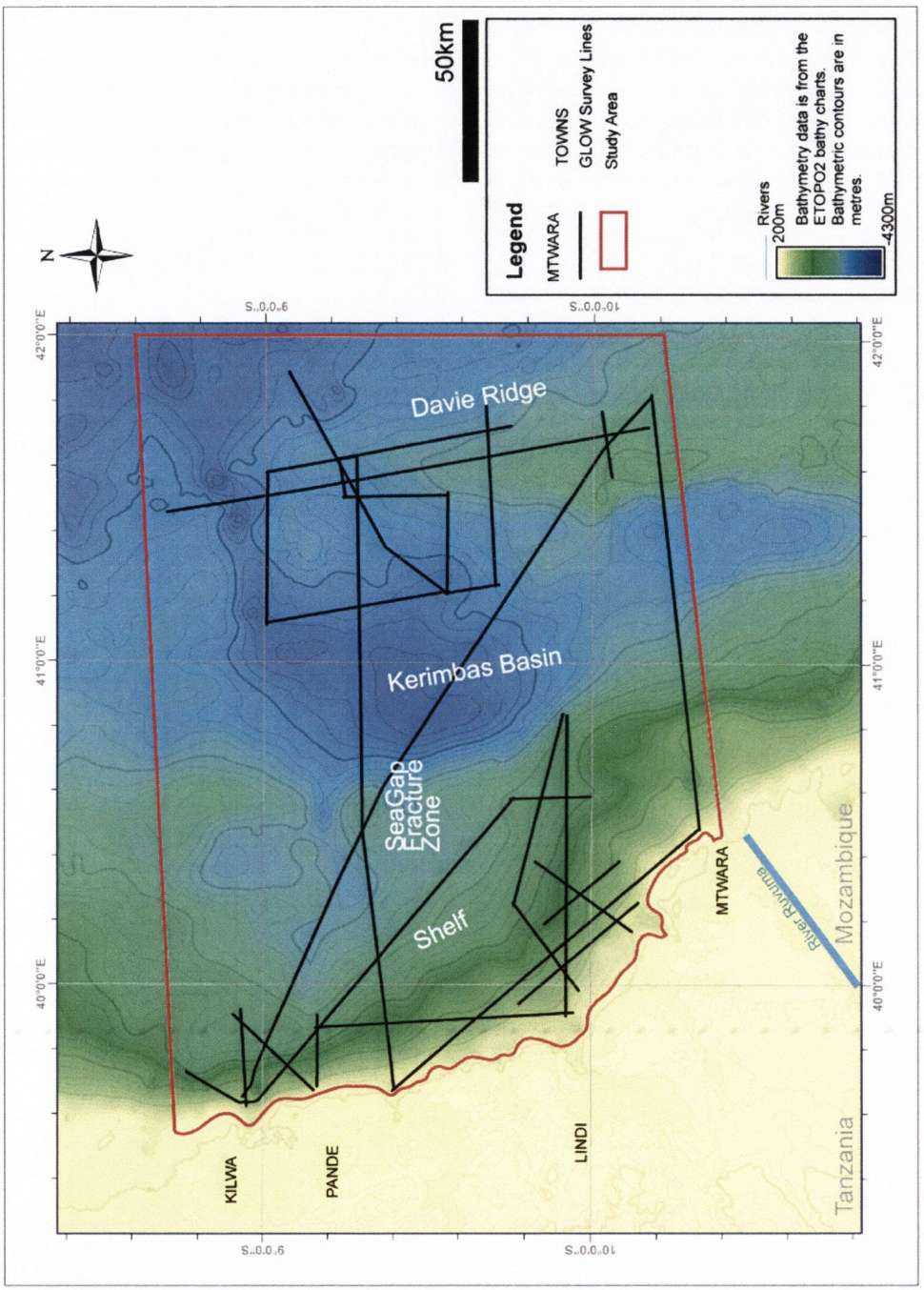

Figure 4.2: The GLOW Seismic Survey location offshore Tanzania. Bathymetry and topography is GEBCO data with contour lines at 100m intervals. The location of the figure is highlighted in Fig. 4.1.

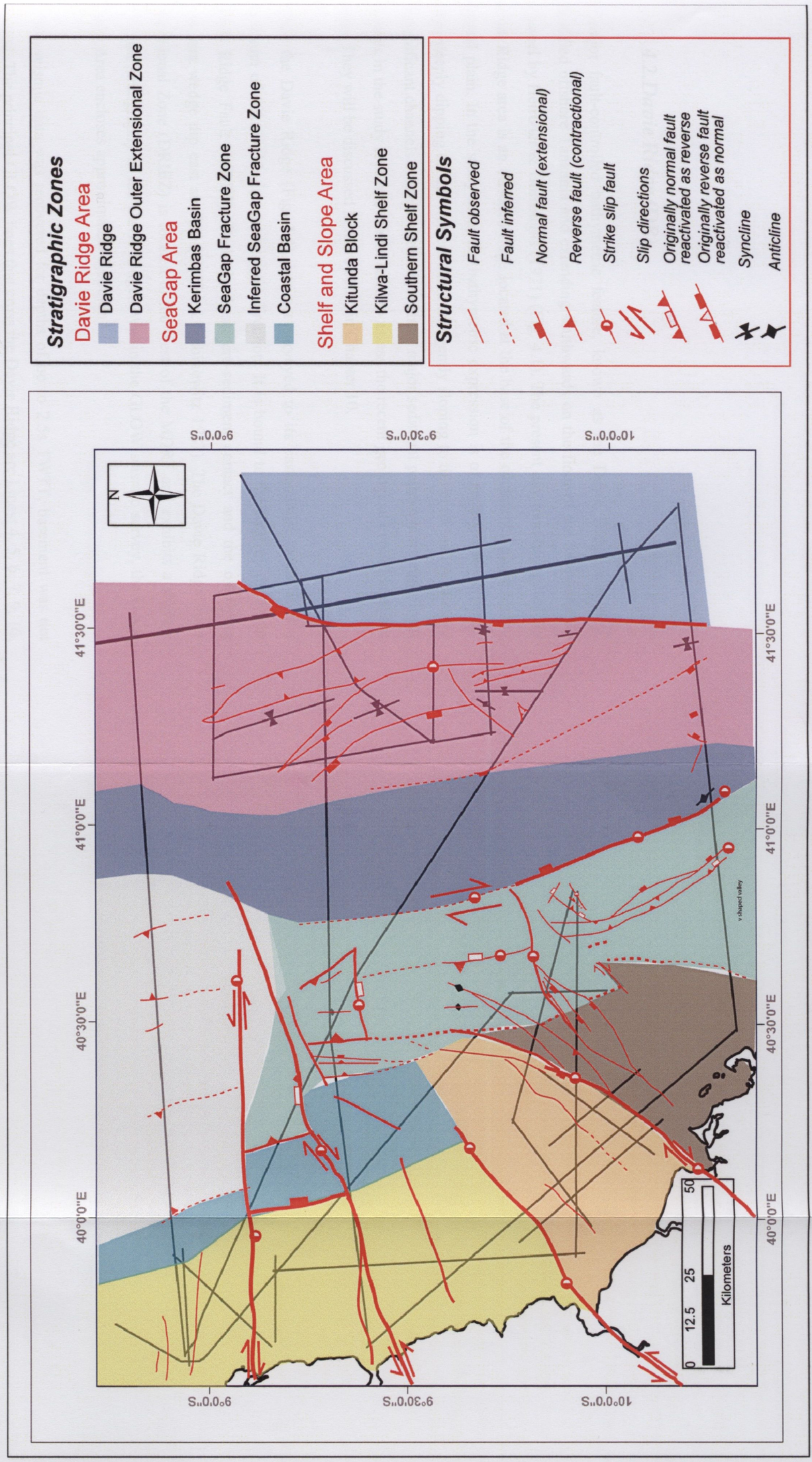

Figure 4.3: Structural zonation of the study area. The stratigraphy of the Davie Ridge and DRIEZ zones will be discussed in this chapter. The stratigraphy of the SeaGap and Kerimbas Basin Areas will be discussed in Chapter 5. Age control for the above areas will be assigned in Chapter 6. The remaining zones are discussed in Chapter 8.

4.2.Davie Ridge (DR)

A major fault-controlled bathymetric feature, known as the Davie Ridge was first identified offshore Tanzania and extending southwards on the floor of the Mozambique Channel by Heirtzler & Burroughs (1971) (Fig. 4.1). The present day morphology of the Davie Ridge area is an elevated ridge located at the base of the continental slope on the abyssal plain. In the study area, the bathymetric expression is of an asymmetric ridge, more steeply dipping on the western flank and gently sloping to the northeast. A number of significant channels crosscut the Ridge. These major sediment pathways are significant features in the study area and can be used to assess the recent geological evolution of the ridge. They will be discussed in more detail in Chapter 10.

While the Davie Ridge (Fig. 4.4) was not surveyed to its easternmost extent it is a minimum of 60km wide in an east-west direction. It is bound to the west by the Main Davie Ridge Fault (MDRF). Both the basement-sediment contact and the overlying sediment wedge dip east at ~15° (Coffin & Rabinowitz 1987). The Davie Ridge Inner Extensional Zone (DRIEZ) is located to the west of the MDRF and exhibits a slightly different stratigraphy to the Davie Ridge.. Within the GLOW seismic survey, the Davie Ridge Area encloses approximately 3,000km^2.

While seismic data was recovered for depths of up to 2.5s TWTT, basement was not imaged. The principal GLOW lines that cross the Davie Ridge are Lines: 4, 5, 6, 7, 9, 10, 11, 12, 13, 14, 15, 16, 17, 18, and 19 (Fig. 4). However, Line 6 has poor quality data and Lines 4, 5, 7 and 9 only transect the ridge in part. Good coverage was thus obtained for this region to enable the erection of a seismic stratigraphic scheme. In the following sections a description of each unit and seismic marker will be given.

Firstly the seismic characteristics are described and interpreted, then the seismic marker characteristics are described and interpreted and finally a seismic stratotype (Fig. 4.5) is proposed to summarise the framework of each locality.

Three seismic sequences are identified in this zone. Labelled DR Units I, II and III, they are separated by seismic markers DR SM 01 and DR SM 02. Largely composed of parallel to subparallel, wavy reflectors with high amplitudes decreasing with depth there are minor internal variations as described below that can differentiate between them.

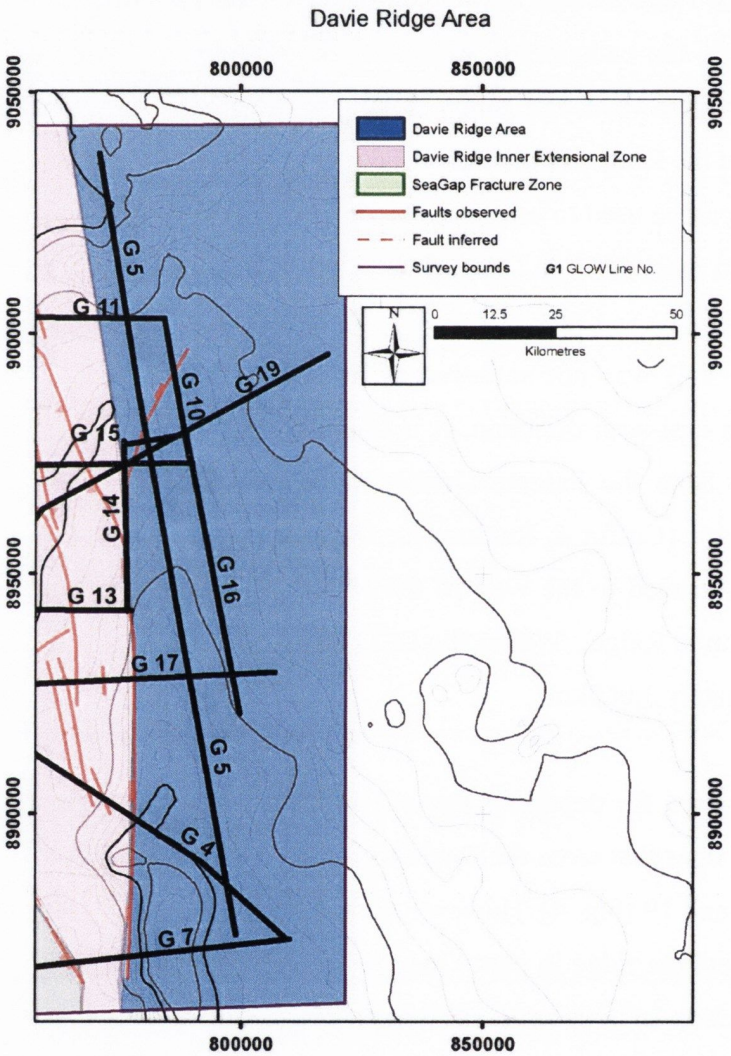

Figure 4.4: The Davie Ridge Area and GLOW Lines that traverse it.

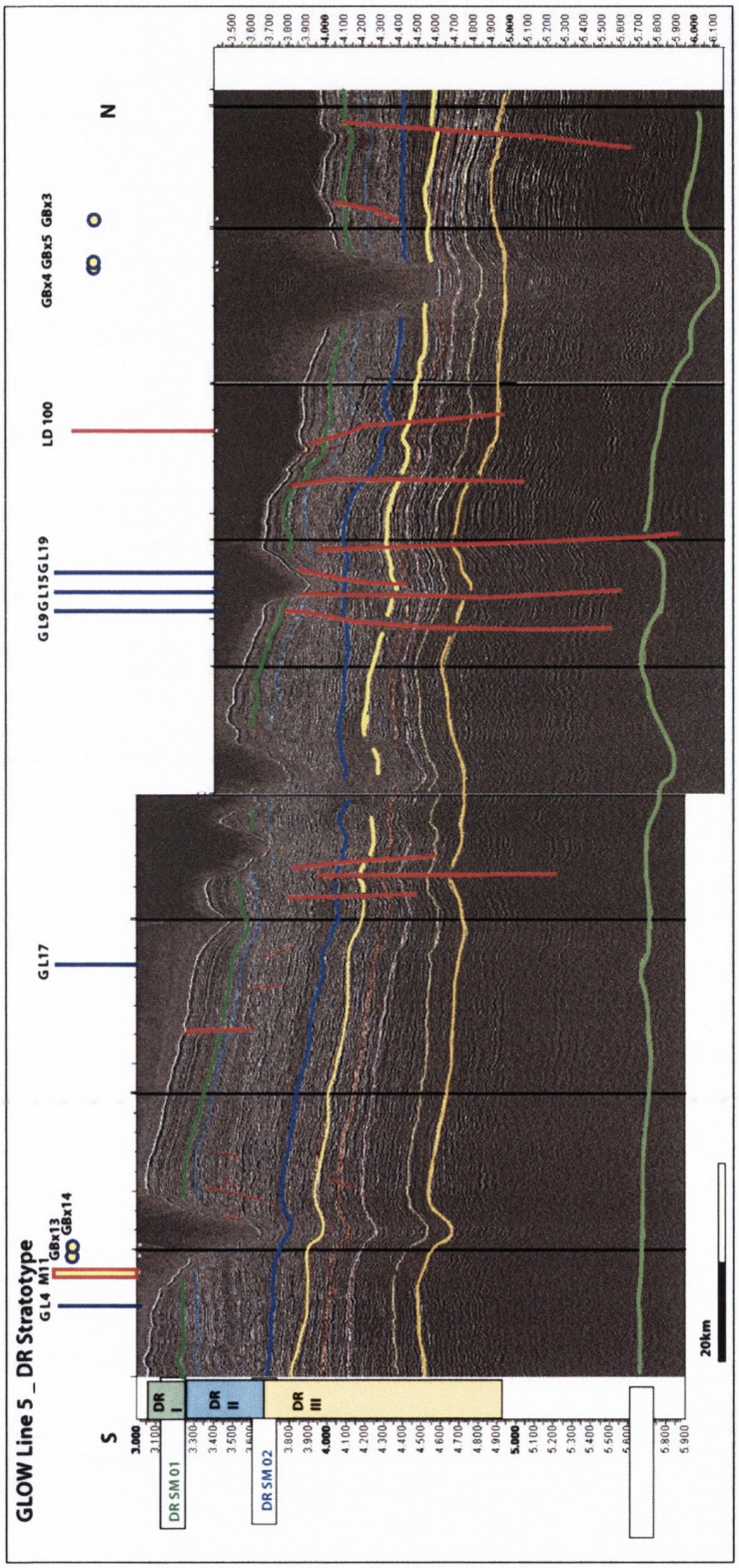

Figure 4.5: A stratotype of the seismic framework of the Davie Ridge Stratigraphy (GLOW Line 5).

4.2.1. DR Unit I

DR Unit I occurs over an interval of 0.4 to 0.5s TWTT and consists of two seismic sub-units. The seismic sub unit I/1 is locally developed with variable interval depth while seismic sub-unit I/2 is a well stratified unit present throughout the Davie Ridge Area.

The seismic sub-unit I/1 is a rubbly, chaotic, high amplitude, non-continuous layer. Localised to the south of the Davie Ridge Area, it varies in thickness from 0 to 0.6s. Bound by the seabed above, it has an erosional base which truncates the parallel reflectors below, as indicated by the pink reflector in Fig. 4.6.

The seismic sub-unit I/2 is well stratified with high frequency, parallel, continuous reflection horizons (Fig. 4.6). The interval over which it occurs increases overall to the south and southeast, reaching a maximum interval of 0.18s TWTT at its southeasternmost extent on Line 4. The base is conformable with the underlying Unit II (green reflector in Fig. 4.6) and is laterally concordant in a N-S direction as shown in the GLOW lines; 10-16 and 5 (Appendix 2).

4.2.2. DR SM 01

The horizon DR SM 01 is picked on a black continuous reflection (peak, positive reflection coefficient) and is represented by the continuous green reflector in Fig. 4.6. The time map of surface DR SM 01 is shown in Fig. 4.7 and occurs between times 3.2 and 4.2s TWTT. Located between Unit I and II, it is laterally continuous and traceable.

The seismic marker DR SM 01 is interpreted to represent a marked sea level rise and the establishment of a classic deep water, hemipelagic depositional environment.

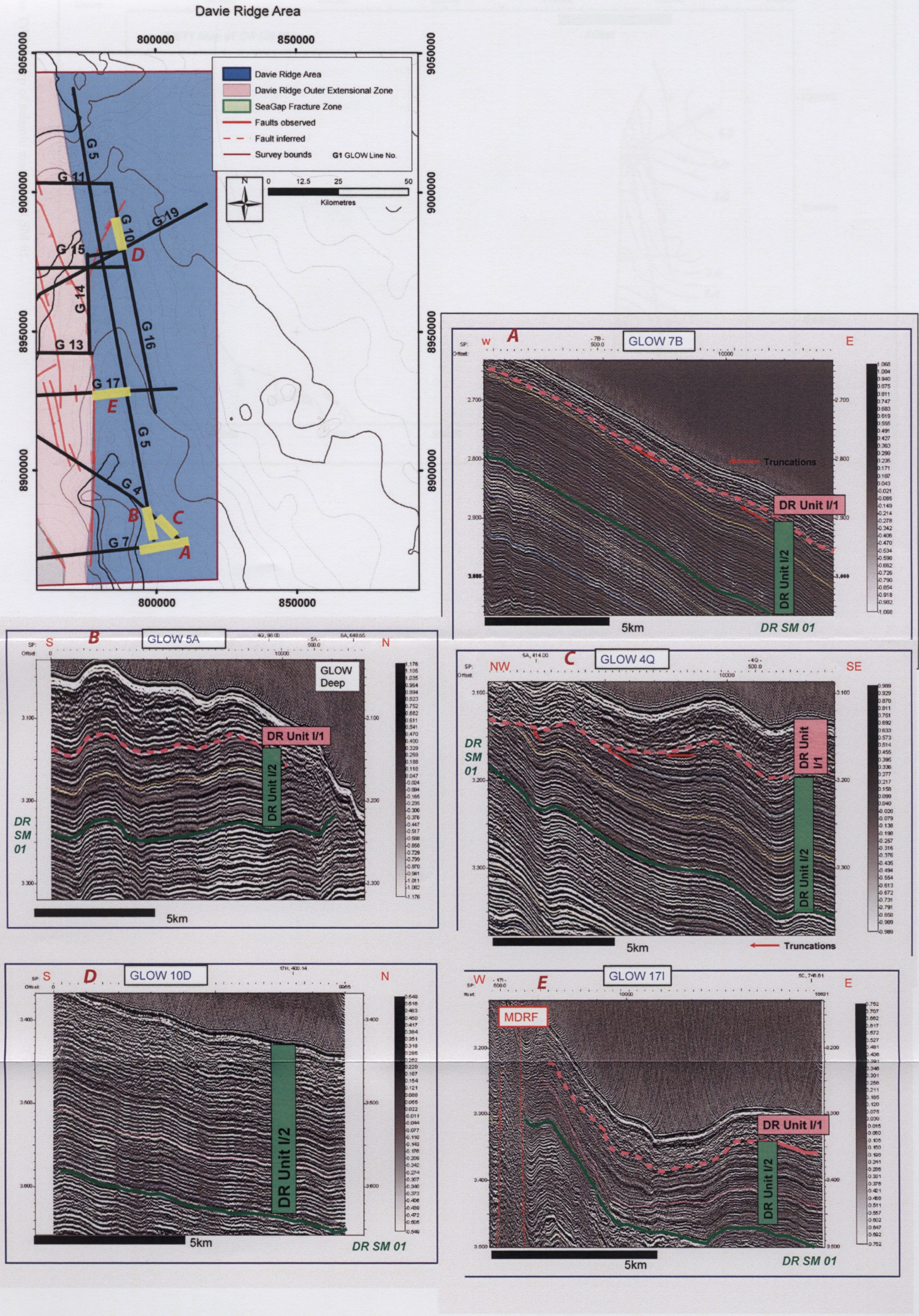

Figure 4.6: A compilation of the seismic characteristics of Davie Ridge Seismic Unit I, comprising I/1 and I/2. The location of figures shown is highlighted on the inset map.

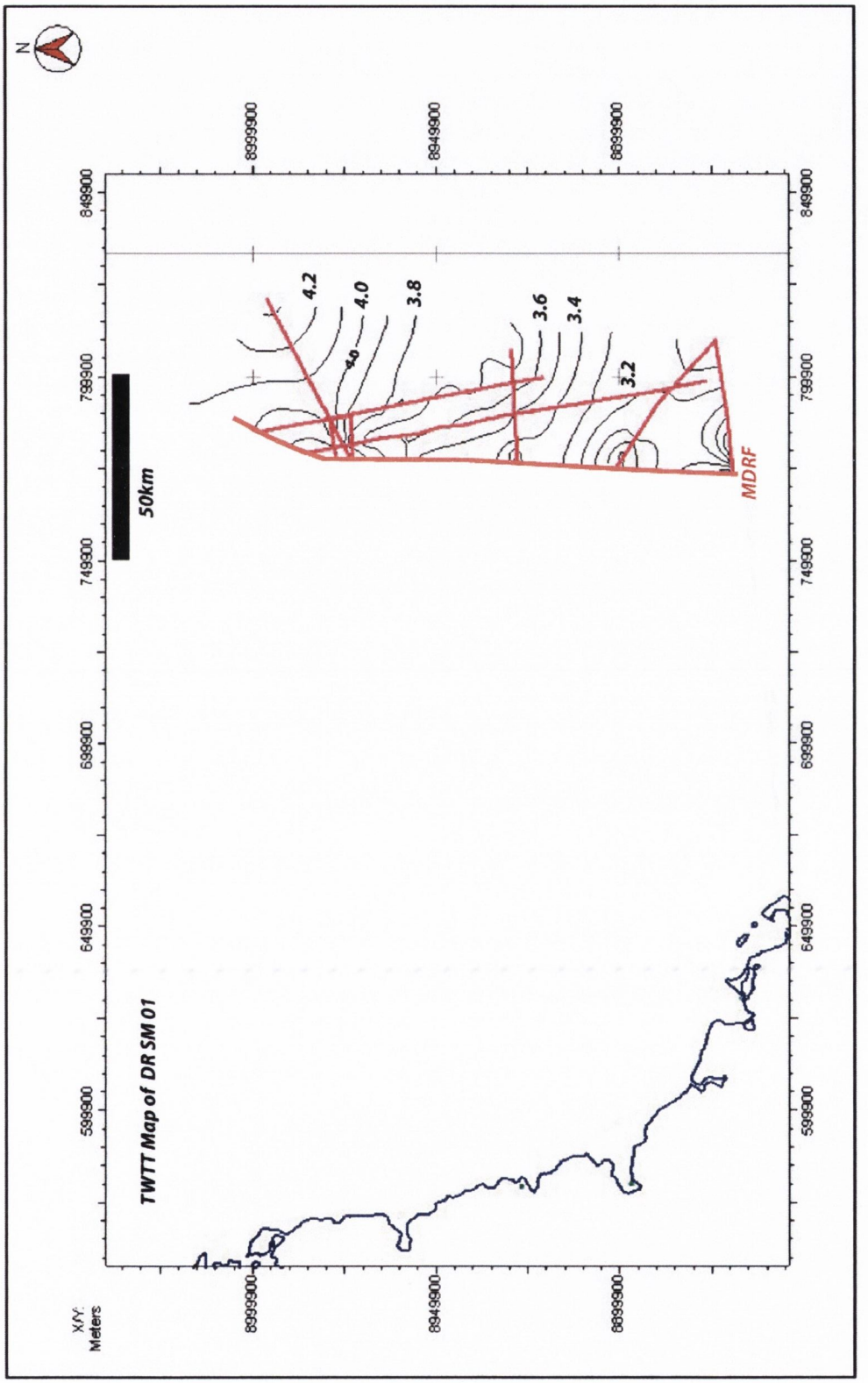

Figure 4.7: The TWTT map of seismic marker DR SM 01.

4.2.3. DR Unit II

DR Unit II occurs over an interval of approximately 0.4sTWTT and consists of two seismic sub-units; seismic sub unit II/1 and seismic sub-unit II/2. DR Unit II encompasses a series of well stratified reflectors, subparallel transparent facies, and channel and sediment wave facies. There is a marked unconformity between II/1 and II/2.

Subsequence II/1 has very similar facies to DR Unit I; high frequency, parallel, continuous reflection horizons and occurs over an interval of approximately 0.25s (Fig. 4.8). The top of the unit is concordant with the overlying Unit I and the principal difference with the overlying Unit I is a marked increase in amplitude of the even, subparallel, wavy reflectors. Within DR II/1 there is some lateral variation in amplitude, usually apparent on the crests of the waves. This is probably due to either differential compaction or variation in lateral sediment composition. The base of subsequence II/1 is marked by the first downward occurrence of numerous minor scale channel-lenses in the lee of migrating sediment waves (blue dashed line in Fig. 4.8). The internal channel reflections are broadly parallel with those of the surrounding reflections; however occasional downlap onto the basal reflector and chaotic fill occurs. While the minor channel lenses are visible on Lines 4 and 5, they are not seen on Line 7. This may indicate a SW-NE channel direction, orthogonal to both Line 4 and Line 5 while parallel to Line 7. These channel lenses create the mounded topography that is replicated in younger units.

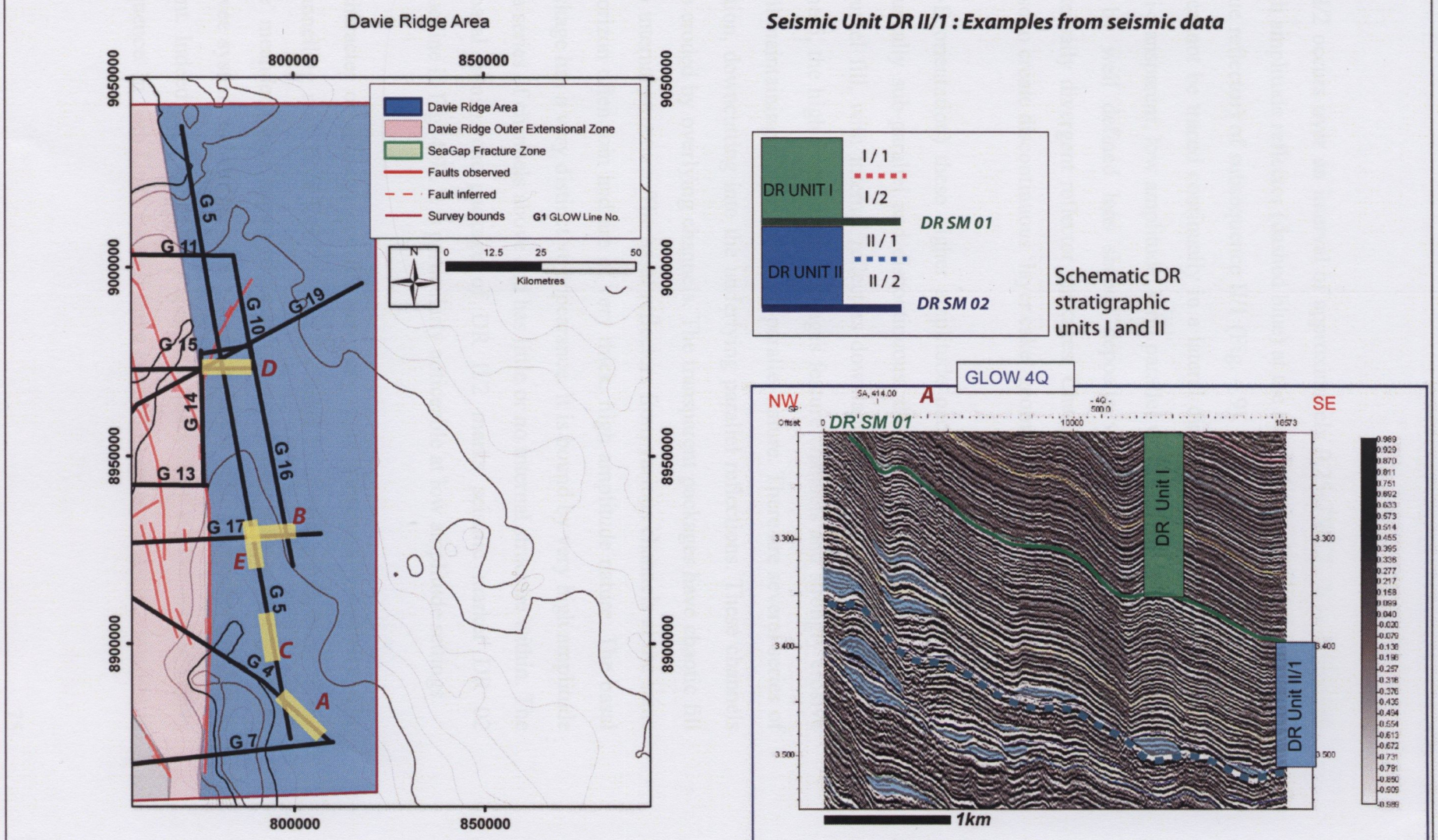

Figure 4.8: A compilation of the seismic characteristics of Davie Ridge Seismic Unit II/1. The location of figures shown is highlighted on the map.

Subsequence II/2 occurs over an interval of approximately 0.25sTWTT. It is defined at its top by a high amplitude reflector (dashed blue) at the base of the minor channel lenses (continuous blue reflector) of subsequence II/1 (Fig. 4.9). Several cycles appear evident, although they cannot be traced continually in a lateral direction. Broadly speaking, II/2 comprises semi-transparent, low amplitude, semi parallel wavy reflector packages which are separated by well defined lens shaped deposits with higher amplitude, semi-continuous, internally divergent reflector packages. Chaotic, near transparent facies are interspersed also to create discontinuous 'layer cake' geometry.

In Line 7 (W-E orientation) these higher amplitude packages exhibit various seismic facies. While usually sub-parallel and discontinuous, there is occasionally sub-parallel prograding channel fill, with internal reflectors downlapping to the west. However, in Line 4 and Line 5, the higher amplitude packages feature channels and strongly erosive bases while still maintaining a reasonably sub-parallel nature. There are several series of channel formation, downcutting into the underlying parallel reflections. These channels are in turn also eroded by overlying channels. The transparent packages have chaotic fill and little or no internal structure. The basal reflectors from various channels at the same stratigraphic horizon often join and are of very thick, high amplitude nature. The basal transparent package has a very distinctive appearance. It is bound by very high amplitude reflectors and a series of channels above and has little or no internal structure within. The base of the basal transparent package of DR II/2 marks seismic marker DR 02 (continuous blue line in Fig. 4.9). It is particularly noticeable at low amplitude settings.

The internal character of subsequence II/2 can vary quite substantially laterally. The amount of channelling may be a local feature, localised to certain zones. Near to the 'GLOW Snake' meander (See Chapter 10 for more details) there is some evidence of an old channel levee system and further to the north the basal semi transparent package is not as dominant. Indeed the base of the sequence is marked by a condensed intensely channelled sequence. In both Units I and II there appears to be some lateral variation in

amplitude that may be due to compression or levee deposition. In summary it is a highly variable sequence.

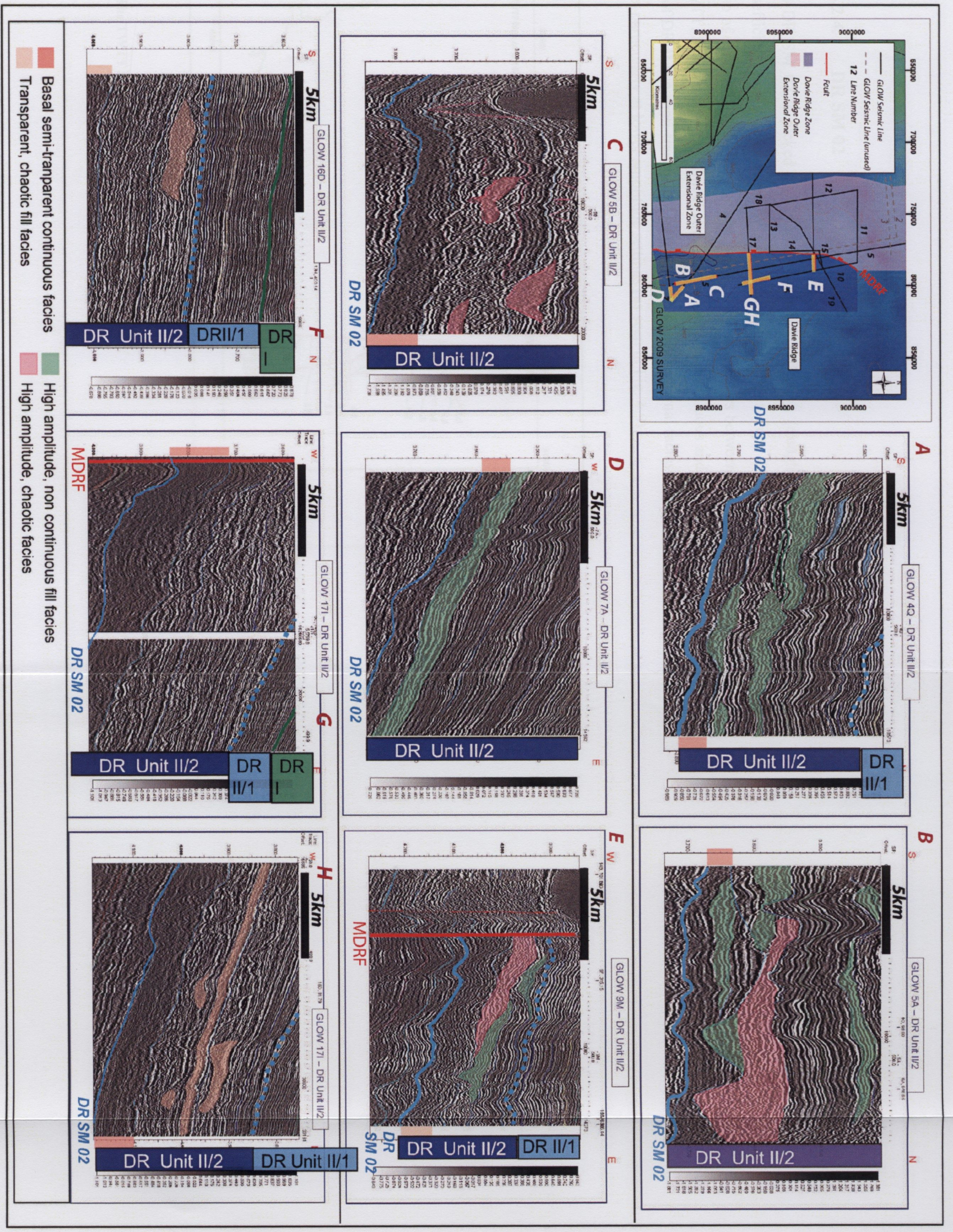

Figure 4.9: A compilation of the seismic characteristics of Davie Ridge Seismic Unit II/2. The location of figures shown is highlighted on the map. Note the highly channelled sequence overlying a largely transparent package, the base of which marks DR SM 02 (continuous blue line).

4.2.4. DR SM 02

The horizon DR SM 02 is picked on a white continuous reflection (trough, negative reflection coefficient) and is represented by a continuous blue line in Figs. 4.8 and 4.9. The time map of surface DR SM 02 is shown in Fig. 4.10, and occurs between times 3.4 and 4.6s TWTT. Located between Unit II and III, it is laterally continuous and traceable. At the base of DR II is a semi-transparent package with chaotic internal facies fill which is distinctive, particularly at lower amplitude settings (as seen in Fig. 4.9).

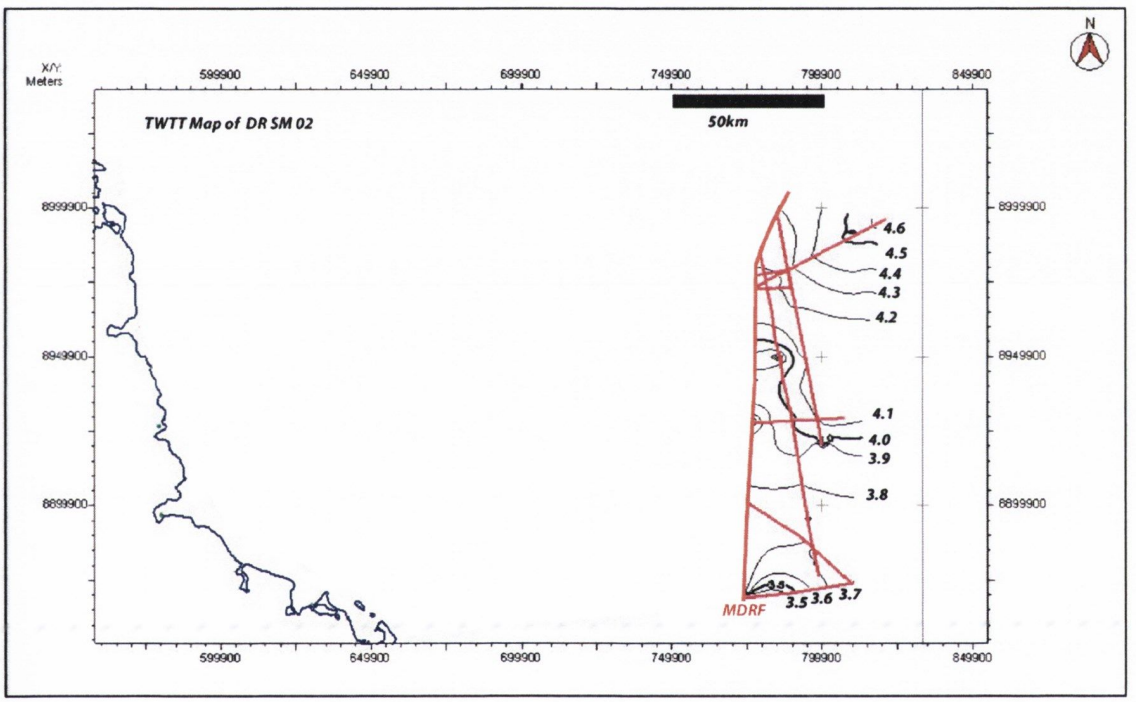

Figure 4.10: The TWTT map of seismic marker DR SM 02.

4.2.5. DR Unit III

Davie Ridge (DR) Seismic Unit III has a minimum interval of 0.9s as the base of this unit is not seen, exceeding the limit of seismic resolution. It consists of five seismic sub-units. Generally speaking however, they are predominantly composed of semi-continuous, sub-parallel, low – mid amplitude reflectors. The principal difference in facies between DR II and DR III is the marked decrease in amplitude and lack of major channelling or erosive features. The amplitude decreases substantially with time over the unit. Although no very distinct seismic surface is seen that can be laterally traced and recognised in all locations, some attempt is made to subdivide this extensive unit into subsequences III/1, 2 3 and 4. However, given that they are largely conformable and of very similar character no description is given of the seismic surface separating each sub-unit. The top of DR III is defined by DR SM 02 (blue continuous reflector) and a conformable semi-transparent package exhibiting erosive channels at its top. A compilation of the seismic features seen in DR Unit III is shown in Fig. 4.11.

DR III/1 is approx. 0.12s TWTT thick and displays a change in seismic facies when compared to DR Unit I and II. The overall geometry of reflectors is semi-continuous, sub parallel and medium frequency. Channelling is evident towards the top while there are two high amplitude reflectors in the middle of the unit. It appears to thin slightly towards the SE as evidenced on Line 4.

DR III/2 is approx. 0.1s TWTT thick and is predominantly parallel-subparallel mid amplitude, laterally continuous reflectors. This unit thickens slightly to the southeast with some internal divergence of reflectors. The unit is somewhat more chaotic towards the southeast. Some high amplitude couplets are visible. The base of the subsequence is almost semi-continuous into the quite similar DR III/3 It is however unconformable towards the SE.

DR III/3 is approximately 0.15s TWTT thick and is largely similar to the description given for subsequence DR III/2. However the seismic reflections are semi-continuous and medium amplitude. Variations in amplitude may be attributed to the development of sediment waves as seen in E-W lines.

DR III/4 is approximately 0.65s TWTT thick and consists of semi-parallel, semi-continuous, low amplitude reflectors. Patches of higher amplitude reflectors can be seen and are possibly attributable to the development of sediment waves in this unit. The limit of seismic resolution is reached above the base of this sub-unit.

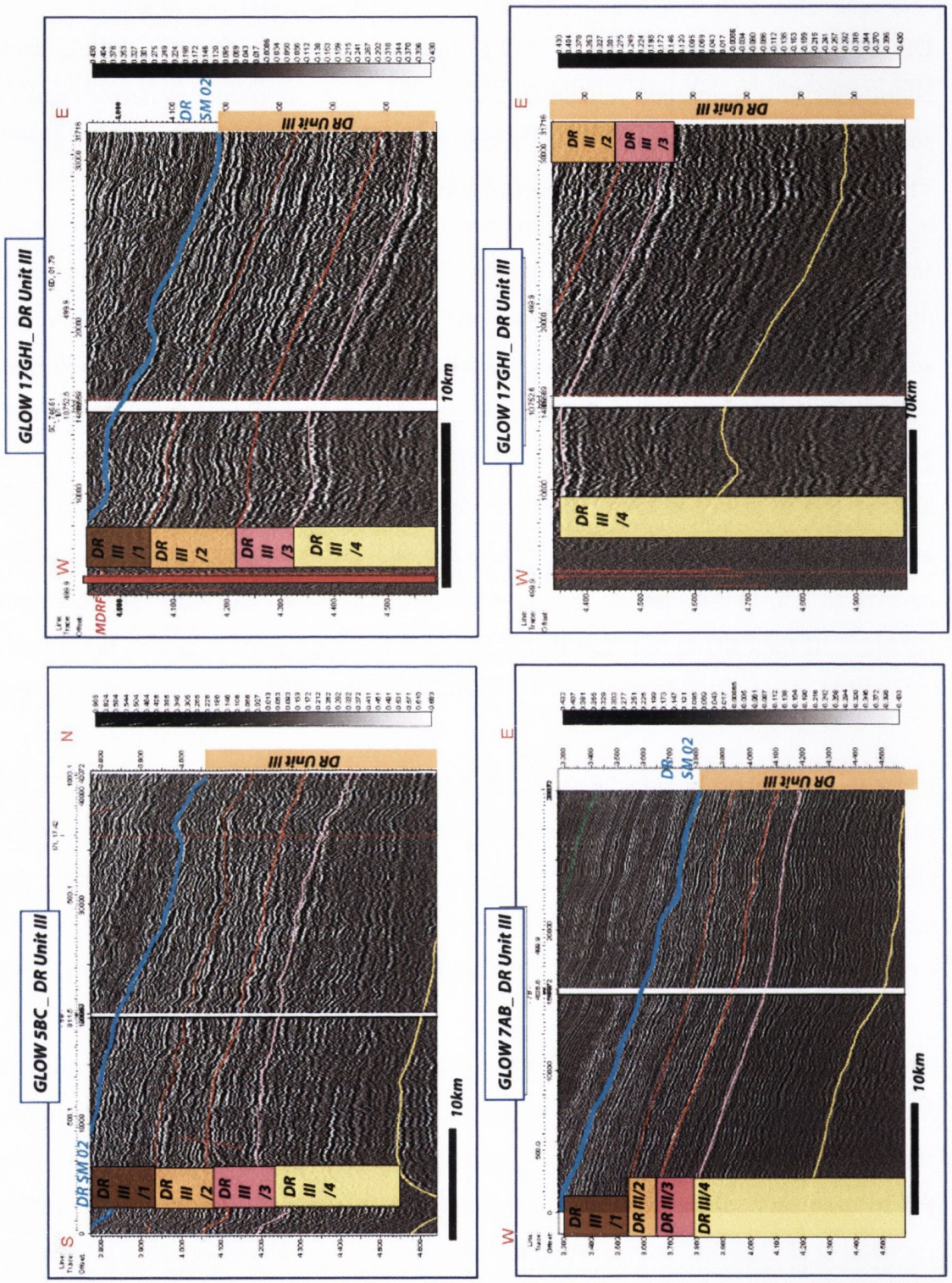

Figure 4.11: A compilation of the seismic characteristics of Davie Ridge Seismic Unit III, comprising III/1, III/2.III/3 and III/4. The location of seismic profiles shown is highlighted on the map in Fig. 4.8.

4.2.6. Davie Ridge Summary Seismic Stratigraphy

The seismic stratigraphy of the Davie Ridge Area can be summarised in Fig. 4.12. The seismic markers can be traced with confidence northwards along GLOW Line 5 (Fig. 4. 13) and correlate well within tied loops of seismic data. Although there are some lateral facies changes and the MDRF crosses GLOW Line 5 towards the north, there is no significant throw at this location and the seismic markers can be traced laterally across it.

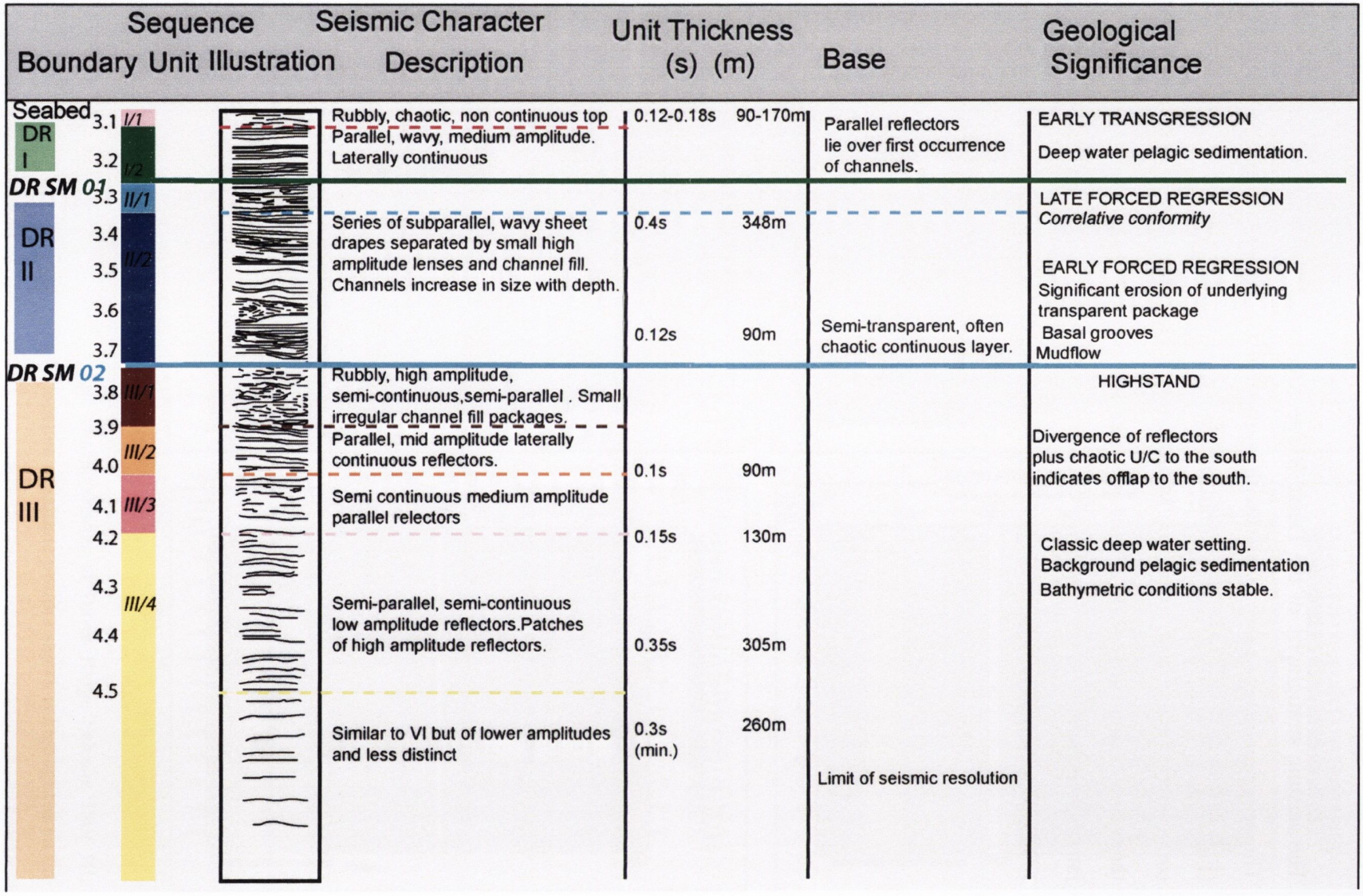

Figure 4.12: Summary of the seismic facies characteristics of the Davie Ridge Area.

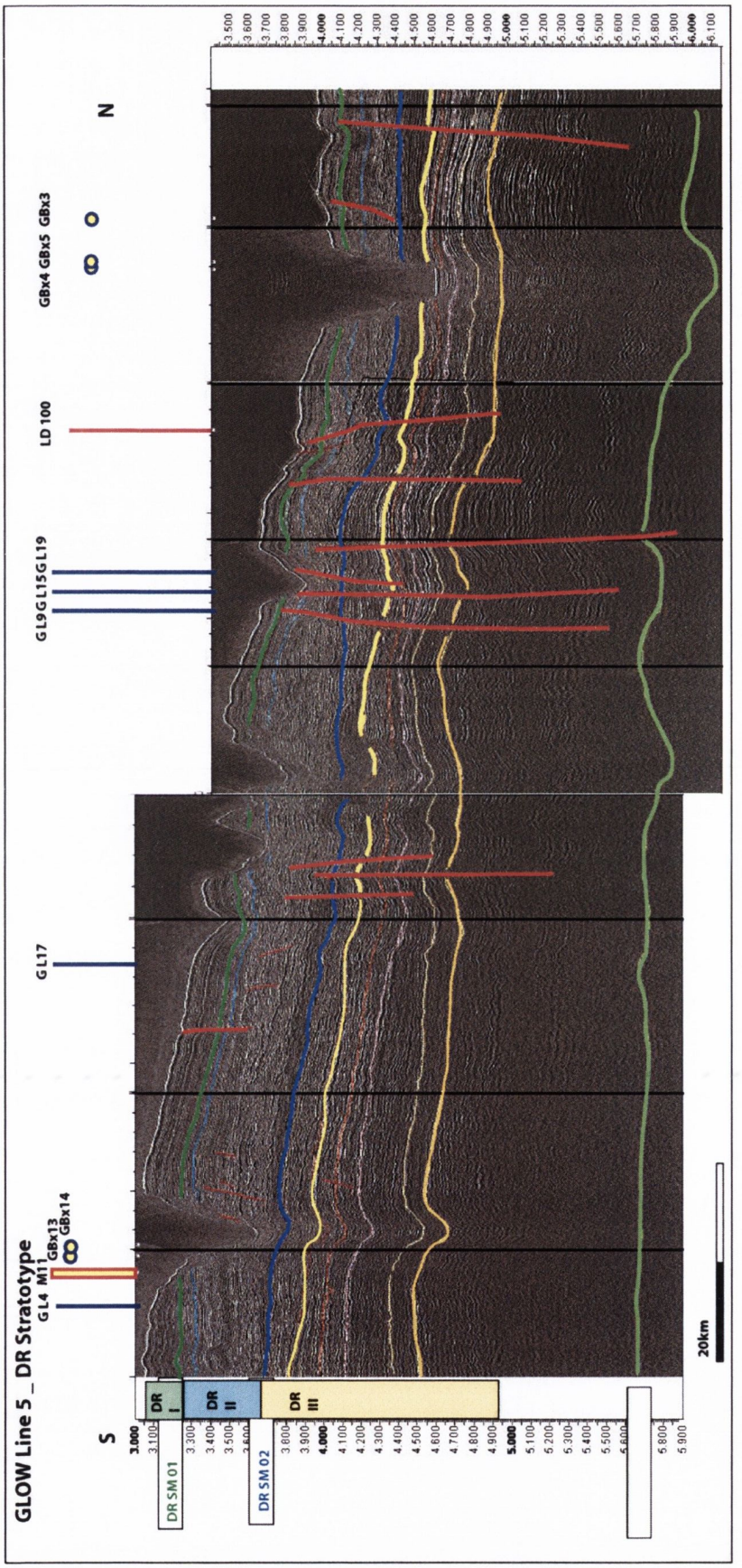

Figure 4.13: Seismic stratotype GLOW Line 5

4.2.7. Sedimentological Interpretation of the Davie Ridge Seismic Facies.

The seismic facies described in previous sections are interpreted as representations of a sedimentary system in a particular environment. Sedimentary environments are assigned to the Davie Ridge seismic units and markers in this section. A model of sedimentological evolution is produced in Fig. 4.14.

During the time of deposition of DR Unit III, the Davie Ridge area was relatively flat and sediment accumulated through suspension settling and pelagic rain out (Fig. 4.14). The sediment accumulation was relatively consistent with no major breaks in deposition. Sandier material and muddy facies interfinger occasionally, particularly towards the top of Unit III.

At the time of deposition of horizon DR SM 02, the Davie Ridge Area was located in shallower water depths than today in a relatively high energy environment (Fig. 4.14).

At the base of DR II/2 the almost-transparent package represents a cohesive debris flow or mudflow in a sheet-like geometry. Instability on the shelf edge region during a base-level fall may have led to the manifestation of a mudflow. The contorted chaotic facies observed may be explained by the fact that mudflows tend to freeze on deceleration (Posamentier & Kolla 2003), due to the discrete shear strength of the sediment/water mixture. Thus the mudflows travel shorter distances than turbidity currents. While they tend to erode on the continental slope the sediment accumulates towards the toe of the slope and in the proximal basin floor settings. As the transparent, chaotic facies becomes less distinct towards the north it is possible that the source of this mudflow was located closer to the south of the Davie Ridge.

Intense erosive bases and channelling features directly overlying the chaotic muddy facies indicate a large amount of sediment bypass and erosion. In contrast with the underlying mudflows the turbiditic, sandier facies are characterised by higher amplitude reflections and well defined layer cake architecture. Channels cut through the Davie Ridge area in a roughly W-E orientation indicating a sediment source from the shelf to the west. A large amount of terrigenous sediment was likely being

delivered to the deep basin via high density turbidity currents. The semi-transparent packages observed in-between probably represent muddy facies draping over the channelled sediments below. Although this environment was prevalent for a substantial amount of time, the Davie Ridge Area was still aggrading sediment. This sequence was deposited when sea level was relatively low and a large amount of sand material was passing into the deep basin, probably during an early regression.

With gradual sea level rise and/or less material reaching the Davie Ridge Area the channels became less intermittent. A significant rise in relative sea level marks a transgressive surface between DR II 1 and DR II 2. This may be referred to as a 'correlative conformity'; a correlative surface that is present during the shift from late regression to early transgression. Less sand is reaching the Davie Ridge Area as predominantly pelagic sedimentation took place with some coarser shelf-derived sediments occasionally interspersed leading to high amplitude zones of reflectors. The parallel continuous reflectors are pushed into sediment waves climbing W/NW. This may indicate the existence of a slope and associated contours formed as strong bottom currents pushed sediment into slope perpendicular waves. As the amplitudes decrease towards the conformable DR SM 01, it is likely that the sediment being accumulated was finer grained and more homogenous.

At the time of deposition of horizon DR SM 01, the Davie Ridge Area was located in the deep sea with pelagic sedimentation (Fig. 4.7). It is likely that there was a small high to the north; a slight divergence of internal reflections to the southeast reflects this difference in accommodation space. During the deposition of DR I/2 the Davie ridge area was located in deep water and deep water hemipelagic sedimentation was taking place. The bathymetric conditions were stable and the energy regime was low. The ridge was tilted, possibly during uplift along the adjacent MDRF. The environment experienced an increase in energy and/or sediment influx as the parallel reflectors of DR I/2 were eroded. The rubbly chaotic cap of DR I/1 was laid down parallel to the existing bathymetry. The evolution of the major channels that erode DR I was either post or syn-deposition of DR I. However, the presence of the meandering GLOW Snake indicates a sinuous submarine high density turbidity current once flowed through the Davie Ridge Area. This would most likely have been located on the continental slope. Thus, due to its present elevation, the Davie Ridge Area has

been uplifted a considerable amount. The timing of this tectonism and related fault activity will be discussed in more detail in Chapters 9 to 11.

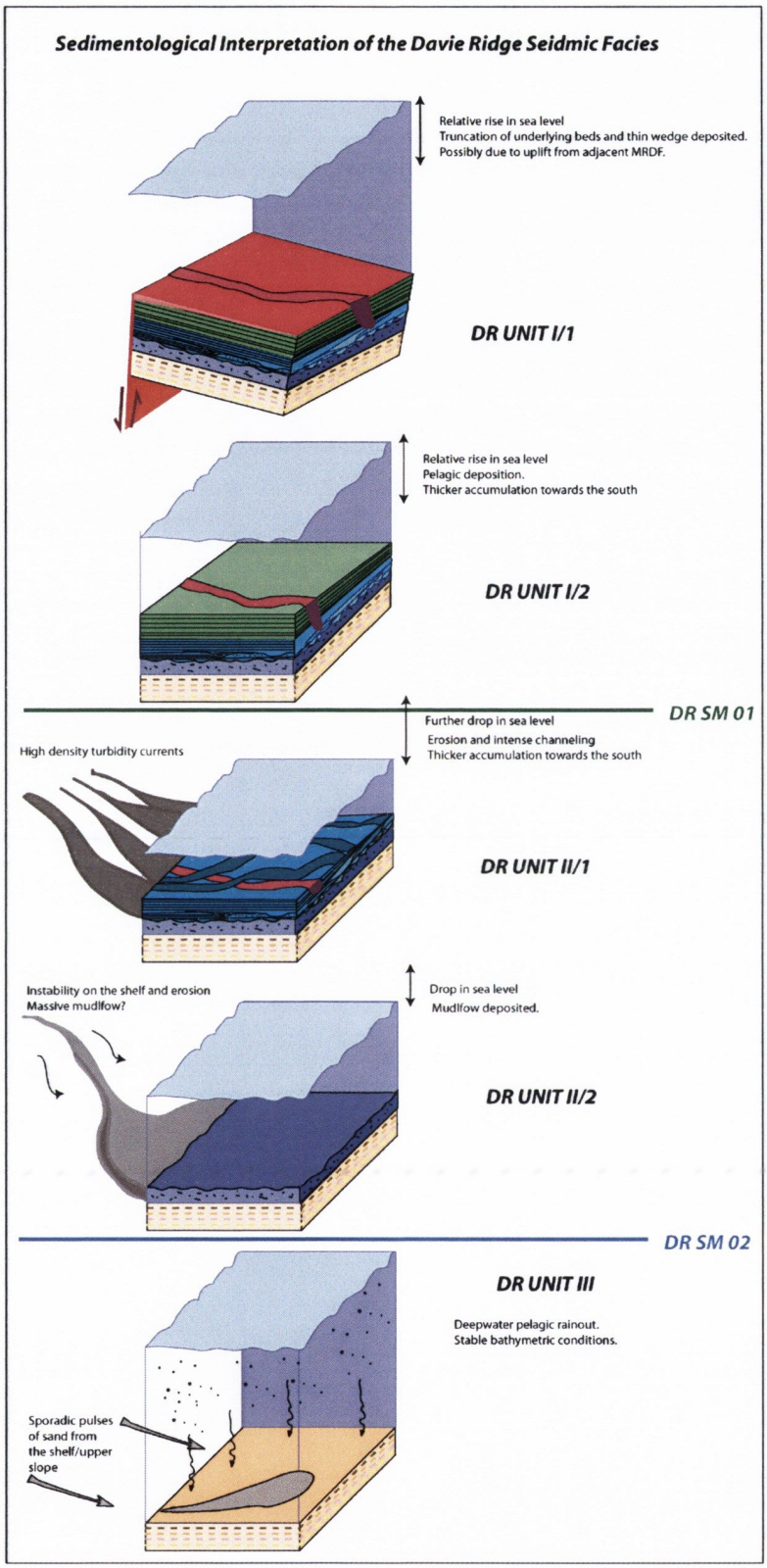

Figure 4.14: Schematic diagram illustrating the sedimentological and palaoegeographical evolution of the Davie Ridge Area. The dark purple represents the earliest possible timing of channel development on the Davie Ridge.

4.3.Davie Ridge Inner Extensional Zone (DRIEZ)

The Davie Ridge Inner Extensional Zone (DRIEZ) is an active extensional zone bound to the east by the normal west-dipping Main Davie Ridge Fault (MDRF) and to the west by the Kerimbas Basin and the West Davie Ridge Extensional Fault (WDEF) (Fig. 4.15). Normal and strike slip faults that were originally normal and are now experiencing some reverse activity are all found in the DRIEZ, predominantly trending NW-SE. Synclines and anticlines are present in fault bound slivers with axes approximately parallel to the NW-SE fault orientation. This shall be discussed more in Chapter 10.Within the GLOW Seismic Survey, the DRIEZ encompasses ~ 8000km^2.

Seismic data was imaged for depths of up to 2s TWTT, although basement was not imaged. The principal GLOW lines that cross the DRIEZ are 7, 17, 13, 9, 11 (E-W orientation), 12-18, 14 (N-S), 4 (NW-SE) and 19 (SW-NE). In the following section a description of the seismic character of units DRIEZ I and II and seismic marker DZ SM 01 will be given.

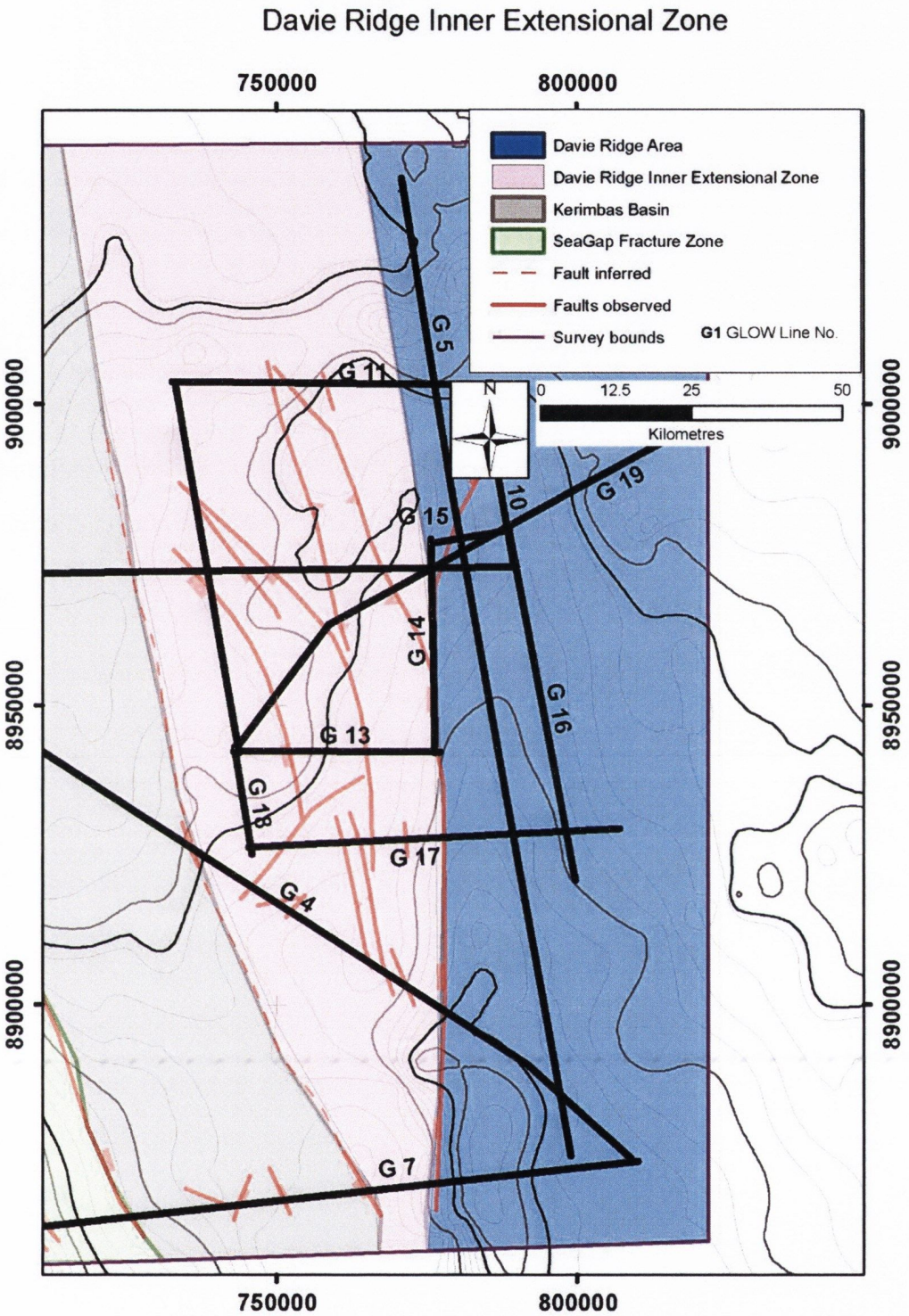

Figure 4. 15: The Davie Ridge Inner Extensional Zone (DRIEZ) Area and GLOW Lines that traverse it.

4.3.1. DRIEZ Unit I

DRIEZ Unit I has an interval of approximately 0.2s but is of variable thickness. It is bound above by the seabed and below by the (green) seismic marker DZ SM 01. Comprising high amplitude, smooth, parallel, continuous reflectors, it is well imaged in most lines (Fig 4.16). It exhibits three morphologies; flat-lying, folded and syn-sedimentary growth wedges. In GLOW Lines 9 and 19 it exhibits a bowed shape within a syncline with some internal onlaps. In GLOW Line 9 the reflectors diverge significantly to the west. In GLOW Lines 7 and 4 this unit can be seen exhibiting diverging reflector packages that grow thicker towards the normal faults. Further north the reflectors are less smooth and continuous, as seen in Line 11 (Fig. 4.16)

4.3.2. DZ SM 01

The horizon DZ SM 01 is picked on a black continuous reflection (peak, positive reflection coefficient) and represented by a green reflector in Fig. 4.16. The time map of surface DZ SM 01 is shown in Fig. 4.17 and occurs between times 2.9 and 4.2s TWTT. Located between Unit I and II, it is moderately laterally continuous and traceable. However, it is significantly dislocated by post DZ SM 01 faulting.

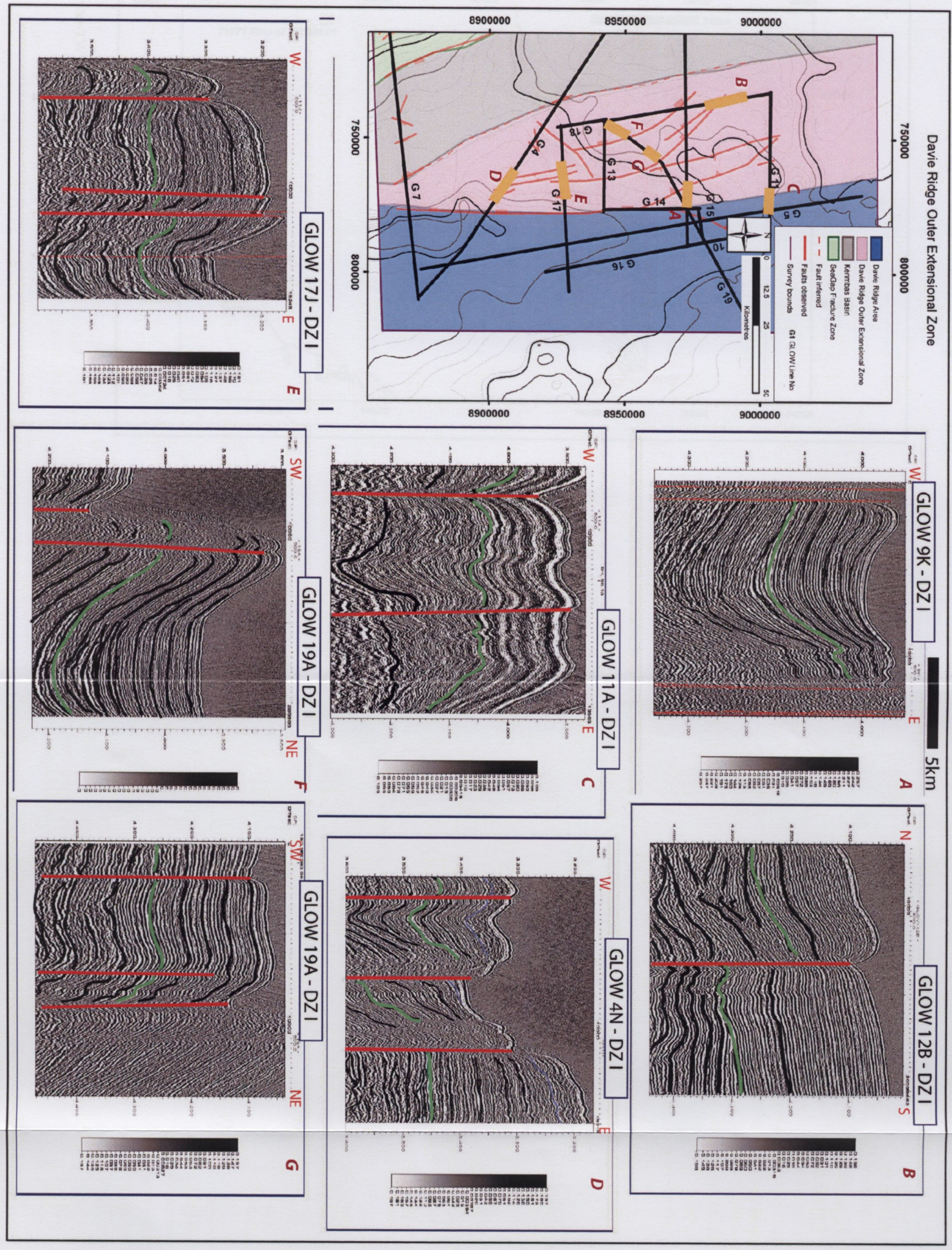

Figure 4.16: A compilation of the seismic characteristics of the Davie Ridge Inner Extensional Zone (DRIEZ) DZ I.

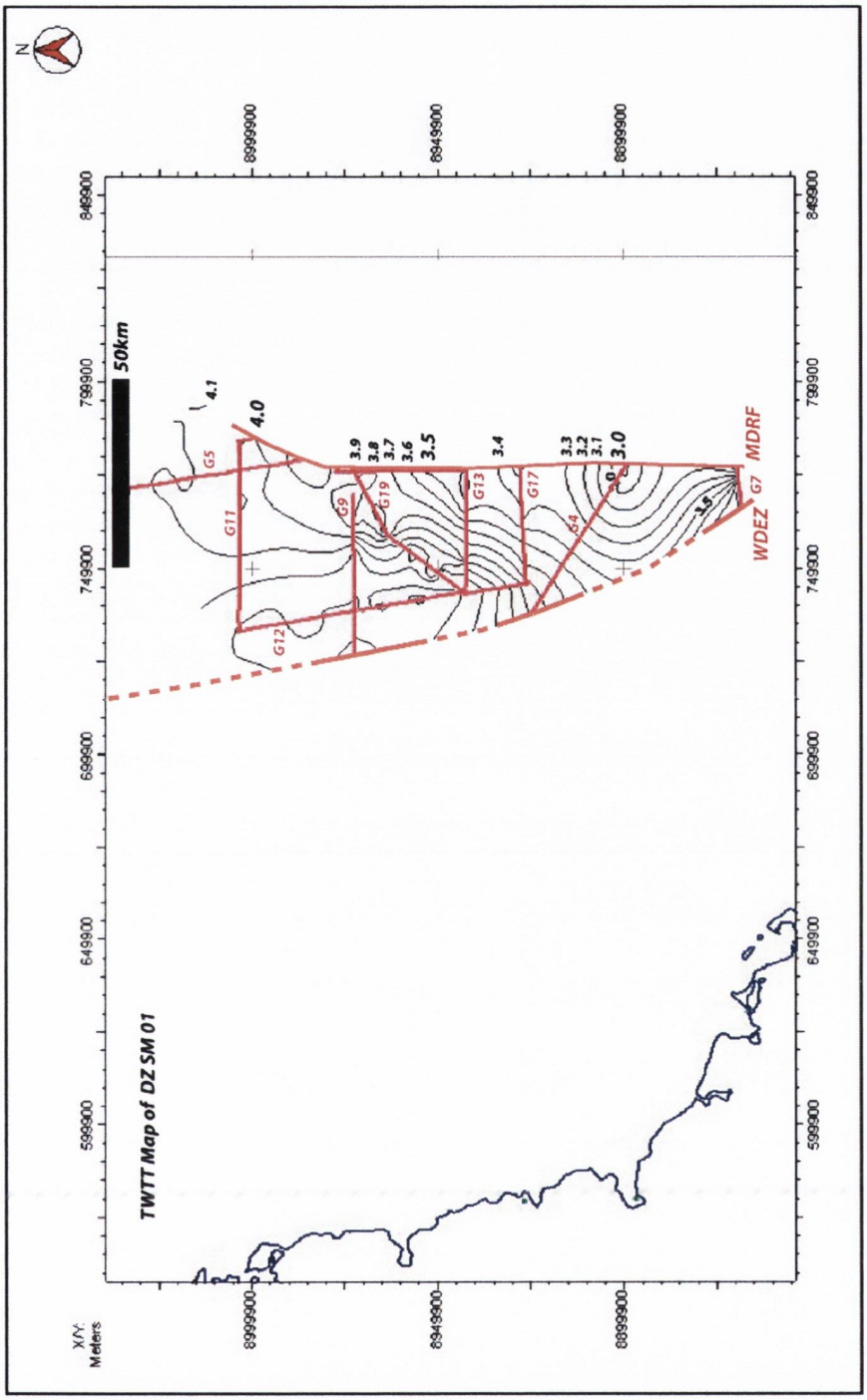

Figure 4.17: The TWTT map of seismic marker DZ SM 01.

4.3.3. DRIEZ Unit II

DRIEZ Unit II has an interval of 0.45s to 0.6s TWTT and is bound above by DZ SM 01 (green) and below by the limit of seismic data. It may be subdivided into three sub-units: DRIEZ II/1/2/3, although there are not enough distinctions between them to allow for a formal designation. DR Unit II exhibits a divergent internal reflection configuration towards the west. Examples of the seismic characteristics of DRIEZ Unit II are shown in Fig.4. 18 with the informal subdivisions also highlighted as per this example.

DRIEZ II/1 is of variable thickness but has an average interval of approximately 0.15s TWTT. It is bound above by the seismic marker DZ SM 01 (green) and conforms downwards into DRIEZ II/2. Comprising high amplitude, smooth, parallel, semi-continuous reflectors, it contrasts with the overlying DRIEZ I by the semi-continuous nature of the high amplitude slightly wavy reflectors. There is some evidence of minor channels and erosion and thin semi-transparent layers. It could be considered a slightly more sandy and energetic facies than DRIEZ I. It is more distinct on the flat-lying sections of the DRIEZ than the inclined fault related sections. Similar to DRIEZ I, there is evidence of significant divergence to the west, particularly in sections abutting the MDRF (Fig. 4.18).

DRIEZ II/2 is 0.15s TWTT thick and consists of smooth, medium amplitude parallel continuous reflectors. It is somewhat transparent in nature compared to the overlying seismic sub-unit.

DRIEZ II/3 is a minimum of 1.5s TWTT thick as the base of it is not imaged (Fig. 4.18). It is a variable unit with high amplitude, non-continuous reflectors, internal divergence and minor truncations. Intermittent transparent layers occur throughout while amplitude markedly decreases with depth.

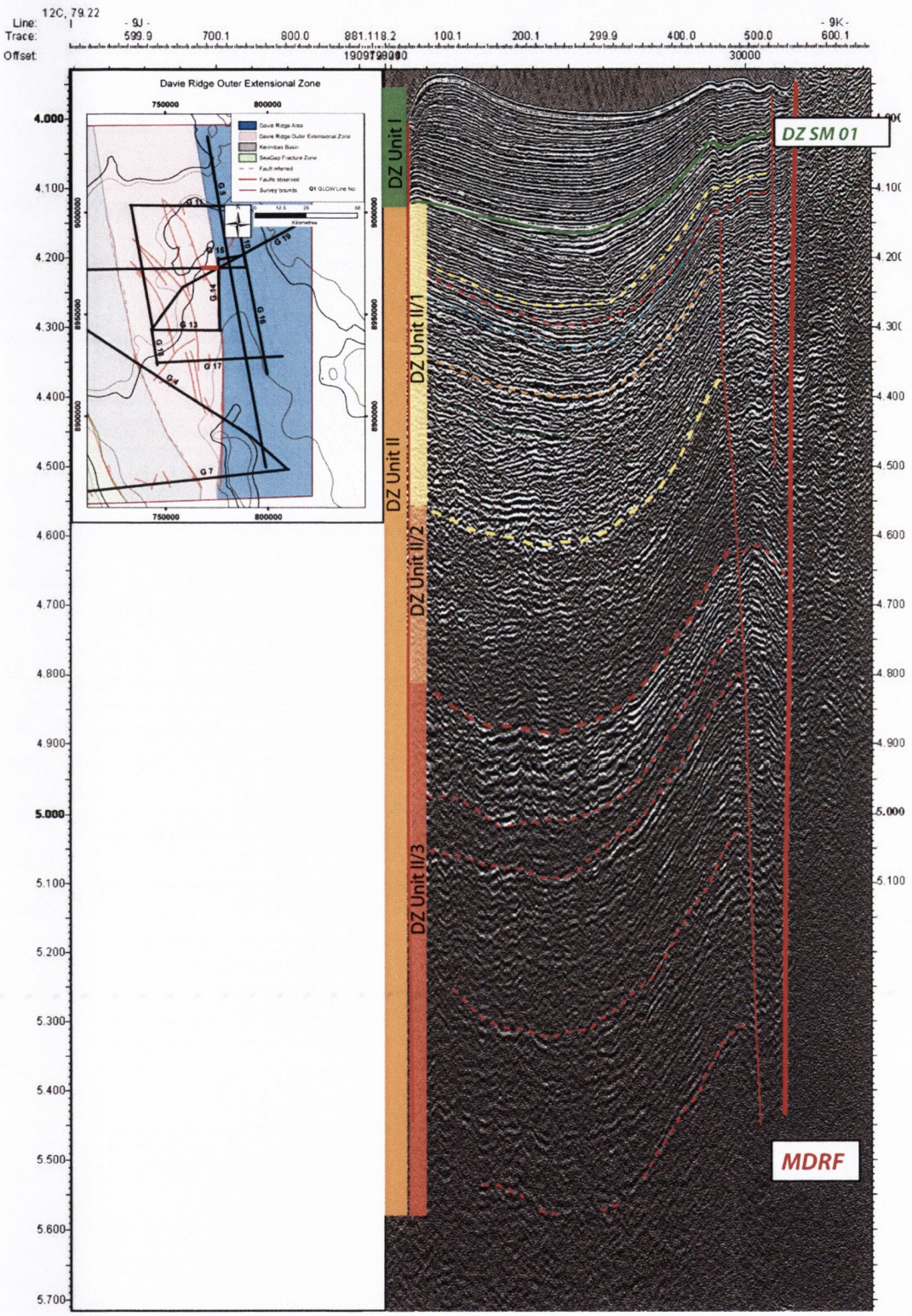

Figure 4.18: An example of the morphology and seismic characteristics of DZ Unit I and II in a section of GLOW Line 9 (Location highlighted on map) immediately adjacent to the Main Davie Ridge Fault (MDRF). The dashed lines highlight the bowed nature of the continuous reflectors.

4.3.4. DRIEZ Summary Seismic Stratigraphy

The seismic stratigraphy of the DRIEZ is summarised in Fig. 4.19.

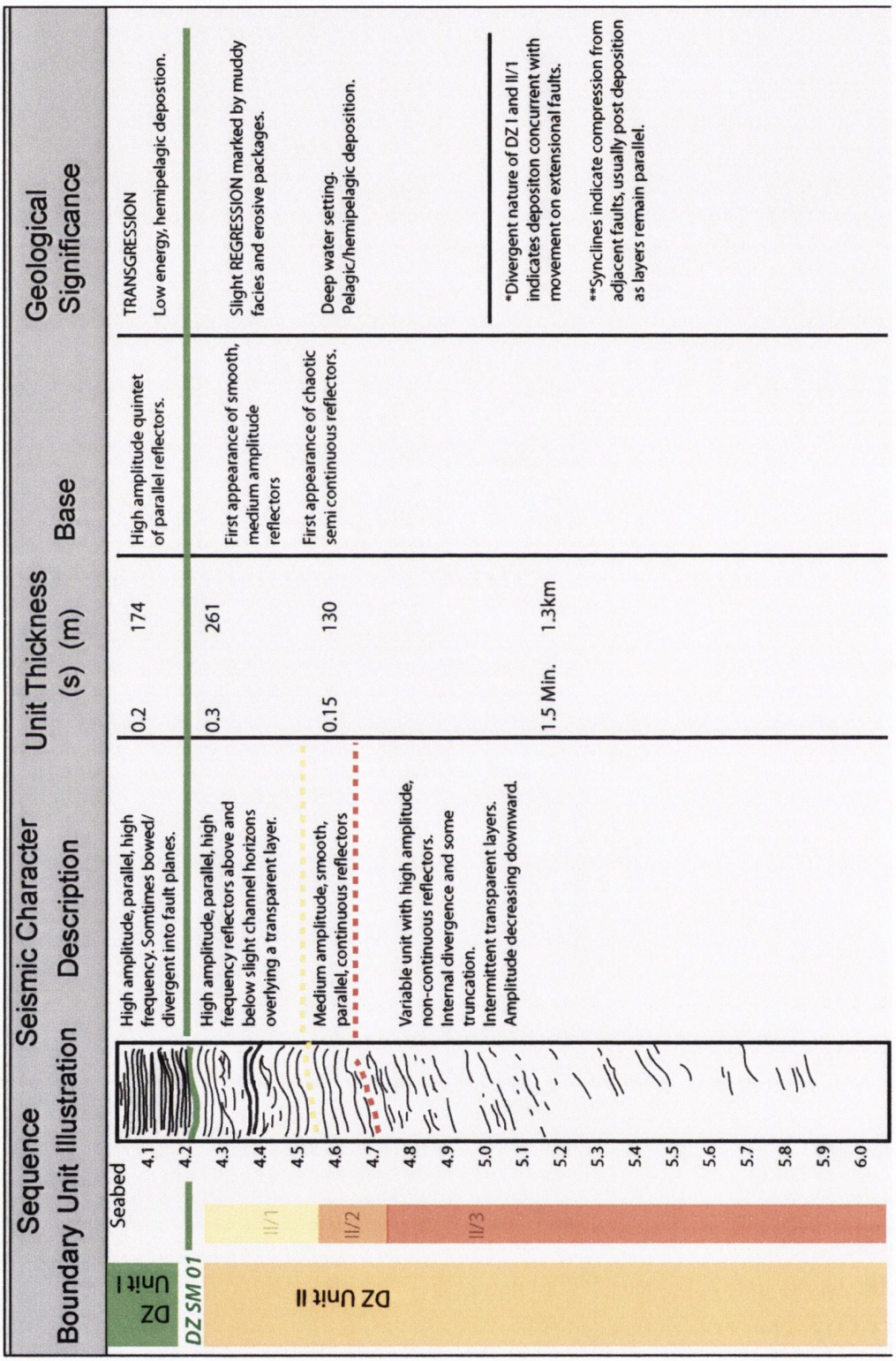

Figure 4.19: Summary of the seismic characteristics and features of The Davie Ridge Inner Extensional Zone(DRIEZ) Stratigraphy.

4.3.5. Sedimentological Interpretation of Davie Ridge Inner Extensional Zone Seismic Facies.

During the deposition of DZ II, the area was located in deeper water and hemipelagic/pelagic sedimentation was dominant. More accommodation space was available to the west of the area, as indicated by internal divergence of reflectors. Slight influxes of coarser material from the shelf environment led to the slightly higher amplitude, non-continuous reflectors of DZ II/3. A drop in the amount of this coarser material, possibly due to a relative sea level rise led to the deposition of DZ II/2. Sea level appears to have fallen during the deposition of DZ II/1 as there is evidence of a mudflow and coarser turbiditic splays. A major rise of sea level and subsequent transgression led to a low energy, quiet hemipelagic environment.

N-S trending normal faults were active during the deposition of DZ I and II, and some are active still to the present day, with their fault traces visible on the seafloor bathymetry. It is worth noting that there are minor amounts of post-rift sediments in DZ I and II indicated by their relatively flat nature overlying growth faults. Within the DRIEZ, the major channel feature is the Tanzania Channel which traverses GLOW Line 11. This shall be discussed in more detail in Chapter 9.

4.4. Sedimentological Correlations between the Davie Ridge Area (DR) and the Davie Ridge Inner Extensional Zone (DRIEZ).

In terms of correlating across the MDRF, there are three options for the DRIEZ in relation to the DR; (1) that the DR stratigraphy is older than the DRIEZ, (2) the stratigraphy in the DRIEZ is older than the DR. and (3) the DR and DRIEZ stratigraphy is age equivalent.

Firstly, it is possible that movement on the MDRF has uplifted the Davie Ridge Area relative to the Davie Ridge Inner Extensional Zone. The precise timing of this fault motion is unclear at this stage. However, it is unlikely that the stratigraphy observed in the DRIEZ accumulated post-DR deposition. This would mean an extensive period of deposition on the DRIEZ and a corresponding lack of deposition on the adjacent DR. As there is no evidence of a hiatus of that magnitude on the DR, this option is considered unlikely.

Secondly, it is clear from the geometry of the fault that the MDRF has uplifted the shoulders of the Davie Ridge and downthrown the adjacent DRIEZ. Therefore unless there was a massive amount of erosion that would remove younger stratigraphy from the upper layers of the DRIEZ, it is highly unlikely that the DRIEZ stratigraphy is older than that of the DR. Thus this option is considered highly unlikely.

Finally, there is some evidence that the DRIEZ exhibits similar stratigraphy to the DR. However, the effects of recent extension and compression arising from its location inside an active fault zone, have overprinted it. By examining the nature of the surfaces bounding the seismic facies some correlation has been possible and hence timing of fault movement elucidated.

As can be seen in Fig. 4.20, there are similarities between a number of the DR and DZ seismic facies. Thus we may conclude that they are part of the same sedimentary

system as described in Figure 4.14. The tectonic overprinting of recent fault movements in the DRIEZ indicates some information on the timing of these faults. A summary of the correlation between the DR and DRIEZ units, from oldest to youngest is described below.

The low-medium amplitude, discontinuous reflectors of both DZ II/3 and DR III are very similar in character. A relatively quiet environment with consistent pelagic rainout and no major breaks in deposition is inferred. Sandier material and muddy facies interfinger occasionally, particularly towards the top of Unit III. DR SM 02 may be correlated with the base of DZ III/2. In the Davie Ridge Area this marks a change in environment from quiet, hemipelagic rainout to a muddy, erosive channelled sequence.

It is notable that the basal transparent package of DR II/2 is not distinct in the DRIEZ, as it is in the DR. However, the highly channelled erosive sequence described in DR II/2 may be correlated with DZ II/1. As a major mudflow was interpreted to have occurred in the Davie Ridge Area at this time, its lack of representation in the DRIEZ may indicate (1) a depocentre in the Davie Ridge for sediment accumulation, (2) that this broadly correlates with the area in which the viscosity of the flow 'froze' it or (3) this very thin, semi transparent package, though distinct in the Davie Ridge may simply be overprinted by tectonic activity.

The dominance of pelagic sedimentation in both DZ I and DR II is highly comparable. Hence DZ SM 01 marks the same transgressive seismic surface as DR SM 01. This is referred to as a correlative unconformity in sequence stratigraphy. The divergent geometry of DZ I and DZ II/1 indicates syn-sedimentary deposition concomitant with this area being downthrown due to fault movement to the west. The bowed geometry of all the DZ stratigraphy, bound by adjacent faults, indicates a post-depositional phase of compression. Most of the strain in the Davie Ridge area seems to be taken up by the MDRF with little or no obvious sedimentary response. However, the same post-DZ depositional phase of compression may have led to a minor amount of uplift of the DR inducing subsequent erosion of DZ I/2 and unconformable deposition of DZ I/1.

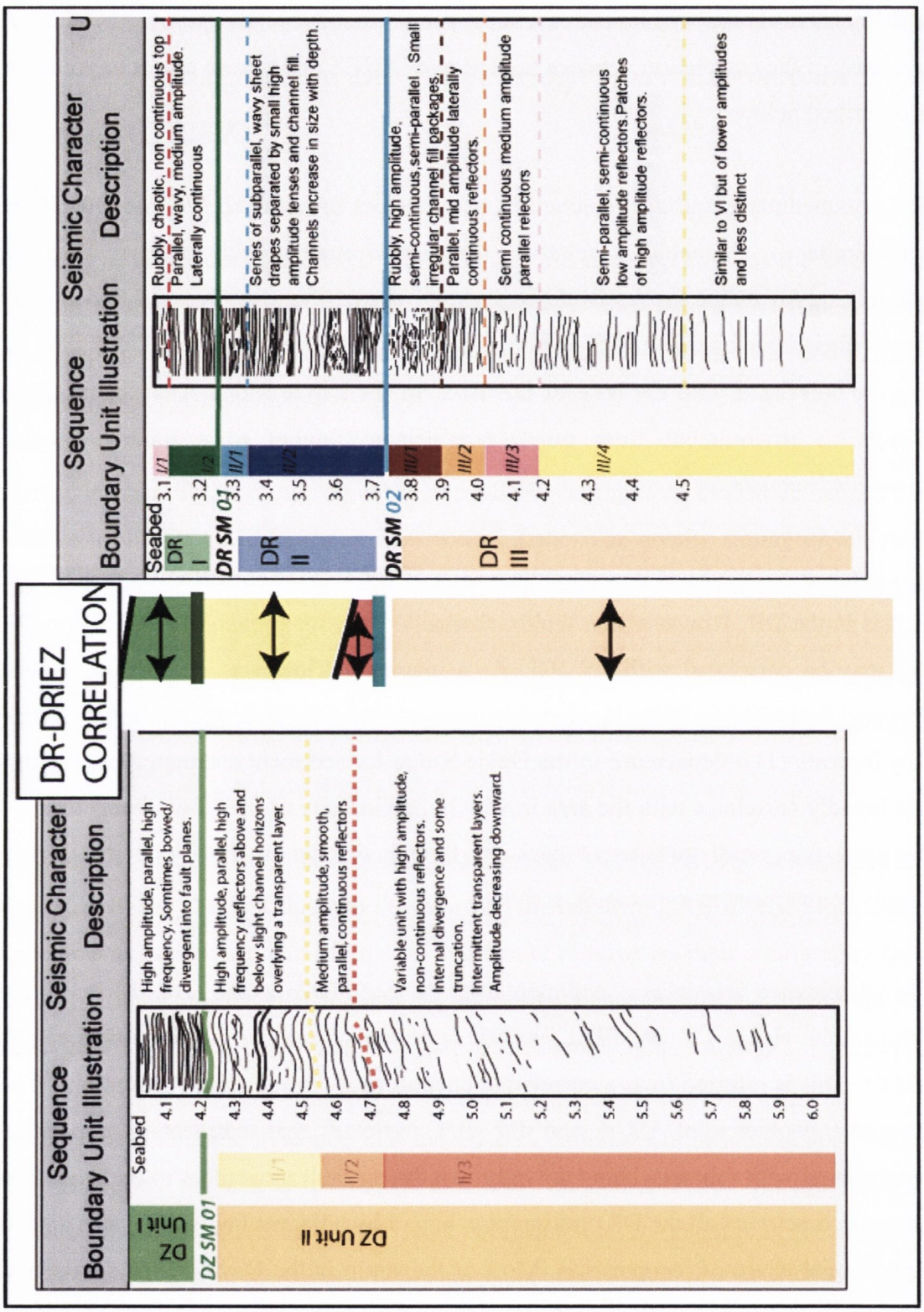

Figure 4.20: Proposed sedimentological correlations between the summary seismic stratigraphies of both the DR and DRIEZ areas.

4.5. Summary

The seismic data traversing both the Davie Ridge (DR) and the Davie Ridge Inner Extensional Zone (DRIEZ) were interpreted using the methods described in Chapter 3. Thus, seismic stratigraphic schemes (Fig. 4.12 & 4.19), TWTT maps to seismic markers and sedimentological interpretations of the seismic facies were produced.

In the Davie Ridge, three seismic units (DR I, II and III) and eight seismic subunits (DR I/1, I/2, II/1, II/2, III/1-4) were recognised. The seismic surfaces DR SM 01 and DR SM 02 were defined and traced laterally. The total sediment accumulation imaged was calculated using the depth conversion method described in Chapter 3 and in total 1.3km of remarkably concordant stratigraphy was imaged. A sedimentological interpretation of the seismic facies indicated a pelagic depositional environment prevailed during DR III. A regressive sequence of mudflows and channels were interpreted as DR II with the regressive seismic surface DR SM 02 in between. DR SM 01 marked a transgressive surface and similarly, DR I represented deposition in a calm, pelagic environment.

In the DRIEZ, two seismic units (DZ I and II) and three seismic sub-units (DZ II/1-3) were recognised. The seismic surface DZ SM 01 was traced laterally throughout the area. Correlation was more difficult in the DRIEZ area due to the prevalence of shallow faulting and folding. The total sediment thickness imaged was 1.8km based on a velocity profile of 1.65-1.8 km/s over the area ofinterest, which is biradly similar to that of DSDP 242 (discussed in more detail in Chapter 6). A sedimentological interpretation of the seismic facies in the DRIEZ zone indicated a hemipelagic setting with a slight increase in coarser material before a return to a hemipelagic setting after DZ SM 01.

Based on the sedimentological interpretations, a correlation was attempted between the DR and DZ stratigraphy. There was a broad similarity noted between the DZ SM 01 and DR SM 01, both representing a transgressive surface. DR SM 02 was correlated to the base of DZ II/2, the onset of regressive channel features. A model of sedimentological evolution was proposed for the Davie Ridge area (Fig. 4.14) and the

evolution of the DZ is thought to be comparable using the above correlations (Fig. 4.20).

It is not possible to say precisely from this interpretation when the Main Davie Ridge Fault (MDRF) was active. However, from the nature of the steep bathymetric scarp present in the south of the study area (GLOW Line 7), it was relatively recently. To the west of the MDRF, syn-sedimentary deposition was initiated at the base of DZ II/1. Easterly dipping normal faults led to increased accommodation space and a divergent geometry of the reflectors. Post deposition of DZ I, the entire sedimentary sequence underwent compression (in the DRIEZ area only) with harpoon structures and synclines evident. It is inferred that the DRIEZ area is undergoing compression, while there is possibly present-day extension on the MDRF accommodating all the strain of the Davie Ridge area, as there is no evidence of fault activity to the east of the MDRF.

5. Seismic Stratigraphy of the Kerimbas Basin (KB) and the SeaGap Fracture Zone (SGFZ); The GLOW Seismic Survey 2009.

5.1.Introduction

The aim of this chapter is to define the general stratigraphy of part of the offshore study area (Fig. 4.1) by studying the available seismic data (Appendix II, IV) using the methods described in Chapter 3. The entire offshore seismic survey area lies on the continental rise of the southern Tanzanian coastline containing approximately 2,000km of original 2D seismic data (Fig. 4.2).

The stratigraphy of individual 'structural zones' or areas are described in separate chapters (Fig. 4.3) relating to seven zones:

1) Davie Ridge (DR), [Chapter 4]
2) Davie Ridge Inner Extensional Zone (DRIEZ), [Chapter 4]
3) **Kerimbas Basin (KB), [Chapter 5]**
4) **SeaGap Zone (SG), [Chapter 5]**
5) Coastal Basin (CB), [Chapter 8]
6) Shelf and Slope (SS), [Chapter 8]
7) Kitunda Block (KTB), [Chapter 8]

This chapter shall establish the seismic stratigraphy for the Kerimbas Basin and the SeaGap Fracture Zone. By establishing the stratigraphy and estimating the age of horizons, tectonic and sedimentological information is extracted in subsequent chapters.

Seismic reflection configuration, seismic features and distinct surfaces were used to divide the stratigraphy of each zone into distinct seismic units. Sedimentary processes, sedimentological evolution and palaeogeographic maps for each seismic unit are described and produced.

5.2. *Kerimbas Basin (KB)*

The Kerimbas Basin is a broad semi-confined deep-water basin, located on the Tanzanian and Mozambican continental margin. It was first described by Mougenot *et al.*, (1986) as a Miocene extensional basin with a Mozambican equivalent called the Lacerda Basin. It is open in the northeast to the Somali Abyssal Plain and in the south to the Mozambique Channel. It is bound to the west by the uplifted Davie Ridge Inner Extensional Zone (DRIEZ) and to the west by the SeaGap Fracture Zone located on the Tanzanian continental slope (Fig. 5.1). Basin margin uplift is an important factor in the basin evolution and has a significant impact on the present day basin architecture. The narrow, steep margins of the Kerimbas Basin are characteristic of a tectonically controlled basin (Fig. 5.2).

The Kerimbas Basin is part of the passive continental margin that formed as a result of extension associated with Jurassic Gondwana rifting and the subsequent Upper Jurassic – Mid Cretaceous right lateral movement of Madagascar along the Davie Ridge strike slip fault (Mougenot *et al.* 1986; Nicholas *et al.* 2007). Subsequent uplift of the Davie Ridge and the concomitant formation of grabens along the continental slope led to the creation of accommodation space. The Kerimbas Basin trapped terrestrial and shelf-derived sediments transported from the shelf and slope. Turbiditic, contouritic and deep sea fan deposits fill the north-northwest southeast striking basin floor bathymetric depression that formed above the hanging wall of underlying, extensional faults and strike slip faults. Thus, the basin is a regionally significant feature.

It is however also of wider importance for three principal reasons. Firstly, because of its nature as an intracontinental strike-slip basin it offers insights into the early rifting process and associated depocentres. Secondly, the axis of the Tanzanian section of the Kerimbas Basin is occupied by a major deep sea channel, the Tanzania Channel (which subsequently traverses the Davie Ridge before entering the Somali Abyssal Plain). Third, basin floor and deep sea fan sediments comprise an important source of East African palaeoclimatic and palaeo-oceanographic information.

The Kerimbas Basin occupies an area greater than 5,000km^2 and is traversed by GLOW Line 4, 7 and 9. The stratigraphy of the Kerimbas Basin has previously been studied by single channel seismic data (SCS), published by Mougenot *et al.* (1986). The seismic data presented here constitutes the first direct attempted constraint on the stratigraphy of the Tanzanian sector of the Kerimbas Basin and allow for a new stratigraphic definition for seismically defined units occupying the basin to be proposed. The Kerimbas Basin stratigraphy is based on the GLOW Seismic Lines 9, 4 and 7 (Fig. 5.1).

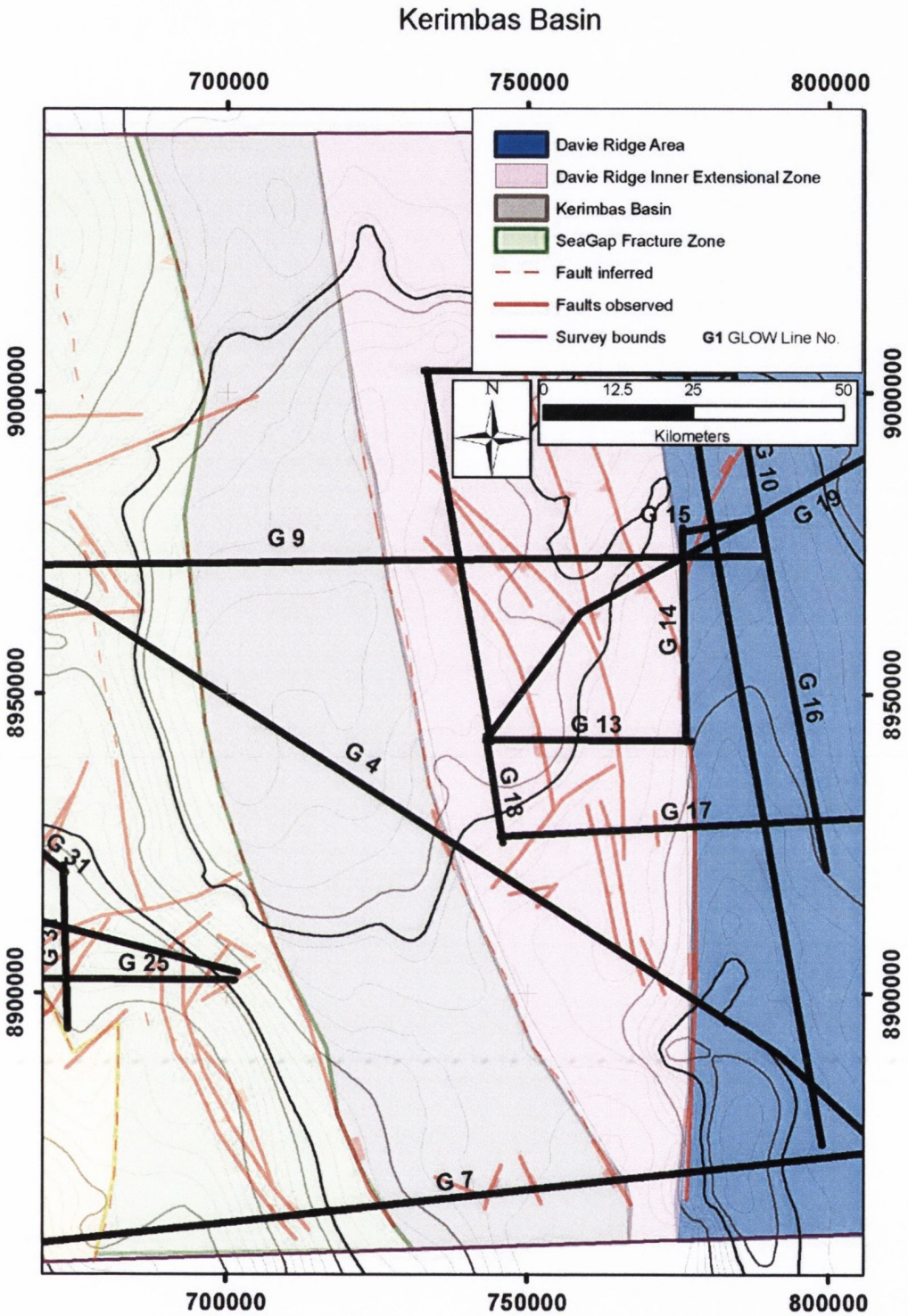

Figure 5.1: The Kerimbas Basin Area (grey) and GLOW Lines that traverse it.

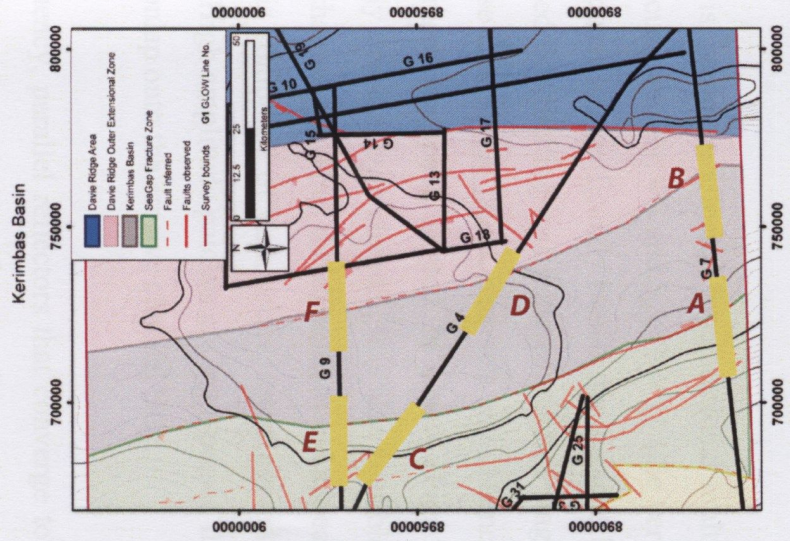

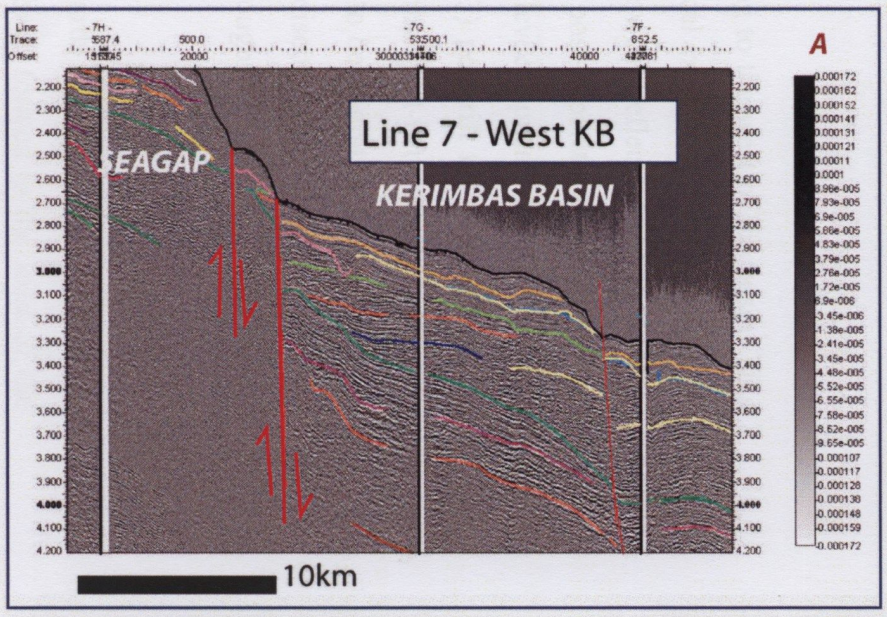

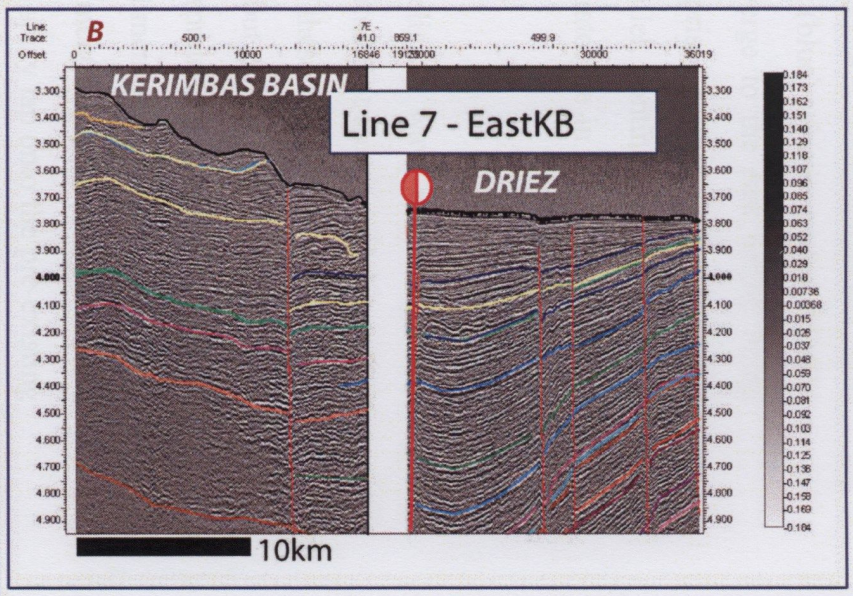

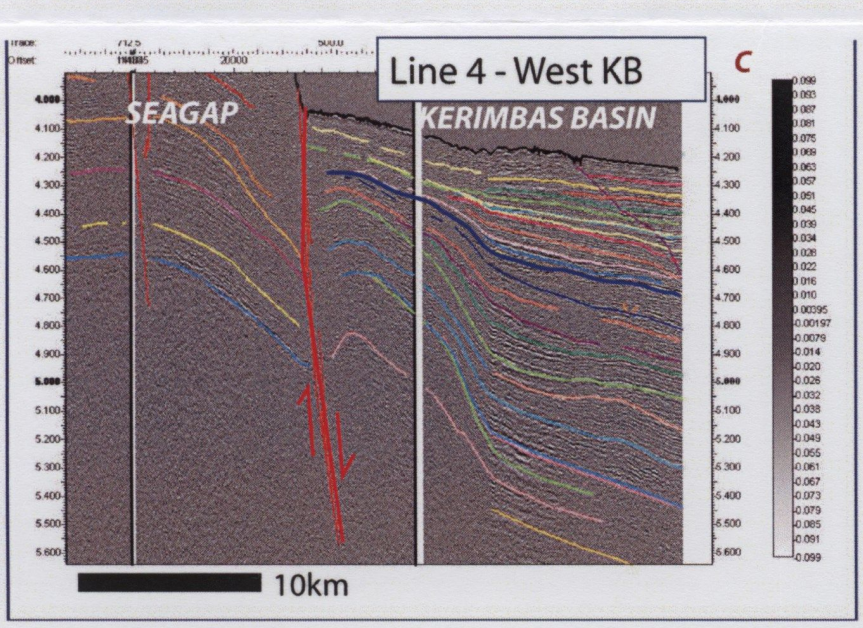

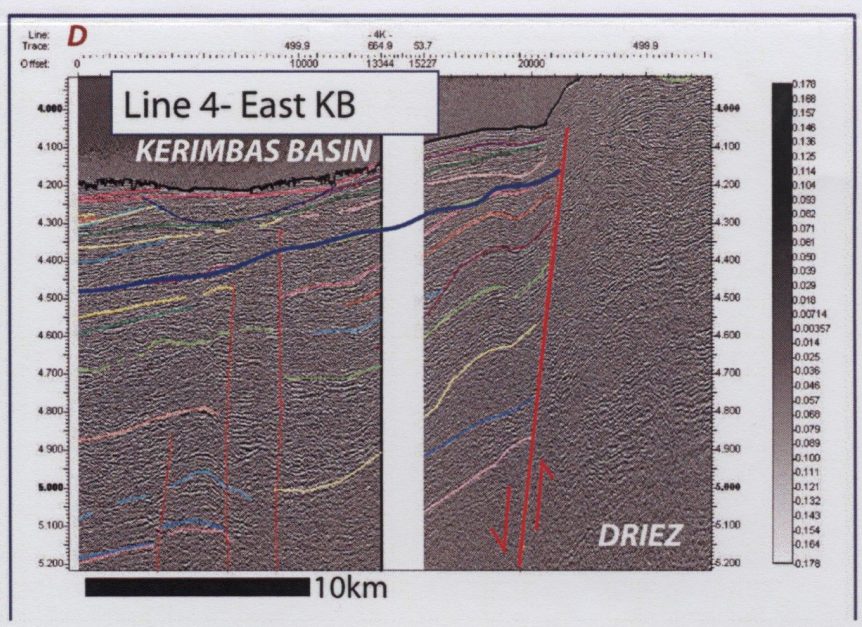

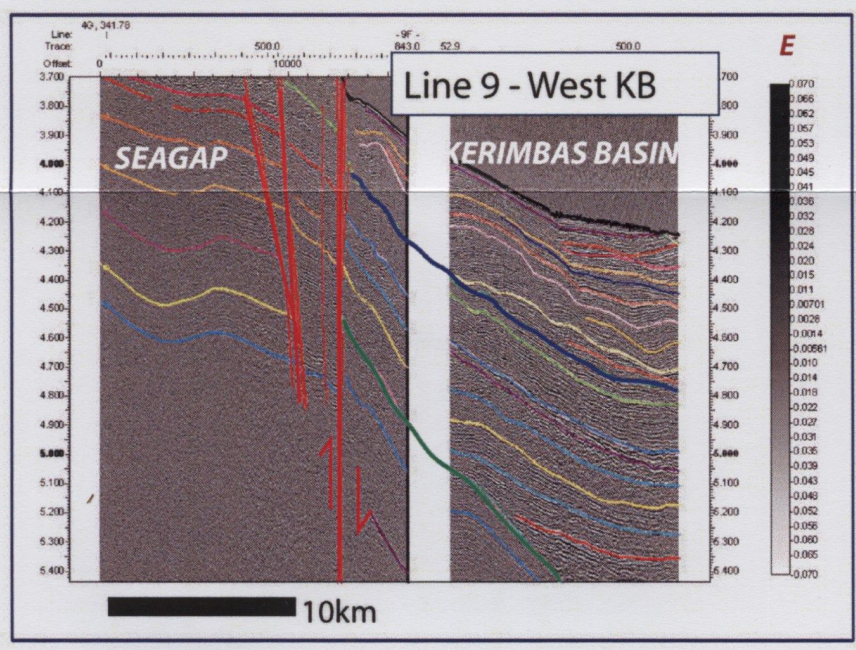

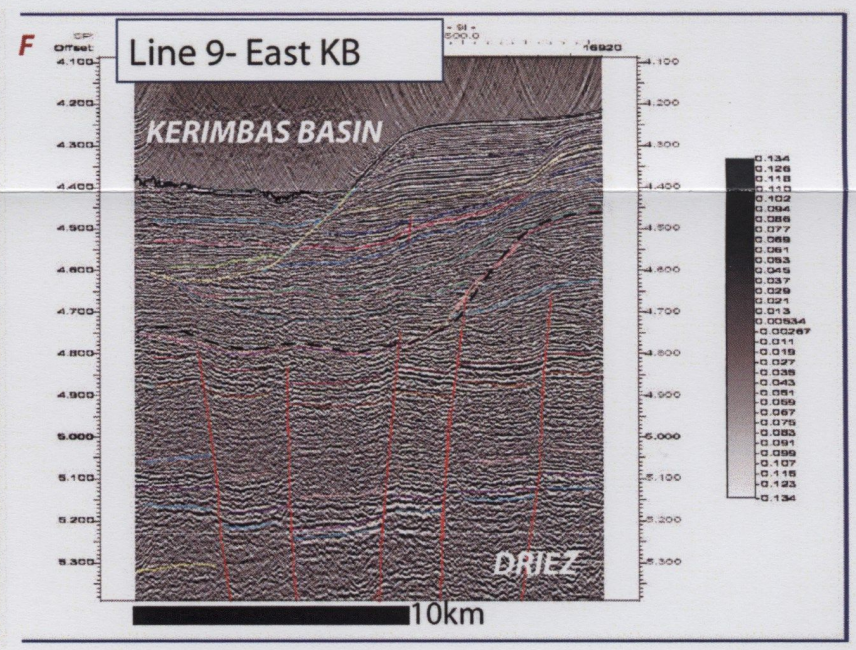

Figure 5.2: The basin margins of the Kerimbas Basin, bounding the SeaGap Fracture Zone to the west and the Davie Ridge Inner Extensional Zone to the east.

5.2.1. KB Unit I

KB Unit I has an interval of 0.4s to 1.5s TWTT, reaching a maximum in the basin axis. It is bound above by the seabed and below by the (blue) seismic marker KB SM 01. The reflectors laterally thin to the west and diverge to the east before being truncated by the West DRIEZ fault. KB unit I comprises several different facies: sediment waves; slightly wavy, high frequency, parallel, continuous turbiditic fill; channel fill and lastly channel levees. The seismic stratotype in Fig. 5.3 shows the geometric relationships of these facies within the unit.

The majority of KB Unit I is composed of parallel, slightly wavy reflectors which occur in layers approx. 0.2s thick exhibiting high amplitudes at the top and decreasing downwards. Downlap is regularly visible in the base of these layers. In some locations a small amount of downcutting and erosion is visible but on the whole, this facies is fairly homogenous and aggradational. It may be interpreted as pulses of turbiditic-current splays that involved a gradual decrease in sediment size and of energy until the flow energy was depleted. The coarser, initial sediment flux ponded in the centre of the basin while the less dense, finer elements of the splay lap onto the pre-existing morphology created by previous splays.

KB Unit I is, however, affected by extensional faulting to the west of the basin. This faulting occurs between 4.3 and 5.5s TWTT (the vertical extent of the fault trace) and does not appear to significantly hinder the distance between reflector packages. Thus it is assumed this faulting was initiated at some stage post-deposition of these layers. Above these extensional faults, channels and channel levees appear to have exploited the accommodation space created. In Line 4 (Fig. 5.3) post-rift fill is indistinct but immediately overlain by a channel. It is also possible this post-rift fill may have been an earlier channel fill. Thus the channel would appear to be migrating westwards. The fill facies is composed of hummocky, interfingered, discontinuous and semi-chaotic reflectors. High amplitude patches are interspersed throughout the fill and the channel fill facies onlap onto the erosive channel base.

High frequency, parallel reflectors that converge towards the channel are present to the east of the channel. Significant sediment waves have formed to the west of the

channel in Line 9, with axes climbing towards the SeaGap Fracture Zone. A similar channel and levee is developed in Line 9, but is much thinner.

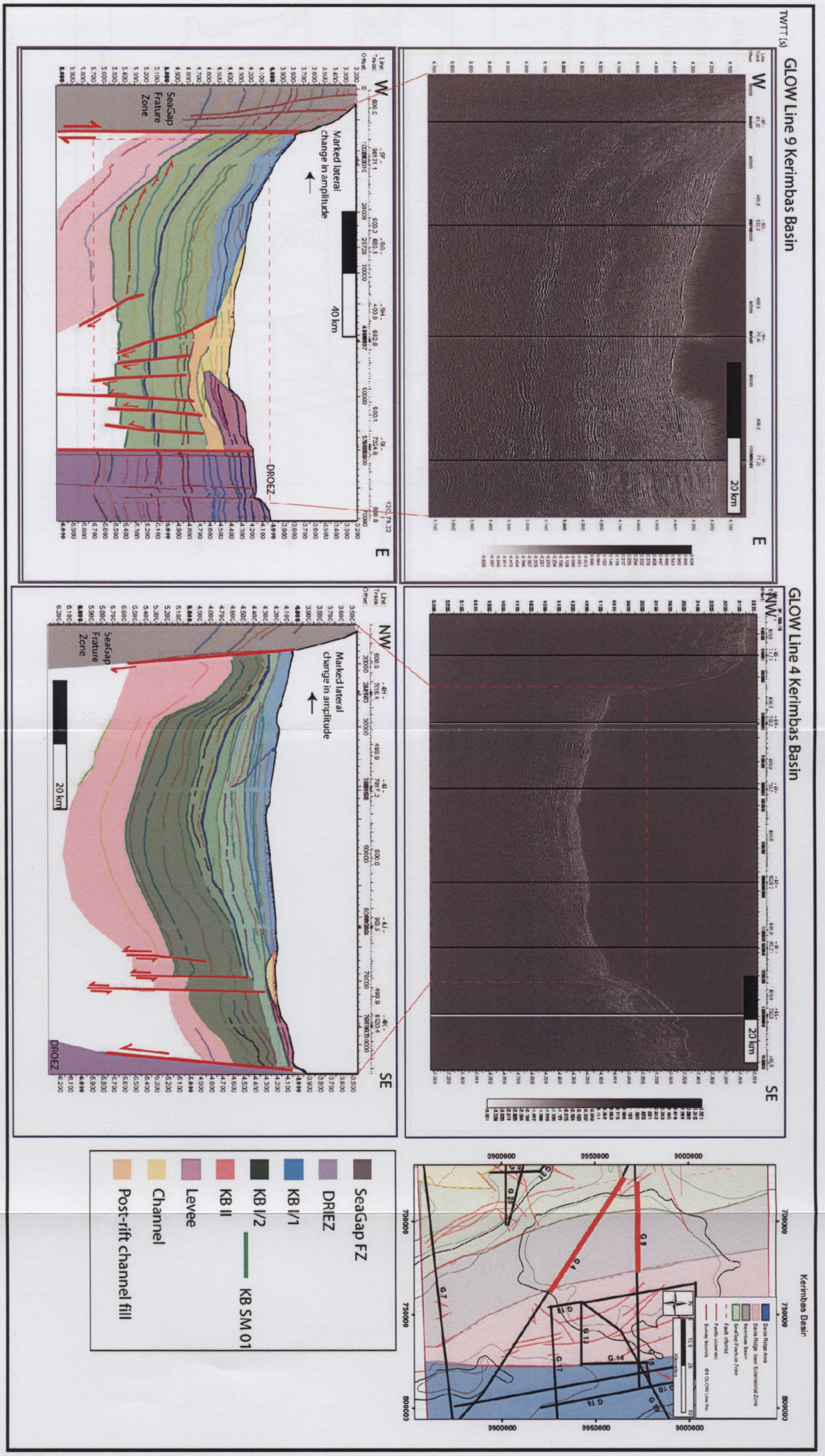

Figure 5.3: Uninterpreted and interpreted sections of GLOW Lines 9 and 4. KB Unit I and II and associated features are highlighted.

5.2.2. KB SM 01

The horizon KB SM 01 is picked on a black continuous reflection (peak, positive reflection coefficient) and is represented by the blue continuous reflector in Fig. 5.3. The time map of surface KB SM 01 is shown in Fig. 5.4 and occurs between times 3.1 and 6s TWTT. Though largely conformable, there is evidence of an unconformity towards the west of GLOW Line 9 where significant onlap onto KB SM 01 can be seen from the overlying KB I.

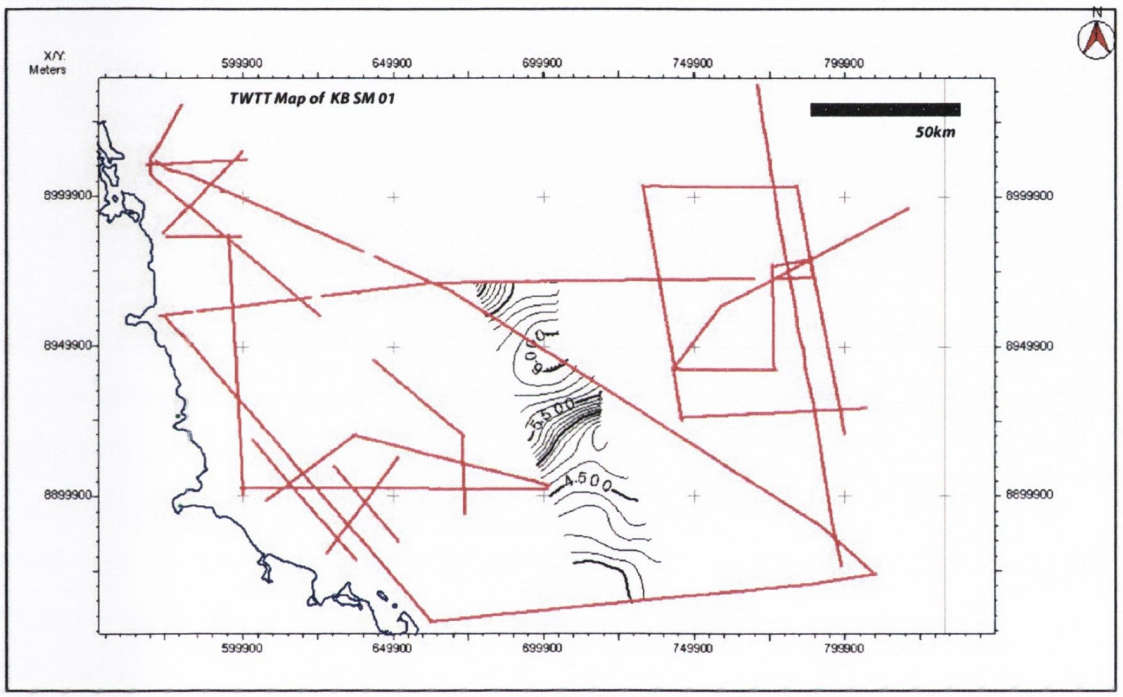

Figure 5.4: The TWTT map of seismic marker KB SM 01.

5.2.3. KB Unit II

KB Unit II has an interval of at least 0.5s TWTT. The base is not imaged, as it is beyond the limit of seismic resolution. The internal reflection configurations are very similar to the turbiditic facies of KB Unit I. The reflectors are lower amplitude and more steeply inclined away from the SeaGap Fracture Zone (Fig. 5.3). The limit of imaged data is reached at approximately 1.6s TWTT beneath the seabed.

Lateral Amplitude Variations in the Kerimbas Basin

Towards the SeaGap Fracture zone there is a noticeable decrease in seismic amplitude. This is shown in Fig. 5.3 and also illustrated at the basin margins of Fig. 5.2. Tracing reflectors laterally from the centre of the basin to the western extent, the amplitudes and thickness drop and the reflectors exhibit a higher frequency, lower amplitude and a slight tilt basinwards. This may be due to a number of reasons: (1) there is a lateral change in sediment type from a highly mixed, turbiditic, sand/mud flow in the centre of the basin to a more homogenous, cleaner, maturer sand of a more distal fan type; (2) there is a fault at this locality and west of this fault is a graben related to the SeaGap FZ and not strictly part of the Kerimbas Basin, or lastly; (3) there has been some shearing of the Kerimbas Basin sediments against the Davie Ridge leading to fault drag folds and a more compressed section of stratigraphy exhibiting a different seismic character. From our limited data, it appears the reflectors can be traced across this point so they have not been offset by a fault. It is most likely related to the difference in sediment supply to the more distal section of a turbiditic splay.

5.2.4. Kerimbas Basin Summary Seismic Stratigraphy

The Kerimbas Basin seismic stratigraphy is summarised in Fig. 5.5.

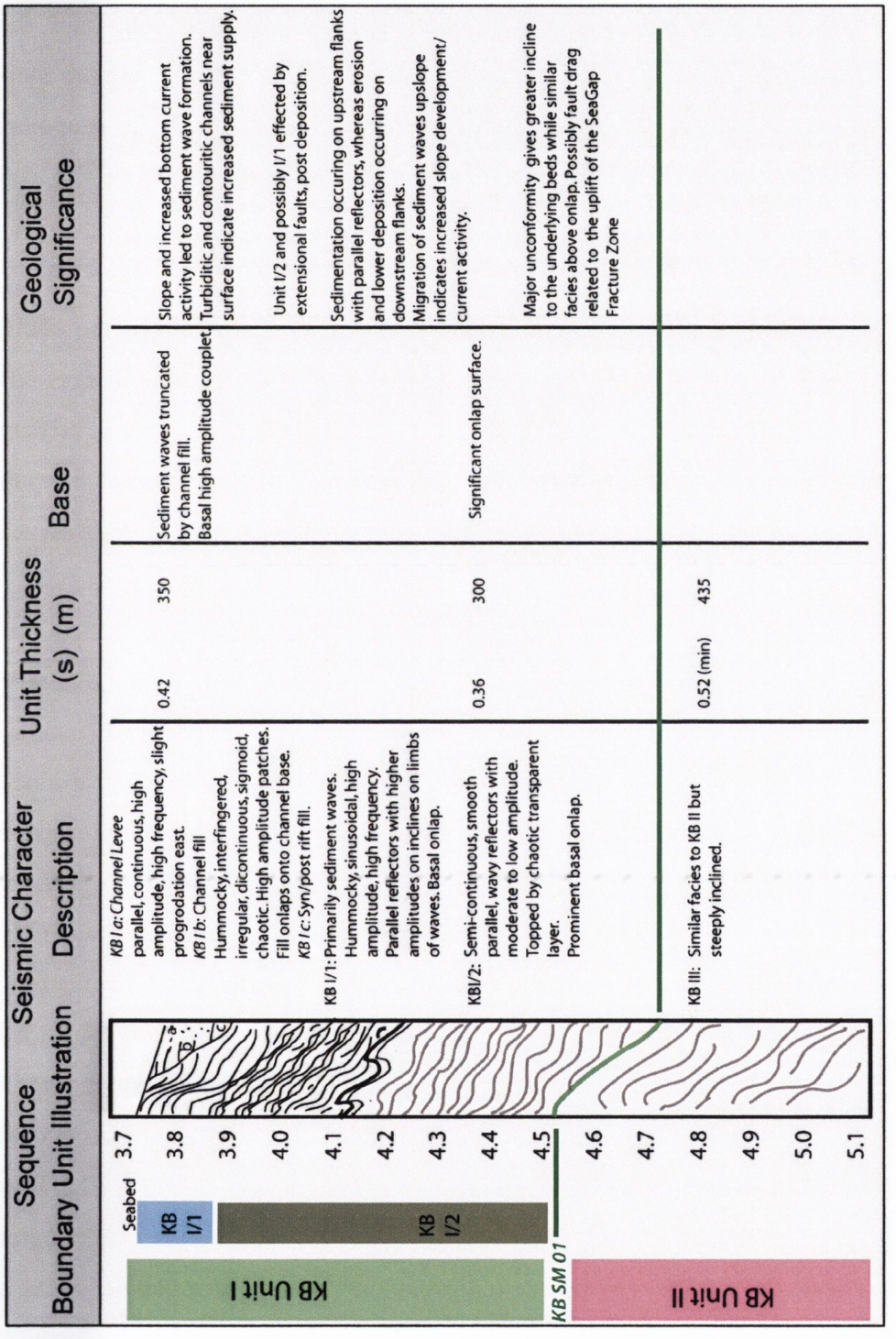

Figure 5.5: Summary of the seismic characteristics and features of The Kerimbas Basin Zone stratigraphy.

5.2.5. Sedimentological Interpretation of the Kerimbas Basin Seismic Facies.

Accommodation space was created between the SeaGap Fracture Zone and the DRIEZ, pre-deposition of the KB seismic facies. Thus it is likely that there are syn-rift and early post-rift sediments beneath the KB units imaged here. The proposed sedimentological evolution of the Kerimbas Basin facies is summarised in Fig. 5.6 and outlined below.

During the deposition of KB II, turbiditic flows entered the basin from the shelf, prograding in a SW to NE direction. Prior to the deposition of the seismic marker KB SM 01, an unconformity was formed in the west of Glow Line 9. The overlying reflectors onlap the tilted surface. This inclined surface may have formed as a result of either a) increased subsidence to the east of the basin or b) a relative increase in sea level.

During KB I/2 deposition, pulses of turbidity currents aggraded in the basin onlapping onto firstly KB SM 01 and secondly towards the SeaGap Fracture Zone. Lenses of material fill in the central axis of the basin while larger flows aggraded finer grained material to the edges of the basin. It is possible there was more accommodation space to the east of the basin as the sediment sheets thicken slightly in this direction. Normal extensional faults are active during the deposition of KB I. However they are only active in the eastern part of the basin and don't significantly offset KB I reflectors. Channel deposits and associated levees began to develop in the newly subsided eastern section of the basin at the same time as turbiditic facies were still aggrading in the west of the basin. The channel developed in GLOW Line 9 is asymmetric with thicker fill towards the east and levee development confined to the east also. This may indicate the development of a meandering channel with levee formation on the outer band. Levee deposits tend to be thicker and coarser at outer channel bends as a function of flow momentum and the associated spillover patterns (Piper & Normark 1983; Posamentier 2003).

Significant sediment wave formation on the western slopes of the basin is possibly related to either a) the overbank environment of the channel-levee system or (b) the development of contouritic sediment waves arising from the presence of a significant slope and bottom current activity parallel to the contours of the basin sides. This distinction will be discussed on more detail in Chapter 10.

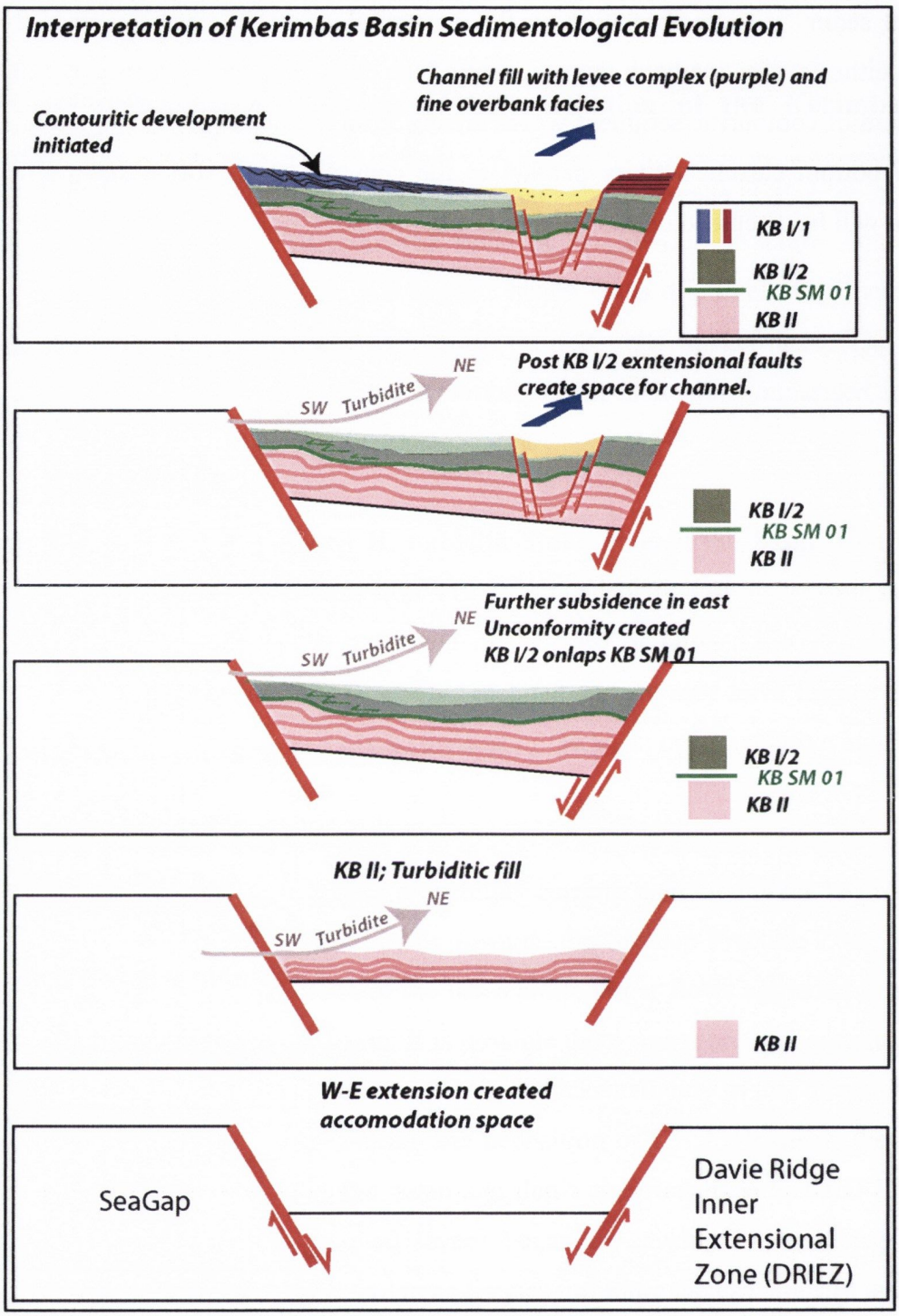

Figure 5.6: A schematic diagram illustrating the sedimentological evolution of the Kerimbas Basin seismic facies.

5.3. *The SeaGap Fracture Zone (SG)*

The SeaGap Fracture Zone has been previously described as a fault controlled inverted flower structure to the west of the Kerimbas Basin, located on the Tanzanian slope (Mougenot *et al.* 1986; Nicholas *et al.* 2007). The stratigraphy of the most prominent bathymetric expression of the Fracture Zone is imaged by GLOW Lines 4 and 9 (Fig. 5.7). There is some evidence from this study that the SeaGap structure continues south, albeit with less surface expression and abuts the Kitunda Block before almost crossing the coastline near GLOW Line 7. Due to the complex structural architecture of the Zone, it is difficult to establish a cohesive stratigraphy for each constituent sliver. The structural relationship between the SeaGap Fracture Zone and the shelf area will be discussed in more detail in Chapter 9.

In the following section three seismic units; SG I, II and III are described for the most prominent section of the Fracture Zone, located at the intersection between GLOW Lines 4 and 9. Two seismic surfaces SG SM 01 and SG SM 02 are described. A sedimentological interpretation of the seismic facies of this section is proposed. Finally the southern expression of the SeaGap Fracture Zone is described.

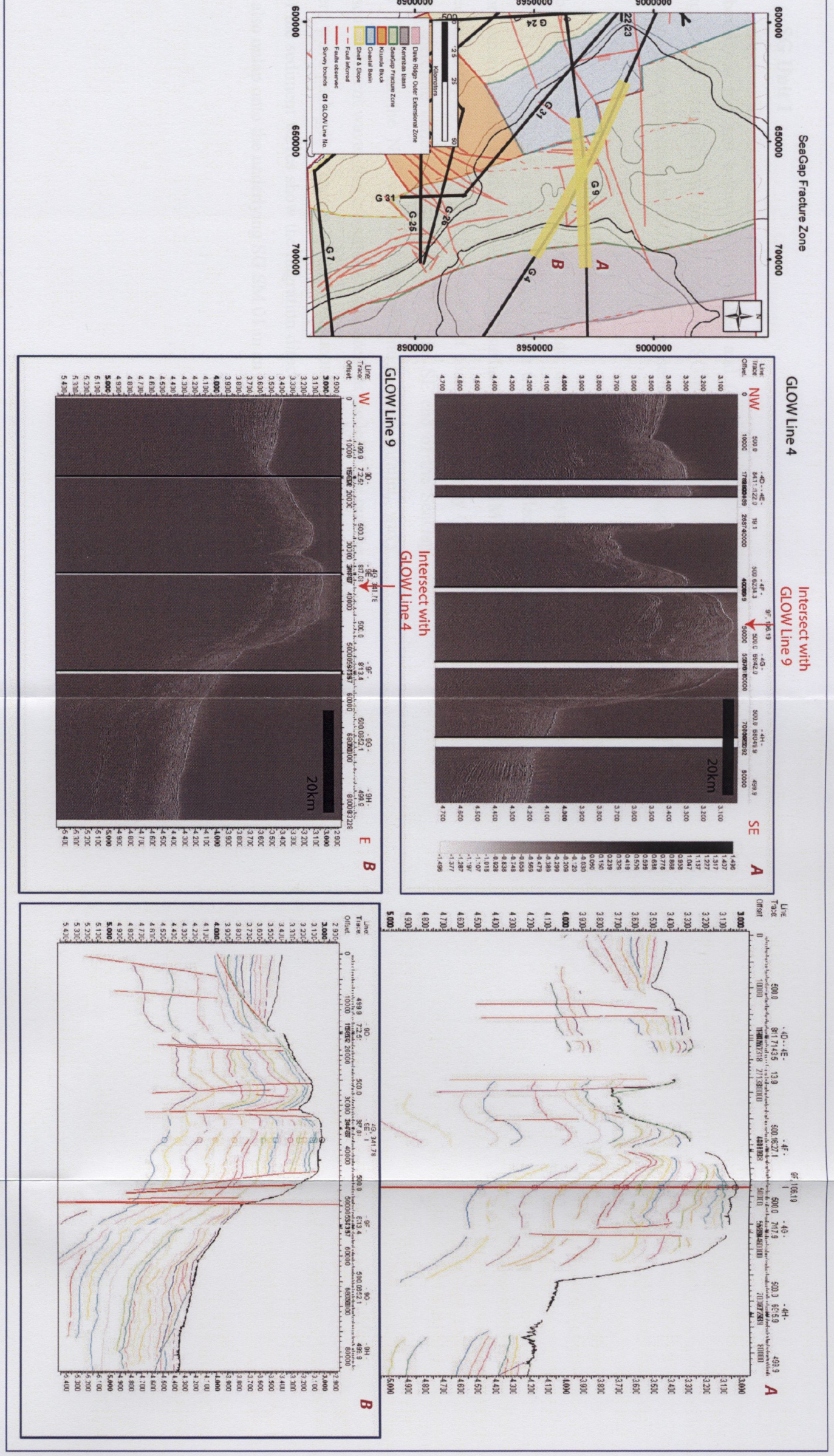

Figure 5.7: The SeaGap Fracture Zone and the GLOW seismic lines that traverse it (inset) Uninterpreted seismic profiles of the GLOW seismic lines 4 and 9 that image the principal bathymetric and subsurface expression of the SeaGap Fracture Zone.

5.3.1. SG Unit I

SG Unit I is bound on top and below by the seabed and (orange) SG SM 01 respectively (Fig. 5.8). It comprises two seismic sub units; SG I/1 (represented at the base by a continuous green reflector) and SG I/2 (base represented by the orange SG SM 01).

The seismic sub-unit I/1 is a rubbly, chaotic, high amplitude, dis-continuous layer. It varies from 0 to 0.1s thick and has an erosional base which truncates the reflectors below. Reflectors onlap a southeasterly dipping seismic surface below (SG SM 01) and are truncated at the top by a thin rubbly layer that just coat the topography (Fig. 5.8). The interval therefore varies from 0.2s TWTT at the SE end of the SeaGap structure to 0s TWTT in the NW section. High amplitude, semi-parallel, wavy reflectors represent sediment waves that are almost transparent in the lees. The outline of these sediment wave packages is shown by the continuous blue reflectors in Fig. 5.8. The axes of the sediment waves show the migration direction is westwards. The basal reflectors also onlap onto the underlying SG SM 01 in an east to west direction.

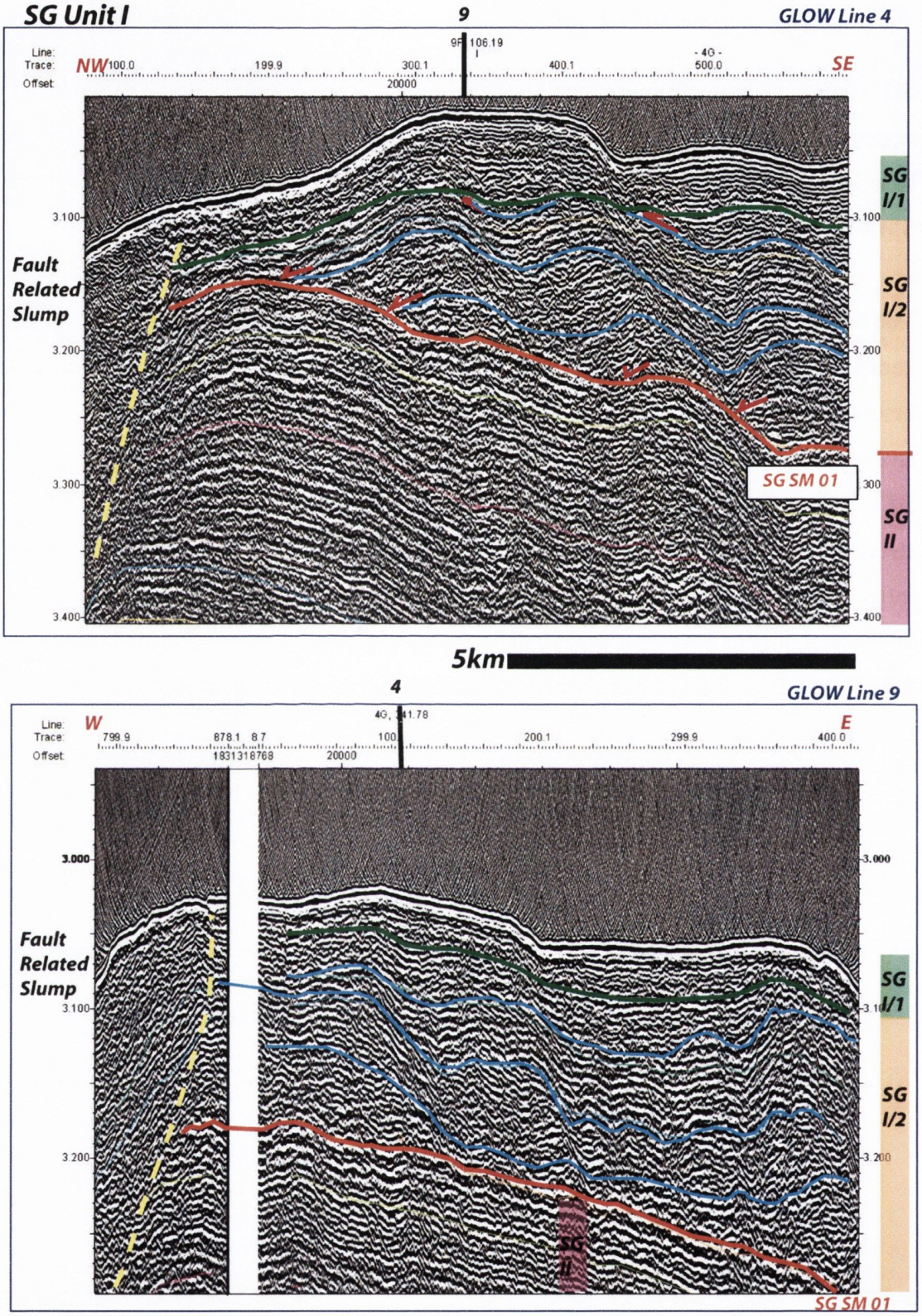

Figure 5.8: A compilation of the seismic characteristics of the SeaGap Fracture Zone seismic Unit I: SG I.

5.3.2. SG SM 01

The horizon SG SM 01 is picked on a black continuous reflection (peak, positive reflection coefficient) and is represented by the orange reflector in Fig. 5.8. The time map of surface SG SM 01 is shown in Fig. 5.9, and occurs between times 3.1s and 3.3s TWTT. Continuous and laterally traceable, this seismic marker is defined by the significant onlap surface of the overlying SG Unit I towards the SW. The overlying sediment waves of SG Unit I then migrate upslope of the surface.

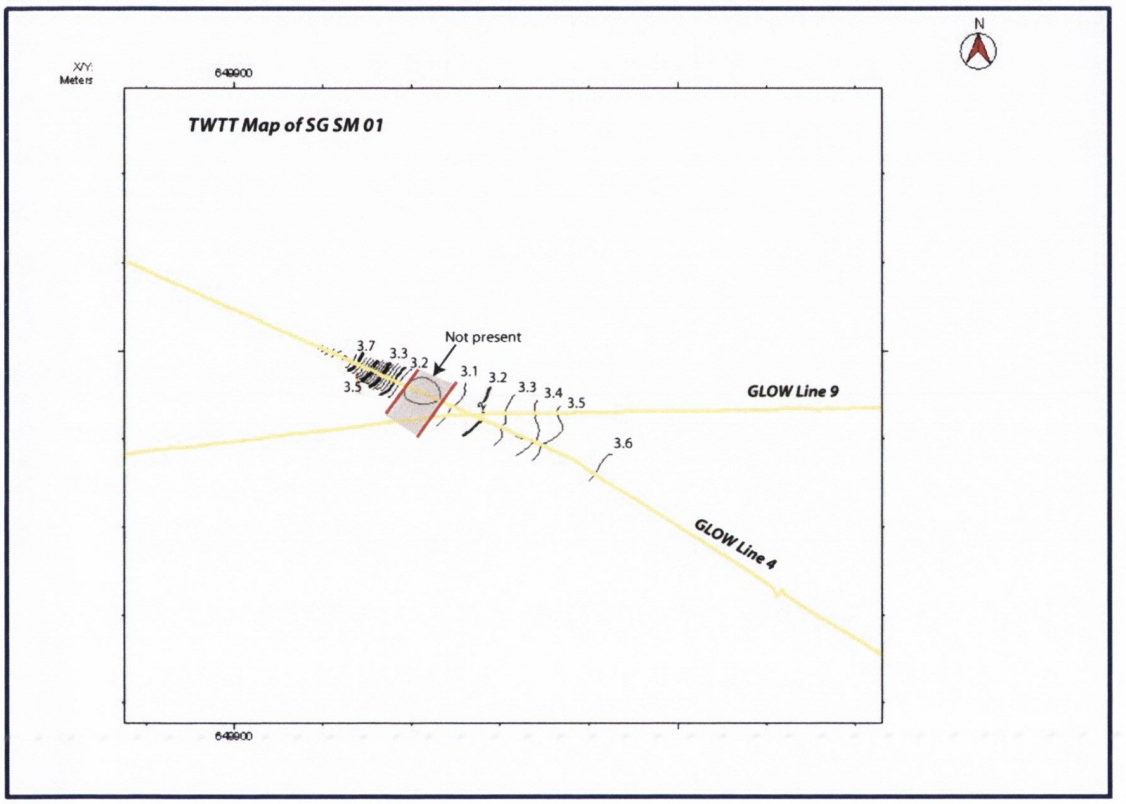

Figure 5.9: The TWTT map of seismic marker SG SM 01.

5.3.3. SG Unit II

SG Unit II has an interval of 0.4 to 0.5s TWTT and comprises two seismic subunits; SG II/1 and SG II/2 (Fig. 5.10).

Seismic subunit SG II/1 has an interval of 2.5s TWTT with homogeneous wavy, continuous, medium amplitude reflectors that are parallel to the overlying SG SM 01. Seismic subunit SG II/2 has an interval of 1.5s TWTT with high amplitude, divergent, semi-continuous reflectors interspersed with chaotic patches. This unit becomes increasingly chaotic towards the base and particularly to the east, where its interval increases by 0.2s TWTT. At the base of SG II/2 reflectors onlap onto the underlying SG SM 02 towards the NE. It is of some significance that in one particular section of Line 4, a high amplitude, continuous, parallel triplet of reflectors approximately 0.05s thick can be seen (Fig. 5.10). The triplet mirrors the seabed trace and reflectors immediately beneath it have higher than average amplitudes, which fade with distance from this triplet. However the amplitude strength is possibly related to a bottom simulating reflector (BSR) imaged. Thus it is possible that the strength of the returned signal of this seismic reflector is not in fact lithological but instead related to the presence of methane gas hydrates.

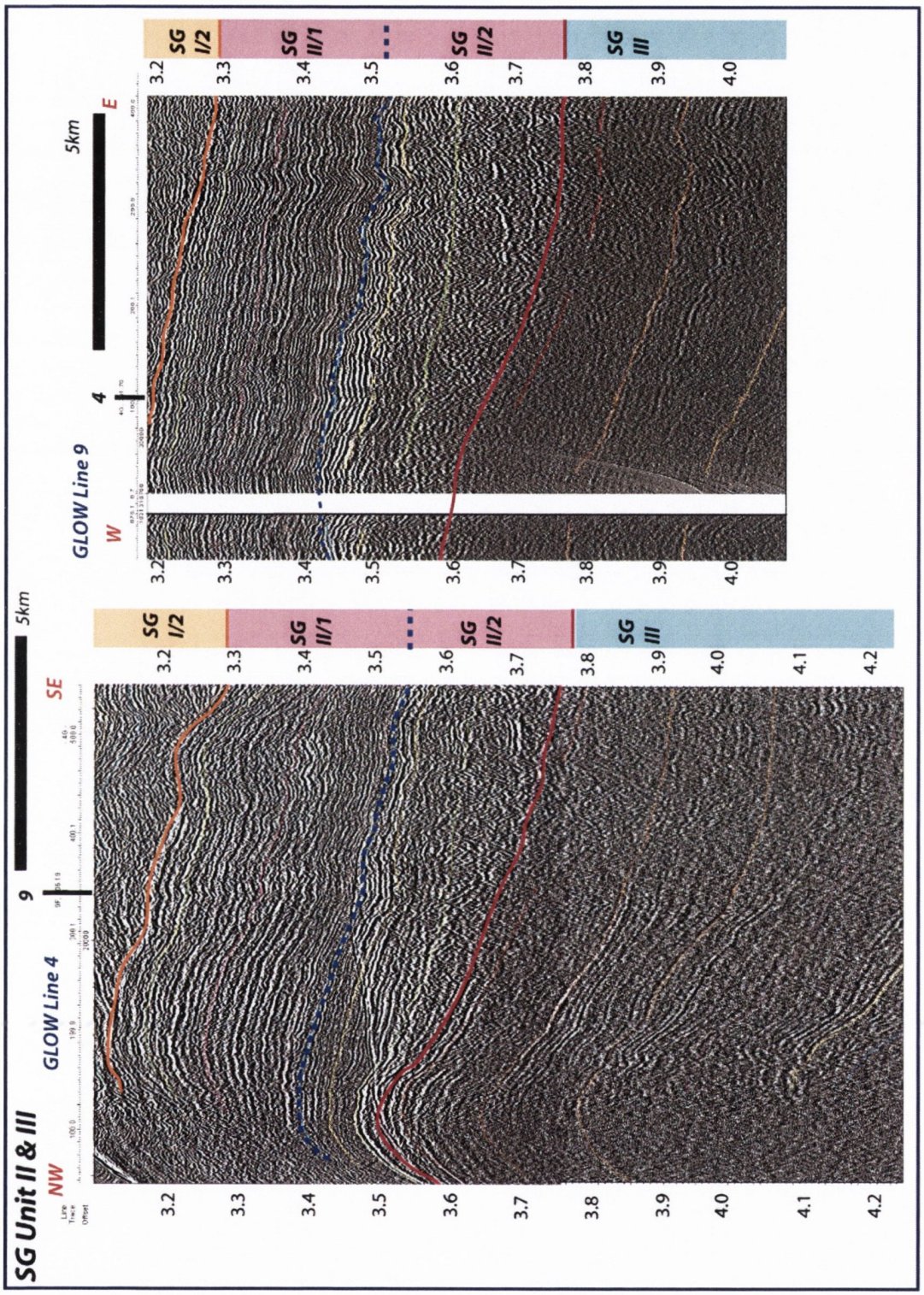

Figure 5.10: A compilation of the seismic characteristics of SeaGap Seismic Units II and III, separated by SG SM 02 (pink-purple).

5.3.4. SG SM 02

The horizon SG SM 02 is picked on a black continuous reflection (peak, positive reflection coefficient). The time map of surface SG SM 02 is shown in Fig (5.11) and it occurs between times 3.4s and 3.75s TWTT. Continuous and laterally traceable, this seismic marker is defined by the significant onlap of the overlying basal reflectors to the west of the SeaGap structure and the distinct change in seismic character from high amplitude, chaotic above to low amplitude, smooth, parallel reflectors below.

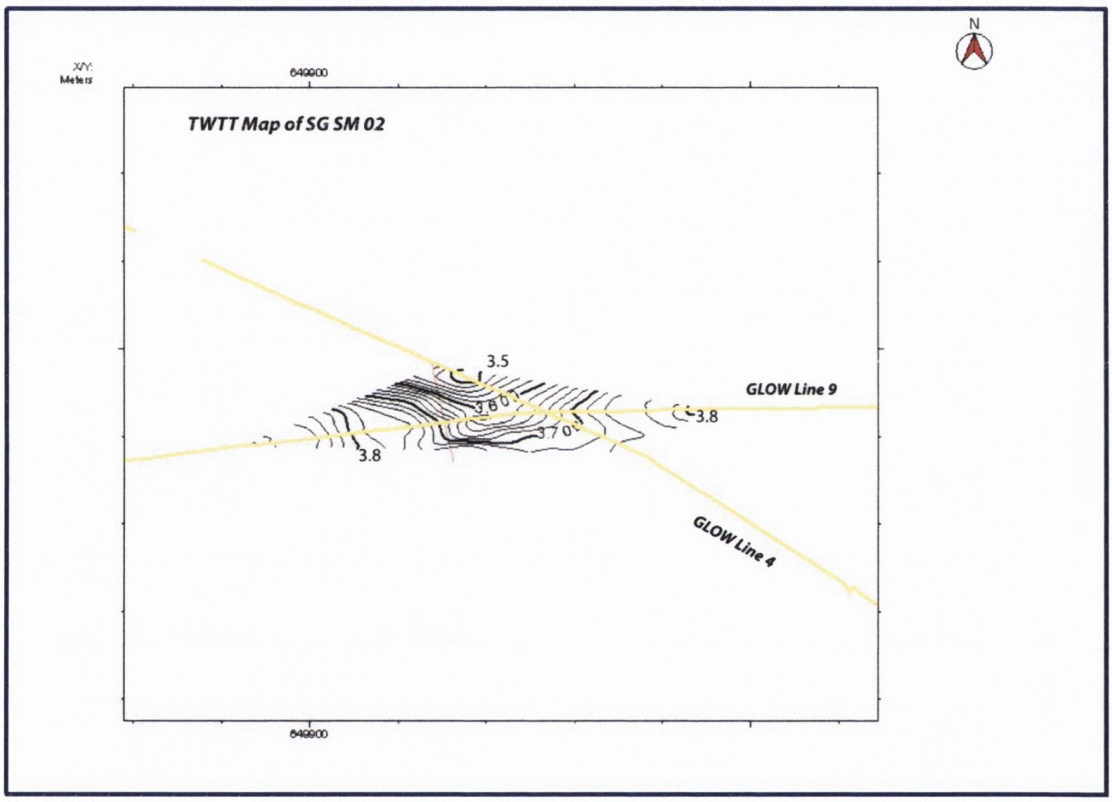

Figure 5.11: The TWTT map of seismic marker SG SM 02.

5.3.5. SG Unit III

SG Unit III is at least 0.9s TWTT thick (the base is not imaged). There is a distinct change in seismic reflection character above (chaotic) to below (parallel, continuous, smooth, low-med amplitude) (Fig. 5.10). Reflectors are slightly divergent towards the east with an internal geometry similar to clinoforms building out in a south-easterly direction. Alternatively they could be slightly wavy facies that laterally pinch out to the west. With decreasing amplitudes, the last imageable data is located at 4.7s TWTT.

5.3.6. SeaGap Summary Seismic Stratigraphy

A panel of both GLOW Lines 4 and 9 (Fig. 5.12) show the highlighted seismic markers while the seismic stratigraphic units are summarised in Fig. 5.13.

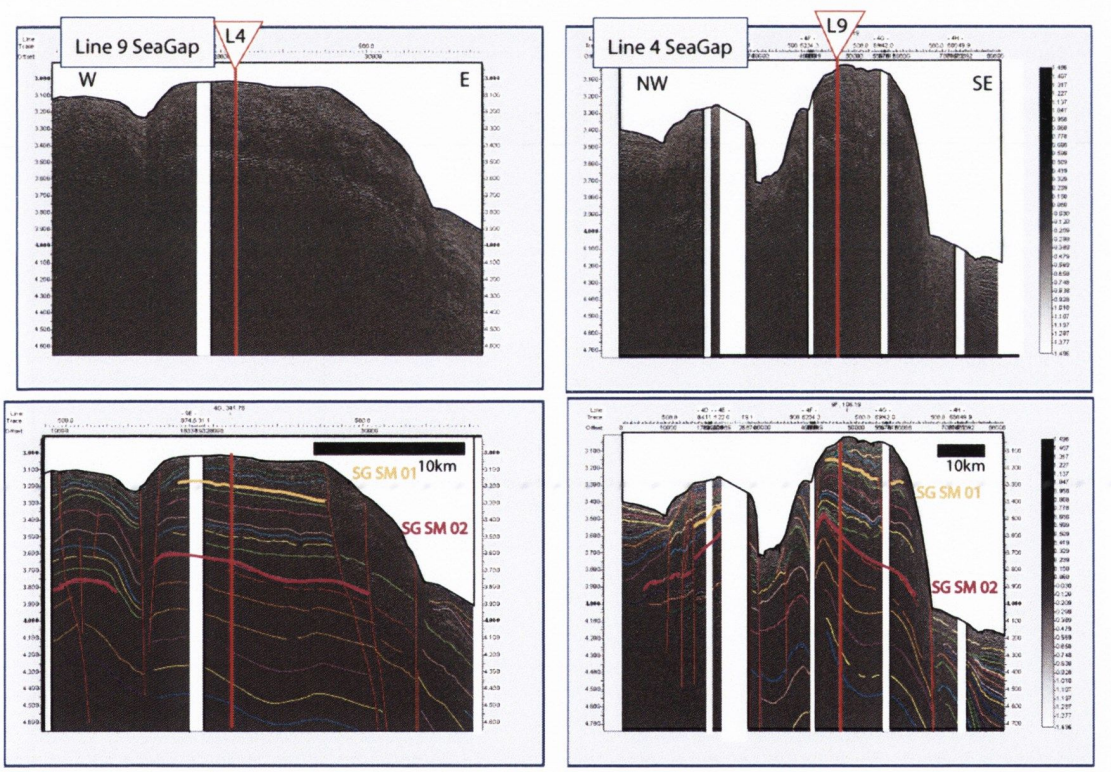

Figure 5.12: Interpreted sections of GLOW Line 4 and 9 that traverse the main bathymetric expression of the SeaGap Fracture Zone.

Figure 5.13: Summary of the seismic characteristics and features of The SeaGap Fracture Zone Zone stratigraphy.

The SeaGap Fracture Zone Extension to the South.

The stratigraphy established in this section for the SeaGap Fracture zone is largely specific to the section traversed by GLOW Line 4 and 9. Thus there is some surveying bias as there is not the same level of coverage across either the Kerimbas Basin or SeaGap Fracture Zone as there is across the Davie Ridge and DRIEZ areas. The SeaGap area is segmented into different fault bound slivers, each with varying complex seafloor morphologies and differing levels of displacement. This is discussed in more detail in Chapter 9. The SeaGap FZ is hypothesised as a partitioned strike slip fault zone. The area with the most obvious seafloor morphology and displacement on the bounding faults is that imaged by both GLOW Lines 4 and 9. There is some evidence however of similar fault activity further south, but this is technically offsetting the stratigraphy of the Kitunda Block area (Chapter 8). Thus establishing a stratigraphy for the entire SeaGap Fracture Zone is not possible, but the stratigraphy for the most bathymetrically prominent and possibly oldest section is established here. The SeaGap structural evolution shall be discussed in more detail in Chapter 9.

5.3.7. Sedimentological Interpretation of the SeaGap Seismic Facies.

During the time of deposition of SG Unit III, in the SeaGap Area, sediment accumulated through suspension settling and pelagic rain out. The sediment accumulation was relatively consistent with no major breaks in deposition. There was probably a low located to the eastern section of the area due to the divergent geometry of the reflectors in this direction.

SG seismic marker 02 marks a change in environment and a possible regressive event. At the base of SG Unit II/2 an influx of high energy, muddy internally chaotic facies overlies the homogeneous, condensed SG Unit III.

During the time of deposition of SG Unit II/2, the sediment reaching the area from the shelf was a quite inhomogeneous sand/mud mix with some erosion and redeposition occurring. Passing upwards, the sand content is increased This may indicate a continued decrease in sealevel and a subsequently more proximal location to the coastline and terrigenous material. SG II/1 has slightly wavy, continuous, medium-amplitude reflectors representing a deepening environment or reduction in sandy shelf material. The initiation of sediment waves may be related to a nearby channel, slope creation and/or intensification of bottom current activity. Overall, SG II records an initial influx of sandy material followed by a gradual reduction in energy and sandy content.

At the time of deposition of SG SM 01 the SeaGap Area had been tilted post depositon of SG II and there was a hiatus in deposition. As SG I/2 was deposited the SeaGap Area was probably located near the bottom currents that sweep the continental slope and contouritic sediment waves were formed climbing the slope towards the west. The sediment reaching the location from the shelf has a relatively high sand/mud ratio. Post SG I/2 deposition, the area experienced an increase in energy and the top of SG Unit I/2 was eroded. The base of SG I/1 truncated the underlying reflectors and a rubbly cap was deposited. Overall, SG I, represents a slope related contouritic facies, with a recent erosional and redepositional event.

5.4. *Correlating between the sedimentology of the Kerimbas Basin and the SeaGap Fracture Zone.*

Correlations between the stratigraphic schemes of the SeaGap Fracture Zone and the Kerimbas Basin are difficult due to the faulted contacts between the 'zones'. There is some similarity between the basal units imaged; SG III and KB II. Both units are interpreted as turbiditic facies. However these turbiditic splays are not necessarily age equivalent.

Both zones also display a similarity in interpreted contouritic deposits in the youngest units, SG I/2 and KB I/1. As discussed previously, contouritic deposits initiate when the bottom water circulation intensifies and/or there is a slope creation. As the sediment wave facies is not common throughout the packages seen here, it is possible that the first occurrence of contourites on both SeaGap and Kerimbas Basin are age equivalent. This could indicate significant uplift of the SeaGap structure since this time, if they were both deposited on the seafloor at the same time.

5.5. *Summary*

Interpretation of the GLOW seismic data that traverses the Kerimbas Basin and SeaGap Fracture Zone areas via the methods described in Chapter 3 led to the production of a seismic stratigraphic scheme for the Kerimbas Basin and SeaGap Areas.

In the Kerimbas Basin, two seismic units (KB I and II) and two seismic subunits (KB I/1 and I/2) are recognised. Lateral age equivalent channel facies are also recognised. The total sediment thickness imaged in the KB is approximately 1.5km using an average velocity of 1.74 km/s. A sedimentological interpretation of the seismic facies indicates a largely turbiditic dominated facies with concurrent subsidence to the east of the basin leading to a thickening sediment wedge towards the east and the onlap of KB I onto KB SM 01. Extensional faults active during deposition of KB I provided the accommodation space for channel development and the associated channel overspill and levee development.

In the SeaGap Fracture Zone area, clear structural control of the complex seafloor expression was identified and the stratigraphy was established for the segment imaged by both GLOW lines 4 and 9. Three seismic units (SG I, II and III) were recognised and subunits SG I/1, I/2, II/1 and II/2 were also recognised. The total sediment thickness imaged was approximately 1.3km. A sedimentological interpretation of the seismic facies indicated a uniform turbiditic environment (SG III) topped by an incursion of coarser material (base of SG II/2) which passes vertically upwards into a section with a higher sand/mud ratio (SG II/1). SG SM 01 marks the creation of inclined surface against which the SG I/2 sediments onlap in a sedimentary wave geometry. Uplift from the west occurs once more, with erosion to create the unconformable surface onto which the SG I/1 sediments onlap.

Correlation between the SG and KB facies based on sedimentological interpretations wasn't possible. However, it is hypothesised that SG III and KB II represent a similar

environment and that SG SM 02 and KB SM 01 represent the same coarsening up sequence. Sediment wave facies are evident on KB II, KB I and SG I. If these similar seismic facies are age equivalent, that indicates major uplift of the SG relative to the KB since the deposition of SGSM01, providing the first evidence of fault activity. The top of the SeaGap segment imaged by GLOW Lines 4 and 9 is approximately 950m above the seafloor of the Kerimbas Basin.

6. The Stratigraphy of Offshore Southern Coastal Tanzania-Incorporating Pre-Existing Data and New Biostratigraphic Controls.

6.1. Introduction

As there are no exploratory wells drilled on the south Tanzanian margin, assigning ages to seismic markers involved incorporating a wide array of data; onshore outcrop and shallow boreholes, academic and industry seismic surveys, deep coastal boreholes with proven biostratigraphy and a box and piston coring campaign during the GLOW cruise which targeted outcropping reflectors. No single line of evidence was definitive; therefore, a rigorous analysis was undertaken of all available data.

In this chapter, wells, well ties to surveys, survey intersections with GLOW and GLOW box core data will be discussed in turn. As the GLOW seismic stratigraphy of the Davie Ridge, Davie Ridge Inner Extensional Zone, Kerimbas Basin and SeaGap Fracture Zone are described in Chapters 4 and 5, this chapter results in ages being ascribed to the various seismic stratigraphic schemes. Synthesising all of the above data, a summary GLOW seismic stratigraphy was constructed (See Summary Fig. 6.38). Furthermore, correlations between onshore and offshore geology including the land to ocean transition zone are assessed in both Chapter 7 and 8 to complete this summary chronostratigraphic synthesis (See end of Chapter 8).

The results of Chapter 7 and 8 enabled a detailed geological, chronostratigraphic and sedimentological evolution of the study area to be proposed in Chapter 11.

6.2. *The Deep Offshore GLOW Seismic Stratigraphic Scheme*

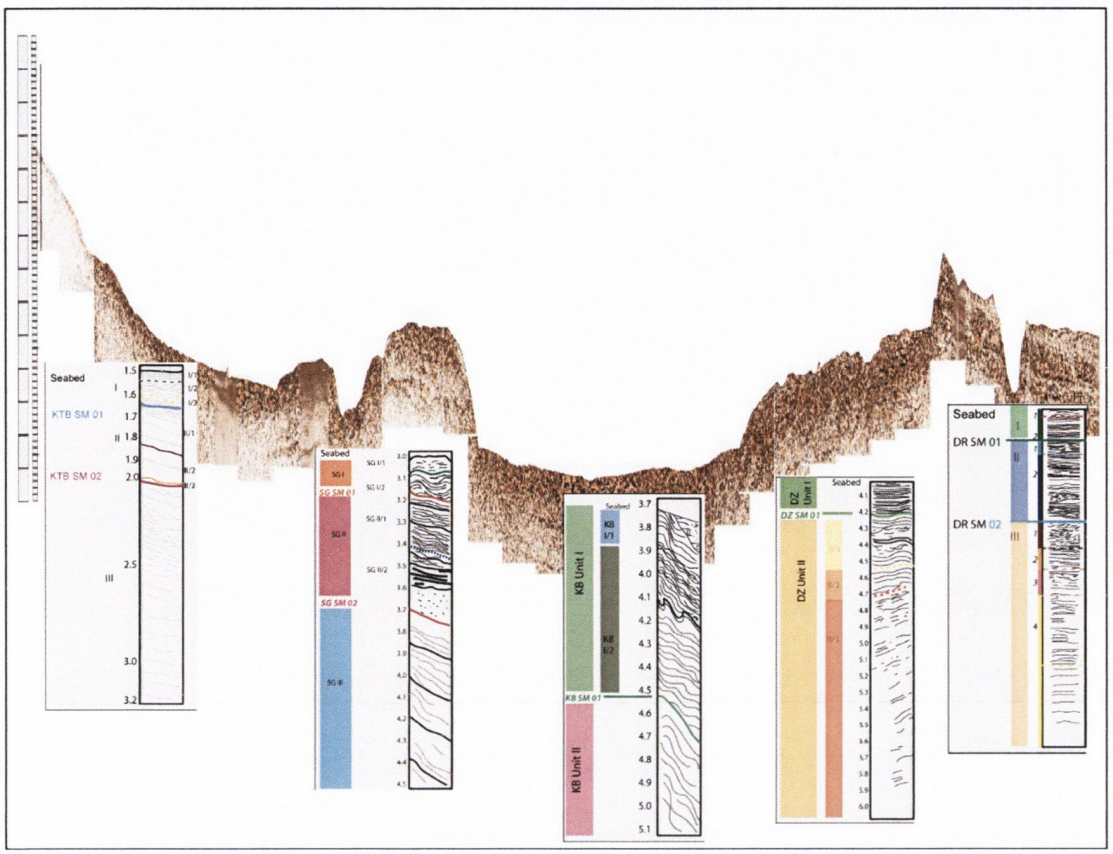

Figure 6.1: An illustration of the GLOW seismic stratigraphy erected for each 'structural zone'. The line shown is GLOW Line 4, which running NW-SE, traverses all of the zones except the Kitunda Block.

In the previous two chapters the seismic stratigraphy and interpretations of the sedimentological evolution of the deep offshore GLOW 'Zones' were presented; Davie Ridge, Davie Ridge Inner Extensional Zone, Kerimbas Basin and SeaGap Fracture Zone. Tentative correlations were attempted based on the sedimentology and depositional environment inferred. In Fig. 6.1 the schematic seismic stratigraphy summaries are compiled along GLOW Line 4, which traverses the study area from NW to SE, and in turn the four structural 'zones' discussed in Chapters 4 and 5. In this chapter, by incorporating pre-existing data, as illustrated schematically in Fig. 6.2, ages are assigned to these GLOW Seismic Units and seismic markers.

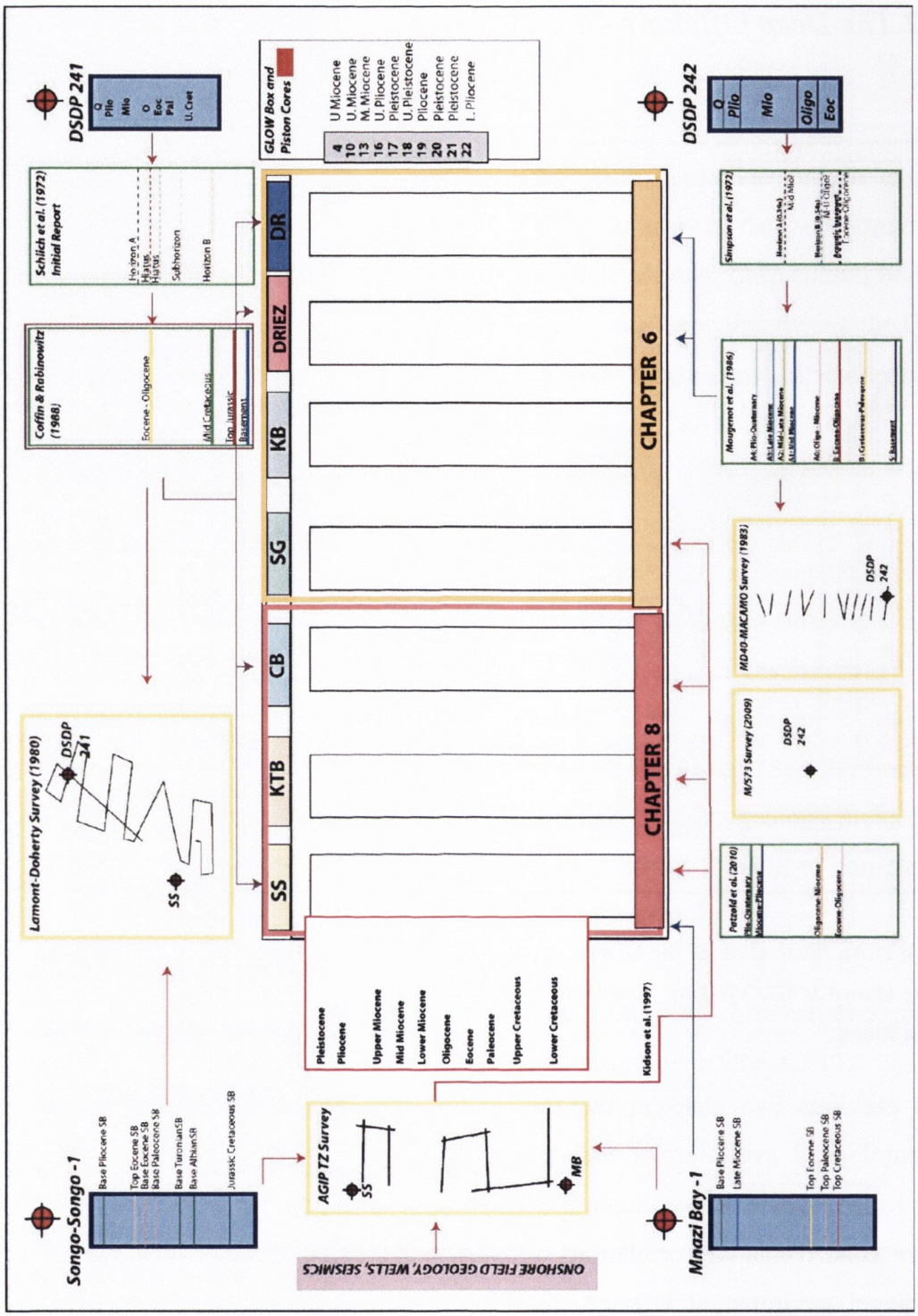

Figure 6.2: Schematic diagram of the data available for this study. The orange and pink columns willl be filled in by the end of chapters 6 and 8. Wells (DSDP 241, 242, Mnazi Bay-1 and Songo-Songo-1(shown in blue boxes); pre-existing seismic data (yellow boxes) and the associated seismic markers (grey boxes) from published data are correlated to the seismic stratigraphy as defined in Chapters 4,5,8.

No exploratory wells exist in southern offshore Tanzania. The nearest wells with proven stratigraphic control can be thought of in three categories; onshore, coastal (Mnazi Bay-1 and Songo-Songo-1) and deep offshore (DSDP 242). (Fig. 6.3). DSDP 241 is located 400km north of the study area and cannot be shown on the Fig. 6.3 but is shown on Fig. 6.5.

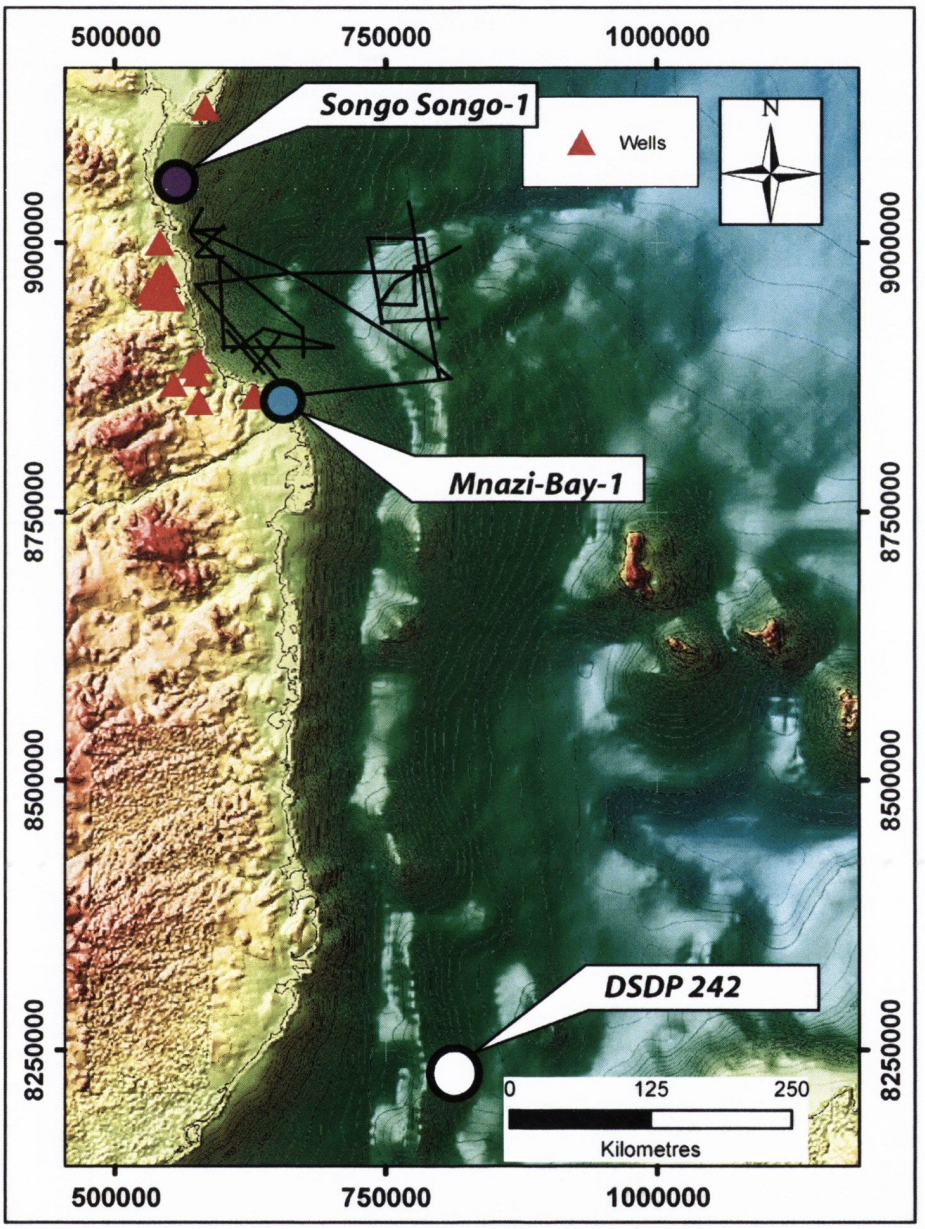

Figure 6.3: The GLOW Survey Area with nearby wells highlighted. Coastal wells Mnazi Bay 1, Songo Songo-1 and offshore DSDP 242 on the Davie Ridge in the Mozambique Channel is shown. Site 242 offshore Kenya is located 400km north and not shown on this scale

Onshore Tanzania there are over 20 deep boreholes drilled with proven stratigraphy and a dense network of industry seismics, extending to the coastal area. Coastal wells, located less than 25 metres above sea level, include Mnazi Bay-1 and the Songo-Songo wells and are located to the south and north of the survey areas respectively. DSDP Sites 241 and 242 were drilled on Leg 25 (1972) on the Kenyan margin and Davie Ridge in the Mozambique Channel. While located a considerable distance from the survey area (~ 600km), major regional surveys cross these wells, traversing the East African margin and eventually intersecting the GLOW survey area, enabling ties to be made.

6.2.1. Coastal Wells

Mnazi Bay -1

Mnazi-Bay 1 is located on the Tanzanian coast, just north of the River Ruvuma and the Mozambican border (Fig.6.3). Located at the site is a producing gas field, the trap formed by a rollover syncline of interbedded clays and sands overlain by a seal of clays. Several key bounding surfaces were identified within the 3.85km deep Mnazi-Bay 1 borehole; Base Pliocene SB, Late Miocene SB, Top Eocene SB, Top Paleocene SB and Top Cretaceous SB (Completion Log) (Fig.6.4). GLOW Lines 7 and 8 approach to less than 10km from Mnazi Bay.

Songo Songo 1

Songo-Songo-1 is located within the Tanzanian Coastal Basin, just north of the survey area (Fig. 6.3). This basin was formed due to Neogene normal faulting approximately parallel to the coast, thus creating a depocentre. Many key bounding surfaces were identified within the 4.42km deep Songo-Songo 1 borehole; Base Pliocene SB, Late Miocene SB, Top Eocene SB, Top Paleocene, Top Cretaceous SB and Jurassic/Cretaceous SB (Fig. 6.4). Songo-Songo-1 is located less than 30km from LD 98 and TZ- Lines 6 and 7 which in turn intersect with the GLOW Survey.

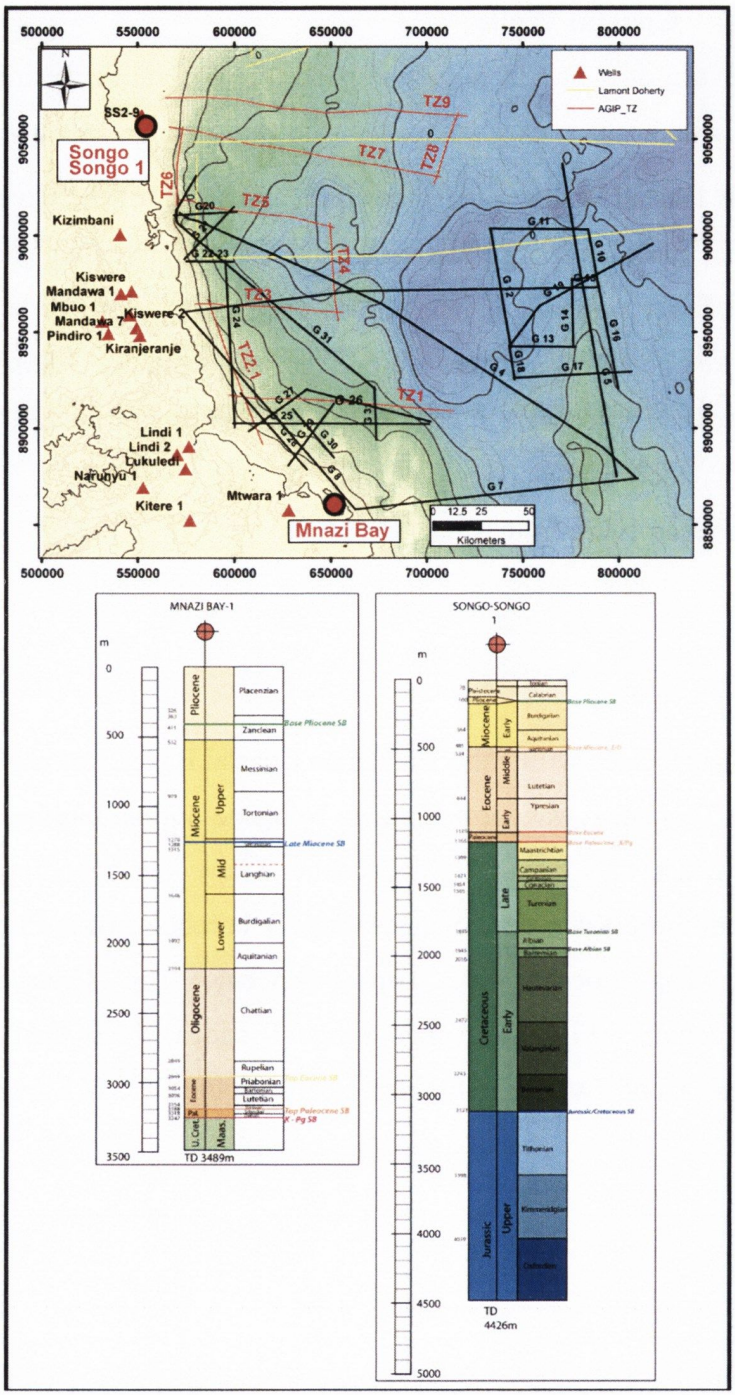

Figure 6.4: Coastal wells Songo-Songo 1 and Mnazi Bay 1. Located less than 25m above sea level, Mnazi Bay-1 is less than 10km from GLOW Lines 7 and 8, while Songo-Songo-1 is located less than 30km from the Lamont Doherty (yellow) and AGIP-TZ (red) surveys which in turn intersect with the GLOW seismic survey. Sedimentary logs (Completion reports reference) with principal sequence boundaries highlighted.

6.2.2. Offshore Wells

DSDP 241

DSDP 241 was drilled during DSDP Leg 25 offshore the Kenyan margin (Fig.6. 5) in 1972 (Schlich *et al.* 1974). Located at 2° 22.24'S, 44° 40.77'E, it was drilled in a water depth of 4,054m. Quaternary to Early Turonian sediments at 1,174m were recovered (Schlich *et al.* 1974). The primary objectives were to; 1) determine the stratigraphic succession in order to identify seismic layers, composition and age; b) sample and date the seismic horizon at 1.2s TWTT seen on Gallieni 4 Cruise (1970) for possible correlation to onshore geology and c) establish any evidence available to deduce possible palaeopositions of Madagascar.

The shipboard party (Schlich *et al.* 1974) documented several well-defined reflectors (Fig. 6.5). Horizon A at 0.5s TWTT, a subhorizon (unnamed) at 1.0s TWTT and Horizon B at 1.2s TWTT. Above Horizon A, lithological Unit I comprises greenish clay – nano ooze with minor clays. Horizon A marks the upper limit of silt and a marked increase in sonic velocity from 1.64km/s to 1.73km/s. The strong reflector at the subhorizon (1s TWTT) corresponds to the appearance of calcareous sandstones and calcarenites (at 835-844m) within lithological Unit II. Unit II is composed primarily of claystones, silty clay and calcareous sandstone. Horizon B at 1.2s TWTT is the top and most persistent of a series of strong reflectors that extend to about 3.0s. These reflectors are possibly due to the changes in composition and degree of lithification (Schlich *et al.* 1974).

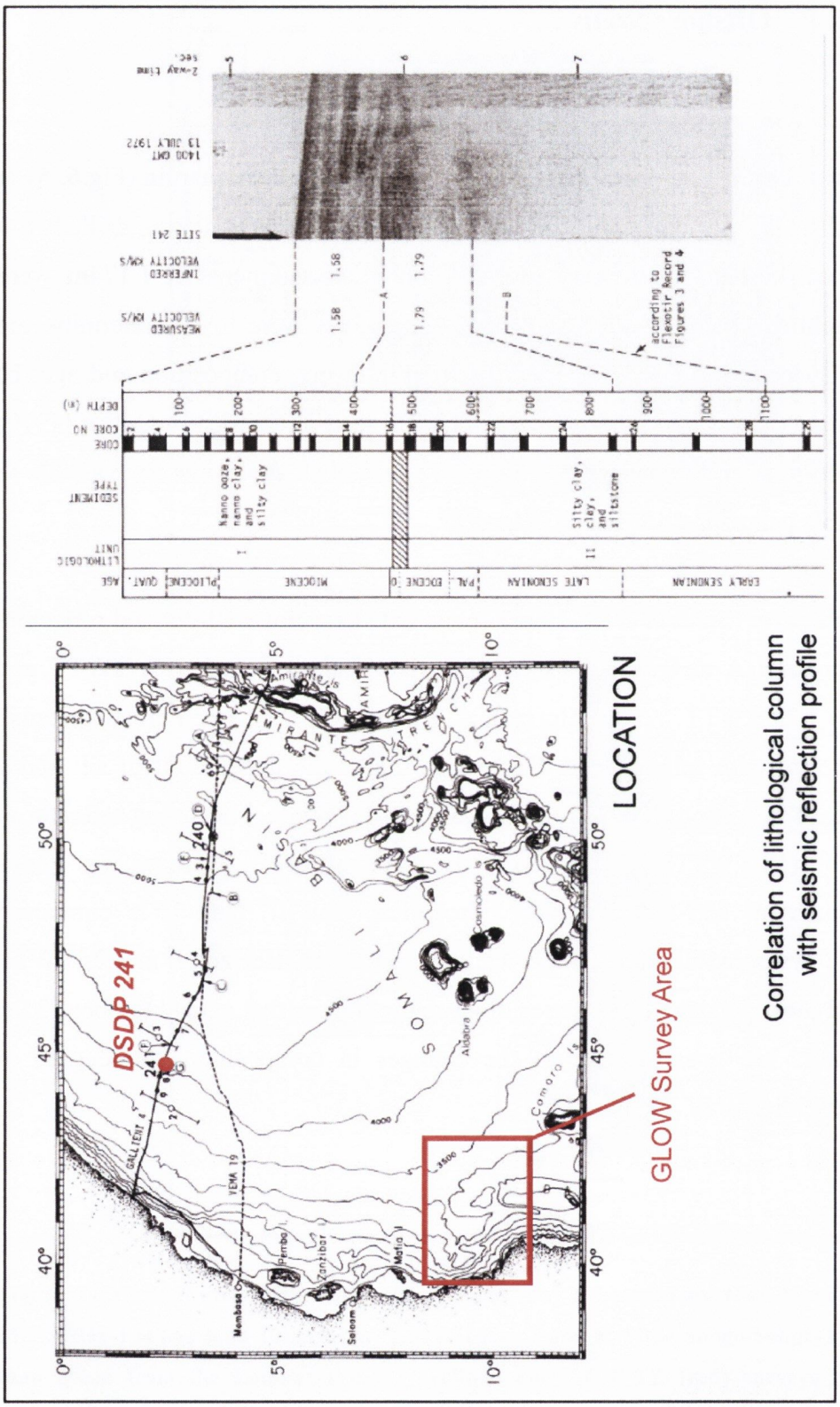

Figure 6.5: The location of DSDP Site 241 offshore Kenya and the accompanying correlation to seismic reflection profiles (Schlich *et al.* 1974).The location of the GLOW survey relative to DSDP 241 is highlighted.

DSDP 242

DSDP 242 was drilled during DSDP Leg 25 on the Davie Ridge in the Mozambique Channel in 1972 (Fig.6.6). Located at 15 50.65'S, 41 49.23'E, it was drilled in water depth of 2275m, penetrating Upper Eocene chalk at its total depth of 676m bsf (Simpson *et al.* 1972). The primary objectives were to; (a) sample, identify and date the ridge basement, (b) establish a stratigraphy for the presumably pelagic sediment cover and (c) determine the structural nature of the Davie Ridge and hence the palaeopositions during the separation of Madagascar from East Africa.

The Shipboard Party documented the consistency throughout the lithological column of nanno-oozes. The seismic stratigraphy was largely composed of a 0.75s TWTT thick semi-acoustically transparent layer overlyinge 'acoustic basement' is somewhat disingenuous however, as crystalline basement was not reached. The reflectors sampled do not correspond to any obvious lithological or stratigraphic change but to sharp variations in physical properties, such as a change in carbonate comensation depth (CCD). Simpson *et al.* (1972) tentatively correlated the reflector at 0.54s to the break in lithology between Units I and II and the acoustic basement to a lateral equivalent of basement.

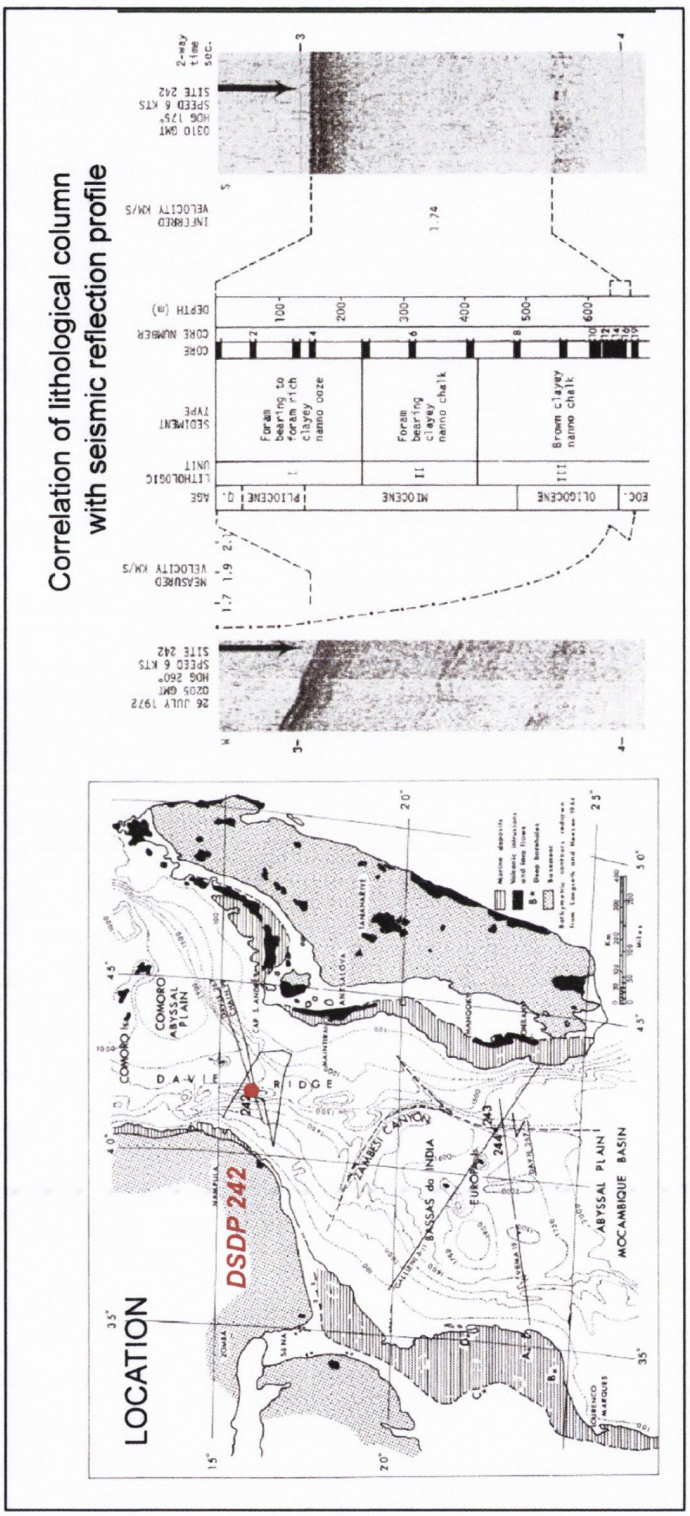

Figure 6.6: Location of DSDP 242 in the Mozambique Channel. The correlation between the lithological column and the seismic reflection profile is shown. (Simpson *et al.* 1972).

6.3.Pre-Existing Seismic Surveys

6.3.1. Lamont-Doherty Survey (1980) Coffin *et al.* (1988)

From November 1980 to January 1981, R/V Vema cruises 3618 and 3619 studied the East African margin and evolution of the Western Somali Basin. Seismic lines V3618 LD 81 and 84 were shot over DSDP Site 241 to aid with the seismic stratigraphic correlations (Fig. 6.7) of LD (79-103) (Shipley *et al.* 2005).. Extending from southern Somalia to southern Tanzania this survey is the principal reference for studies of the East African margin. Seismic data was obtained from the University of Texas (Shipley *et al.* 2005)

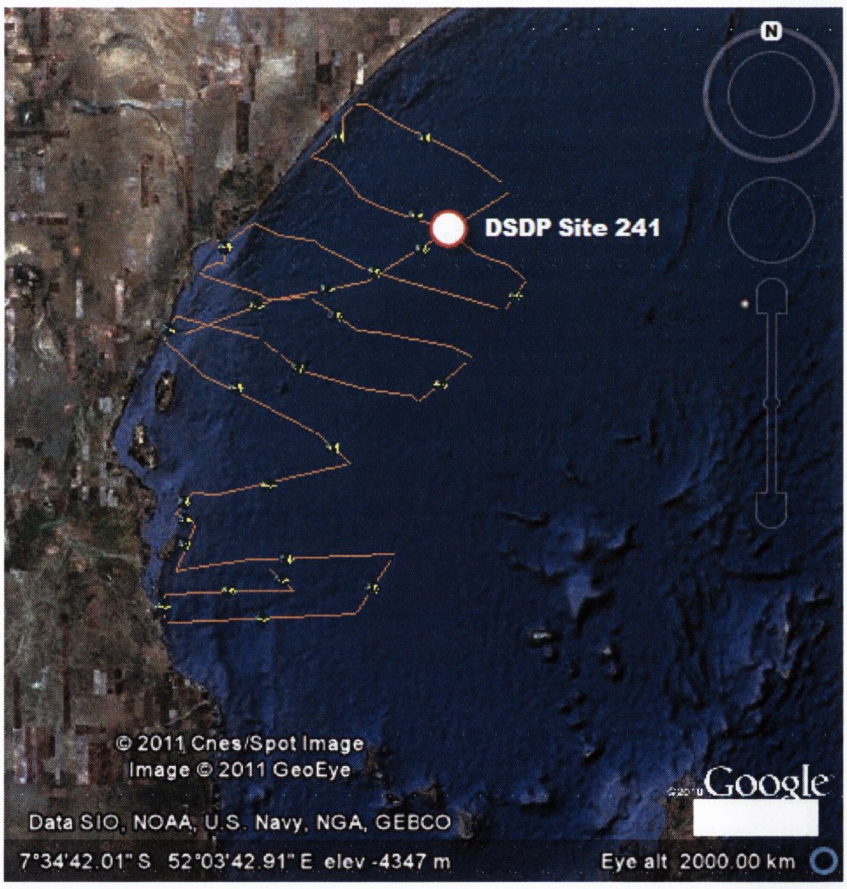

Figure 6.7: Location of the V3618 Lamont-Doherty Lines extending from southern Somalia to southern Tanzania. (Shipley *et al.* 2005) DSDP Site 241 is highlighted.

6.3.2. TZ-AGIP Phillips Survey (1976)

In September 1976, the Phillips Petroleum Company contracted AGIP and Seagap contractors to survey the shallow offshore to offshore area of Tanzania (Fig. 6.8) (Kidson *et al.* 1997). Nine profiles (labelled TZ-1 to 9) were obtained from the offices of TPDC in Dar es Salaam in paper format. Partly previously published in Kidson *et al.* (1997), the regional scale dip and strike lines reach up to 7s TWTT and are between 50 and 150km long. They extend from the shelf to the SeaGap Fracture Zone area (Fig. 6.8).

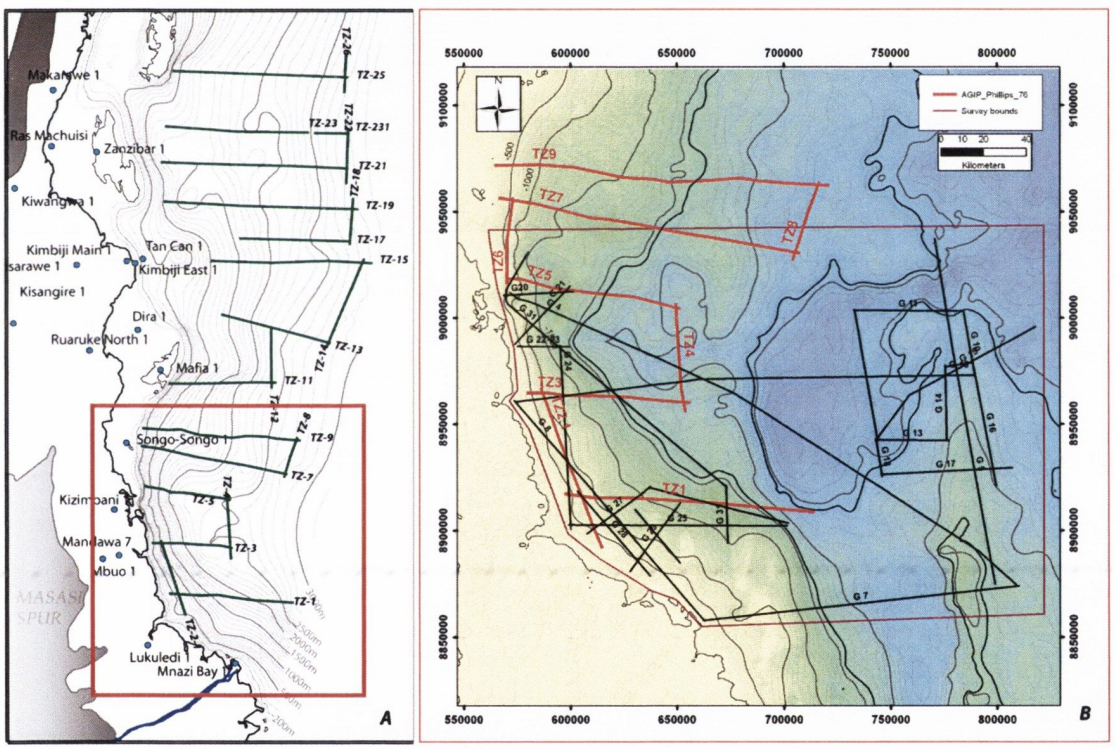

Figure 6.8: The AGIP-Phillips-TZ Survey Lines; (a) in total extending along the Tanzanian coast and b) the TZ-lines used in this study that intersect with GLOW survey and LD Lines. Location is highlighted on inset Fig. (a).

6.3.3. MACAMO-MD40 Survey (1983) Mougenot *et al.* (1986)

In June 1984, 7500km of single channel seismic data was obtained within the Mozambique Channel (Fig. 6.9), primarily surveying the Davie Ridge. The results were published in Mougenot *et al.* (1986) and Mascle & Blarez, (1987). The survey traversed the DSDP Site 242 and subsequently intersects with the GLOW survey area to the north.

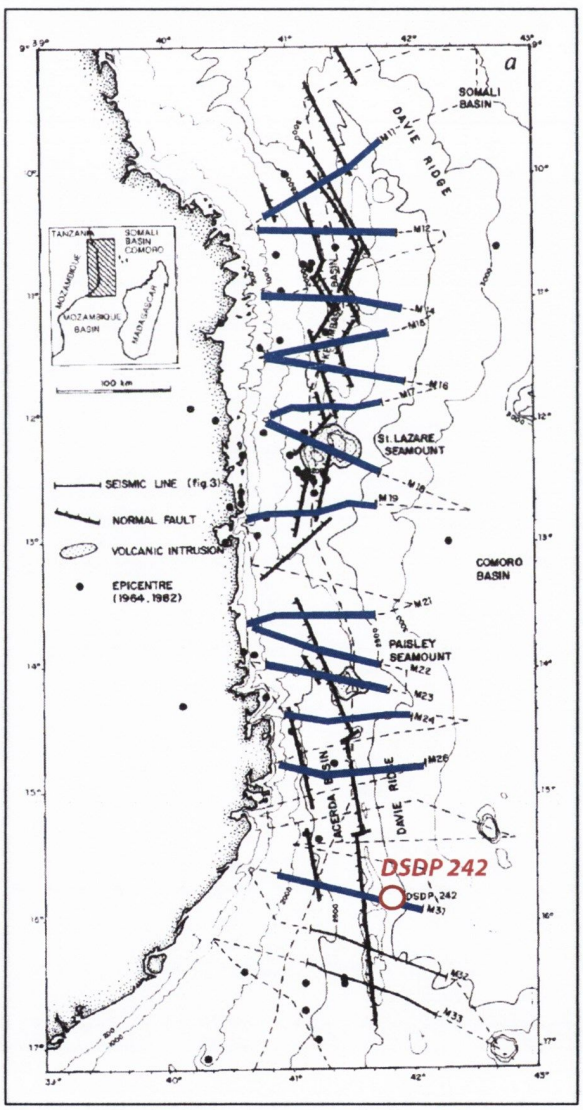

Figure 6.9: The 2-D seismic lines surveyed in MD40-MACAMO published in Mougenot *et al.* (1986). Site 242 is highlighted.

6.4. Correlating coastal wells to the GLOW, LD and TZ-AGIP Surveys.

6.4.1. Mnazi Bay-1 to GLOW 7 and 8.

Mnazi Bay-1 is located 10km and 8km from GLOW Lines 7 and 8 respectively (Fig. 6.4). Although the GLOW lines were shot in very shallow water, with multiples obscuring data beneath 0.8sTWTT closest the coast, some extrapolation of the sequence boundaries can be made (Fig. 6.10). The Base Pliocene and Mid-Late Miocene Sequence Boundaries can be extended onto both GLOW Lines 7 and 8, while the Mid-Late Miocene and Base Miocene SBs may be extended by eye, assuming regular geological contacts in the non-seismic data zone (with inherent error in this method) into the dip GLOW Line 7.

As the stratigraphy from the shallow shelf is poorly imaged, these ages do not necessarily correlate to any particular seismic units or markers. Rather they may be taken as a guideline to the depth of age boundaries in the GLOW Lines 7 and 8. Subsequently, these results are incorporated when the onshore to offshore transition zone correlations are made in Chapter 8.

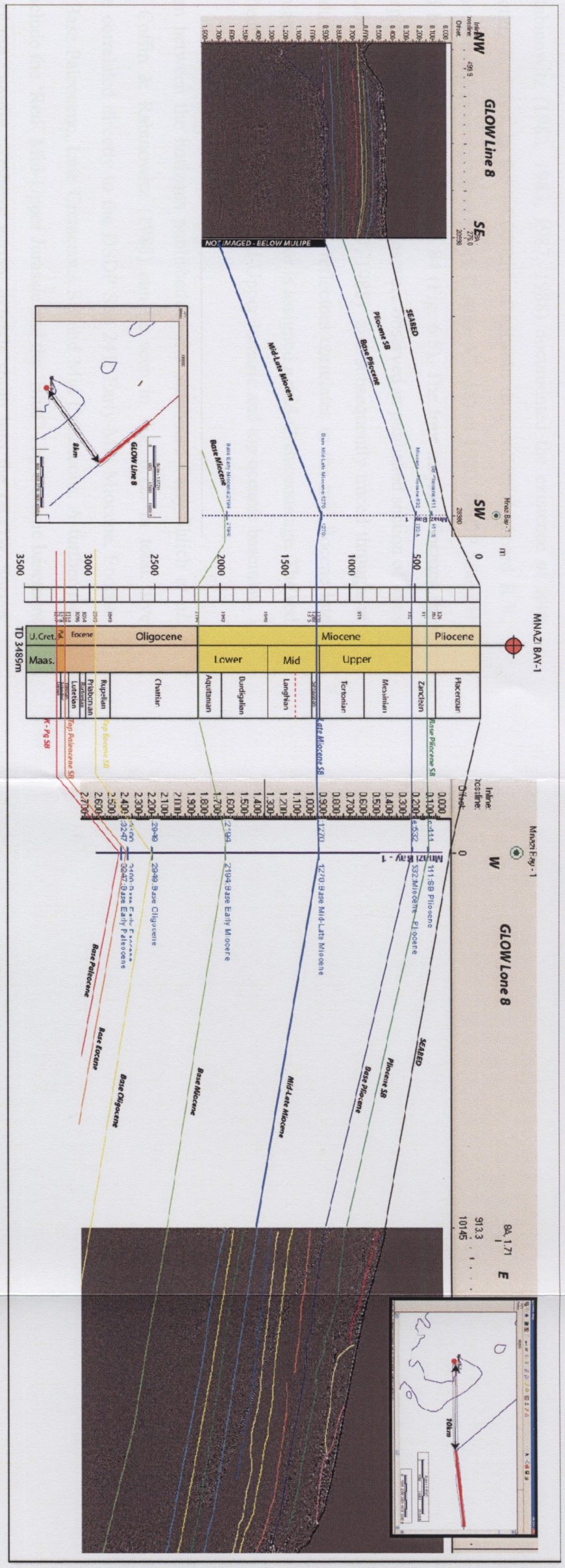

Figure 6.10: Guideline correlations of sequence boundaries in the Mnazi Bay-1 well with nearby GLOW Lines 8 and 7. Locations inset.

6.5. *Uninterpreted and Interpreted Pre-Existing data*

6.5.1. DSDP 241 – Lamont Doherty (& Songo Songo-1)

Coffin & Rabinowitz (1982, 1983, 1987, 1988) documented the existence of four major reflecting horizons in the ~6,000km of seismic data collected aboard R.V. Vema by the Lamont-Doherty Observatory (Cruise V3618) in 1980. DSDP Site 241 was crossed by survey lines LD 81 and 84 (Fig. 6.5). The four major reflectors, the 'green', 'purple', 'red' and 'blue' horizons were observed in published section of lines Coffin & Rabinowitz (1982, 1983, 1987, 1988) and subsequently traced throughout the survey during this study .The green reflectors correlates to the mid Eocene-late Oligocene hiatus, while the purple reflector is assigned a mid-Cretaceous age. The red and blue reflectors are assigned to the Mid-Upper Jurassic and top oceanic basement.

A correlation between the horizons published by the Shipboard Party-Shlich *et al.* (1972) and Coffin & Rabinowitz (1988) can be seen in Fig. 6.12. In total, five horizons are correlated directly to the DSDP Site 241; Early-Mid Miocene, Eocene-Oligocene, Base Paleocene, Late Cretaceous SB and Mid Cretaceous. A further two reflectors include the 'Red' Mid-Upper Jurassic and the 'Blue' Top Oceanic basement reflectors. As the Lamont –Doherty survey extends south into the GLOW Survey Area, these horizons can be extrapolated to the GLOW Lines.

A compilation of west-east profiles and north-south profiles of the Lamont-Doherty Cruise (Coffin & Rabinowitz 1988) is shown in Figures 6.13 and 6.14. Interpretations are based on those published by Coffin & Rabonowitz (1988) and incorporating the correlation of Songo-Songo 1 to LD 101 and 102 .LD Lines 98, 99, 100, 101, 102 and 103 traverse the Tanzanian margin, surveying the shelf, slope, SeaGap Fracture Zone, Kerimbas Basin, Davie Ridge and east of the Davie Ridge.

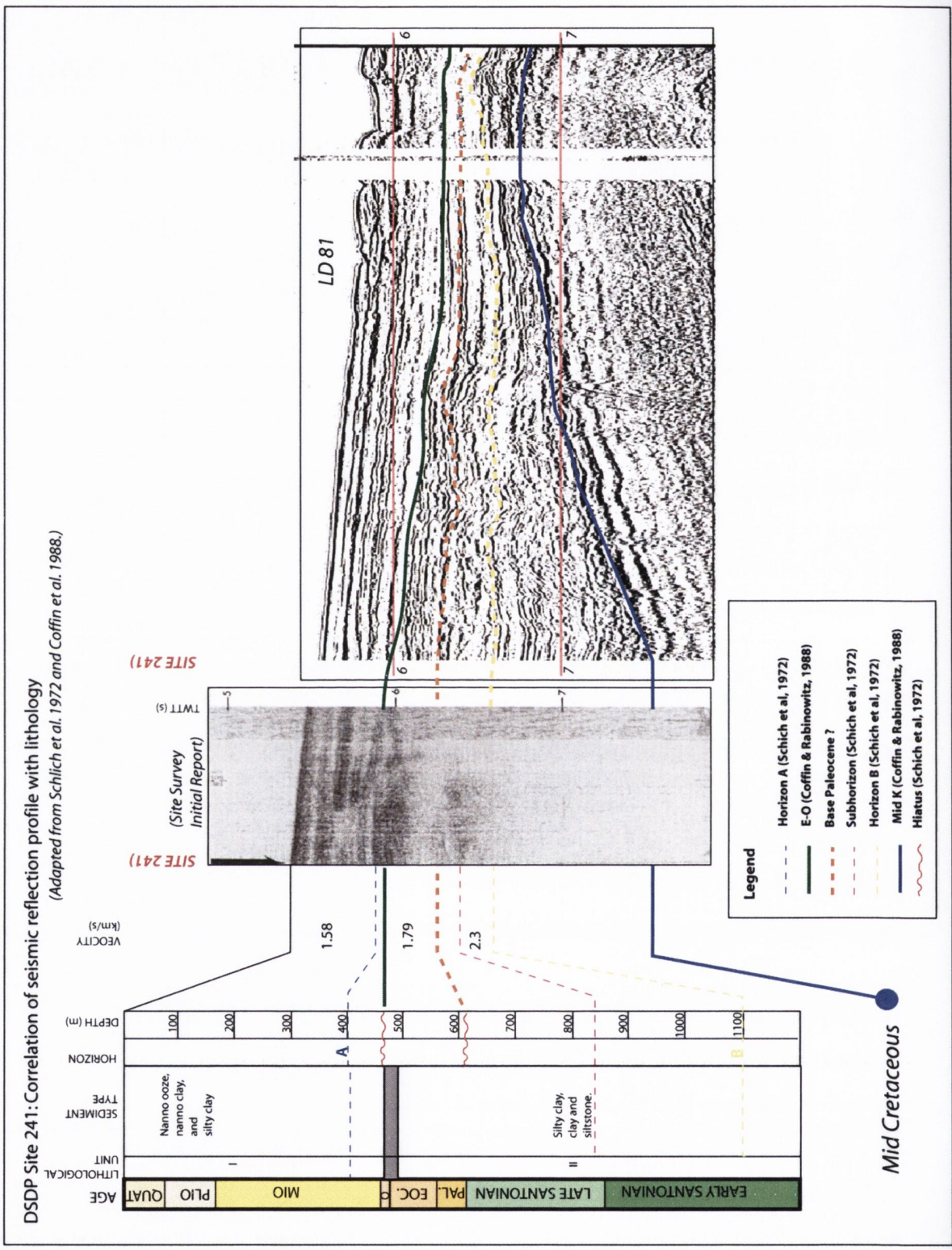

Figure 6.12: Correlating the stratigraphic column of DSDP Site 241 with the seismic reflection profile of Lamont-Doherty Line 81. Adapted from Schlich *et al* (1972) and Coffin & Rabonowitz (1988).

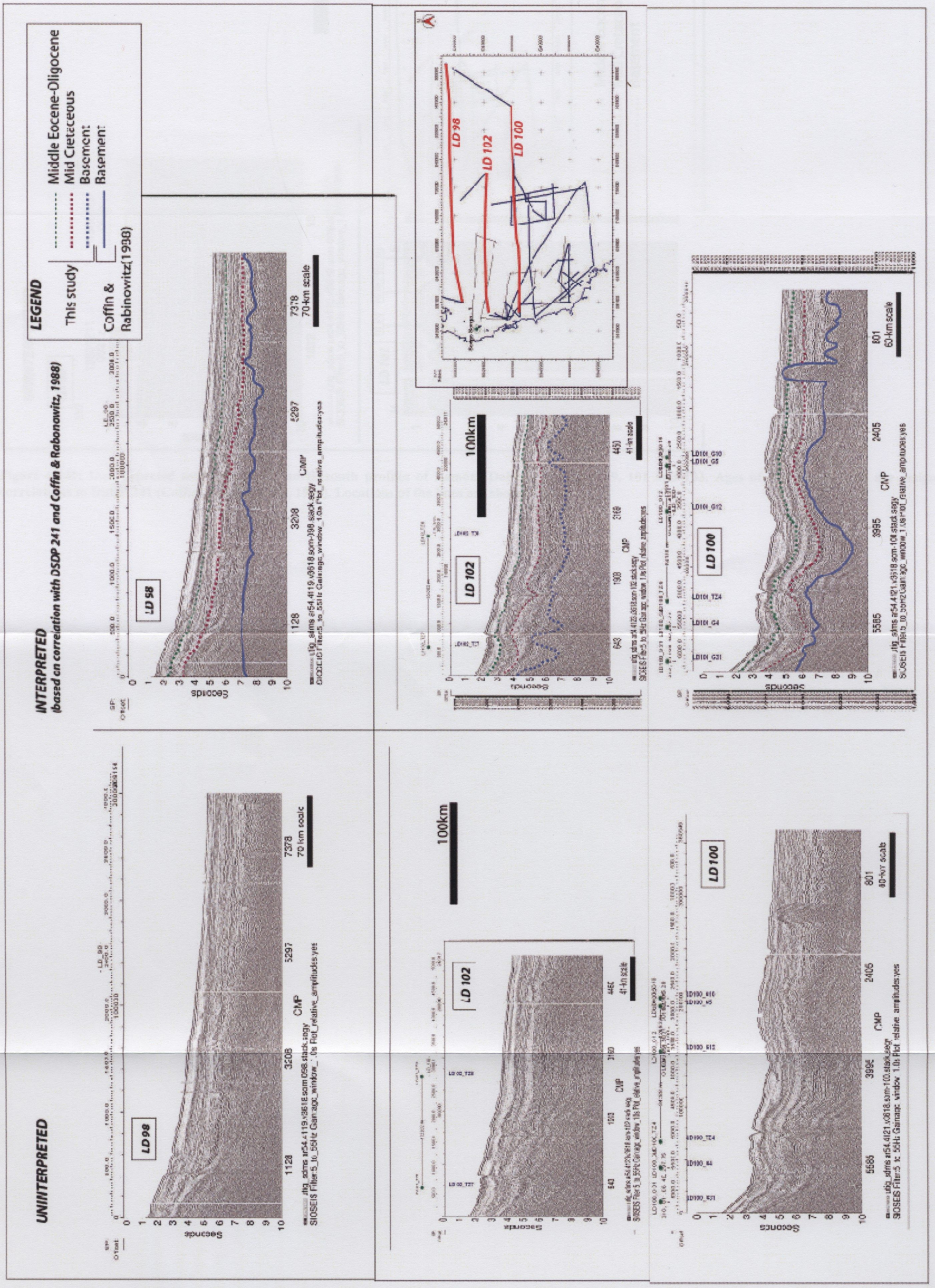

Figure 6.13: Uninterpreted and Interpreted west to east profiles of Lamont-Doherty lines LD 98, 101 and 102. Ages of seismic markers are assigned from correlations to DSDP 241 (Coffin & Rabinowitz, 1988). Locations of the lines are shown inset.

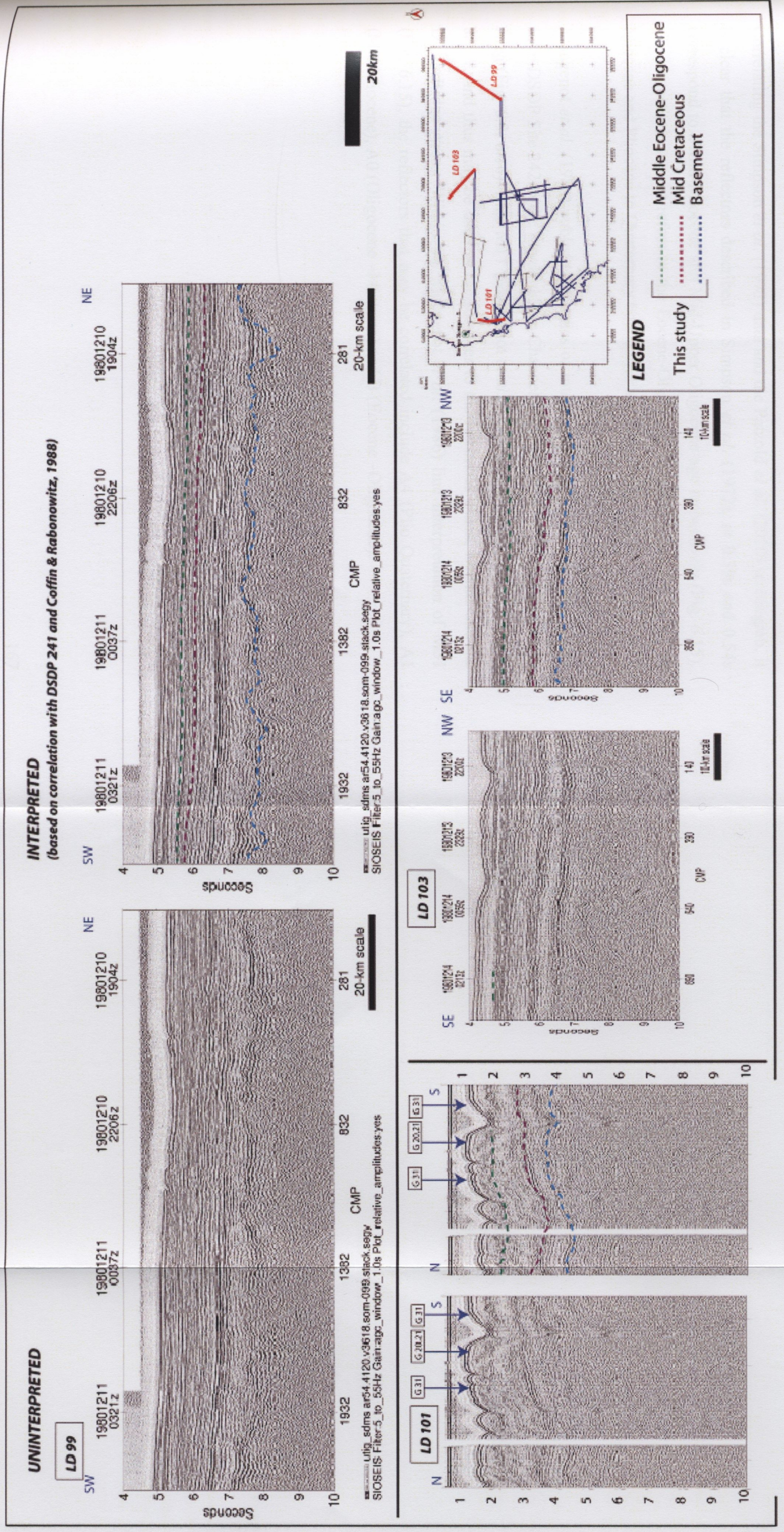

Figure 6.141: Uninterpreted and interpreted north south profiles of Lamont Doherty lines LD 99, 101 and 103. Ages of seismic markers are assigned from correlations to DSDP 241 (Coffin & Rabinowitz, 1988). Locations of the lines are shown inset.

6.5.2. DSDP 242 – Mougenot *et al.* (1986)

DSDP Site 242 was traversed by at least two academic surveys; the MD4-MACAMO cruise (1983) and the M/573-Bremen survey (2009). A screengrab from a DSDP 242 crossing line of M/573 (Patzold *et al.* 2010) displays a similar stratigraphy to that of the initial Site 242 report (Simpson *et al.* 1972) (Fig. 6.15), in which four seismic horizons marking key chronostratigraphic boundaries are identified; Pliocene to Quaternary (Green), Miocene to Pliocene (Orange), Oligocene-Miocene (Dark blue) and Eocene-Oligocene (pink).

Correlating the Simpson *et al.* (1972) data and the Patzold *et al.* (2010) screengrab, it is clear that the reflectors described in Simpson *et al.* (1972), at 0.39s and 0.54s correspond to a Mid-Miocene and Mid-Upper Oligocene age respectively (Fig. 6.15). The acoustic basement refers to the Eocene-Oligocene boundary. The Oligocene to Miocene and Pliocene to Quaternary boundaries are also established.

Mougenot *et al.* (1986) published a series of interpreted seismic profiles that extend from DSDP Site 242 in the Mozambique Channel, northwards into the GLOW Survey Area (Fig. 6.9; 6.16). Line M11 (Mougenot *et al.* 1986) intersects GLOW Lines 4, 5, and 7, and thus may be used to ascribe ages to the Kerimbas Basin, DRIEZ and the Davie Ridge Areas. Within the Mougenot *et al.* (1986) line interpretation of M31 (Fig. 6.15), the reflectors that may be correlated include A4 (Plio Quaternary), A1 (Mid Miocene), A0 (Oligocene –Miocene) and B (Eocene –Oligocene).

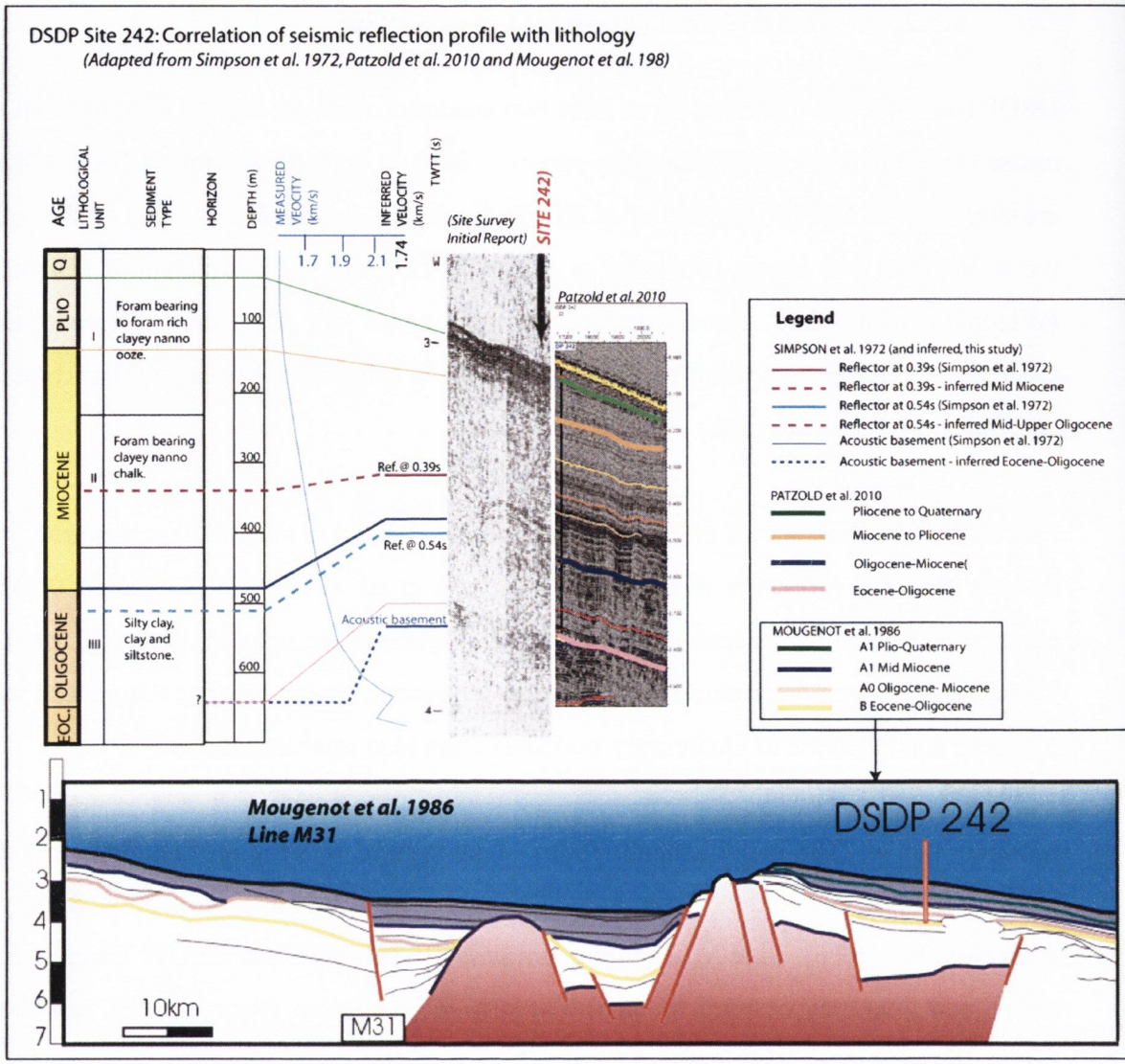

Figure 6.15: Correlating between the biostratigraphic and chronostratigraphic controls of DSDP Site 242 and intersecting seismic data (Schlich *et al.* 1972; Patzold *et al.* 2010; and Mougenot *et al.* 1986). Shown below is an adapted interpretation of Line M31 of the MD40-MACAMO survey which traversed DSDP 242 and the interpreted ages of reflectors (adapted from Mougenot *et al.* 1986).

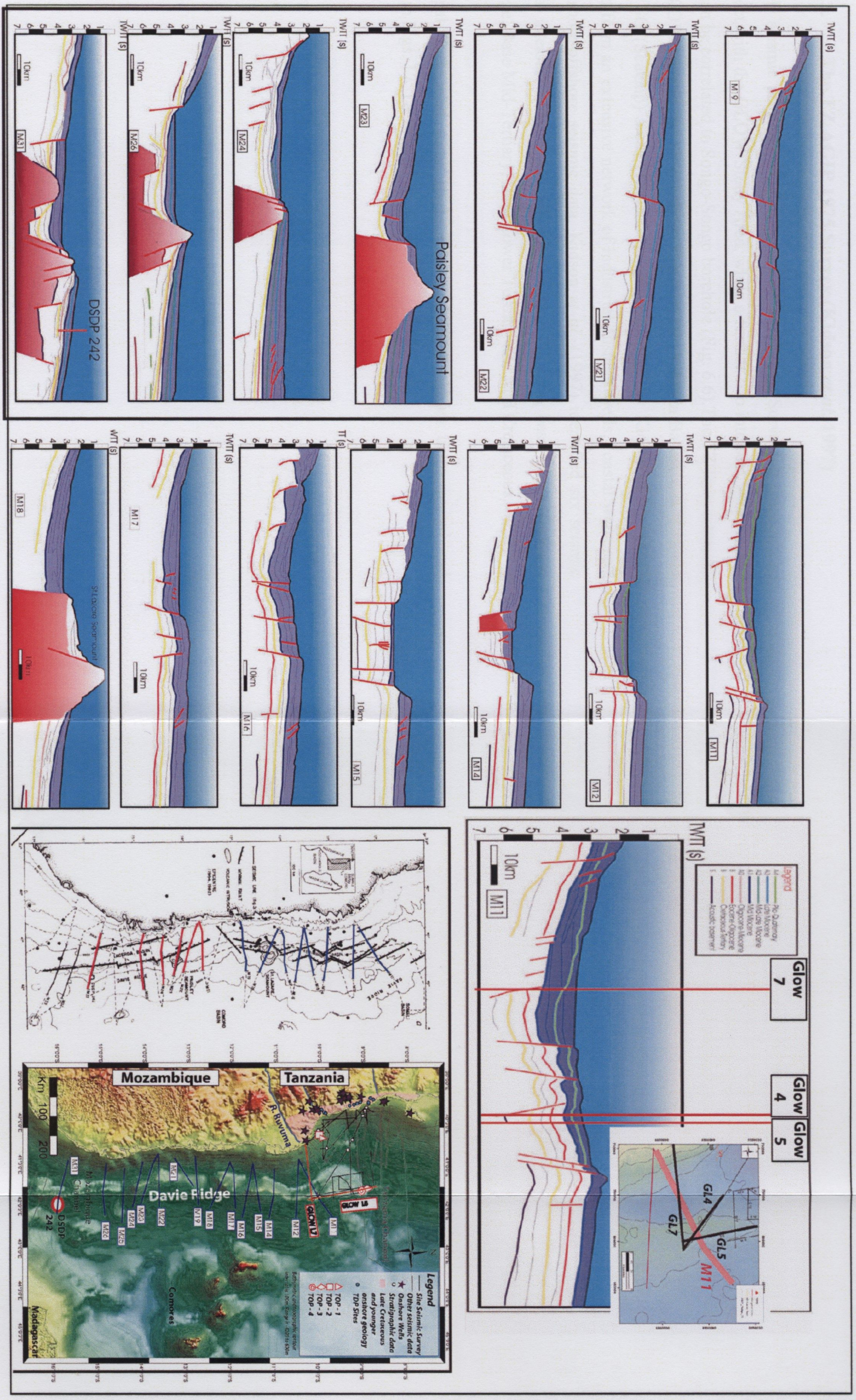

Figure 6.16: Line interpretations from cruise MD40-MACAMO (Mougenot *et al.* 1986) and the intersection of M11 with Glow Line 5 in the Davie Ridge Area. The highlighted blue and pink sections indicates Mid Miocene and younger and basement respectively.

.

6.5.3. The TZ AGIP 1975 Survey (Kidson *et al.* 1997)

Five TZ 2-D seismic profiles recorded by the AGIP Phillips Surveying company in 1976 intersect with the GLOW Study Area, while a further two intersect with the LD Lines and can be correlated to Songo-Songo borehole (Fig. 6.6).The TZ-lines intersect with the GLOW lines in the SS (Shallow Shelf), KTB (Kitunda Basin), CB (Coastal Basin) and SG (SeaGap) areas. The stratigraphy published by Kidson *et al.* (1997) was derived from an extensive network of industrial onshore wells, coastal wells and shallow onshore-offshore seismic data. Kidson *et al.* (1997) identified six seismic markers that intersect with the GLOW survey; Base Pliocene, base Upper Tertiary, base Miocene, Base Mid-Tertiary, Base Lower Tertiary and Mid Cretaceous.

The principal lines used were TZ-1, TZ-3 and TZ-4 shown uninterpreted and interpreted in Figs. 17, 18 and 19.

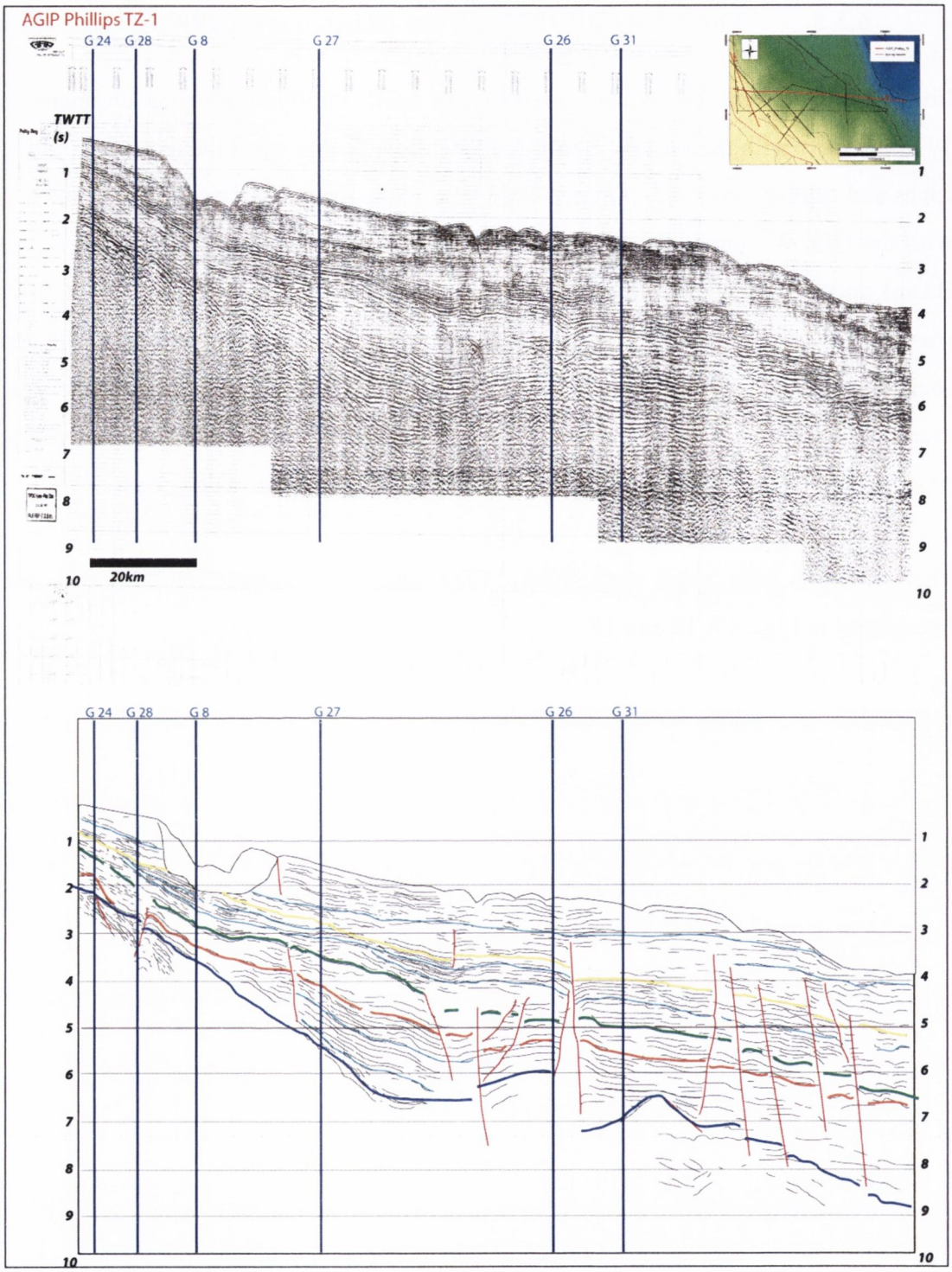

Figure 6.17: Uninterpreted and interpreted profiles of TZ-1. The ages of the reflectors are Mid-Upper Tertiary/Mid Miocene (pale blue), Base Mid Tertiary/Top Eocene (yellow), Base Lower Tertiary/Top Cretaceous (green), Mid Cretaceous (brown) and Basement (dark blue).The location of profile is shown inset and the blue vertical lines represent the locations of the intersecting GLOW lines (e.g. G24). Interpretations are based on those published in Kidson *et al.* (1997).

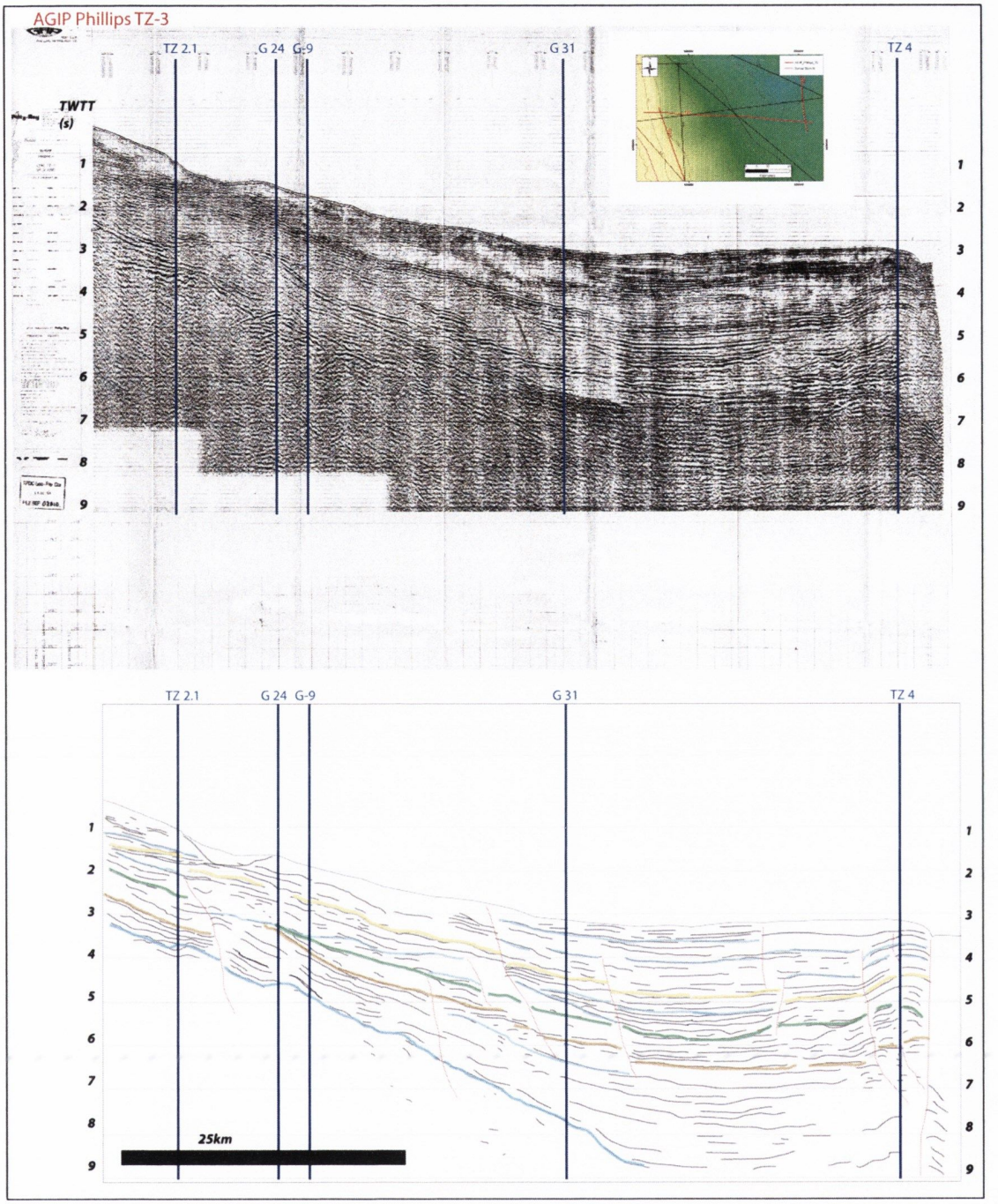

Figure 6.18: Uninterpreted and interpreted profiles of TZ-3. The ages of the reflectors are Mid-Upper Tertiary/Mid Miocene (pale blue), Base Mid Tertiary/Top Eocene (yellow), Base Lower Tertiary/Top Cretaceous (green), Mid Cretaceous (brown) and Basement (dark blue). The location of the profile is shown inset and the blue vertical lines represent the locations of the intersecting GLOW lines. Interpretations are based on those published in Kidson *et al.* (1997).

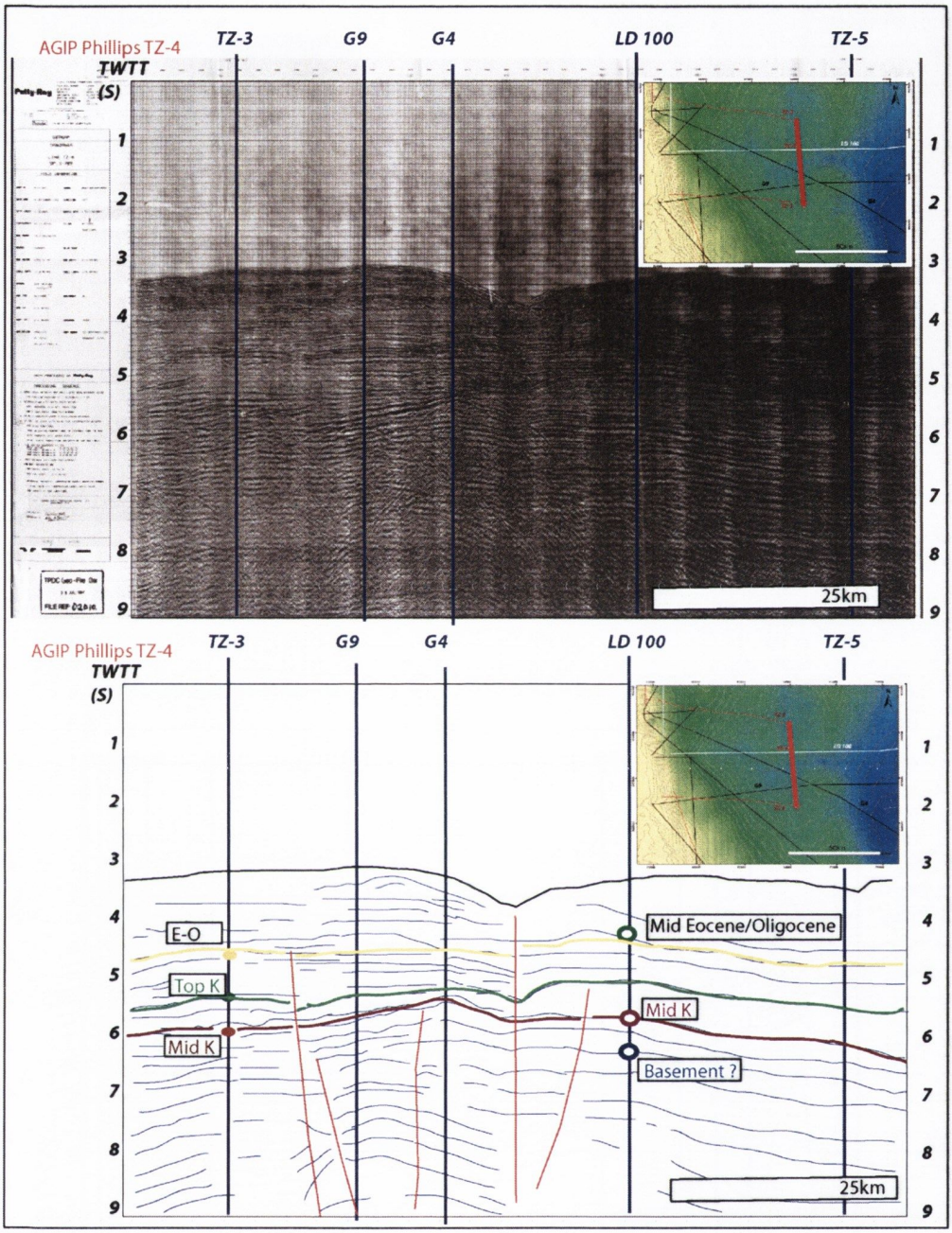

Figure 6.19: Uninterpreted and interpreted profiles of TZ-4. The ages of the reflectors Base Mid Tertiary/Top Eocene (yellow), Base Lower Tertiary/Top Cretaceous (green), Mid Cretaceous (brown) and Basement (dark blue). As there are parallel reflectors seen below the LD basement intersection and the basement is below 9s TWTT on TZ-3, this is interpreted a probably erroneous. The location of profile is shown inset and the blue vertical lines represent the locations of the intersecting GLOW lines and LD line 100. Interpretations are based on those published in Kidson *et al.* (1997).

6.6. GLOW Piston and Box Core Age Data.

During the GLOW Cruise, eighteen box cores retrieved sediment from the sea bottom (Fig. 6.20). The objective of this coring was to target outcropping reflectors as seen in the single channel output onboard and to furthermore, assign dates to these specific reflectors by biostratigraphic dating of the sediment from the core. An example of the single channel output obtained on board and the targeted location of coring is shown in Appendix III. Of the eighteen, 50cm deep cores obtained, eleven revealed an age of Recent (0-0.65Ma). However, the remaining seven revealed ages ranging from Pleistocene to Miocene (1-9.82Ma) based on the presence of key species of planktonic foraminifera. Full details of the box and piston cores can be seen in Appendix III.

The new box core data confirmed the ages of several outcropping reflectors located within the GLOW Survey.

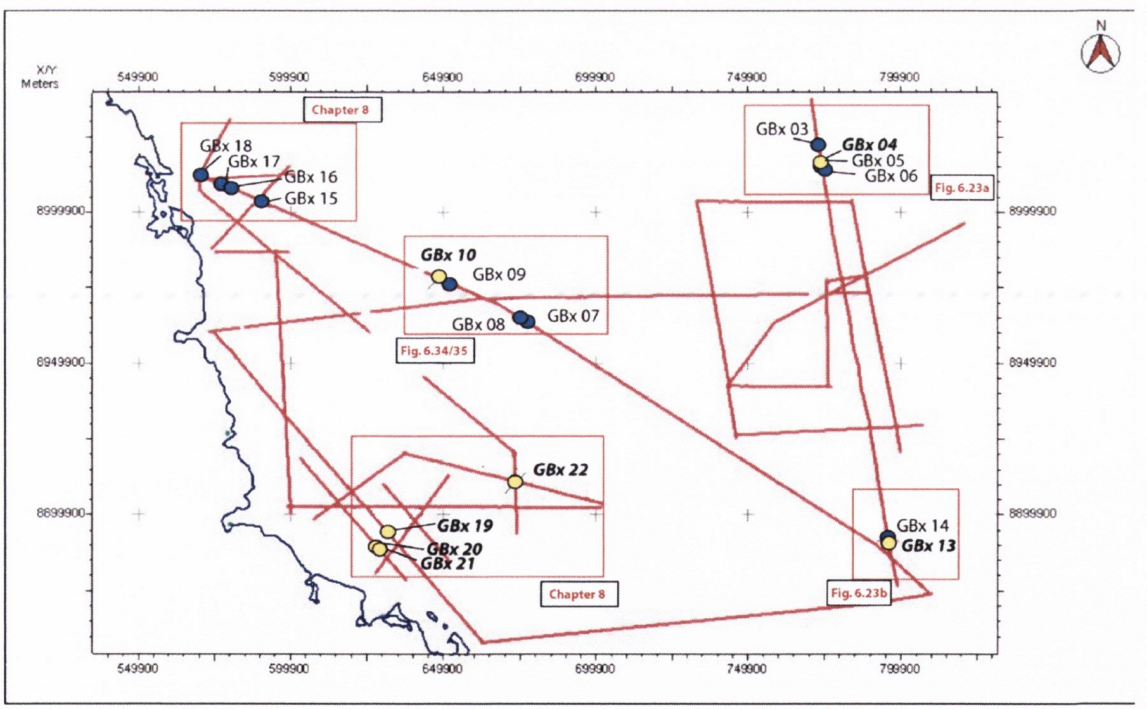

Figure 6.20: GLOW Box Core locations. Red boxes refer to later figures.

6.7.Assigning ages to the Seismic Stratigraphy of the Structural 'Zones'

6.7.1. The Davie Ridge Area

The seismic stratigraphy of the Davie Ridge Area was constructed in Chapter 4. The Davie Ridge Area is intersected in the north by seismic profiles LD100 and in the south by seismic profile M11, and it was box cored in the Tanzania Channel and GLOW Deep Areas. A table of results indicating the location of intersections and the depth of the assigned age is shown (Fig. 6.26). The location of the intersections and the depths of the assigned ages were input into the Kingdom project as wells, thus enabling easier correlation. A summary of the newly age-constrained Davie Ridge stratigraphy is also shown (Fig. 6.27). A more detailed description of the intersections and correlations are given below.

Lamont-Doherty (LD) Seismic Reflection Profiles

In the Davie Ridge Area, the LD 100 line intersects with GLOW Lines 5 and 10 at SP 626 [777405, 8895203] and SP 415[785402, 8995465] (Fig. 6.21). The yellow Base Pliocene SB (from Songo-Songo 1) occurs at 3.95s TWTT (GLOW Line 10) and 4s TWTT (GLOW Line 5). This assigns a Base Pliocene Age to the seismic marker DRSM01. The LD 'Green' Eocene-Oligocene horizon occurs at ~4.45sTWTT and corresponds to the base of DR Unit III/1. The LD 'Purple' Mid Cretaceous horizon occurs at ~5.7s and corresponds to the limit of seismic resolution at the base of seismic unit III/4. Based on these observations, DR SM 02 probably relates to the Mid-Upper Miocene, while DR SM 01 is Base Pliocene in age. It is worth noting that the basement 'Blue' reflector occurs at ~6.3s, deeper than any of the age constraints and the resolution of seismic refletion data (Fig. 6.21).

Mougenot *et al.* (1986) Seismic Reflection Profiles

Line M11 (Mougenot *et al.* 1986) intersects with GLOW Lines 4 and 5 in the Davie Ridge Area and GLOW Line 7 in the DRIEZ area (Fig. 6.22). The A4 Plio-Quaternary and A1 Mid Miocene reflectors are assigned to mid DR seismic unit II and DR SM 02 respectively. The Eocene-Oligocene reflector occurs at or near the base of seismic unit DR III/1. The Cretaceous-Paleogene transition correlates with an undefined horizon in the middle of DR III/4. Thus almost all of the imageable seismic straigraphy on the Davie Ridge, for this study is Paleogene and Neogene in age (Fig. 6.22).

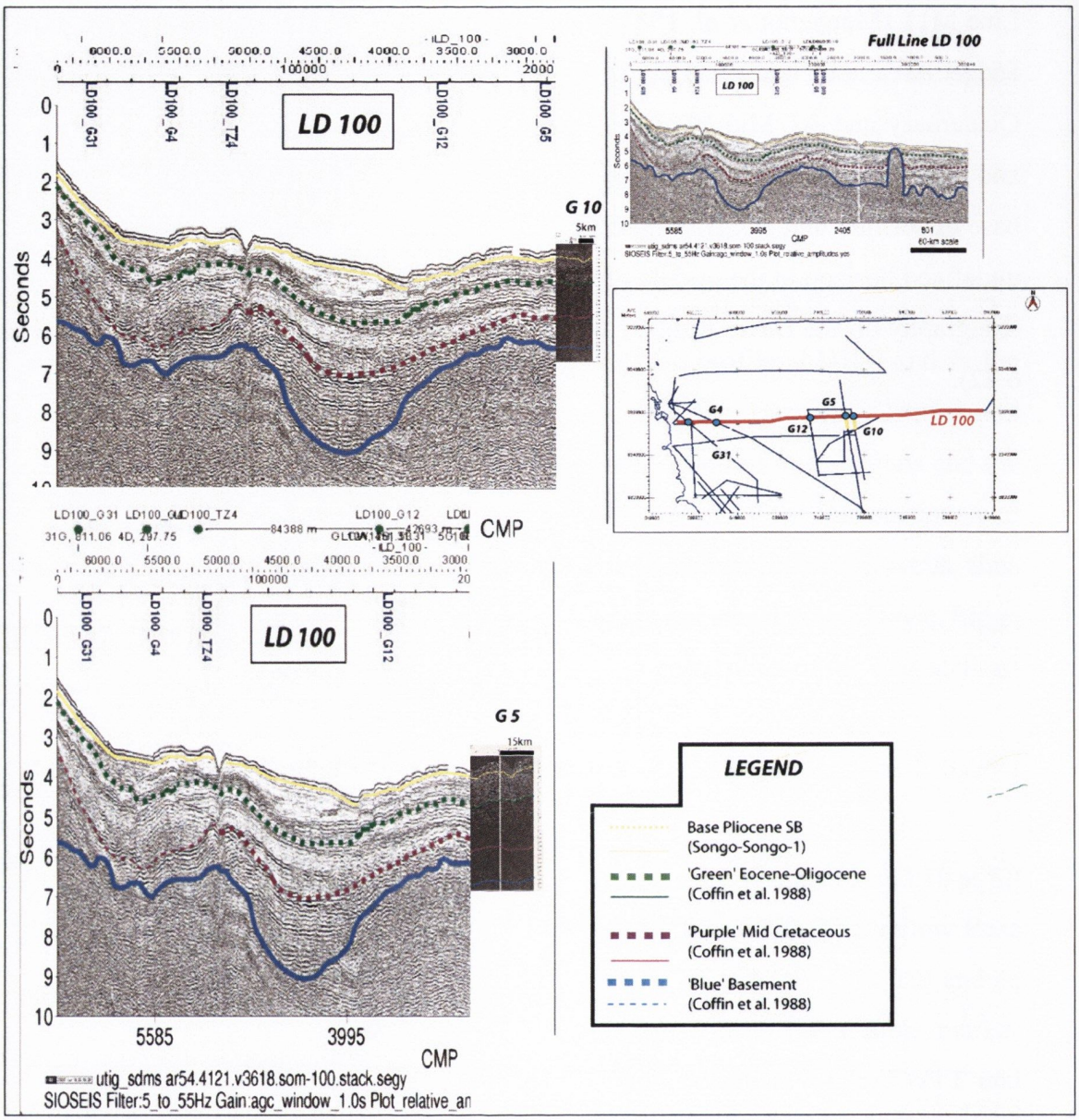

Figure 6.21: The intersection and correlation of seismic markers from LD 100 to GLOW Lines 5 and 10 in the Davie Ridge Area. Shown inset are the complete interpreted line and the location of LD 100 and intersects with GLOW Lines.

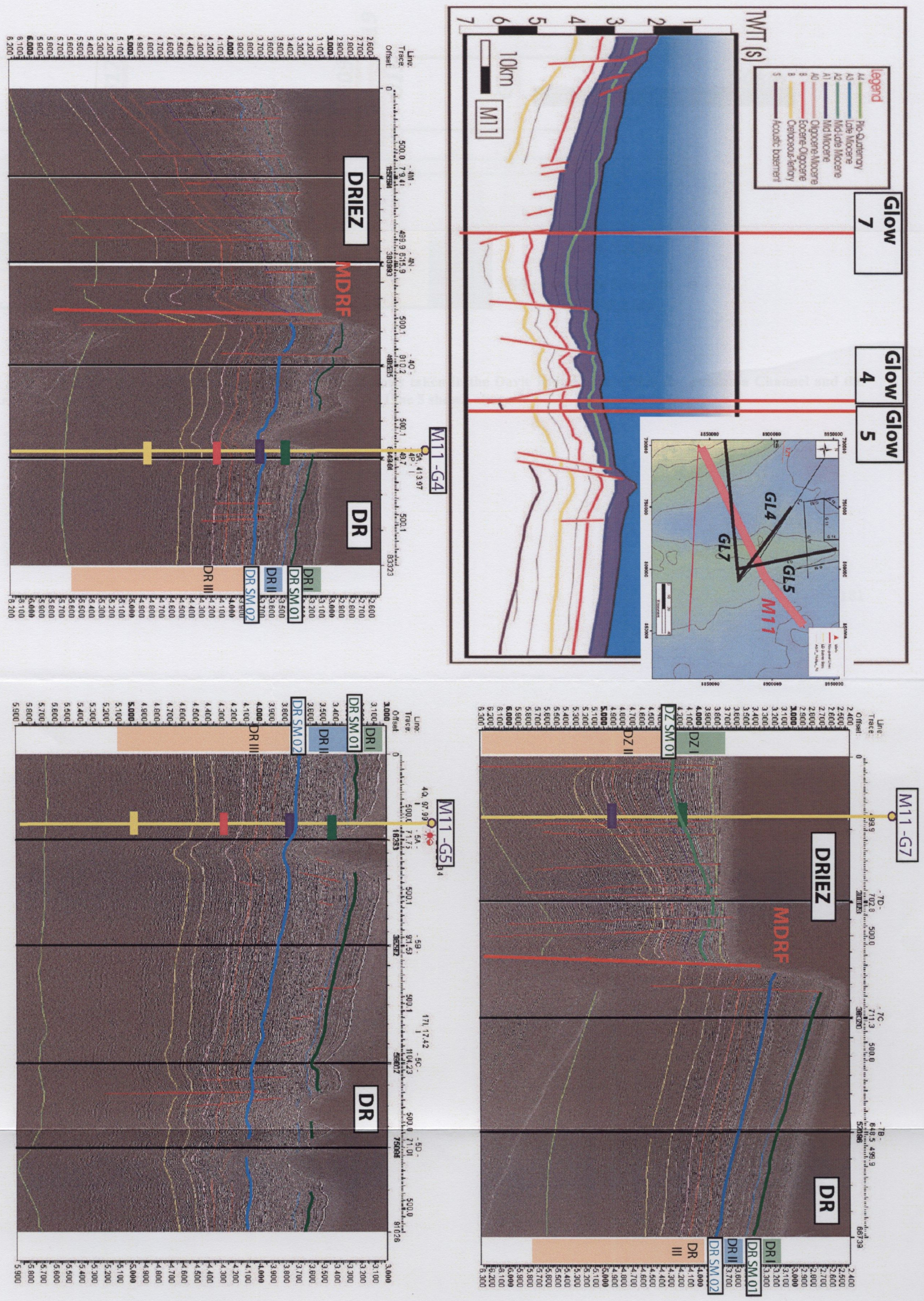

Figure 6.22: Correlating from M11 to GLOW Lines 4, 5 and 7 (within the DR and DRIEZ Zones). The colours refer to the ages of the M11 reflectors; green (Plio-Quat), dark blue (Mid-Miocene), pink (Eocene-Oligocene) and yellow (K-Pg). The colours on the seismic profiles correspond to the colours used in the GLOW seismic stratigraphy (Chapter 4).

.

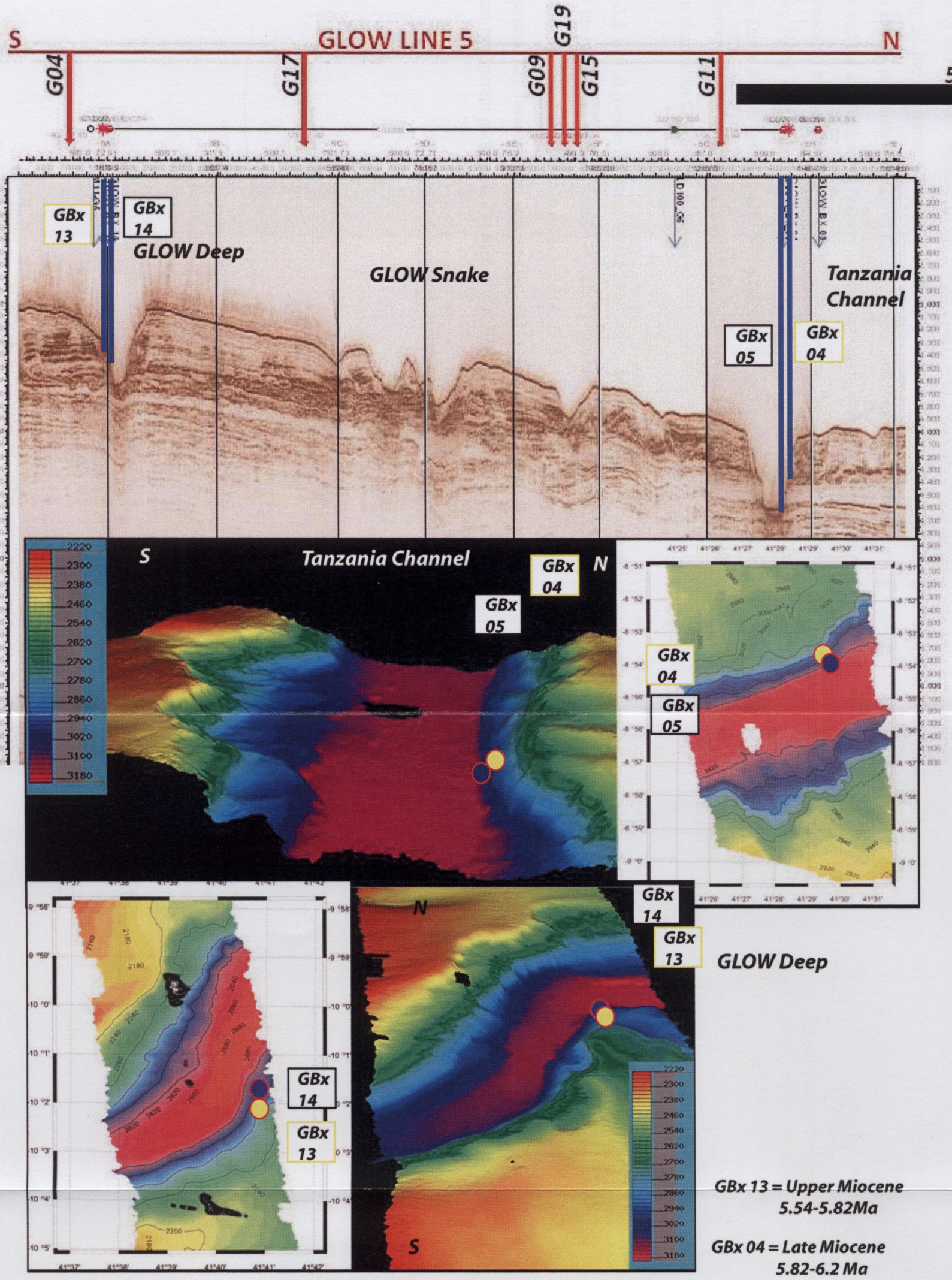

Figure 6.23: Bathymetric and seismic profiles of locations of the GLOW Box core samples taken in the Davie Ridge Area within the Tanzania Channel and the GLOW Deep. Location of figures shown in Fig. 6.20 and an uninterpreted line of GLOW Line 5 shown above.

.

Box cores

Two ages, Late-Miocene and Uppermost Miocene, were recovered on the basis of their planktonic assemblage of box cores retrieved in the channels transecting the Davie Ridge. In the northern segment of the Davie Ridge, four box cores were taken in the vicinity of the Tanzania Channel; GLOW BX 3,4,5 and 6 (Fig. 6.23). The Channel was chosen primarily because of the unslumped and winnowed nature of the canyon walls and the single channel outputs showed reflectors over the entire depth of the canyon truncated by the canyon walls. In locations such as the Tanzania Channel a 50cm boxcore could punch through to much older sediment than exposed on the surface of the Davie Ridge, for example. While GBx 3, 4 and 5 were located directly on the positioning of GLOW Line 5, a site was identified within the canyon a suitable distance from slumps for GBx6 (Fig. 6.23)

GLOW Bx 3,5 and 6 yielded Recent (0-0.65Ma) ages. However, GLOW Bx 4, located on the northern canyon wall of the Tanzania Channel produced a biostratigraphic age of Late Miocene M13b/M14 (5.82 - 6.2Ma) based on the presence of several key foraminiferal species (Fig. 6.24). This age corresponds to the top of the semi-transparent package at the base of DR II/2, located immediately above DR SM 02.

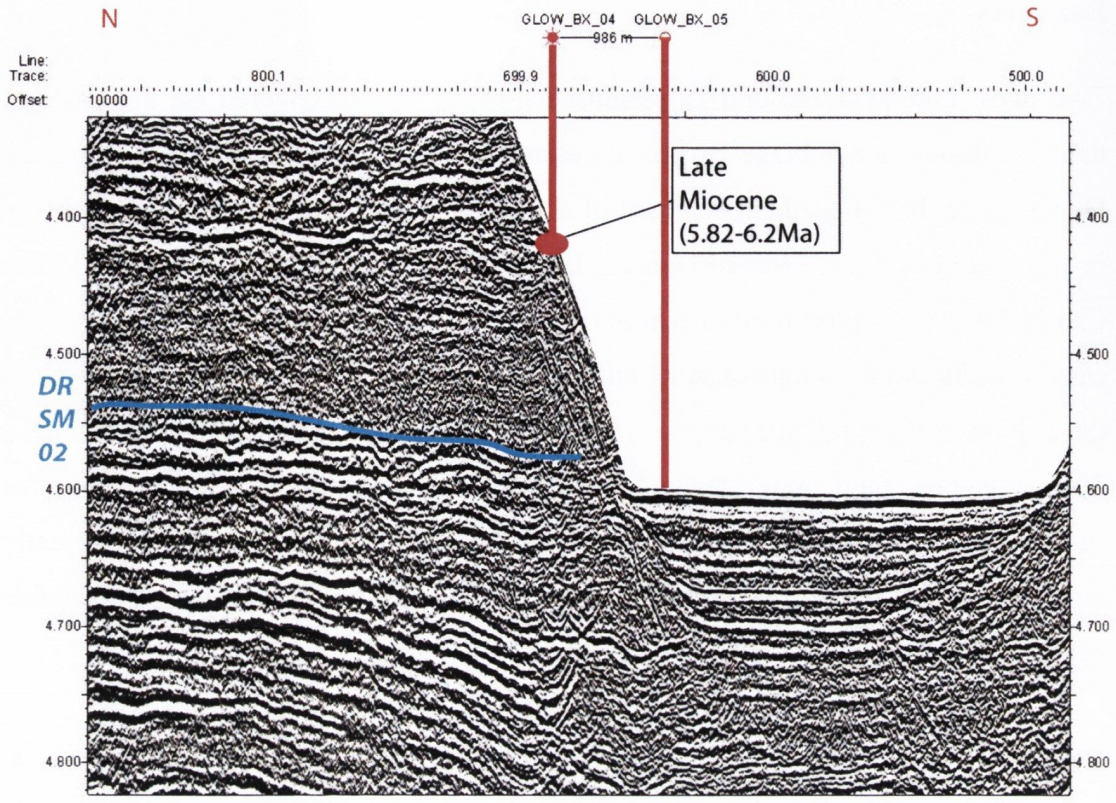

Figure 6.24: Location of GBx 04 and 05 on the northern flank of the Tanzania Channel. GBx 04 sampled the base of the seismic unit DR II/2.

In the southern extent of the Davie Ridge, within the survey area, GLOW Box cores 13 and 14 were sited within the southern walls of the GLOW Deep Canyon (Fig. 6.23). While GBx 14 was Recent in age, GBx 13 was uppermost Miocene; 5.54-5.82 Ma in age (PL1/N18). A piston core was also located at this site with penetration of 3.2m. The reflector package this box and piston core sampled was the top of DR II/1, just beneath DR SM 01 and it is therefore above the package dated as Mid Miocene in GBx 04 (Fig. 6.25). The similar ages for these two box core located over 160km from one another verifies the remarkably laterally consistent Davie Ridge stratigraphy.

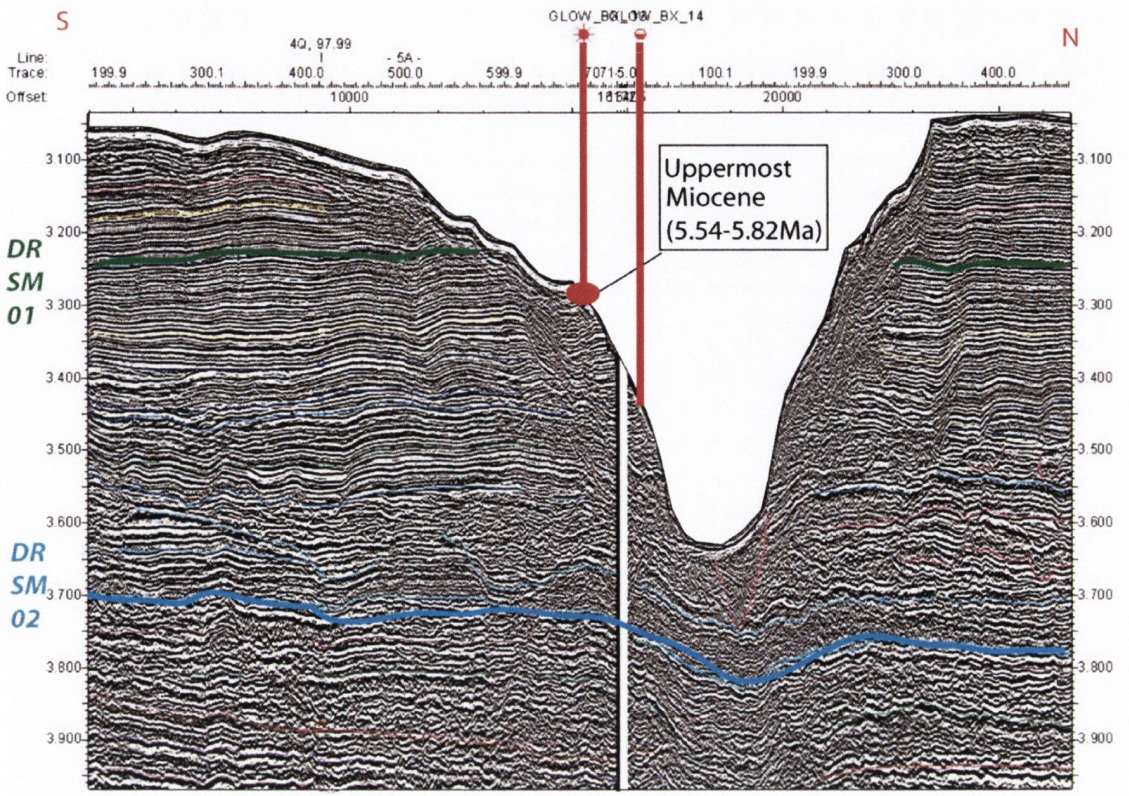

Figure 6.25: GBx Cores 13 and 14 located in GLOW Deep in the southern Davie Ridge Area. GBx 13 samples the top of DR II/1, stratigraphically above the layer sampled in the Tanzania Channel by GBx 04 (Fig. 6.24).

Results and Interpretation

Survey Name	SP	GLOW Line	SP Location	X	Y	Age of horizon	TWTT(s)	Corresponding seismic marker/unit
LD 100	2933	5	5G, 625.86	777405.72	8995205	Base Pliocene	4	DR SM 01
						Eocene-Oligocene	4.45	Base DR Unit III/1
						Mid-Cretaceous	5.7	Base DR Unit III/4
	2789	10	10B, 415.29	785409.7	8995465.35	Base Pliocene	3.95	DR SM 01
						Eocene-Oligocene	4.6	Base DR Unit III/1
						Mid-Cretaceous	5.45	Base DR Unit III/4
M11	~	5	5A, SP 586.5	795987	8889471	Plio-Quat	3.45	Upper DR Unit II/1
						Mid Miocene	3.7	DR SM 02
						Eocene-Oligocene	4.25	Base DR Unit III/3
						Cretaceous -Paleogene	4.95	Mid DR Unit III/4
		4	4Q, SP 672.1	793767	8888292	Plio-Quat	3.5	Mid DR Unit II/2
						Mid Miocene	3.7	DR SM 02
						Eocene-Oligocene	4.15	Base DR Unit III/3
						Cretaeous -Paleogene	4.85	Mid DR III/4
G Box Core 14	~	5	4Q, SP 672.1	795409	8892921	Late Miocene; M13b/M14 (5.82 - 6.2Ma)	4.4	Mid DR Unit II/2
G Box Core 13	~	5	5A, SP 680.7	795624.24	8891635.56	uppermost Miocene; PL1/N18 (5.54-5.82 Ma)	3.28	Top DR Unit II/1

Figure 6.26: Results of intersection analysis in the GLOW Deep Area of the Davie Ridge.

The following ages were assigned to the Davie Ridge stratigraphy and are summarised in Fig. 6.27. DR SM 01 corresponds to the Base Pliocene. Thus DR I is Pliocene-Holocene in age. DR SM 02 corresponds to the Mid Miocene. DR seismic unit II is interpreted as Mid-Upper Miocene in age. The change in seismic facies from DRII/2 to DR II/1 probably represents the Mid-Upper Miocene boundary. The base of DR seismic unit III/1 corresponds to the Eocene-Oligocene transition, therefore it is inferred that unit III/1, bound above by DR SM 02, is Oligocene-Lower Miocene in age. The Cretaceous –Paleogene transition occurs in the middle of the homogenous DR III/4 seismic unit while a Mid Cretaceous age is assigned to the base of the imageable data in DR III/4.

A summary synthesis chronostratigraphic diagram for the entire offshore area is found at the end of Chapter 9. Quantitative sedimentation rate analysis and chronostratigraphic interpretations were enabled by assigning ages to reflectors and this is discussed in terms of the margin as a whole in Chapter 11.

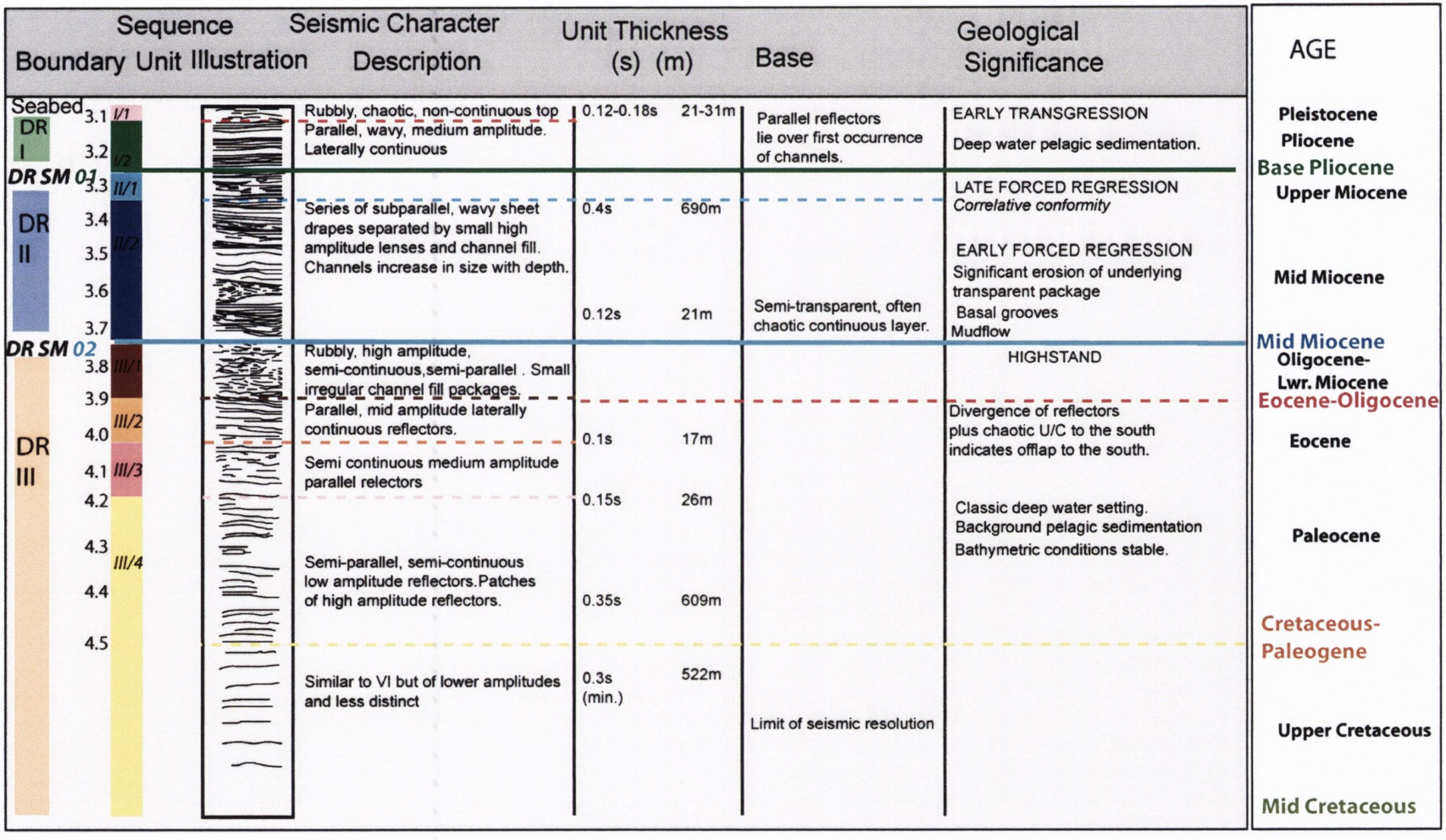

Figure 6.27: Age constrained seismic stratigraphy of the DR Area

6.7.2. The Davie Ridge Inner Extensional Zone (DRIEZ)

The seismic stratigraphy of the Davie Ridge Inner Extensional Zone was constructed in Chapter 4. The DRIEZ is intersected in the north by LD100 and in the south by M11. A summary of the newly age-constrained DRIEZ stratigraphy is shown in Fig. 6.30.

Lamont Doherty (LD100)

LD 100 intersects with GLOW Line 12 in the Davie Ridge Inner Extensional Zone (DRIEZ) (Fig. 6.28). The LD 'Green' Eocene-Oligocene horizon occurs at ~4.9s TWTT (Fig. 6.28) and corresponds to the base of seismic unit DZ Unit II/1. The LD 'Purple' Mid Cretaceous horizon occurs at ~6.4s and corresponds to the limit of seismic resolution at the base of seismic unit DZ II/3.

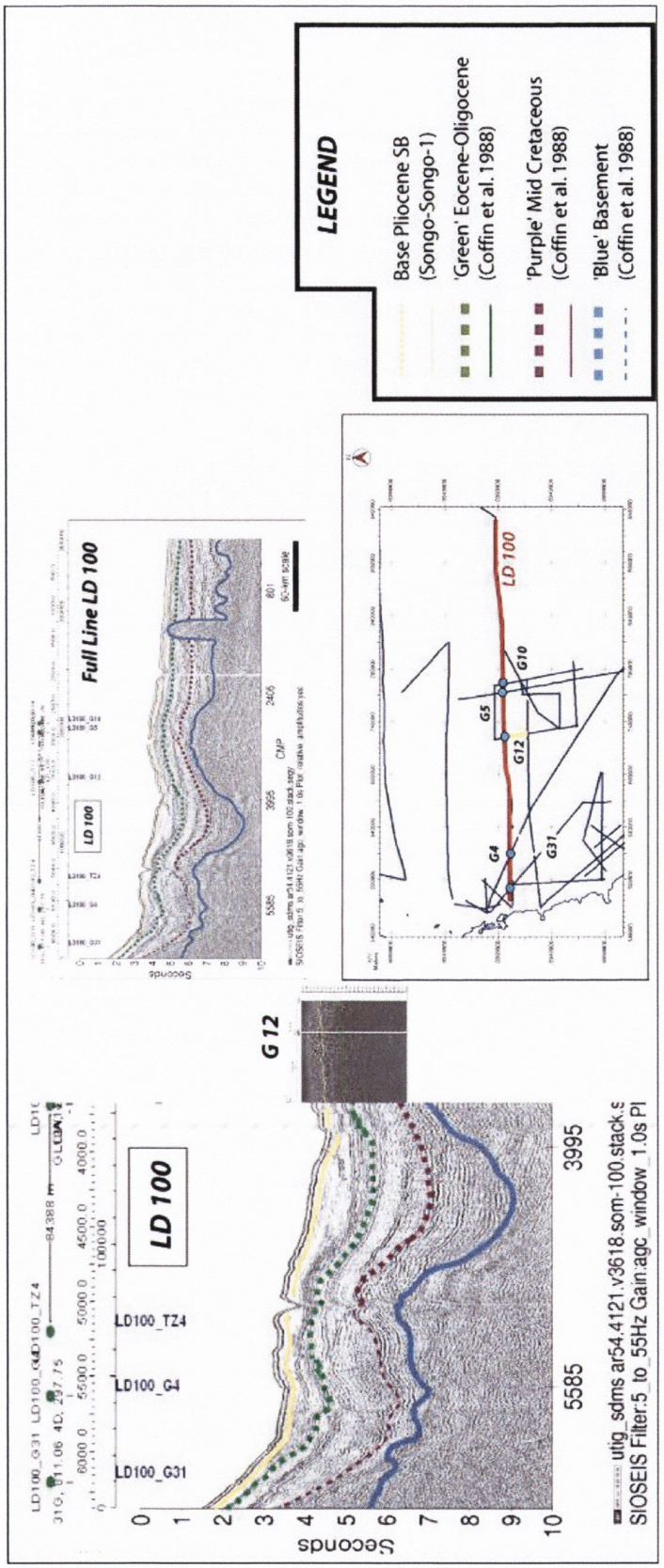

Figure 6.28: The correlation from LD 100 to the GLOW Line 12 in the DRIEZ.

Mougenot *et al.* (1986); Line M11

The intersection of M11 (Mougenot *et al.* 1986) with GLOW Line 7 is shown in Fig.6. 29. The depths at which the seismic markers for the Plio Quat, Mid Miocene and Eocene-Oligocene are shown in Fig.6. 29

Survey Name	SP	GLOW Line	SP Location	X	Y	Age of horizon	TWTT(s)	Corresponding seismic marker/unit
LD 100	3685	12	12B, 28.4	734730.72	8993950.32	Base Pliocene	4.35	DZ SM 01
						Eocene-Oligocene	4.9	Base DZ Unit II/1
						Mid-Cretaceous	6.4	Base DZ Unit II/3
M11	~	7				Plio-Quat	4.15	DZ SM 01
						Mid Miocene	4.9	Base of DZ Unit II/1
						Eocene-Oligocene	5.25	Mid DZ Unit II/3

Figure 6.29:TWTT occurrences of seismic markers at the intersection of LD 100 with Glow Line 12 and Mougenot M11 with Glow Line 7. M11 intersects with GL7 at (752280, 8866856 UTM).

There was some discrepancy over the location of the Mid-Miocene and Eocene-Oligocene seismic marker between the LD and M11 interpretations. The highly faulted nature and resolution of these surveys prevented the accurate assignment of ages via this method and the results were inferred as a guide. In Chapter 4 a sedimentological correlation between the seismic stratigraphy of the DR and DRIEZ was proposed and the results of that correlation were incorporated here.

Figure 6.30:Age constrained seismic stratigraphy of the DRIEZ area. (Min. refers to minimum).

6.7.3. Kerimbas Basin

The seismic stratigraphy of the Kerimbas Basin Area was constructed in Chapter 5. Ages of the KB seismic markers were inferred from interpreting nearby LD 100 as there are no intersecting surveys in the basin. A summary of the newly age-constrained KB stratigraphy shown in Fig. 6.32.

The profile of LD 100 in this area was compared with the Kerimbas Basin to assign an age to the stratigraphy. The W-E profile is strikingly similar to the GLOW Line 9 profile and was therefore interpreted to identify similar seismic marker characteristics that could be inferred in the Kerimbas Basin stratigraphy (Fig. 6.31).

The Eocene-Oligocene occurs at 5.5s TWTT in LD100 and coincides with KB SM 01. There is also a similarity in the overlying seismic stratigraphy as the basal reflectors of the next seismic unit onlap the E-O reflectors in LD 100. A base Pliocene age is assigned to the base of KB Seismic unit I/1 (blue in Fig. 6.31) after correlating from Songo-Songo borehole to LD 100. This implies an age of Oligocene-Miocene for KB Unit I/2.

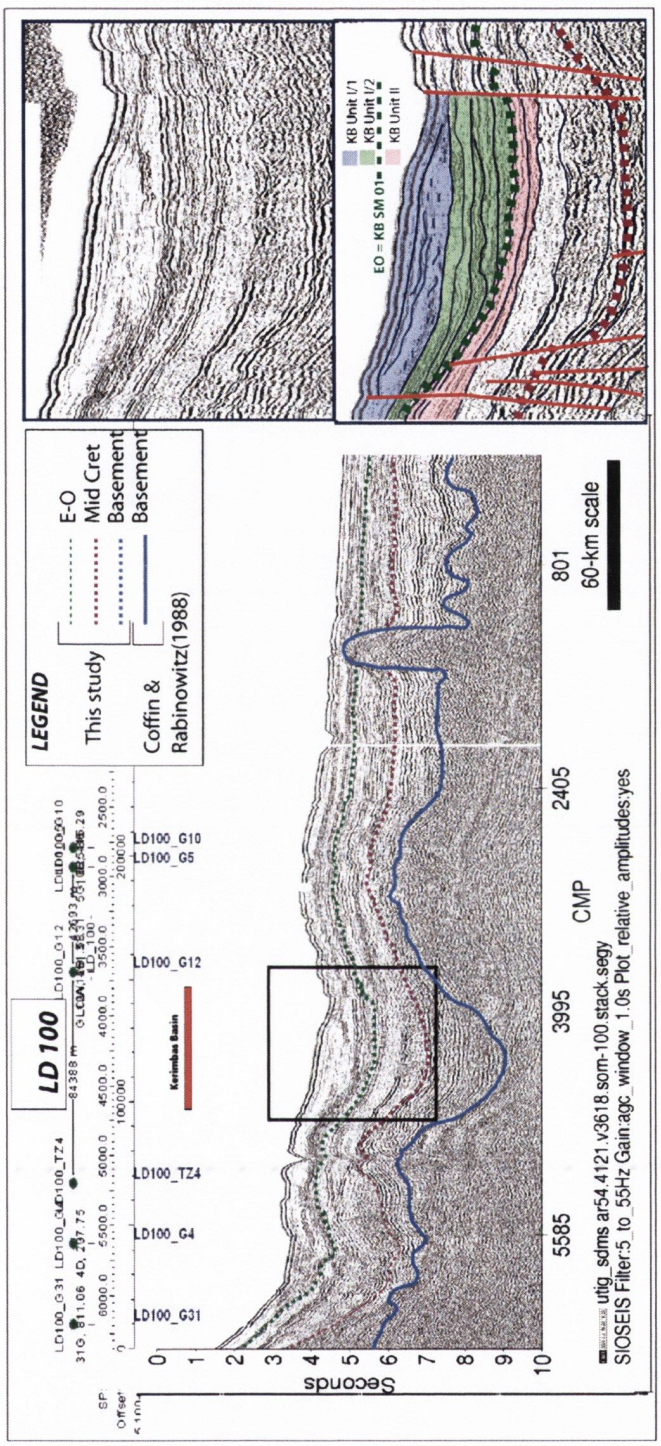

Figure 6.31: Interpreting the Kerimbas Basin facies on LD 100. On the basis of the stratigraphical relationships observed, KB SM 01 is interpreted as Eocene-Oligocene in age, the base of KB Unit I/2 as Oligocene-Miocene and the base of I/1 as Base Pliocene.

Figure 6.32: Age constrained stratigraphy of the Kerimbas Basin Area.

6.7.4. SeaGap Area (SG)

The SeaGap Area is constrained in age by the intersecting TZ-4, nearby LD100 seismic lines and box core data. Given the highly faulted nature of the SeaGap Area, however, correlation across individual faults is difficult.

The intersections of TZ-4 and LD 100 indicate the depth of imaged data in the SeaGap is younger than Eocene-Oligocene, which occurs at approx. 4.7s TWTT in GLOW Lines 9 and 4 (below imaged data in Fig. 6.35). The box core GBx 10 yielded a biostratigraphic age of Miocene M13a/N16 (Age: 8.58-9.82 Ma) from the seafloor of the Mid SeaGap Canyon (Fig. 6.35). The SeaGap stratigraphy is constrained as the SG SM 02 is interpreted to have a Late Miocene age based on the box core data. The limit of seismic data (i.e. the base of SG Unit III) is Eocene-Oligocene in age.

TZ AGIP

TZ-3 (West-East) and TZ-4 (North South) intersect the SeaGap Area (Figs. 6.18 and 6.19). The eastern extent of TZ-3 surveys the SeaGap although it does not intersect with GLOW Lines directly in this area. TZ-4 is unfortunately of poor quality on the paper format, however an interpretation was made that indicates the age of the seismic units on the intersecting GLOW Lines 9 and 4 are younger than Eocene-Oligocene.

LD

Similarly to the coverage of TZ-3 above, although the LD Line 100 does not intersect with any GLOW Lines in the SG area, it does survey the structure to the north of the area, along strike. As similar facies and structural features are observed, LD 100 likely indicates the depth of imaged data in SeaGap corresponds to a package that is younger than Eocene in age.

Box Cores

GLOW Box cores 07, 08, 09 and 10 were retrieved from the SeaGap Fracture Zone (Fig. 6.26, 6.34). GBx 10 yielded the only non-Recent age of Miocene M13a/N16 (Age: 8.58-9.82 Ma). Unlike the other box cores taken in this area, GBx 10 was not

located along GLOW Line 4, but at a site located 380m from GLOW Line 9 and 4.26 km from GBx 9. The site of GBx 10, within the Mid-SeaGap canyon was identified by multibeam bathymetric surveying (Fig. 6.33). Within this segment of GLOW Line 4, AGIP TZ-4 traverses 646m NE of GBx 09 (Fig. 6.34).

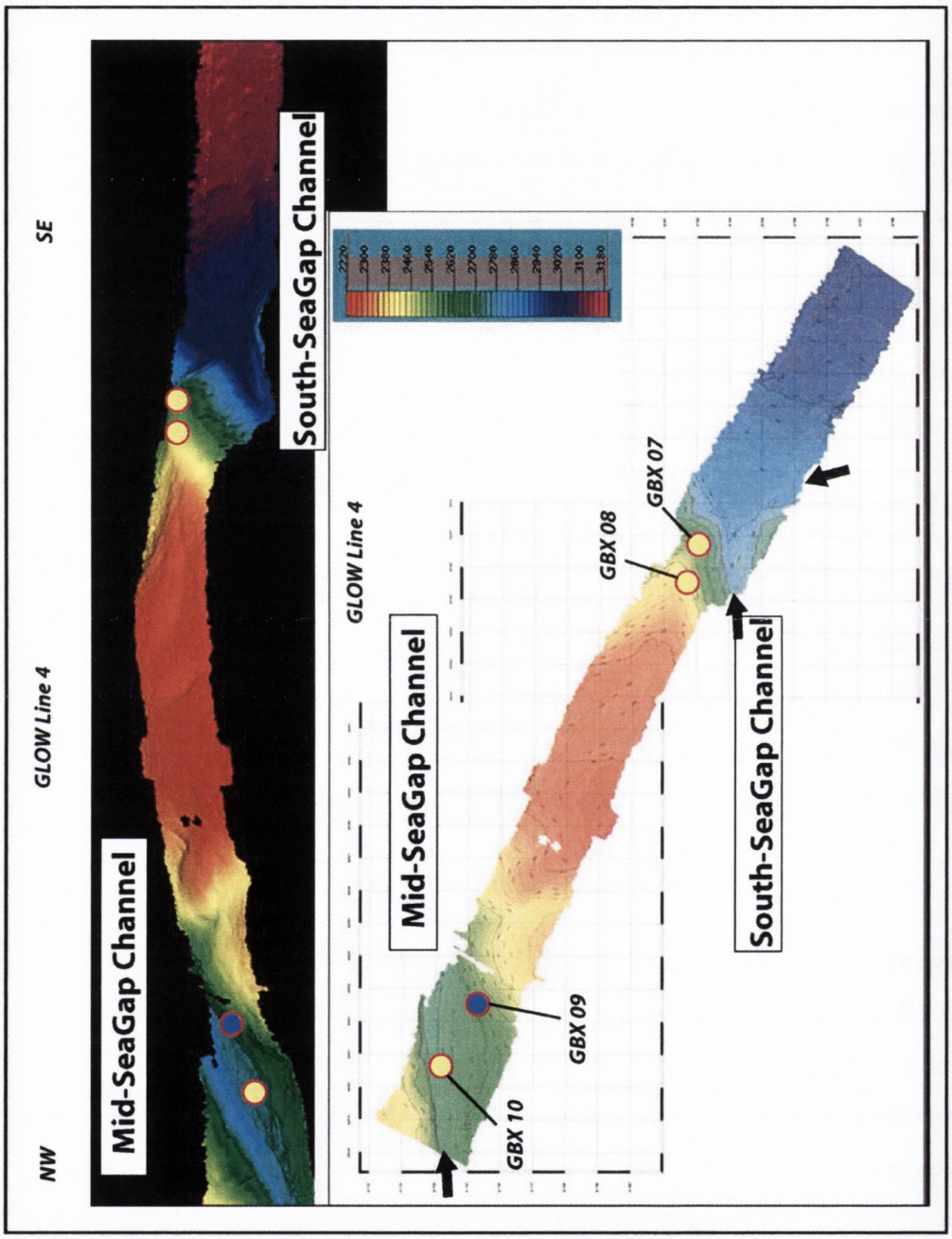

Figure 6.33: Bathymetric profile of the SeaGap Fracture Zone Area with the GLOW Box core locations 7, 8, 9, 10 highlighted. Glow box core 10 yeilded an age of Miocene; 8.58-9.82Ma. Seismic profile of this line 4 is shown in Fig. 6.35 and location in 6.34.

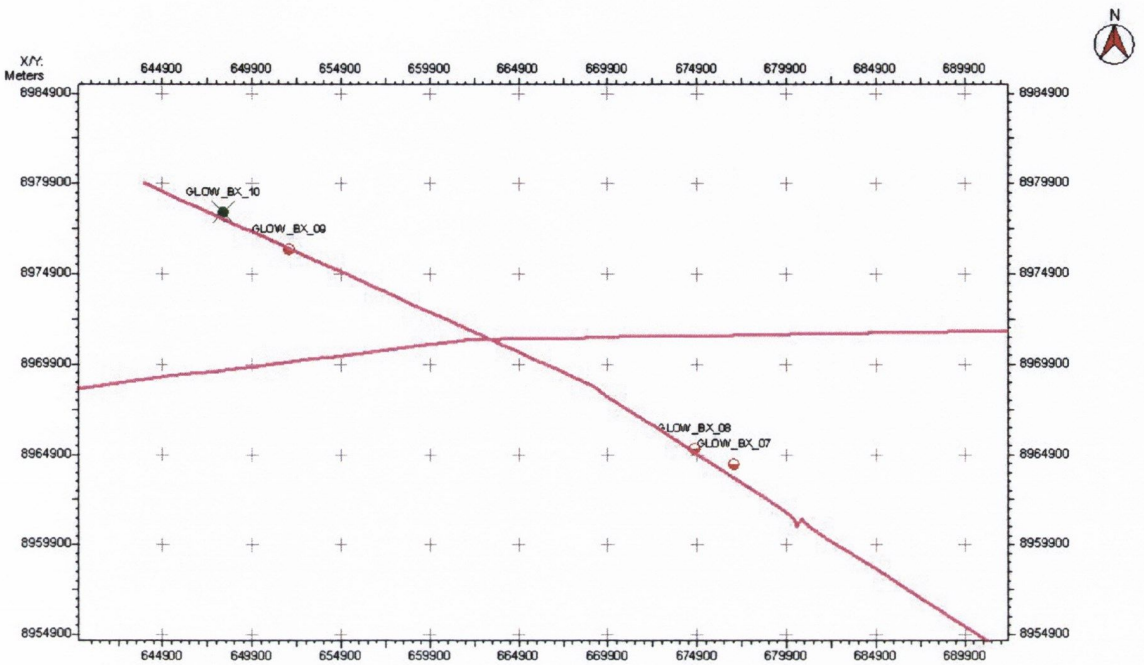

Figure 6.34: Location of box cores taken in the SeaGap Fracture Zone. Location of figure is shown in Fig. 6.20.

As GBx 10 box core was retrieved from the centre of the Mid-SeaGap canyon (Fig. 6.35), its sedimentary origin is less clear than other cores retrieved. It comprised 24cm of coarse foram sand with clay adhering to the bottom of the coring apparatus. The sediment within the core was seen to fine upwards. While the core is assigned an M13a/N16 biozone, the clay found beneath the apparatus is also M13a/N16 but with Lower Miocene and possible Middle Miocene reworked elements. Therefore the age assigned is M13a/N16 but with possible older reworking. Within the core were a small piece of amber with plant inclusions, coral fragments and abundant fragmented benthic foraminifera.

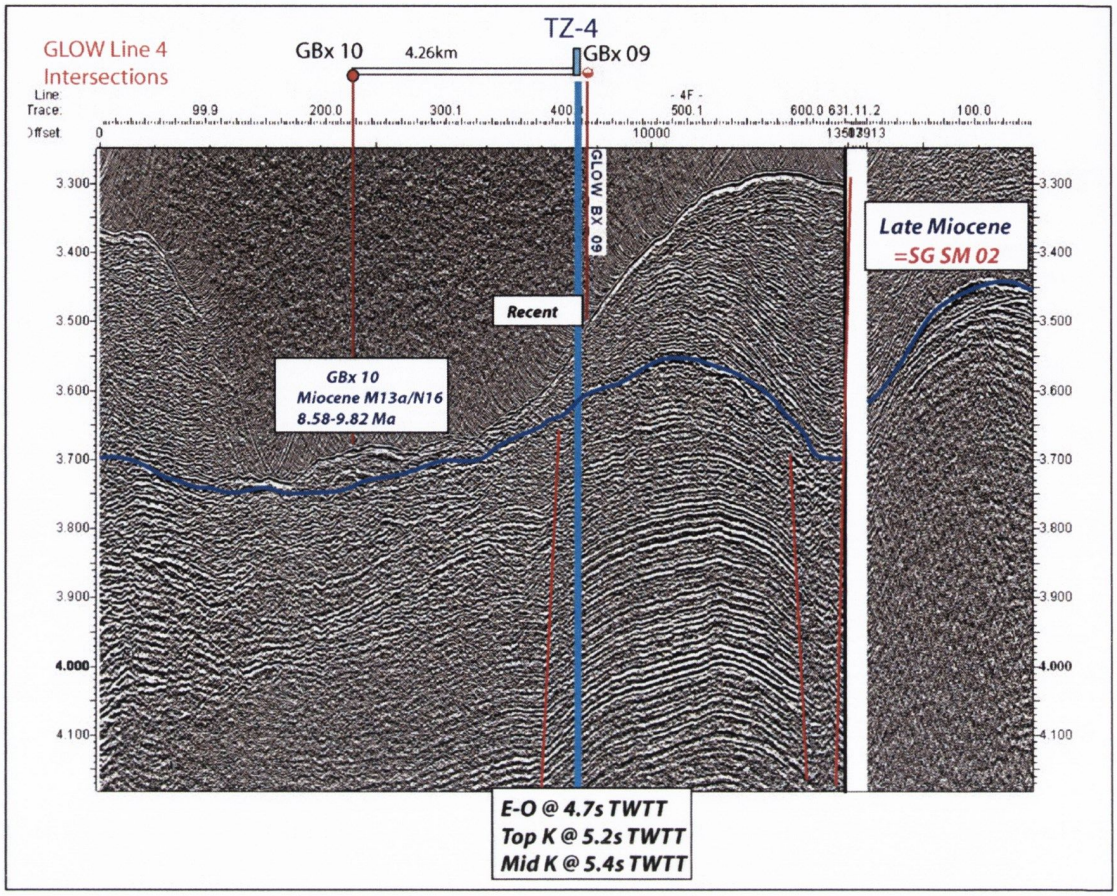

Figure 6.35: The Mid SeaGap Canyon Area and intersections with TZ-4 and GBx 09, 10. The age of Mid Miocene is assigned to SG SM 02. There is an assumption that the material derived from the nearby seafloor has been reworked (Option b discussed in text).

The coarse foram sand may be a) located directly on the canyon floor; b) located directly beneath the canyon floor and reworked within the canyon area; c) slumped material from the canyon walls located higher than the canyon floor d) sediment derived from closer to the shelf and transported here via turbidity currents and the strong flow recorded through the Tanzania Channel or e) a mix of the turbiditic material from the shelf and reworked material from within the canyon. If an element of in-situ reworking is considered, as indicated by the Lower and Middle Miocene elements on the base of the apparatus, it is reasonable to assign an age of Mid-Late Miocene to the reflectors that appear laterally continuous with the base of the canyon floor.

Survey Name	SP	GLOW Line	SP Location	X	Y	Age of horizon	TWTT(s)	Corresponding seismic marker/unit
TZ 4	~	4		651409	8976402	Eocene-Oligocene	4.7	Base of SG III
						Top Cretaceous	5.2	Below imaged seismic data
						Mid-Cretaceous	5.4	Below imaged seismic data
	~	9		651841	8969968	Eocene-Oligocene	4.75	Base of SG III
						Top Cretaceous	5.3	Below imaged seismic data
						Mid-Cretaceous	5.5	Below imaged seismic data
GBx 04				648268.3	8978352.26	Miocene M13a (Age:8.58-9.82Ma)	Base Mid	SG SM 02
						Late Miocene	SG Canyon	

Figure 6.36: Intersection data for the SeaGap Area. GBx 04 occurs at [774176, 9016054].

Considering all the intersection data (Fig. 6.36), the base of SG Unit III is assigned an Eocene-Oligocene age and the seismic marker SG SM 02 is assigned a Mid-Late Miocene age. Therefore SG Unit III is Oligocene-Middle Miocene in age. SG II and SG I are Mid Miocene to Recent in age. A summary of the ages assigned to the SeaGap stratigraphy can be found in Fig. 6.37.

Figure 6.37: Age constrained summary seismic stratigraphy for the SeaGap Fracture Zone.

6.8.Estimated Ages of GLOW Seismic Markers for the DR, DRIEZ, KB and SG Areas.

Based on the correlations between the published data and the nearby wells a reasonable estimate of the age of seismic markers and units may be made. In conclusion a stratigraphic framework for the southern offshore realm may be established (Fig.6. 38).

The following Chapters 7 and 8 define the onshore geology and extend that to assess the age of the transition zone (onshore to offshore) seismic data. A complete margin interpretation of sedimentological and structural evolution is constructed in Chapter 11.

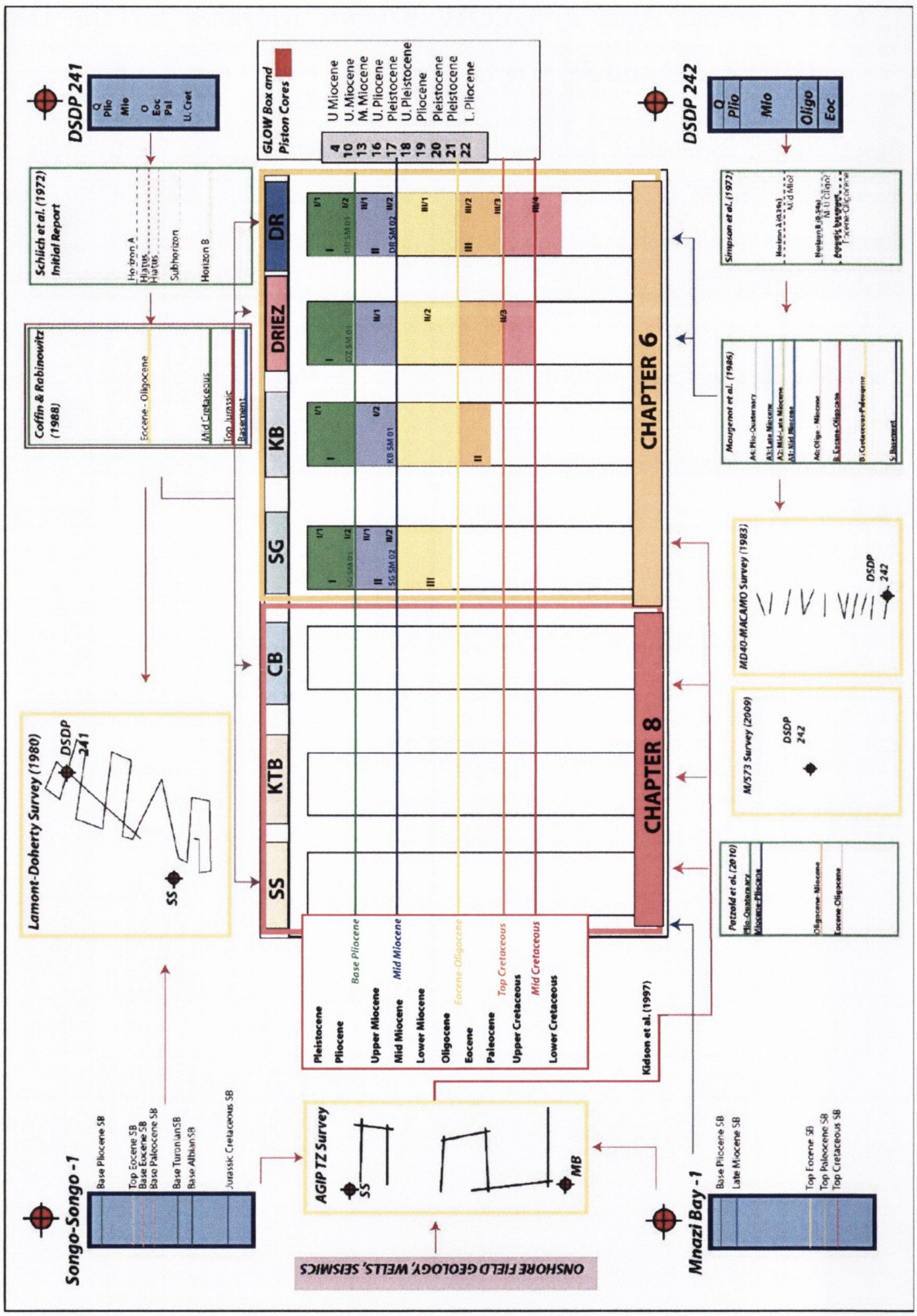

Figure 6.38: Summary of correlating from pre-published data and box core data to the GLOW Seismic survey. The results of this chapter are included in the orange boxes.

6.9.Previous Stratigraphic Nomenclature

Various stratigraphic schemes have been proposed for the offshore Tanzania area. Many have been discussed already in terms of the seismic surveys that accompany the schemes and intersect with GLOW data. Mpanda (1997) produced a seismic interpretation of the Coastal Basins of Tanzania. However, this coastal basin area did not survey south of Songo-Songo Island and therefore is not discussed here. Cope (2000) produced a seismostratigraphic scheme for the 'Mafia Deep Offshore Basin', of which the southern half approximately is represented by this study area.

6.9.1. Mafia Deep Offshore Basin (MDOB) Seismostratigraphy; Cope (2000)

Based on an extensive industrial survey shot by Western Geco, a seismostratigraphic interpretation (Fig. 6.38) of the Mafia Deep Offshore Basin (MDOB) was published by Cope (2000). Five seismic sequences are described. Unfortunately, no specific locations of this dataset are provided. As the sediment thickness appears substantially thicker in the younger sections than seen for previous studies and nearby wells, it may be safe to assume that this scheme represents a deeper water setting than our stratigraphy. Although similar sedimentological characteristics and distinct seismic surfaces exist, because there is no distinct intersection with the data of this study, the results of Cope (2000) are not incorporated in this study.

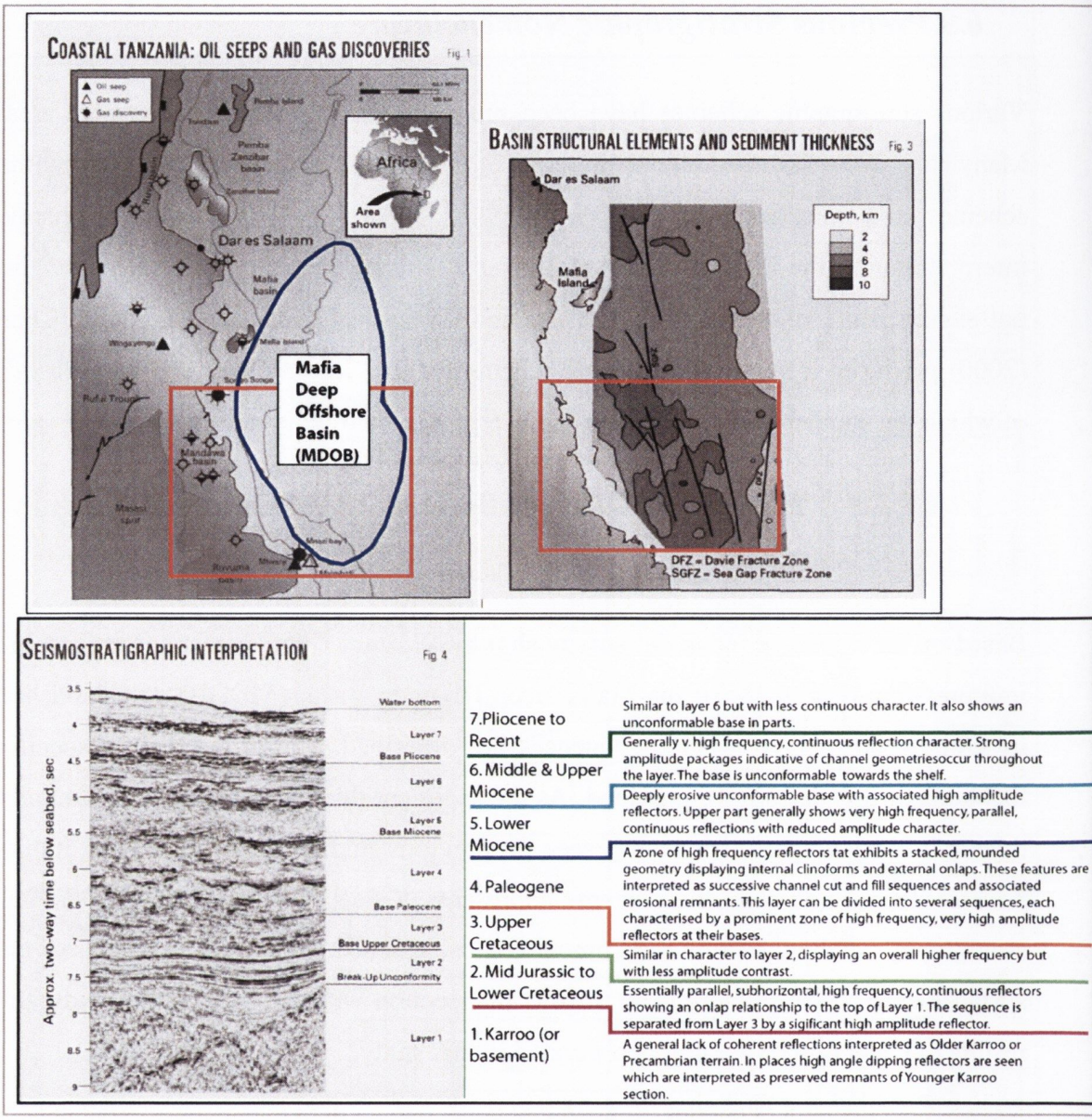

Figure 6.39: Seismostratigraphic scheme of the Mafia Deep Offshore Basin (MDOB). The study area is highlighted in red. Adapted from Cope (2000).

6.10. Summary

Incorporating a range of disparate previously published and un-published seismic and borehole data with new box-core biostratigraphic control, ages were assigned to the stratigraphic schemes established in Chapters 4 and 5. Thus a chronostratigraphic scheme was created. The results of that scheme and the data input are shown in Fig. 6.38. The following regional unconformities are correlated with GLOW seismic markers. Mid-Top Cretaceous corresponds to the base of DRIEZ II/3 and DR III/4. The Paleocene and Eocene are represented by KB II, part of DZ II/3, DR III/2 and DR III/3. The Base Oligocene to Mid Miocene corresponds to SG III, the upper part of KB II, DZ II/2 and DR III/1. The Mid Miocene to Base Pliocene is correlated to SG II/1 and II/2, KB I/2, DZ II/1 and DR II/1 & II. The Base Pliocene to Recent is represented by SG I, KB I/s, DZ I and DR I.

The seismic markers corresponding to the Mid Miocene include SG SM 02, KB SM 01 and DR SM 02. The seismic markers corresponding to the base Pliocene are SG SM 01, DZ SM 01 and DR SM 01.

7. The onshore geology of southern coastal Tanzania; assessing regional unconformities and introducing the Upper Oligocene-Quaternary Tipuli unit.

7.1.Introduction

Field surveys were undertaken to establish the onshore geology adjacent to the offshore survey area. Identification of principal regional unconformities that may extend offshore was used as a method of correlation from the onshore to offshore realm. The stratigraphy has been well established recently for the Mandawa Basin and the Kilwa and Lindi areas (Nicholas 2006, 2007; Hudson 2011). However the Neogene stratigraphy is poorly understood. By establishing the Upper Oligocene to Recent stratigraphy of southern coastal Tanzania sedimentological, stratigraphic and tectonic information could be extracted. Fieldwork was undertaken in August 2008 and 2009. This work was completed in co-operation with palaeontologists from Cardiff University and the age constraints based on planktonic foraminifera assemblages and larger benthic foraminiferal assemblages were invaluable. All the ages herein were assigned to field samples collected and examined both in hand specimen and thin section petrographic analysis by Paul Pearson and Laura Cotton of Cardiff University. Further data relevant to this chapter may be found in Appendix V.

As previously described in Chapter 3, an initial desk study was undertaken to review the previously published data. The study area has not been extensively mapped and much of the available data originates from industrial reports, accessible in the archives of TPDC. Available geological maps included Kent *et al.* (1971); Nicholas *et al.* (2006; 2007); Shell (1990); Texaco (1991); and Hudson (2011). Recent publications include Reuter *et al.* (2009) and Jiminez-Berrocoso *et al.* (2009). Stratigraphic terms used here are those recently consolidated in Hudson (2011).

At the end of this chapter, new terms are introduced for the Neogene and Quaternary; the Upper Oligocene – Pleistocene Tipuli Unit (Tu), including a Pleistocene Mbanja subunit (Msu). This is a chronostratigraphic unit identifiable in the study area, bound above and below by distinct surfaces, which are extended to the offshore via the transition zone. The identification and utilisation of the key bounding surfaces onshore enables the stratigraphy of the problematic transition zone (relatively shallow water and shelf area seismics) to be resolved and correlated to deeper water. The shelf and upper slope are more sensitive to sea level fluctuations and thus sequence

stratigraphic principles have more relevance in this zone. The application of the results of this chapter are therefore found in Chapter 8. Similarly, the structural geology of the onshore realm shall be discussed in conjunction with the structural geology of the margin in Chapter 9. Finally, the geological evolution of the margin as a whole is assessed in Chapter 11.

7.2. Previous Stratigraphic Nomenclature

7.2.1. Geological Maps

The only geological maps for use in the field are those published by Hudson (2011); Kent *et al.* (1971); Nicholas *et al.* (2006; 2007) and the unpublished Shell (1990) and Texaco (1991) maps.

Hudson (2011) reassessed the structural and sedimentological evolution of the Mandawa Basin in the light of new field surveys and produced several excellent structural and geological maps that extend south to the Mchinga area (Fig. 7.1). These maps have been used as the basis for this study and extending this reassessment further south. For a detailed, regional appraisal the Kent *et al.* (1971) 1:1,000,000 map remains the best reference (Fig. 7.2). It was compiled as a result of several expeditions by Shell geologists to the area in the 1950's. Many of the tracks and town names are still accessible. However, the Neogene outcrop is referred to as 'Marine Neogene' and 'Non-marine Neogene', hence further subdivision is required.

The Tanzania Drilling Project, or 'TDP' (1998-2009) successfully drilled twenty six shallow boreholes along the southern Tanzanian coast with the aim of retrieving sediment records of critical climatic intervals, producing geological maps in area of limited exposure and resolving structural issues. Detailed geological maps for the Kilwa, Pande and Lindi areas were produced at a scale of 1:10,000 (Fig. 7.3).

The Ruvuma Basin Field Study was commissioned in 1991 by Texaco and undertaken by consultants ECL. Included in the report detailing the regional geology are 1:250000 maps of the geology of the Ruvuma Basin and sample location plot. Also used as mapping tools are base topographic sheets (Fig 7.4) obtained from the Ministry of Minerals and Surveys and Digital Elevation Models (DEMs) obtained from the NASA website (NASA, 2010) (Fig. 7.5).

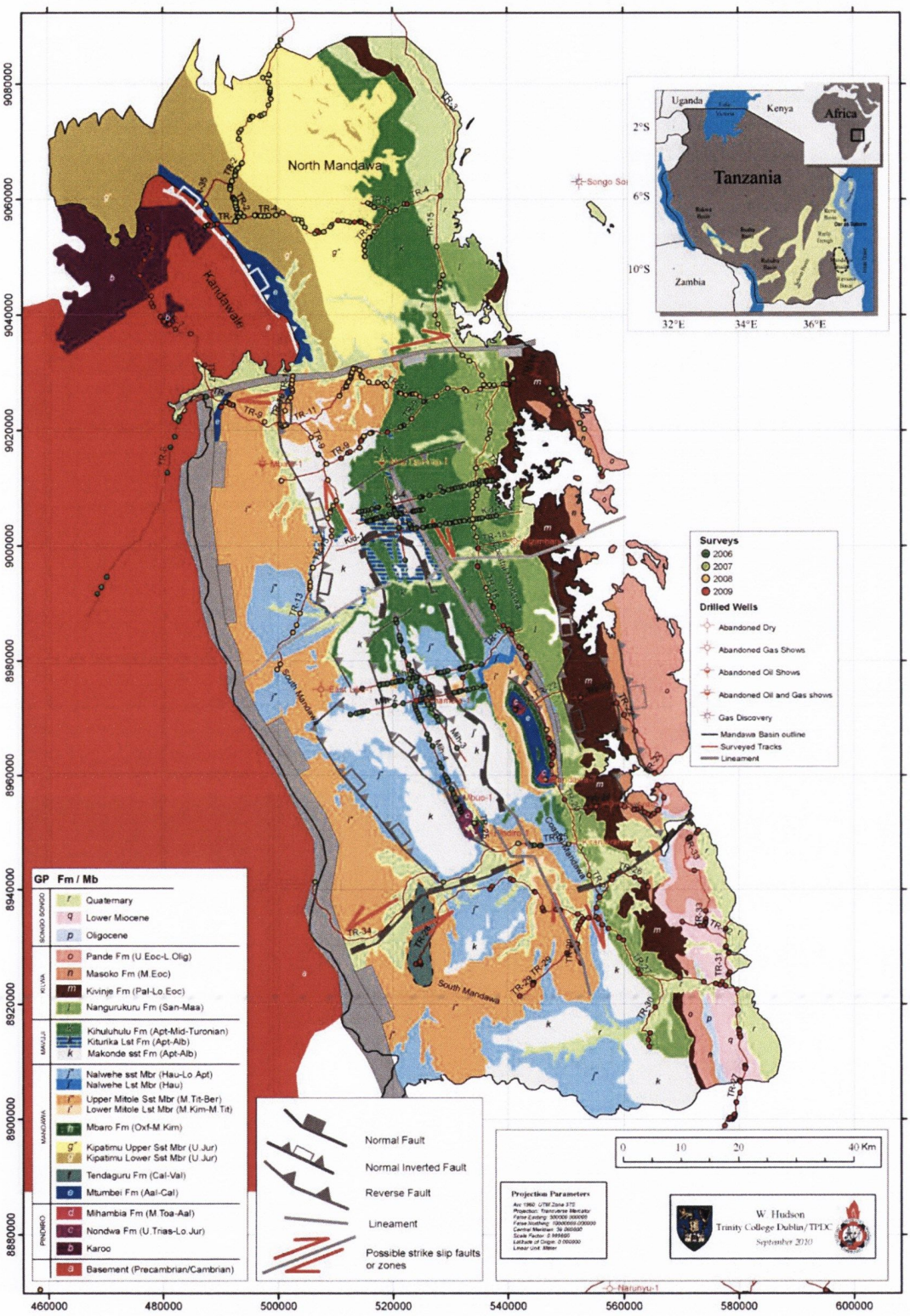

Figure 7.1: Geological map of the Mandawa Basin (Hudson 2011)

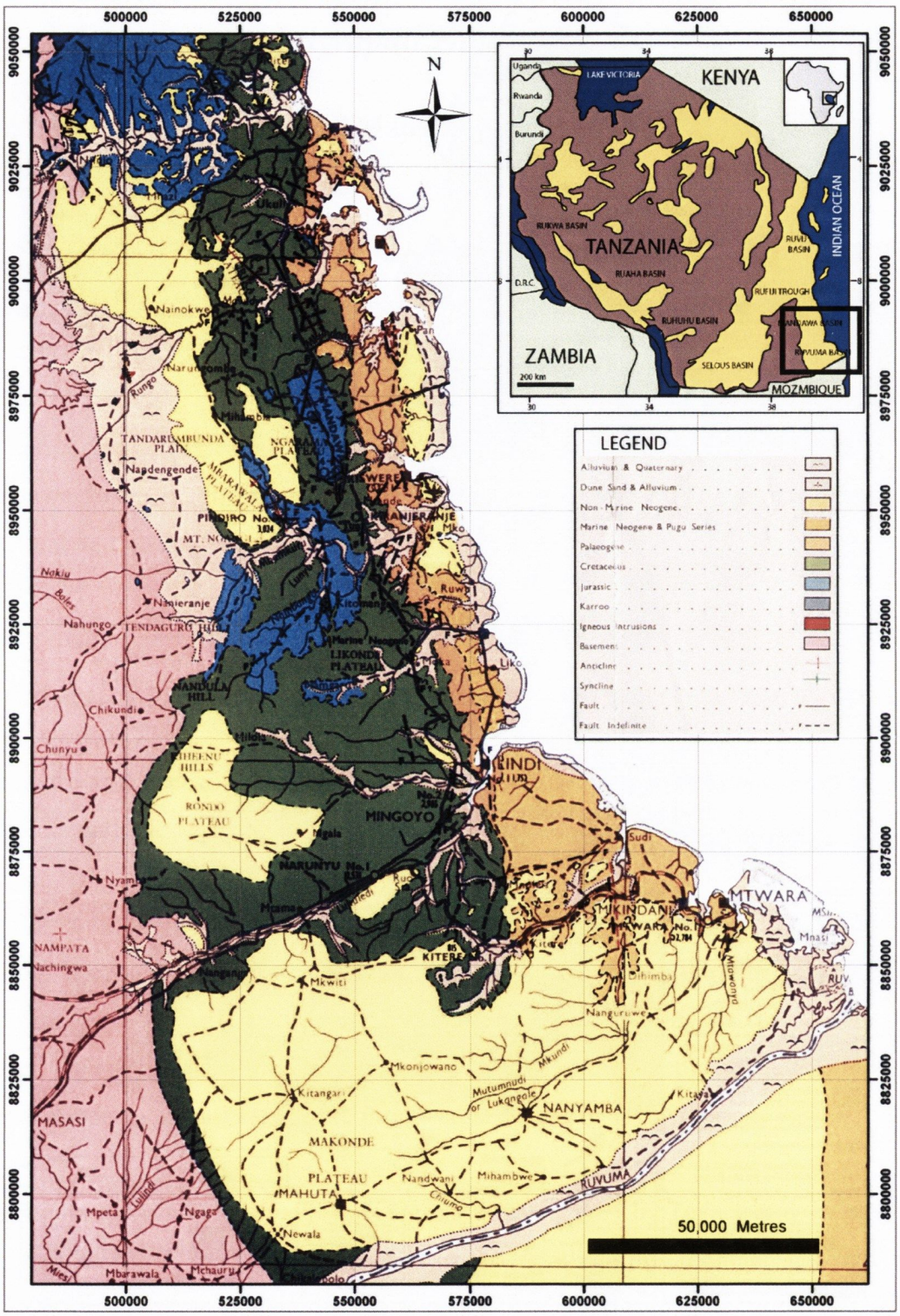

Figure 7.2: Geological map of southern coastal Tanzania (Kent *et al.* 1971)

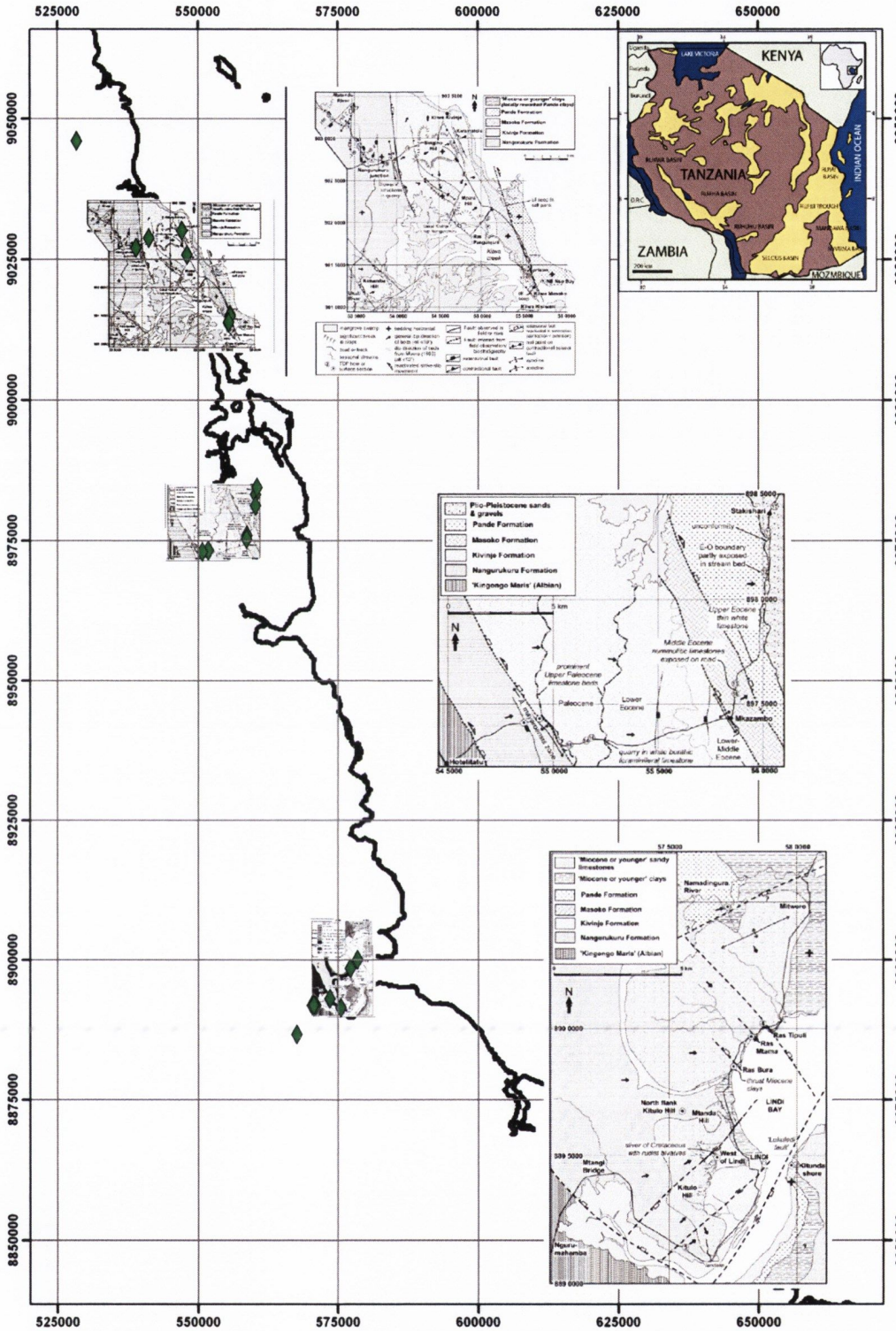

Figure 7.3: Location of TDP boreholes and the geological maps (Nicholas *et al.* 2006, 2007; Jiminez-Berrocoso 2009). The inset maps are shown expanded to the right.

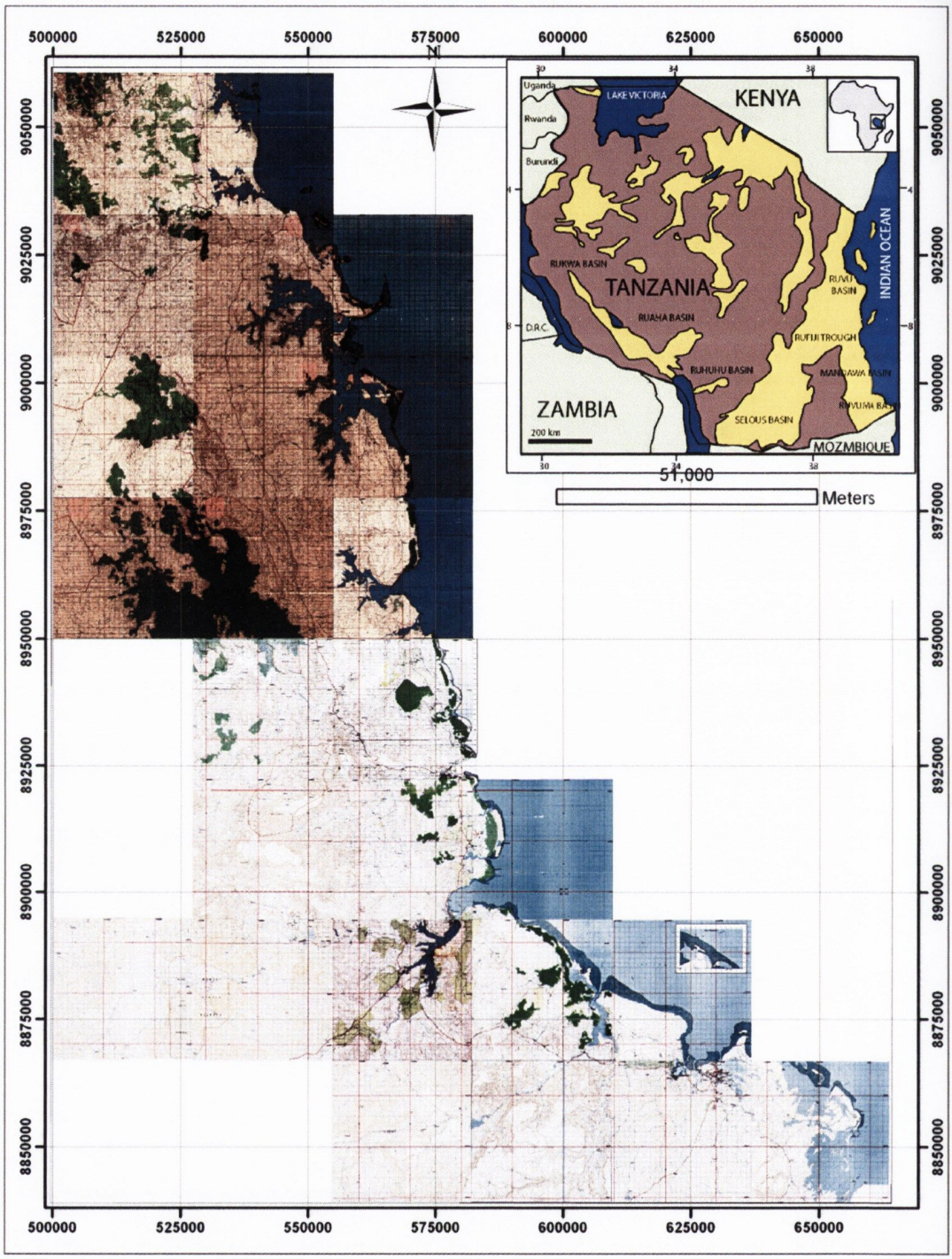

Figure 7.4: Topographic maps obtained from the Ministry of Maps and Surveys, used as basemaps for field operations.

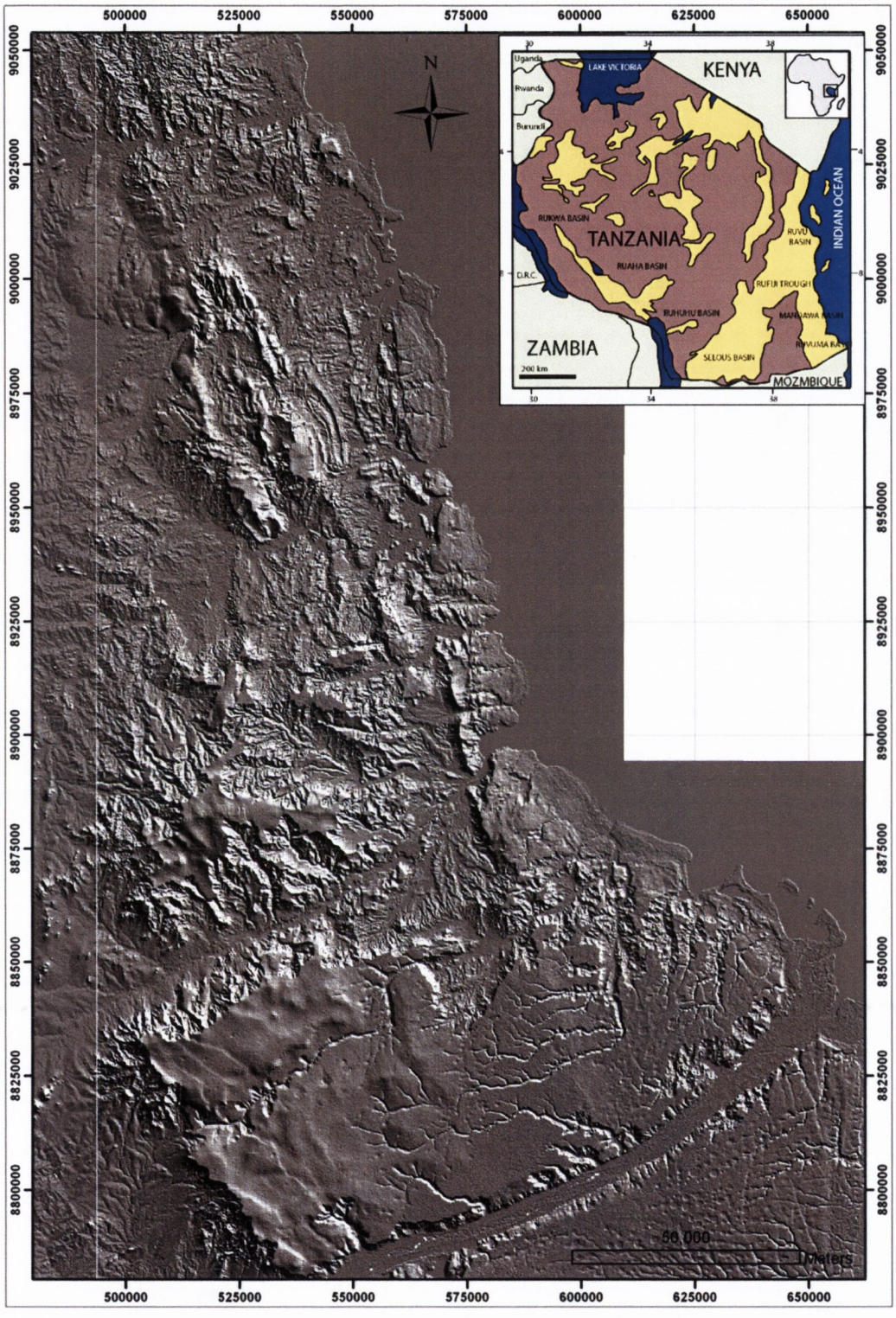

Figure 7.5: Digital Elevation Model (derived from SRTM3 data; NASA)

7.2.2. Onshore Stratigraphy (and Existing Stratigraphic Information)

A synthesis of the stratigraphy and existing stratigraphic nomenclature from published data will be given in this section. References will be made to areas within the study area and finally to the subsurface. A summary of the stratigraphic terms is shown below. The principal bounding surfaces that have been well documented and possibly extend offshore into the GLOW seismics include the following:

a) The Base Pliocene Unconformity
b) The Mid-Upper Miocene boundary Unconformity
c) The Upper Oligocene-Lower Miocene Unconformity
d) The Rupelian (mid Early Oligocene) unconformity
e) The Turonian-Santonian (mid Late Cretaceous) Unconformity
f) The Mid Cretaceous Unconformity

A summary of the established stratigraphic nomenclature with the approximate locations of distribution in both outcrop and subsurface is shown in Fig. 7.6.

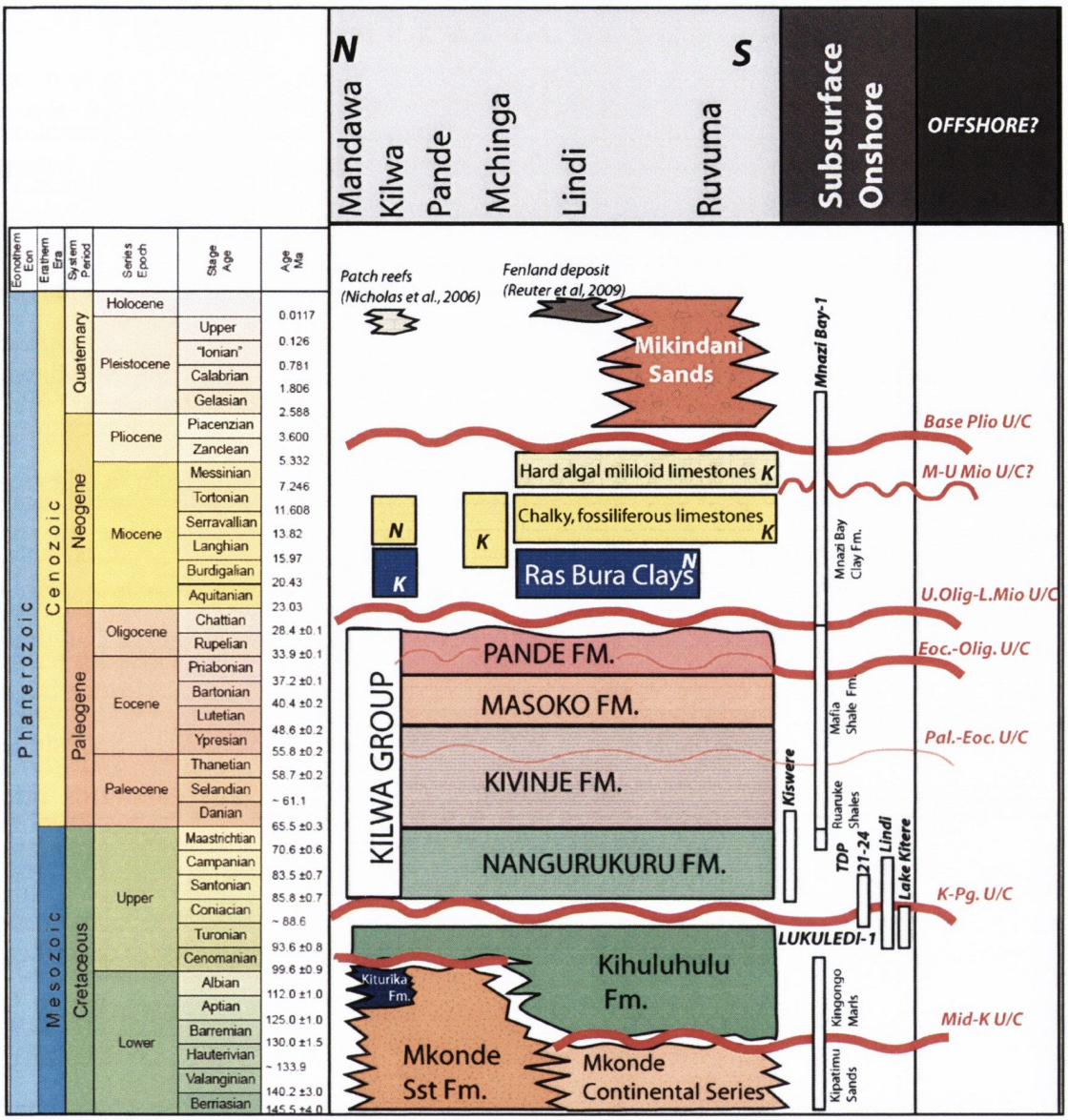

Figure 7.6: A summary of previous stratigraphic nomenclature. Adapted from Hudson (2011), Nicholas (2006)[N], Kent *et al.* (1971)[K], Reuter *et al.* (2009). Subsurface data including stratigraphic terminology is from Kidson *et al.* (1997). Shown projected are proposed unconformities that possibly extend offshore.

Lower Cretaceous (Berriasian to Hautevarian)

Renewed rifting in the Late Jurassic led to the creation of accommodation space within the Mandawa and the Ruvuma Basins (called Rovuma in Mozambique). Active erosion and deposition led to the accumulation of the fluvial clastic dominated Lower Cretaceous sandstones that dominate the margin at this time.

Fluvial sandstones with minor carbonate beds were deposited across the Mandawa Basin from Hauterivian to Lower Aptian times. The Mitole and Nalwehe Formations were described by Hudson (2011). They represent the transition from a clastic-dominated shallow marine environment to an alluvial/fluvial environment. In the Ruvuma Basin the Mkonde Continental Series were deposited (Texaco 1991) extensively across the Rondo and Mkonde Plateaux and extend south of the Ruvuma River into Mozambique. The non-marine mature sandstones and conglomerates have been previously called Mkonde Beds, Mkonde Sandstone and Newala Sandstone (Quennel *et al.* 1956). The Mkonde series appear to pass laterally eastwards into marginal marine rocks in the Mambi Valley west of Lake Kitere. Cenomanian-Turonian fauna from these marine-marginal marine beds and their presence in the Narunyu well log implies a shoreline at least this far west. Key *et al.* (2008) described the fluvio-deltaic Macomia Formation in the Mozambican Rovuma Basin, which is laterally equivalent to the Tanzanian counterparts; the Mkonde Formation. Similarly, in the subsurface the Lukuledi-1 well recorded 3142' of the Lower Cretaceous 'Kipatimu Formation'; thought to be comparable to the Mkonde Continental Series (Texaco 1991).

Mid Cretaceous (Barremian-Turonian)

After the period of active rifting a thermal sag phase and/or eustatic sea level rise led to a shelf wide transgression and homogenous clay deposition in the mid-Lower Cretaceous.

In the Mandawa Basin the fluvial and marginal marine sand-dominated units of the Lower Cretaceous sequences are overlain by a laterally extensive unit characterised by thick olive grey claystones or 'marls' with intercalations of turbiditic sandstones

deposited during the Aptian as the 'Kihuluhulu Formation'. A base Barremian unconformity is suggested from the overview of wells in the area. This is the bounding surface separating the Kihuluhulu and its contemporaneous Kiturika and Makonde Formations from the underlying sands. The Kihuluhulu Formation incorporates the previous nomenclature of the Kihuluhulu and Kingongo Marls defined by Balduzzi *et al.* (1992) in the Lukuledi-1 well. A minor regressional sequence is recorded in the uppermost Aptian. It is likely that the Pande High became exposed in part during this regressional event.

The Makonde, Kiturika and Kihuluhulu formations are contemporaneous in the Mandawa basin representing fluvio-deltaic, shallow marine and shelf environments near an Aptian-Albian palaeoshoreline. In the Ruvuma Basin, marine and marginal marine Cretaceous facies were observed in five localities during the Texaco survey. They range in age from Hauterivian to Turonian. The ages of exposed marine Cretaceous generally young from north to south.The TDP Sites 21-26 record several occurrences of Cenomanian to Turonian marine facies in the Lindi area. There are a series of disconformities or non-sequences from the Cenomanian to Santonian along the coastal zone. Exploratory boreholes Naranyu No.1, Lake Kitere, Lindi No. 1 and 2 yield similar marine/marginal marine Cenomanian – Maastrichtian aged rocks (Kent *et al.* 1971).

A transgression occurred in Aptian-Albian times and the Mid-Cretaceous shoreline extended further west in the Ruvuma than in the Mandawa Basin, possibly as far west as Lake Kitere in the Ruvuma Basin during Cenomanian-Turonian times.

Late Cretaceous (Campanian) – Paleogene (Early Oligocene)

Kilwa Group

A period of relatively uniform subsidence occurred across the shelf during the Late Cretaceous with clay deposition keeping pace with subsidence rates. This has been attributed in the past to the development of a passive margin. However, it is possible that the base Aptian Kihuluhulu Formation transgression and subsequent clay-dominated succession represents the post-rift thermal sag phase, effectively producing an enforced highstand for much of this time.

The Kihuluhulu Formation passes upwards into the Kilwa Group with little or no lithological change. The Kilwa Group outcrops along the coastal belt from The Rufiji River to the Lukuledi River. Extensive Miocene deposition in the Ruvuma Basin extended further inland than the Kilwa Group, effectively masking it onshore within the Ruvuma Basin. Kilwa Group clays have not been reported south of Lindi. However, as Key *et al.* (2008) have defined a lithologically similar Mesozoic to Cenozoic succession in the Mozambican Rovuma Basin and it is most likely that this represents the lateral equivalents of the Kilwa Group.

The Kilwa Group is a heterogeneous group of clays, claystones and marls that is at least 1km thick. Throughout the Kilwa Group turbiditic sands and carbonate beds are intermittent. Carbonate ramps developed along palaeo-strike and periodic storms and/or slope failure triggered debris flows which delivered pulses of clastic sediment dominated by benthic foraminifera to mid and outer ramp environments. In addition to these debris flows, thin distal turbidite sandstones occur with scoured bases, flute marks, graded beds, cross bedding and intensively burrowed tops. In the Pande area there is some evidence that the Kilwa Group may have continued as a minor palaeotopographic high shedding clay slumps and debris flows westwards into the Mandawa Basin and possibly offshore also.

The Pande Formation is the youngest within the Kilwa Group. At Pande, a conformable Eocene-Oligocene boundary was recovered by the TDP. The earliest Oligocene demonstrated a marked shallowing up trend towards the top of the hole. At present, no late Early or mid Oligocene sediments have been recognised along the onshore southern coastal zone. Kent *et al.* (1971) reported the existence of clays on either side of Lindi creek which yielded Oligocene ages, though these clays have not been found since. The limestone cliff on the south of Lindi (which is probably Kitunda cliff) was regarded as Oligocene by Henning (1914) but is now ascribed to the Lower Miocene on foraminiferal evidence (Kent *et al.* 1971). Although shown in the Shell Mandawa map (1990) there are no Oligocene samples recorded. It is possible that an early-Oligocene to Miocene unconformity may have led to the partial or complete erosion of some of the formations prior to the deposition of the Neogene.

At various localities, Miocene sediments unconformably overlie Lower Eocene or Paleocene beds.

Kent *et al.* (1971) also reported the presence of Oligocene in the Kiswere-Mchinga, Lindi and Lake Kitere areas. At Kiswere-Mchinga 70m of algal detrital limestones and grey silty clays with *Lepidocyclina* and *Nummulites* were reported (Kent *et al.* 1971). At Lindi 90m of rubbly silty limestones and clays with *Lepidoclyclina*, *Spiroclypeus* and the diagnostic *Nummulites fichteli-intermedius* occur. Remnants of eroded blocks of limestone with *Lepidocyclina-Nummulites* and *Eulepidina dilatata* have been found near Lake Kitere.

In the subsurface, a number of wells penetrated the Kilwa Group. Kiswere -5 spudded in on Lower Paleocene in the Kiswere area and recovered sediments to Cenomanian-Santonian age. Lindi -1 spudded in on Maastrichtian and recovered sediment to Turonian. It is now well documented that the Eocene-Oligocene boundary correlated with the onset of major northern hemisphere polar ice accumulation. It is therefore likely that the top bounding surface of the Kilwa Group is a significant unconformity onshore and corresponds to this Early –Mid Oligocene lowstand.

Neogene: Miocene

The Miocene stratigraphy has not been formally defined in southern coastal Tanzania. Following the global regression in the early Oligocene, the Miocene is strongly transgressive in coastal Tanzania, as elsewhere in East Africa. The underlying Kilwa Group facies are largely laterally continuous, whereas the post-Oligocene units are highly variable both laterally and stratigraphically. They comprise mainly clays and shallow marine limestones with more extensive coverage reported in the south.

The first recognition of post-Paleogene stratigraphy originated from the original research by Bornhardt (1900); Scholtz (1911) and Oppenheim (1916) who informally recognised the 'Lukuledi Beds'. On the southern side of the Lukuledi River at Kitunda, south of Lindi. Haughton (1938) subdivided the 'impure greyish-yellow to reddish fossiliferous limestone, with angular to little rounded quartz pebbles, grey

porous limestone, light grey hard coral and foraminiferal limestone' into two informal sub-units; Lindi Uppermost Beds and Kitunda Beds. However, Nicholas *et al.* (2006) has suggested that the macro and micro fauna indicate a part Neogene age, most likely a mix of Plio-Pleistocene reef knolls, marine sands and Miocene reef limestones.

A Miocene unit was recognised by Terris and Stonely (Moore *et al.* 1963) in Kilwa. A series of clays were reported occurring in north Kilwa Creek on the large island to the north of the Mavudyi creek system and capping a northward trending peninsula to the east of Namatazu Island. Prolific ostracod fauna led to the age of Miocene, probably Lower Miocene being assigned. A limestone sample from between Singino Hill and the coast was dated as Lower Miocene or younger (Moore *et al.* 1963). Similarly, at Kilwa, Kent *et al.* (1971) reported 55m of Miocene grey clays and coral limestones unconformably overlying Upper Eocene, which are in turn unconformably overlain by Pliocene or Quaternary reef knolls. Nicholas *et al.* (2006) decribed Miocene or younger benthic foraminiferal limestones from Nangurukuru Quarry.

Further south, at Kiswere-Mchinga, Kent *et al.* (1971) reported a significantly thicker sequence of 600m of Miocene interbedded clays and detrital or sandy limestones. Only 150m of Miocene buff-grey and brown grey silts are reported for Lindi with *Eulipidina, Spiroclypeus* and *Miogypsina.* Nicholas *et al.* (2006, 2007) reported Lower to Middle Miocene clays on the north shore of Lindi Bay and Upper Miocene clays with thin limestone stringers exposed in the cliffs at Ras Bura. These Upper Miocene clays were sampled unconformably overlying Paleocene clays of the Kilwa Group in a quarry north of Lindi. A shelf-wide unconformity in the Mid-Oligocene combined with lithological and facies differences means there is a distinct bounding surface at the top of the Kilwa Group and the overlying 'Miocene and younger' beds may be assigned to a different formation or chronostratigraphic unit.

In the Ruvuma Basin, the Lower Miocene is the dominant marine formation at the surface, transgressing beyond the Kilwa Group and Upper Cretaceous clays. The stratigraphy is described as comprising three lithologies (Kent *et al.* 1971). The base comprises clays while the middle beds are chalky limestones often with molluscs, including abundant *Lopha virleti*, frequently echinoids and sometimes *Lepidocyclina* coquinas. Dips are variable indicating shallow water deposition. Lastly, a hard algal-

miliolid limestone forms a capping to the plateau. The thickness of the entirety of the Miocene beds is difficult to assess but is likely ~1100m near Mtwara.

In the subsurface the Miocene is penetrated by Mnazi Bay – 1 and Mtwara No. 1. The Texaco reports identify Mid Miocene foraminifera in calcareous sandstones and reef limestones in the Mambi Valley west of Lake Kitere. Similarly, Kent *et al.* (1971) reported that small outliers exist as far inland as NE Mandawa. They show a shallow facies and frequently contain allochthonous material from the ground over which they spread.

It is clear from the reported occurrences of Miocene lithologies that there was significant subsidence towards the south of the Ruvuma Basin compared to the Mandawa Basin for this thick accumulation of 'Miocene or younger' to form.

Neogene; Pliocene

Compared to the Miocene the Pliocene was a period of major regression in southern coastal Tanzania. The main reported occurrences of Pliocene sediments are of the mainly continental 'Plio-Pleistocene' 'Mikindani Formation' of continental sandstones, gravels and clays. This facies is very similar to the Mkonde Continental Series in the Ruvuma Basin. Variously described, these fluvial strata are not necessarily of one age, and it is very difficult to separate from the Lower Cretaceous sands, particularly in the Ruvuma Basin.

Kent *et al.* (1971) describe the Mikindani Beds resting on an irregular surface and heavily dissected. 'Continental red beds' (Moore *et al.* 1963, after Terris & Stonely unpublished report 1955) were decribed as capping Singino and Mpara Hills in Kilwa and overlying Lower Miocene clays in Kilwa Creek, comprising mainly loose red sand and colour varying from pale yellow-pale white. The sand is mainly coarse grained but silts to conglomerates with pebbles of quartzite and vein quartz are also present. 'Mikindani Beds' sands and gravels become quite extensive further south towards Mtwara (Nicholas *et al.* 2007). Dipping eastward the dips are the same as that of the slope and are thus blanketed on topography not dissimilar to the present day one. Kent *et al.* (1971) claim they are clearly appreciably younger than raised coral

reefs and terraces of the coast so that a Pliocene or early Pleistocene age seems most likely. However, their exact dating and equivalence remain to be established. The fact they overlie Lower Miocene clays in Kilwa indicates a post Lower Miocene age.

Minor marine beds that occur in association with the Mikindani Beds include Pliocene reefal red-bed limestones up to 25m thick in Kilwa Bay (Kent *et al.* 1971). At Kilwa cliffs 7m of reef limestone occur on the western side of the local islands. The rock contains a variety of both simple and compound corals together with a few shells and small foraminifera. They have been broadly assigned a Pliocene age. At Lindi there are 30m of coral limestones, rubbly sandstones and clays with *Pecten vasseli*. South of Lindi chalcedonized sandstones, interbedded with the terrestrial Mikindani sandstones, gravels and clays are believed to be Pliocene in age.

It is interesting to note that Neogene to Recent residual sands, gravels and in some cases, boulder beds are also widespread at lower elevations to the west of the main plateaux in the Ruvuma Basin in particular. It is possible that they represent collapse and/or erosion of the formerly more extensive Mkonde Series. Indeed, it is worth noting that the plateaux of the Ruvuma Basin (Makonde and Rondo) are now significantly higher than the basement to the west, forming a substantial west facing scarp of fluvial red sands. Pebbles and boulders from this lithology were often the source of ancient human stone workings (Texaco 1991).

Neogene; Pleistocene

Pleistocene patch reefs with benthic foraminifers that indicate an Eemian or younger age are scattered across the Kilwa Pensinsula amongst the 'Mikindani Beds' (Nicholas *et al.* 2006). Reuter *et al.* (2009) reported the presence of a Pleistocene fenland deposit at Mbanja Quarry northwest of Lindi. This will be discussed in more detail in subsequent sections.

7.3.Field Geology of the Kiswere Area

The Kilwa and Pande Peninsulas have been well studied by Nicholas *et al.* (2006; 2007) and Hudson (2011) (Fig.7.7) and will not be repeated here. However, new information can be added to the coastal Kiswere area, south of Pande.

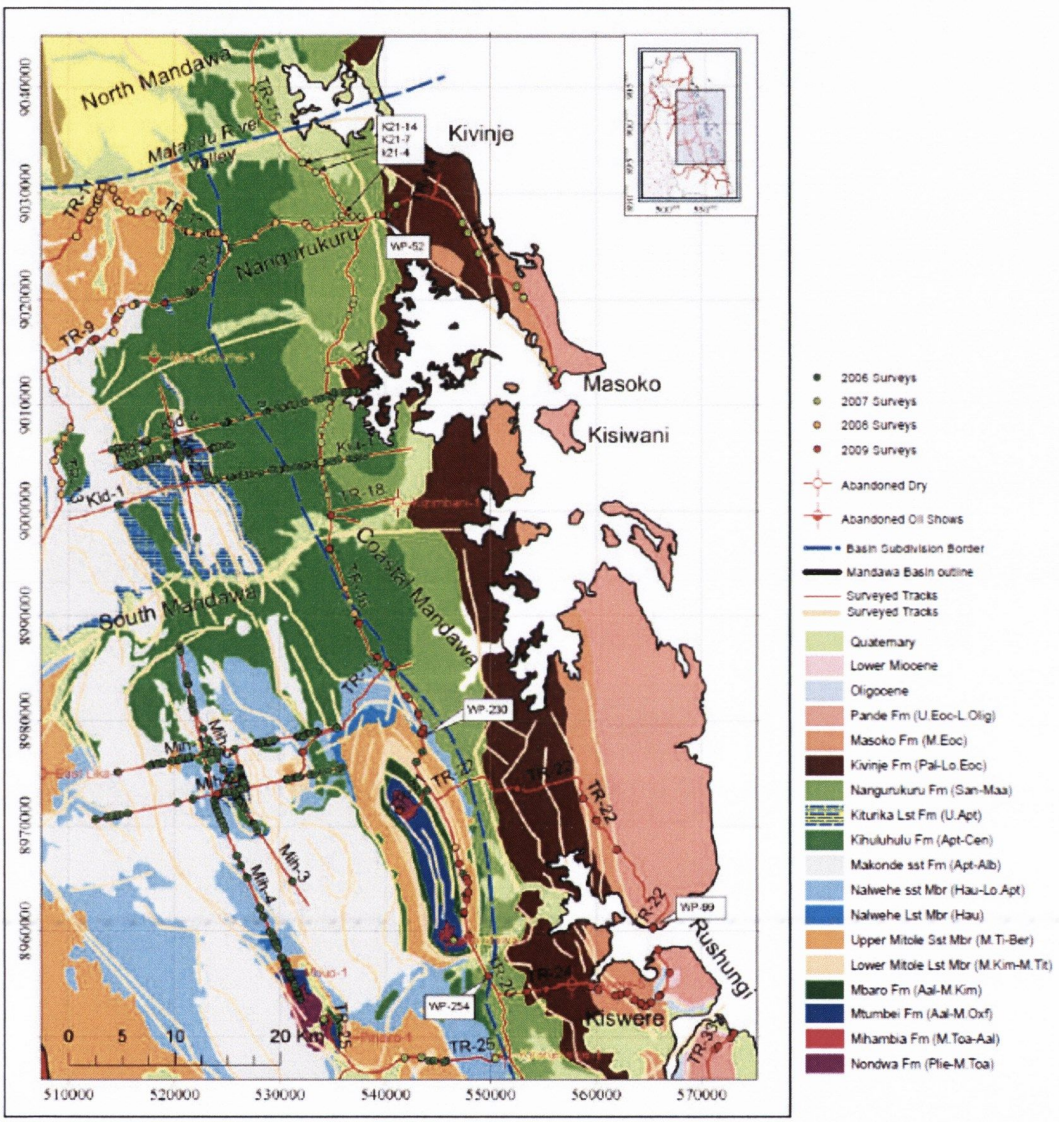

Figure 7.7:Coastal Mandawa bedrock geology (Hudson 2011)

Kiswere is a small peninsula, located south of the Pande Peninsula and is bound above by Kiswere Haven and below by Msungu Bay (Fig. 7.8). It is separated from the Mandawa Basin by a series of faults. A carbonate ramp succession across the critical Eocene-Oligocene transition was recorded at Kiswere (Cotton and Pearson, 2011). The headland was originally thought interesting because it has a series of NW-SE trending hills with an unusual topography and may be offset from Pande by a large right lateral strike slip fault. Thus, it was felt that important structural information could be obtained from re-examining it, particularly as it is located 4km from GLOW Line 9. The geology of Kiswere is fairly unusual in this coastal belt indicating a structural control over the aggradation of sediment here. It is interesting to note that the youngest facies observed on Kiswere were Lower Oligocene, indicating this area has been a relative high since that time.

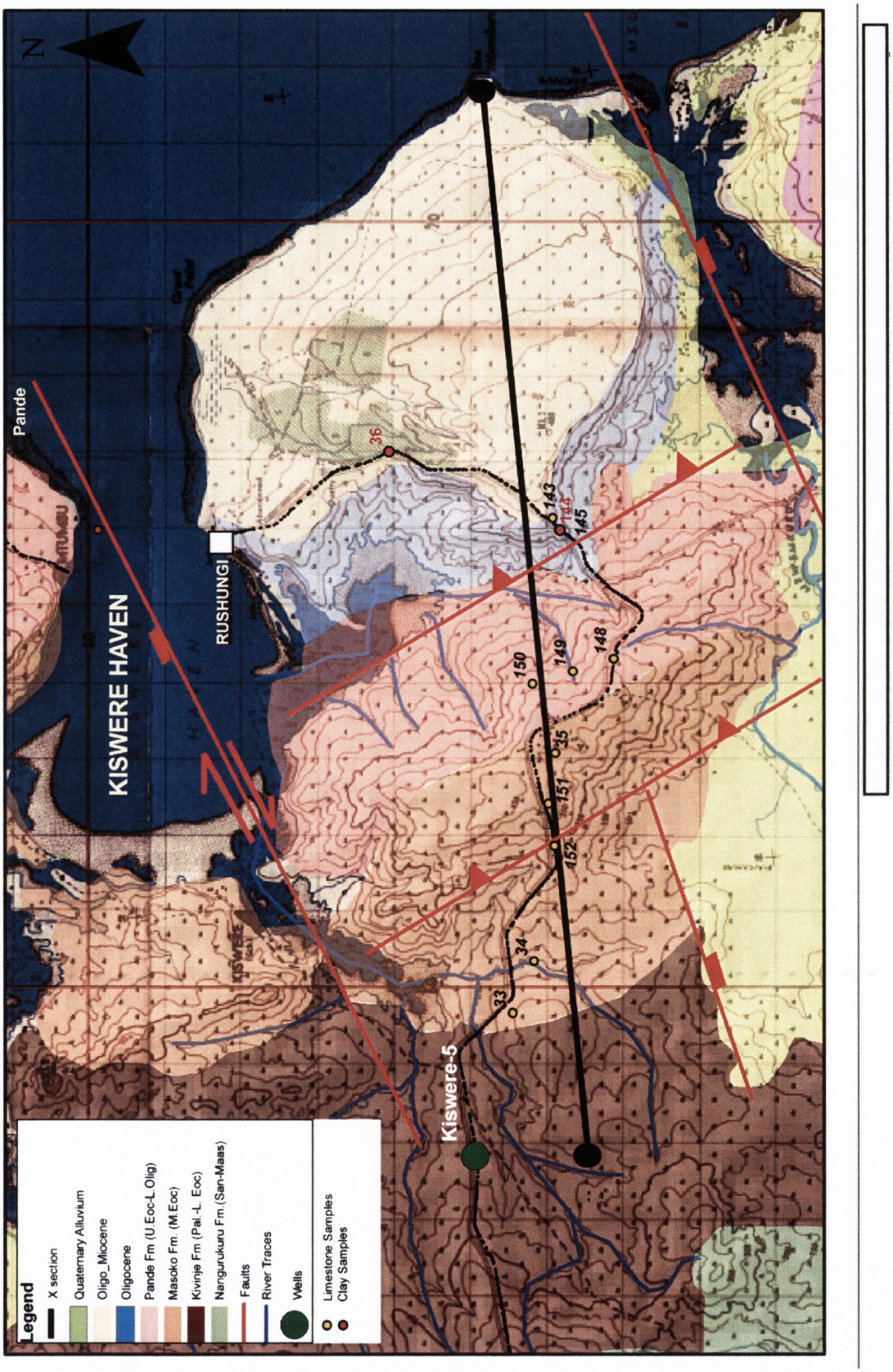

Figure 7.8: Geological map of Kiswere Haven (1:75, 000). Scale bar is 10km. The black line indicates the line of section drawn in Figure 7.9. Numbers refer to samples taken and the colour is representative of limestone (orange) or clay (pink).

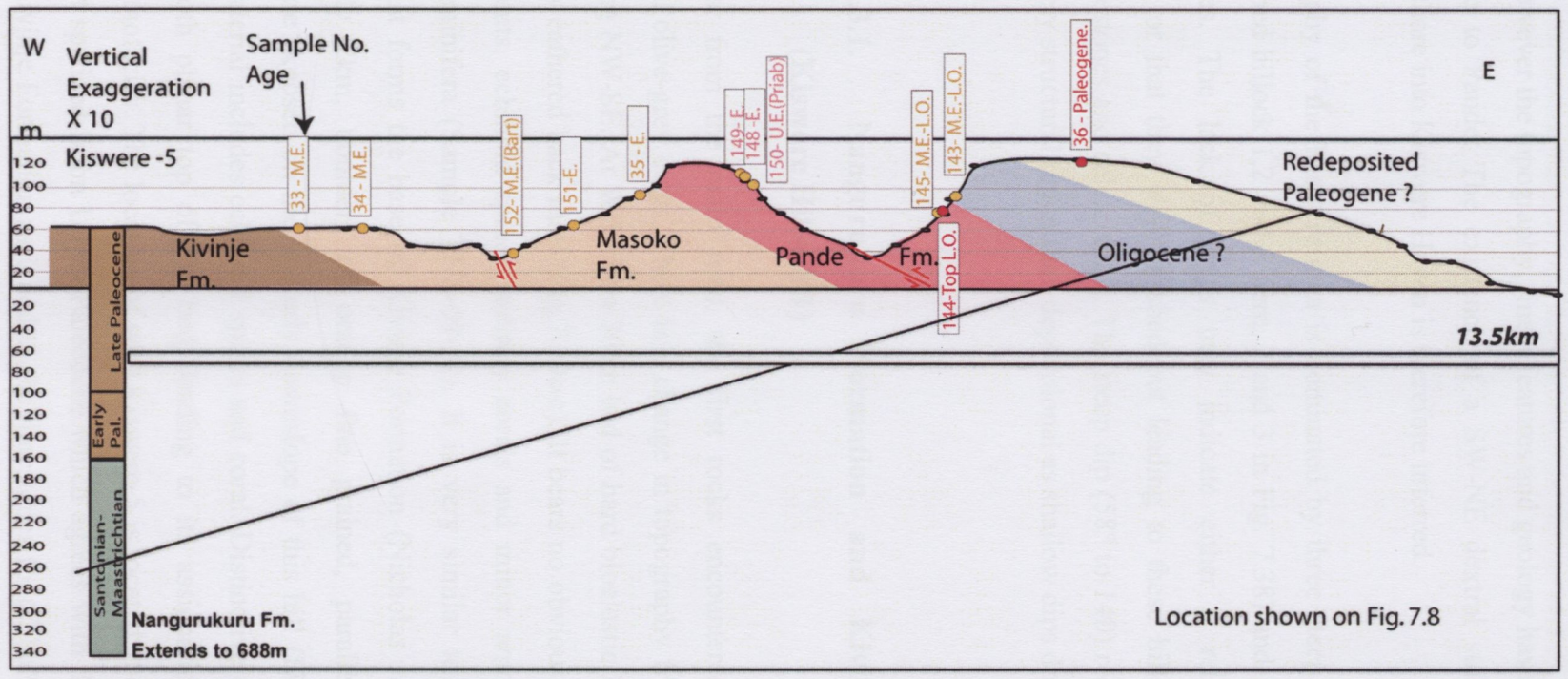

Sample	Large Benthic foraminifera: Pellataspira	Somalina	Nummulites	Alveolina	Discocyclina	Heterostegina	Assilina	Alveolina	Rotalids	Amphistegina	Sphaerogypsina	Linderina	Operculina	Other fossils	Age	
36															Paleogene (redeposited)	Redeposited Paleogene
143 Large benthic foraminifera packstone			x			x							x	Echinoid fragments, miliolids, red algae, smaller benthics.	Eocene-Lower Oligocene	Oligocene
144															Top Lower Oligocene (O3)	
145			x			x							x	Dasyclads, echinoid fragment, miliolids, red algae, ?bryozoan.	Mid Eocene-Lower Oligocene	
150 Shell hash lst	x		x	x	x				x		x	x		Miliolids, bryozoan attached to shell, echinoid fragment, red algae, smaller benthic forams.	Upper Eocene(Priabonian)	Upper Eocene
148 Shelly sparite									x		x			Miliolids, red algae, echinoderm fragments, smaller benthic forams (agg)	Eocene	
149 LBF lst						x				x	x	x	x	Planktonic foraminifera, coral fragments, miliolids, smaller benthic foram (agg), echinoid fragments, red algae.	Eocene	
35			x		x									Miliolids, red algae, benthic foraminifera (agg?), mollusc shell fragments with attached bryozoan.	Eocene	Mid Eocene (Lut-Bart.)
151 Large benthic foraminifera packstone			x		x			x	x	x				Miliolids, smaller benthic forams, red algae.	Eocene	
152			x			x	x	x	x					Miliolids, red algae (+some growing over large Nummulites), echinoid fragments, gastropod, planktonics in one area.	Mid Eocene (Bartonian?)	
34		x	x	x	x									Miliolids, small "spikey" rotaliids gastropod, benthic forams, tube	Mid Eocene	
33		x	x	x										Complex miliolids, Bryozoan fragment dasyclad, smaller rotaliids, red algae (inc Distichoplax type)	Mid Eocene	

Nangurukuru Fm. Kivinje Fm. Masoko Fm. Pande Fm.

Approx. 1km thick

Clay Details

36 Poorly preserved forams, oxidatised material, very sandy. Forams infilled and sparse. Two types of quartz, wind blown sand grains, shell and algal fragments.

Subbolius sp (?)/subolina;
radiate Nummulites sp. (eroded benthic forams)

144 Some glassy forams although preservation variable

Globigerina praebulloides,
Globigerina ciperoensis,
Dentoglobigerina larumi,
?Protentella sp.,
Globoturborotalita woodi,
Globorotaloides,
Chilogwembellina ototara,
?Pararotalinaa pseudokugleri,
Chilogwembellina cubensis

Fig. 7.9: Cross section, stratigraphic column and sample descriptions of Kiswere. Line of section is highlighted on Fig. 7.8; the geological map of Kiswere. N.B. Please note the vertical exaggeration on the cross section is 10.

The Kilwa Group Formations outcrop in the Kiswere area in a broadly similar pattern to Pande. However the topography, linear features and geology have been offset to the west relative to Pande. The existence of a SW-NE dextral strike slip fault that emerges offshore into Kiswere Haven is therefore inferred.

The topography of the Kiswere area is dominated by three steep south east facing scarps (Termed hillock 1,2 and 3 here, 2 and 3 in Fig. 7.38) and gentler north west facing slopes. The lack of clays may indicate either a relatively shallower environment or that they were washed out leading to these hillocks of the more resistant limestones and calcarenites. The steep dip (58° to 140) recorded at WP 325 are more likely structural rather than depositional as shallow dips dominate the coastal belt.

7.3.1. Nangurukuru Formation and Kivinje Formation (Kiswere Hillock 1)

Driving west from the main road, the first rocks encountered in outcrop are Nangurukuru olive-grey clays. There is a change in topography from flat to a steep scarp trending NW-SE. At WP 325 a 30cm bed of hard bioclastic limestone is found overlying a weathered back marl (Fig.7.10a-c). It bears no obvious forams, but some shaly fragments, echinoid spines, solitary corals and minor amount of mm scale benthic foraminifera (Sample TNZ-09-32). It is very similar to the quartz sandy limestone that forms the base of Kivinje Formation (Nicholas *et al.* 2006). After approximately 2km, boulders of orange fine grained, parallel bedded, sandy calcarenite are exposed on the westerly downslope of this hill (Fig. 7.10 d-e). Fine bioclastic material includes echinoid spines and coral. Distinctive trace fossils occur on the smooth planar top of the bed, leading to its assignation to the Kivinje Formation lithofacies. The location of well Kiswere-5 is located at (557776, 8954968 ; Fig. 7.8). It spudded in on Upper Paleocene which agrees with the Paleocene ages and hence Kivinje Formation assigned to the limestones found between here and the Nangurukuru Formation. The sharp change in topography and occurrence of steeply dipping Kivinje Formation limestones and calcarenites indicated the presence of a fault at the base of the hillock.

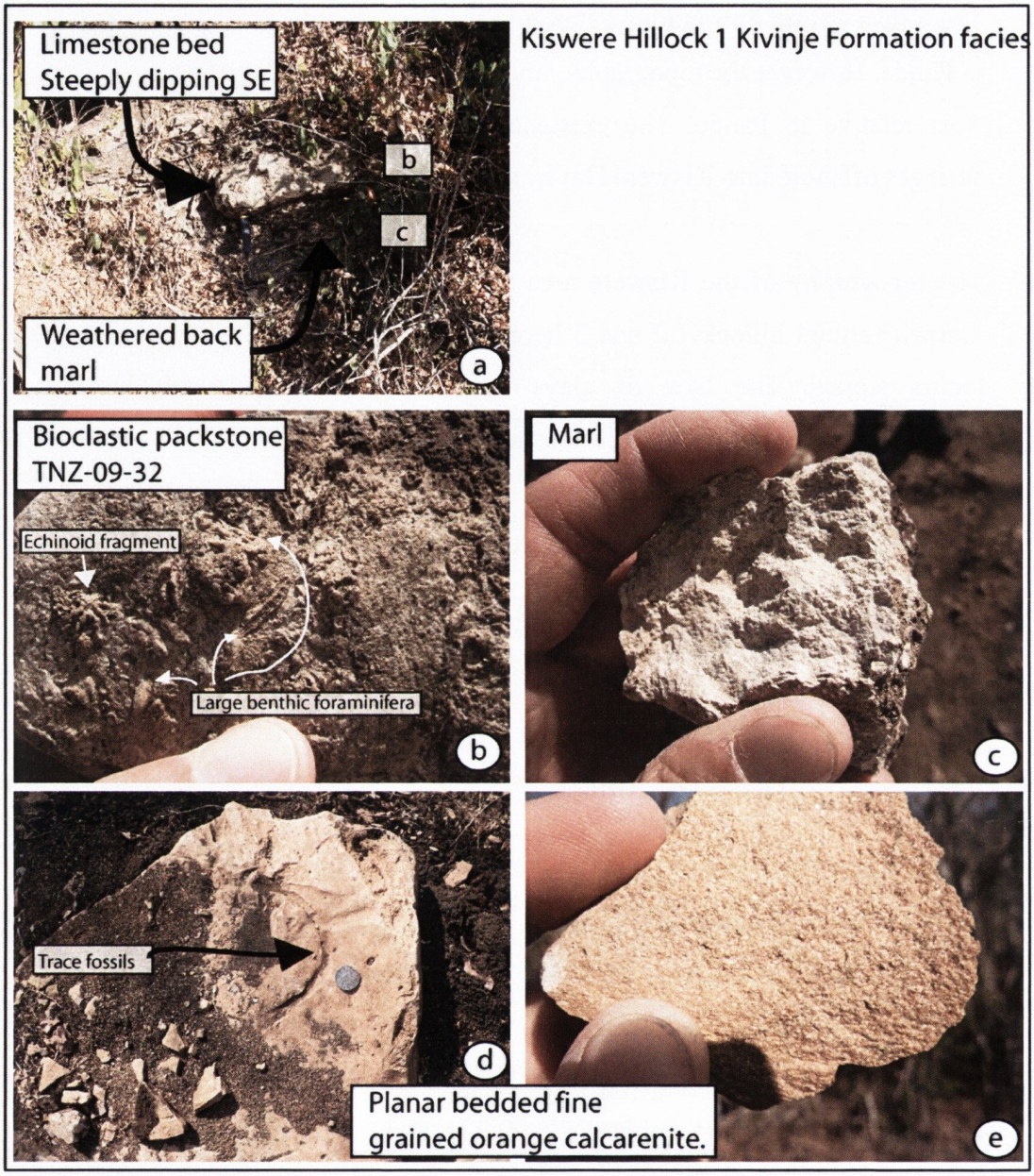

Figure 7.10: Compilation of Kivinje Formation facies in Kiswere. The letters (a-e) are referred to in the text. (a-c) is the oldest Kivinje Formation outcrop at WP 325 at the base of hillock 1; (d and e) classic Kivinje Formation calcarenites with distinctive trace fossils.

7.3.2. Masoko Formation (Kiswere Hillock 2)

After driving downslope eastwards from the Kivinje Formation calcarenites that probably form the dip slope of hillock 1, the topography begins to steeply rise again (Fig. 7.8). A steep scarp is present for approximately 3km, climbing from near sea level to a small plateau at the height of 125m above sea level. Boulders of large benthic foraminifera packstone with sparry cement are scattered along the roadside climbing the steep scarp The limestone outcrops on this hillock have no defined bedding orientation and appear to be weathering out from underfoot. The sedimentary facies is variable and a compilation of the observed facies is shown in (Fig. 7.9). Sample TNZ-09-152 is a sparry limestone rich in large very flat *Nummulites* and *Assilina* with a coiled cross section, small benthic foraminifera, clay intracalasts and micrite. However, , a fine grained white-cream micritic sparite forms a ledge (TNZ-09-151). Near the top of the small plateau, there are two distinct types of lithology; (1) a carbonate cemented sandy limestone with quartz grains, sparse small benthic foraminifera and a burrowed surface; (2) an orange bioclastic packstone dominated by shelly debris, mainly large benthic foraminifera (TNZ-09-35).

Samples TNZ-09-33, 34,152,151 and 35 all lie within the Middle Eocene age range assigned due to the presence of key large benthic foraminifera (Fig. 7.9). In general the Middle Eocene large benthic foraminifera packstones contain a variety of *Nummulites, Somalina, Alveolina, Discocyclina, Heteroestegina, Assilina, Alveolina, Rotalids* and *Amphistegina.* Other fossils include miliolids, bryozoans, dasyclads, red algae, gastropods and smaller benthic forams. They are interpreted as representing an in-situ carbonate platform deposit.

While the sedimentary facies of the western flank of hillock 2 is somewhat varied, the biofacies are remarkably consistent. There is no evidence of reworking and the sedimentary variations possibly reflect varying sediment sources within the carbonate ramp.

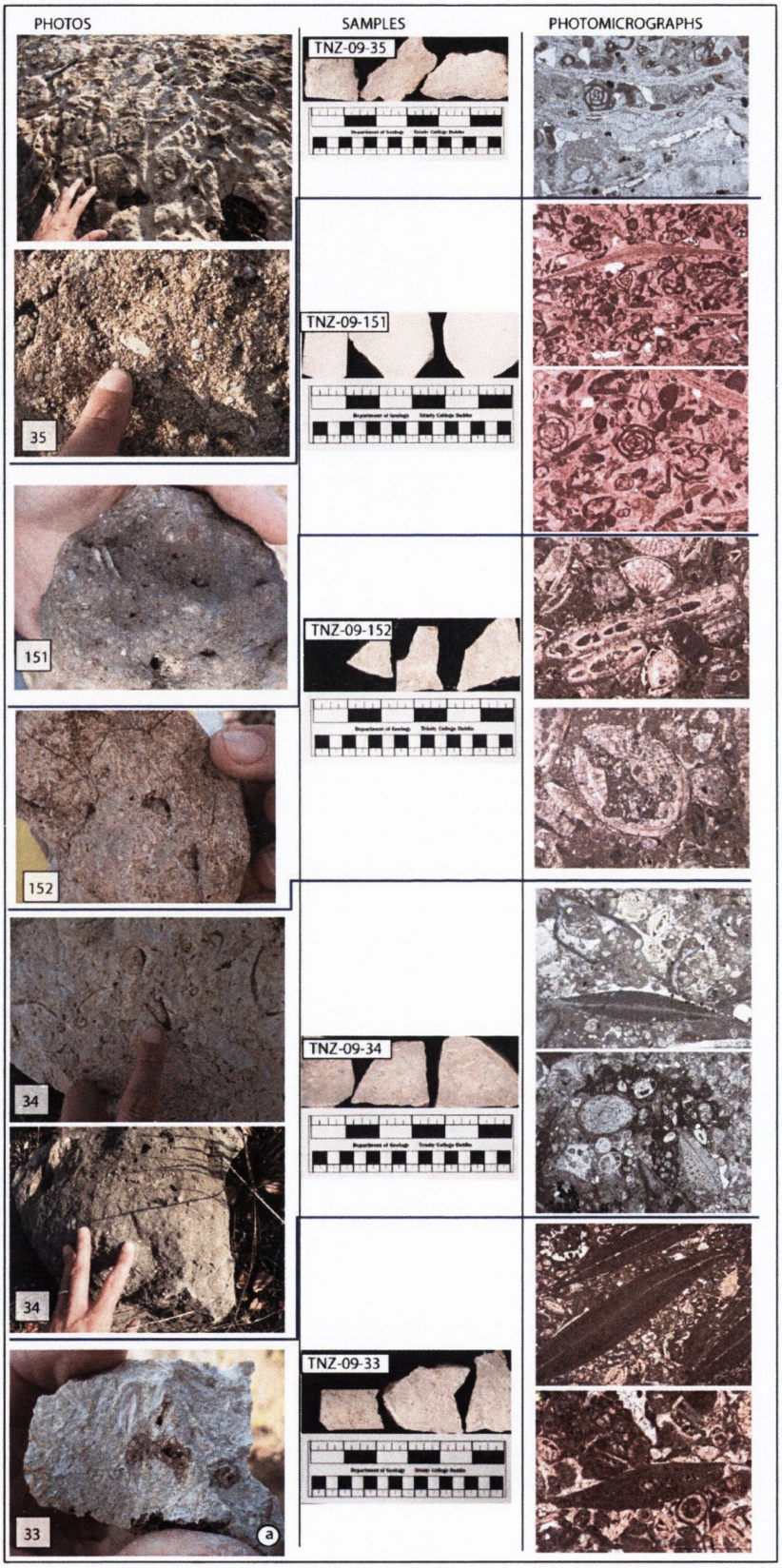

Figure7.11: Compilation of hand samples, cut surfaces and photomicrographs from the Masoko Fm. on Kiswere. The numbers refer to the sample nos. as described in the text. The location of the samples is highlighted in Figs. 7.8 and 7.9. Distinctive benthic foraminifera are evident both in hand specimen samples and in thin section.

7.3.3. Pande Formation (Kiswere Hillocks 2-3)

Coming downslope of Kiswere Hillock 2 (Fig. 7.8), samples 147, 148, 149 and 150 were taken (Fig. 7.7). The lithofacies were quite mixed, but in general comprised bioclastic sparites with echinoid spines, nummulites, corals and shelly debris. A compilation of the observed facies is shown in Fig. 7.10. A shell hash wackstone at (Sample TNZ-09-150) has been dated as Uppermost Eocene (Priabonian) on the basis of the presence of *Pellatispira*, which is largely restricted to the Priabonian and only found very close to Eocene-Oligocene boundary in TDP cores on Pande (Cotton and Pearson, 2011). Thus this transect likely represents an in-situ carbonate ramp accumulation across the Eocene-Oligocene climatic transition. Located immediately above Sample TNZ-09-150 is sample TNZ-09-147;a bioclastic sparite with 15% shelly debris (none intact) and coarse angular quartz grains.

Climbing the western flank of Kiswere hillock 3, a thin clay bed outcrops between two limestone beds. It lies at WP 550 (Sample TNZ-09-144) immediately above a nummulitic limestone (Sample TNZ-09-145). Within the basal limestone above the candidate E-O boundary the *nummulites* are 2-3mm and significantly smaller than those in the older stratigraphy. Large benthic foraminifera (*Lepidocyclinids*) comprise approximately 30% of the sample with minor amounts of echinoid and bivalve shells. One particularly large complete echinoid, approx. 6cm in diameter was seen. Based on the benthic foraminiferal assemblage in Sample TNZ-09-145 and the planktonic foraminiferal assemblage in TNZ-09-144, Mid Eocene-Lower Oligocene and Top Lower Oligocene (O3) were ascribed to these samples respectively.

Overlying the greenish clays (at WP 550,96m asl), are boulders of pale cream pink micrite packed full of *nummulites* (0.5 – 1cm) with rare larger benthic foraminifera and *operculinas* with a distinctive swirly texture. An Eocene to lower Oligocene age was assigned and as the clays immediately below are Top Lower Oligocene, these are likely Uppermost Lower Oligocene. From this location, 96m above sea level to the top of Hillock 3, the surface is coated in black stained rubbly boulders of limestone and calcarenite, reaching a maximum height of 108m. Some are poorly sorted calcarenites; carbonate cemented with coarse quartz grains, pebbles and some coral

fragments and occasional *Lepidocyclinids*. However, it is not immediately clear where the quartz was derived from. This indicates however a possible Upper Oligocene – Lower Miocene section. The northeasterly dip slope of this hillock forms the bedrock as it gently reached the sea at Rushungi where modern day beachrock and quartz rich coral is found (Fig. 7.12 c, d). An outcrop of greenish-grey clay rich soil (Fig. 7.12a-b) was sampled in a roadside gully at [0566999, 8956081]. It was very rich in *Lepidocyclina Amphystigina?,* however yielded a Cenozoic age, and was quite likely redeposited indicating it was most likely derived from the material in the hills above. Finally, red lateritic soils coat the surface.

Due to the occasional steep dip of the limestone beds in an overall gently dipping environment, steep slopes and narrow hills a number of post-depositional reverse faults are interpreted as existing on the Kiswere peninsula in a NW-SE orientation and usually at the base of the prominent topography of the hillocks.

Figure 7.12: Examples of outcrop from the eastern side of hillock 3. (a and b); Very sandy clay with poorly preserved forams, (infilled and sparse) and oxidised material were present. Two types of quartz, wind blown sand grains, shell and algal fragments were also found, (c) Quartz rich coral reef with red coral sand developing in the vugs, (d) modern day beach rock developed near Rushungi, (e) View looking northwest towards Rushungi from the top of hillock 3.

7.3.4. Depositional Environment of the Kiswere Area

The Kiswere succession is interpreted as representing accumulation in a mid-carbonate ramp environment. Ramp facies reflect the protracted offshore energy gradients which are a consequence of gradual water depth change (Burchette and Wright; 1992). Thus, individual ramp depositional zones have different compositions. Mid ramp facies form below the fair weather wave base (FWWB) and therefore represent storm event and deposits. During fair-weather intervals, sediment is formed by suspension fall-out (terrigenous mud or lime) and becomes bioturbated.

The optimal tectonic settings for ramp development are continuous subsidence, slight gradients and relatively shallow water depths. This carbonate ramp likely formed after a phase of extension on the Kiswere Fault. It most likely formed in a quiescent phase post-rift when the relief was relatively low and subsidence was slow. The sea level remained relatively constant for the time of the carbonate ramp facies accumulation. A drop in sea level of a few metres would expose the complete ramp. Thus carbonate ramps are very sensitive indicators of sea level variation.

A shallowing up section is recorded in Kiswere Hillocks 1 and 2, with increasing bioclastic debris content. A major sea level fall is indicated by the presence of inner-ramp grainstones (Sample 143) overlying outer-ramp clays (Sample 144). The whole ramp was gradually exposed and karstified. Sediment was subsequently eroded and redeposited on the dip slope.

7.4.Field Geology of the Mchinga/North Mchinga Area

Mchinga is a village located south of Kiswere and at the mouth of Mchinga Bay. The area between Mchinga and Msungu Bay/Kiswere is referred to here as North Mchinga (Fig. 7.13). The topography is generally of a flat-lying limestone platform dipping gently east and surrounded by areas of lower lying topography; Lake Mkoe and the River Mariki (which enters Msungu Bay) floodplain to the north, the Mbwemkuru River valley to the south (which enters Mchinga Bay) and the relatively low-lying Kitomanga area, located between the Ruawa Plateau and the coastal Mchinga platform.

This area is of interest because it is located to the south of the Mandawa Basin bounding fault and north of the Ruvuma Basin bounding fault, on a basement high referred to as the 'Ruvuma Saddle'. As there has been relatively little petroleum prospecting in this area, its geology is poorly understood.

A number of key outcrops were identified in this area which help to resolve the Palaeogene and Neogene stratigraphy. The outcrop geology is dominated by Early to mid Miocene limestone facies. It is interesting to note that no sediments younger than Mid Miocene were observed, indicating this area has been a relative high since Mid Miocene times. The following areas will be described in turn; Lake Mkoe, Ngomba Quarry, Mchinga Village, Nondo and the North Mchinga Plateau (Fig. 7.13).

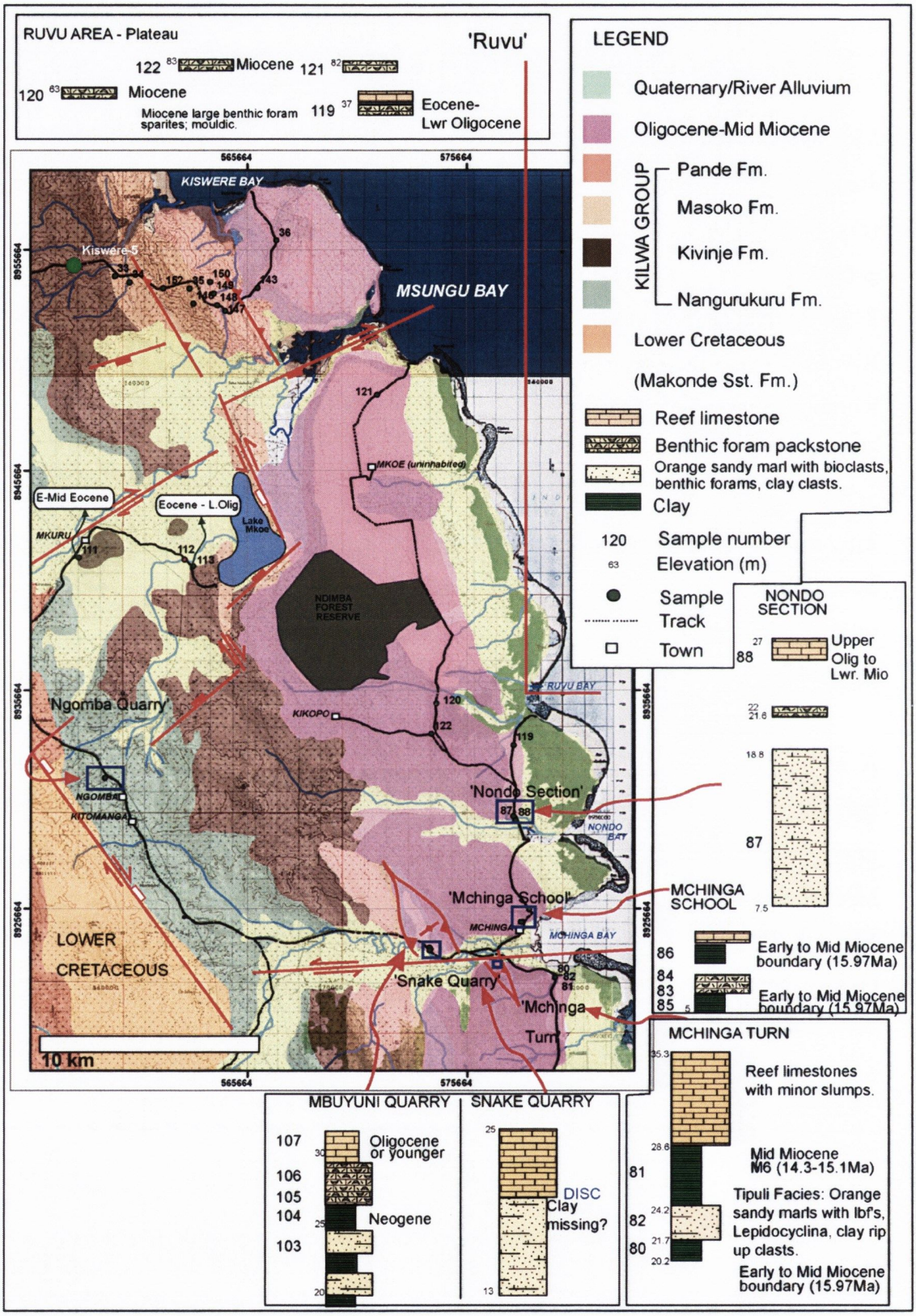

Figure 7.13: Geological map (1:150, 000 scale) of the North Mchinga area with schematic outcrop logged sections inset. The locations referred to in the text are highlighted by blue boxes.

7.4.1. Lake Mkoe Area; Eocene-Oligocene reef knolls

The Lake Mkoe area is located immediately to the southwest of the Kiswere-Rushungi Area (Fig. 7.13). It was reached by turning eastwards from the main road 4km north of Mingoyo at WP 458. It is noticeable that it is of significantly lower elevation and in the floodplain of the Mariki River. Underfoot, lateritic and recent sand overlies brown earth. It is marked on the Hudson (2011) map as Quaternary-River Alluvium. However, the solid geology beneath is probably Upper Cretaceous Nangurukuru Formation (Figs. 7.13; 7.6).

In the flat lowlying topography a number of mounds were apparent (Fig. 7.13). To the east of Mkuru Village, a mound approximately 50 long and 8m high was visible (Fig. 7.17a). No bedding was observed although grey boulders of pale white-orange benthic foram limestone (Fig. 7.17b) were eroding out of the surface (TNZ-09-111). An increase in benthic and echinoid fragments was noted from the base towards the middle of the mound. At the top of the mound nummulites are the dominant biofacies. The presence of key benthic foraminifera (*Discocyclina, Alveolina, Nummulites, rotaliids)* indicates a Mid-Upper Eocene age (Fig. 7.14c). Similar mounds are scattered in the Mkuru Village vicinity. Near the end of the navigable track (WP 464) past Lake Mkoe a small hillock of limestone boulders was seen. Pale orange, nummulitic limestone with echinoid spines and small shelly debris (possibly benthic foraminifera) were sampled (Sample TNZ-09-113). The presence of nummulites indicated an Eocene-Lower Oligocene age.

These mounds are probably isolated reef knolls that formed during background Kilwa Group deposition. None of the lithologies appear to be debris flows and their morphology would be a strong indicator for isolated reef knolls. The surrounding clays were probably washed out and/or covered by Recent river alluvium (Sample TNZ-09-112). At the time of deposition this location was perhaps considerably deeper than the carbonate ramp developed at Kiswere, based on fauna. This indicates a probable normal fault located between the Lake Mkoe reef knolls and the Kiswere

area along strike) to create the accommodation space for clay accumulation with isolated reefs as opposed to the shallow waters for a carbonate ramp at Kiswere.

Figure 7.14: Eocene-Oligocene reef knolls near Mkuru, Lake Mkoe; their appearance in outcrop and photomicrographs.

In the base of the floodplain at WP 461, a sample was taken of the clayey brown earth (TNZ-09-112).This very fine sand is poorly sorted, with rock fragments, pyritised wood and no forams. It is most likely the river alluvium that feeds eventually into Lake Mkoe to the northeast of this location.

At WP 464 the track stopped but the Ndimba scarp east of Lake Mkoe was most noticeable from this vantage point.

7.4.2. Ngomba Quarry; A Pleistocene (?) Fossil Mangrove Deposit

To the west of the main road at WP467, there is a recently excavated quarry, exposing approximately 16m of predominantly marls with calcitic crusts and fossilised mangrove leaves and pneumatophores. Approaching the village of Ngomba from the north there was a noticeable change in lithology from lateritic and recent sands of the area north of the bridge over the Mariki River to the white marly outcrop in the Ngomba area (Fig. 7.15, 7.16a, b).

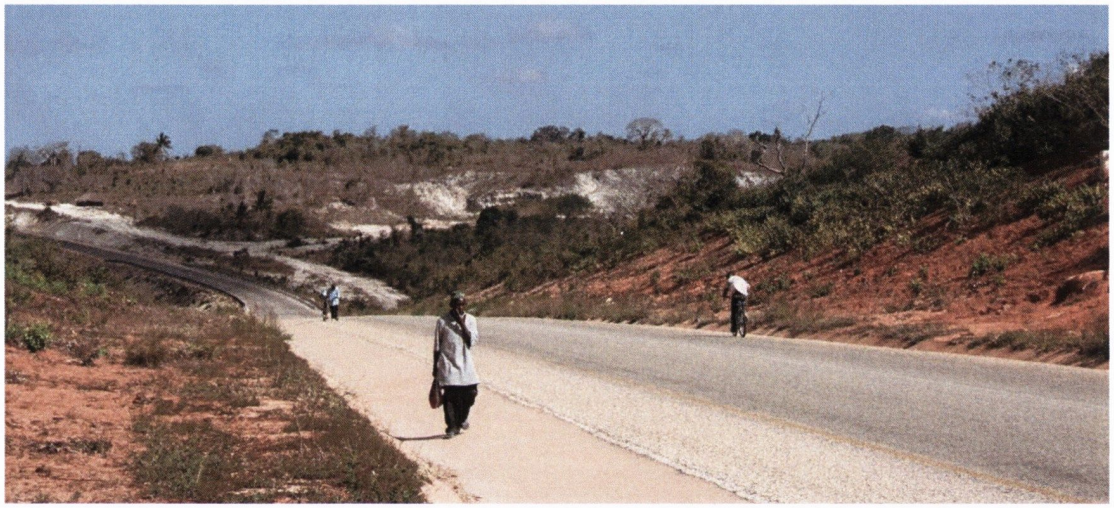

Figure 7.15: Photo taken from north of the River Mariki looking south towards the marl dominated quarry at Ngomba. Note the contrast between the lateritic soil derived from Lower Cretaceous sands nearby and the white argillacous carbonate mud of the Ngomba fossil mangrove deposit. A fault was inferred on the basis of the marked stratigraphic contrast.

There are approximately four lithologies exposed here; (1) a white porous unconsolidated chalky marl with harder brown grey calcitic cemented leaves and leave fragments; (2) A fine sandy brown clay with gastropods (Fig. 7.16c); (3) Fine white marl with gastropods with a karstic surface that forms a ledge (Fig. 7.16d) and (4) An algally bound mouldic limestone with the moulds in the shape of pneumatophores (Fig. 7.16e-g). Some scattered fossilised mangrove leaves occur but they are not abundant.

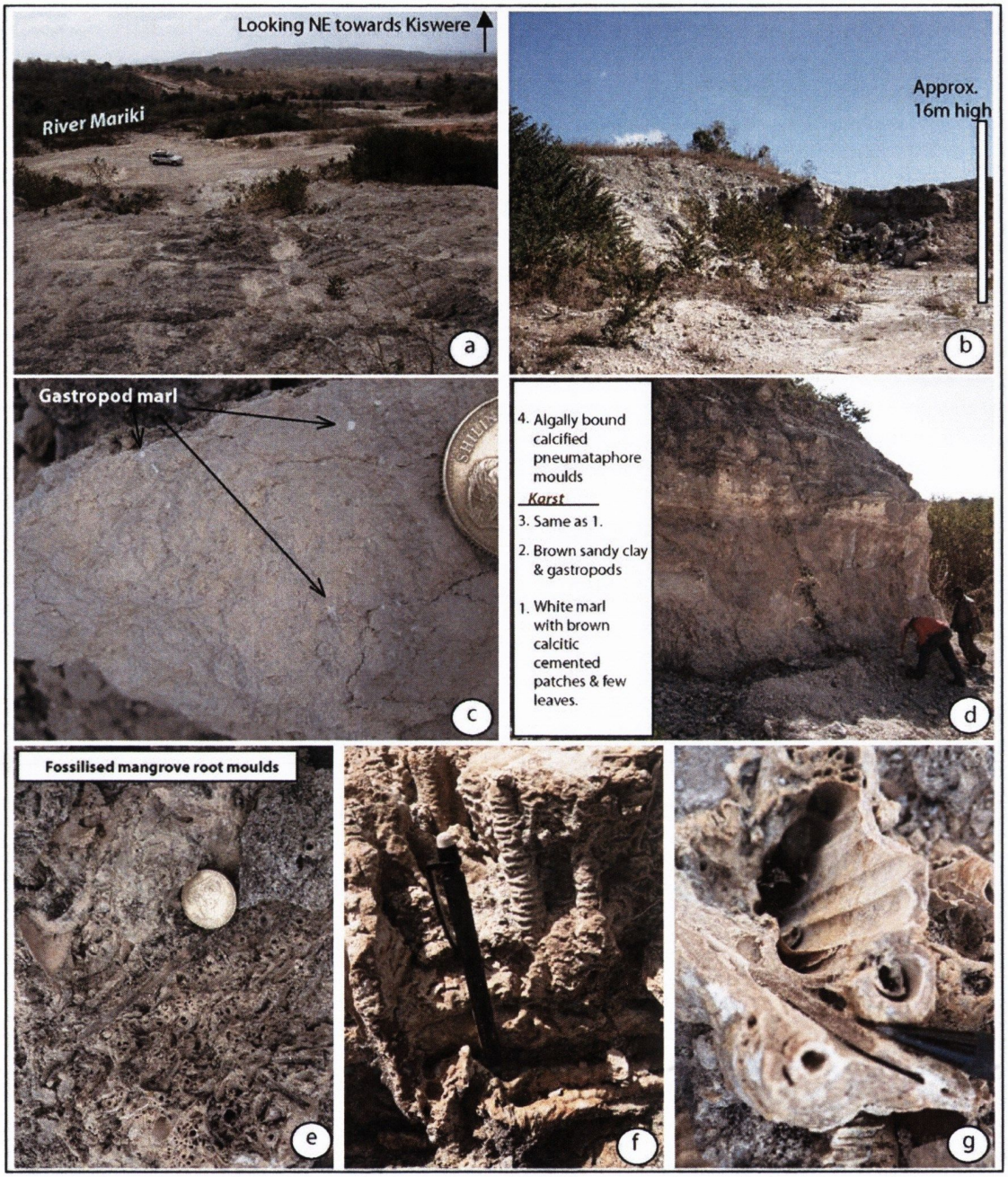

Figure 7.16: Ngomba Quarry (location shown on Fig. 7.11). (a) Looking NE from the summit of Ngomba Quarry across the Lake Mkoe floodplain towards the prominent topography of Kiswere, (b) Ngomba Quarry from the road entrance reaching approximately 16m high, (c) The silty, pale brown marl with mm-scale gastropods (Facies 1 in d), (d) a schematic profile of the clif face in Ngomba with four principal layers identifies, (e) near the summit of the quarry hard calified tube moulds occur (f) the cast of fossil mangrove pneumatophores and (g) the excellent preservation of the interior structure of a pneumatophore.

Driving further south from this locality towards Kitomanga, marls still mark the roadside (WP469). Another small quarry of marl overlain by an 80cm bed of pale brown-white algal limestone with an almost oncolitic texture shows a similar facies to the Ngomba Quarry (Fig. 7.17). The marl reaches up to 3.5m at its thickest and the overlying limestone dips gently to 109° (SE). Thus this facies is laterally extensive in a NW-SE direction for over 8km adjacent to the Ruawa Plateau (Makonde Sst Fm. (Aptian-Albian)).

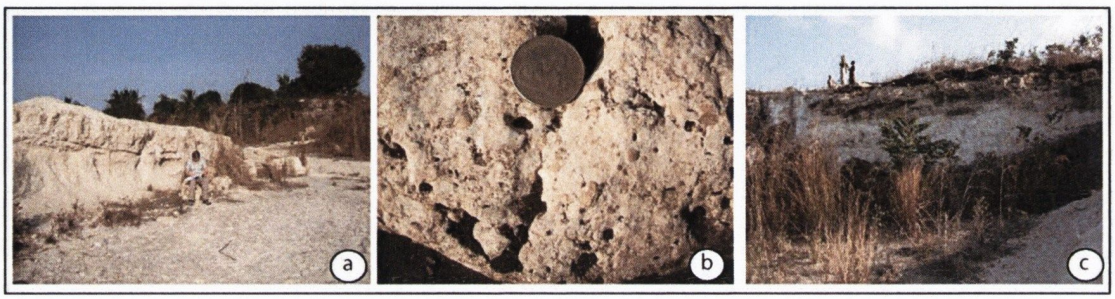

Figure 7.17:Extension of Ngomba Quarry 8km south at WP 469. Similar karstic surface is visible. (a)Limestone beds dip gently ESE, (b) Oncolitic texture of limestone beds, overlying white marls (c) white powdery texture of ledge.

Similar facies were recorded further south in Mbanja (Section 8.5.1) and most likely represent a fossil mangrove setting, as opposed to the published interpretation of a 'fen' (Reuter *et al.* 2009). Usually formed at sea level or slightly inland in river mouths the presence of this section here 22km inland and 134m asl (above sea level) will be discussed later with the description and interpretation of the Mbanja subunit. The presence of the Rivers Mariki and Mbwemkuru and their orientation indicate that the North Mchinga area may have been a palaeo-high while the sea transgressed behind to deposit what is thought to be these Plio-Pleistocene deposits. Alternatively the deposits may represent the furthest point reached by the Miocene-Pleistocene coastline. Indeed the Ruawa Plateau would form a significant barrier to further transgression. The geological map published by Hudson (2011) shows the presence of Nangurukuru Formation clays here.

7.4.3. Mchinga Bay Area –Early to Mid Miocene Facies

Upper Oligocene to Mid Miocene stratigraphy is exposed in the vicinity of Mchinga Village (Fig. 7.13). The plateau north of Mchinga extends to Msungu Bay and can be considered a laterally continuous limestone platform reaching approximately 80m above sea level. It overlies outcrops exposed from sea level to approximately 30m above sea level in the Mchinga village area and also the roadcuts at Mbuyuni, Snake Quarry and Mchinga turn. The exposures at Nondo (N of Mchinga village), Mchinga school and Mbuyuni Quarry are described below. Prominent topographic features including NW-SE linear ridges are present at Mbuyuni Quarry and Snake Quarry. Similarities in outcrop geology indicate they are probably part of the same depositional sequence. The offset of the Snake Quarry ridges by 3km east relative to Mbuyuni and the presence of a linear depression and Mbwemkuru River, indicates the presence of a right lateral strike slip fault that runs though the Mbwemkuru River Valley (Fig. 7.13).

Blue green clays dated by Cotton and Pearson as Early to Mid Miocene boundary in age (15.97 Ma) are recorded at the base of the sections at Mchinga school and at Mchinga Turn. In this area, a compilation of simplified logs is shown in Fig.7.13. Four facies may be considered Early-Mid Miocene in age, shown listed in chronostratigrapic order, (i.e. oldest at base);

1) A powdery white, poorly lithified sandy marl.
2) A coral reef limestone that forms a cap overlying (3).
3) A benthic foraminifera packstone or sparite

[A blue silty clay is present in some localities and appears weathered out in others]

4) a variable unit of orange sandy marl with bioclasts of large benthic foraminifera (often up to 80% of the rock), pecten, echinoid fragments,
5) a blue-green, often silty clay
6) a variable unit of orange sandy marl with bioclasts of large benthic foraminifera (often up to 80% of the rock), pecten, echinoid fragments,

Mchinga Village/School

After turning northeast off the main road towards Mchinga there is a very noticeable dip slope to the west of this road, dipping gently (6°) east and capped by a distinctive 1.5 m blocky limestone bed. At WP 384 it reached road level and could be examined as a pale orange, sandy marl with shelly debris, echinoid fragments and large benthic foraminifera (Fig. 7.18d). This is in turn overlain by a white powdery, algal marl. The limestone/marl extends towards the village.

At Mchinga school, it is not clear whether the limestone/marl dip beneath the road surface and are overlain by the stratigraphy exposed here or are discontinuous and would have overlain the stratigraphy at sea level here. A silty blue-grey clay was sampled from a water well and close by, an algally bound, bioclastic limestone with oyster fragments visible to the eye (Sample TNZ-09-83) forms a rubbly outcrop and ledge (Fig. 7.18c). The presence of *Sphaerogypsina, Lepidocyclinid* and *Miogypsina* indicates a Miocene age. The school is perched on top of this white-grey rubbly outcrop at approximately 5m above sea level. To the north of this outcrop the road swings NW and begins climbing. Very clean clay is exposed in the roadside gullies here and has excellently preserved planktonic foraminifera which also date as Early-Mid Miocene boundary. This appears to overlie the previous clay and limestone. Climbing further, a marly, coralline limestone facies forms the road surface beneath, as exposed in a small quarry adjacent the salt pans on the south side of Nondo Bay.

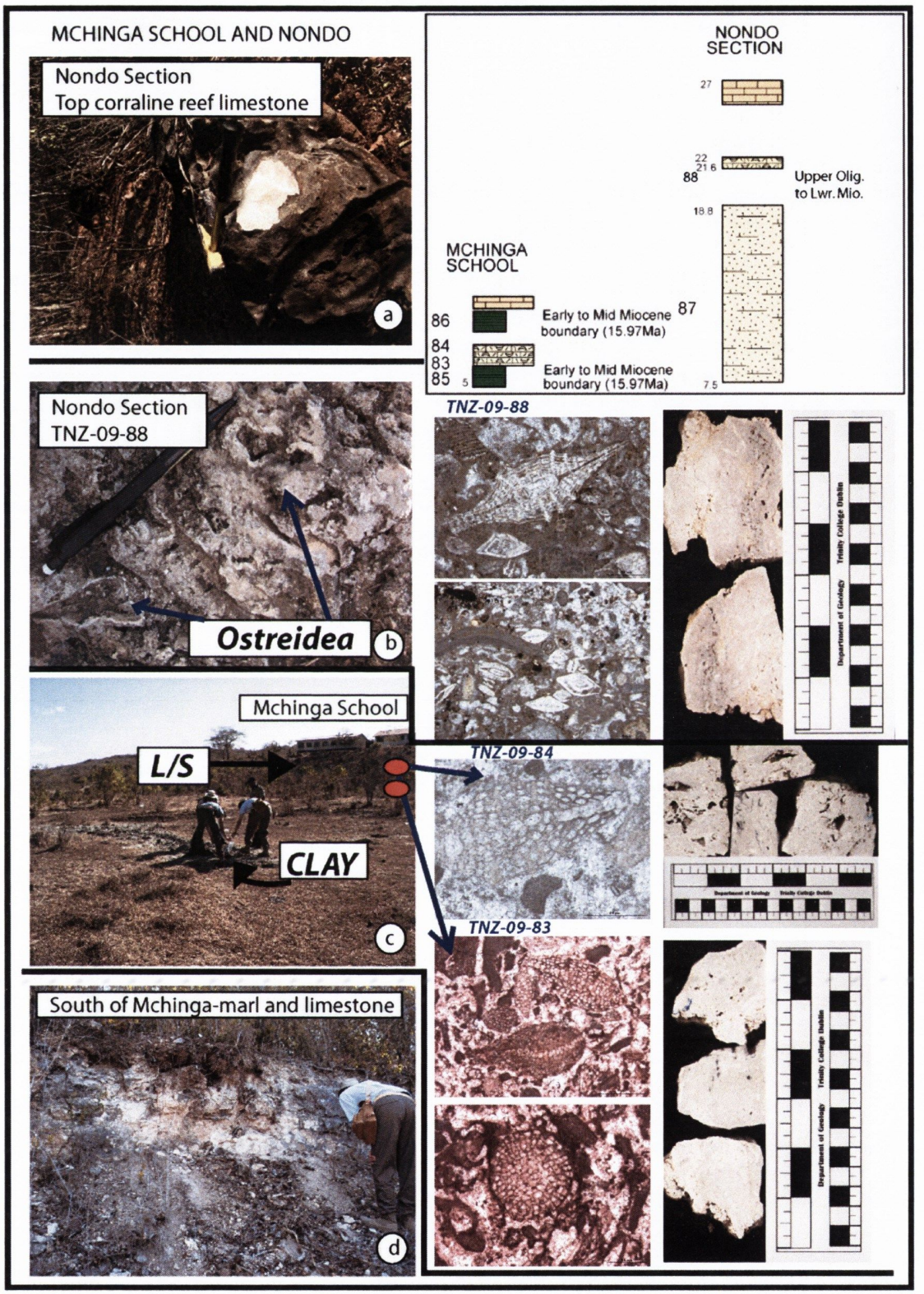

Figure 7.18: Field photos, photomicrographs (scale), cut sections and sketch logs from the Mchinga school and Nondo areas.(a) The coralline reef limestone boulders that cap the Nondo section, (b) ostreidea as seen in Sample 88 of Nondo (Upper Olig-Lower Mio), (c) Mchinga school perched on the topographic high of limestone overlying clay (d) the appearance of the pale orange, sandy, bioclastic marl and limestone facies observed south of Mchinga.

Nondo Bay

At the next inlet, Nondo Bay, the road again climbs from near sea level to a height of 27m asl. At the base of the section is a bioclastic limestone with hard, poorly carbonate cemented sandstone which quickly passes up into a poorly lithified sandy marl with variable shelly debris. The exposure here is somewhat weathered back and extends from 7.5m above sea level to 18.8. There is a gap in exposure where some clays may have been washed out before the next outcrop at 21.6m. A 50cm thick bioclastic packstone bearing shelly fragments, oysters, tube structures and benthic foraminifera in a sandy marl matrix form a bench like structure (Fig. 7.18b). This may be dated as Miocene in age if the presence of *Miogypsina* is confirmed or Upper Oligocene-Miocene if *Miogypsinoides*. A 5m gap of exposure is present and topped by a coral reef limestone which forms weathered ridges of massive dark grey boulders (Fig. 7.18a). This would appear to be the facies that forms the base of the road surface here.

North Mchinga Plateau

The coastline between Msungu Bay to the north and Mchinga to the south is dominated by bioclastic limestone facies (Figs. 7.13 and 7.19). It is approximately 25km long in a N-S direction and extends to about 25km inland where its westernmost extent is usually marked by a distinct westerly facing scarp. Tracks were not well developed in this area and limited coverage somewhat. There was no road north of Ruvu and no bridge across to Rushungi, although both were marked on the 1966 topographic sheets. The Ndimba Forest Reserve limits exposure and the former settlement around Mkoe is no longer inhabited. A red coralline sand overlying a vuggy framework coral limestone is the principal lithology under the road surface (Fig. 7.19a). Where the road cuts down into the plateau at river incisions, a benthic foram sparite is sampled underlying the coral limestone (Fig. 7.19c-e). Beneath the sparite a white, powdery, quartz rich marl extends to the west (Fig. 7.19j).

The benthic foram limestone (Fig. 7.19g) is often mouldic as most of the benthic foraminfera and other fossiliferous material have dissolved out. The majority of the rock comprises the remaining white-grey sparry cement and minor amounts of shelly

debris from gastropods and echinoids. In some localities, angular and poorly sorted quartz infills the benthic foram moulds. The benthic forams that are present include *Lepidocyclina, Miogypsina, ?Operculina, ?Amphistegina* and the absence of Nummulites indicates a Miocene age for Samples TNZ-09-120, 121 and 122. At WP473 the presence of Nummulites in Sample TNZ-09-119 indicates a slightly older Eocene-Lower Oligocene age which possibly indicates a redeposition of the Nummulites. This age has recently been reconfirmed as Miocene.

Driving west the benthic foram limestone appears to pass laterally into a marl with a high quartz content. The more resistant benthic foram limestone appears to form a ledge which then slopes westwards into the marl. At WP 498, near Kikopo village the marl is poorly lithified, soft, white and powdery with approx. 50% well sorted medium grained, subrounded quartz grains (Fig. 7.19j). The nature of this contact appears to be stratigraphic. The contact between the Kilwa Group and the overlying carbonates is not seen in this area.

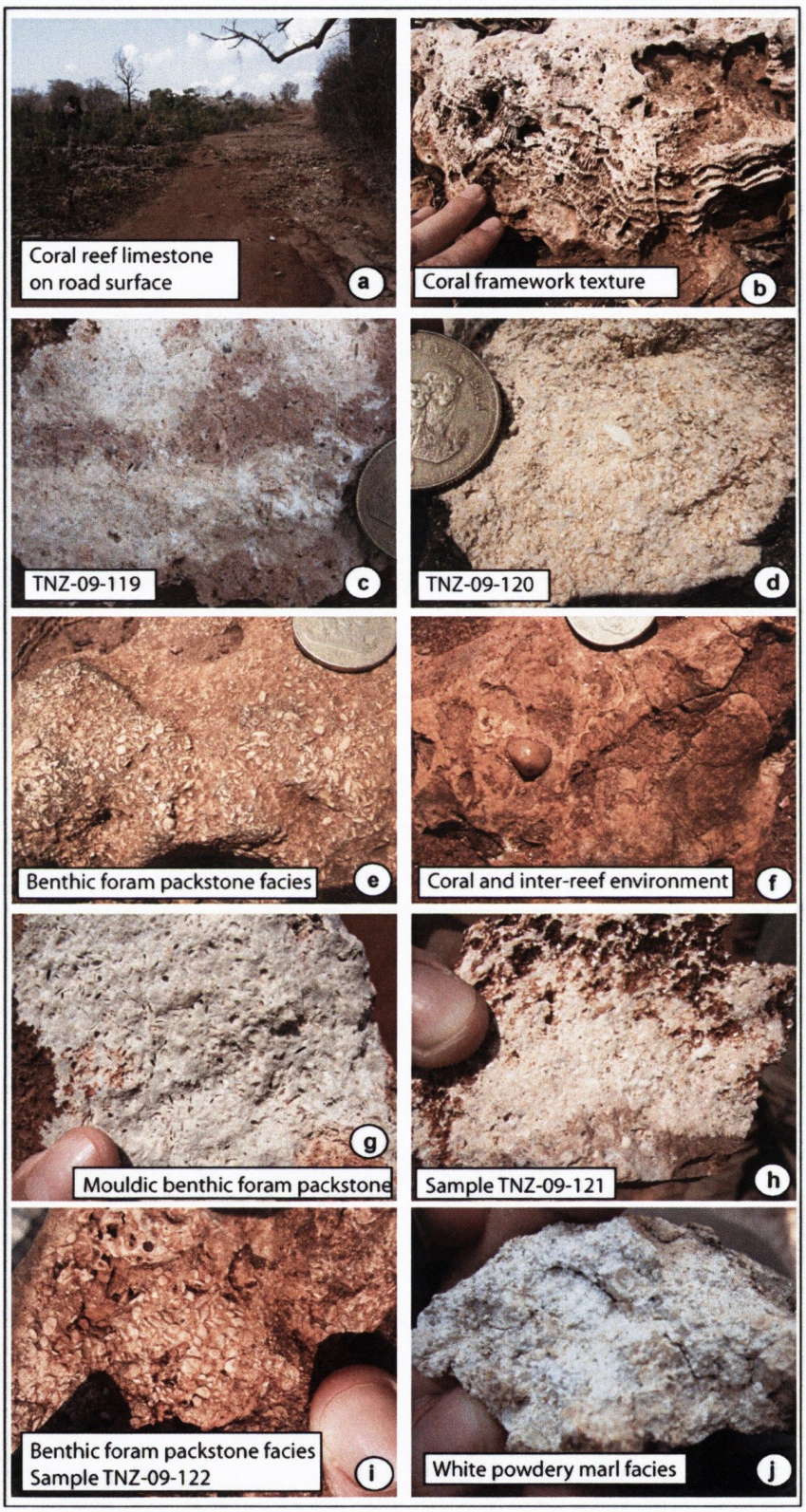

Figure 7.19: Field photos of the facies of the north Mchinga Plateau. (a) Dominant road surface coral reef limestone (b) the texture of the vuggy coral reef facies (c-i); benthic foram packstone which underlies (a) and (j) white powdery quartz rich marl that extends east of the plateau and appears to tbe lateral equivalent of the benthic foram packstone.

Mbuyuni Quarry and Snake Quarry – Proximal Miocene (?) facies

The Mbuyuni Quarry is located on the main road between Kitomanga and Mchinga (Fig. 7.13). The nearest place-name on the topographic map is Mbuyuni and that name is thus assigned to this quarry. 'Snake Quarry' is the name given to an exposure visible from the road to the south of the turn off for Mchinga. At Mbuyuni, three sections were logged within this easterly dipping quarry, named Main Log; East Mbuyuni and Mbuyuni Road (Compilation log in Fig. 19).The litho- and bio- facies observed here are different from those seen in North Mchinga and Mchinga.

The Mbuyuni Main Log (Fig. 7.20) is located to the west of the exposures, where a bank of approximately 12m of well bedded stratigraphy is logged from heights 19m to 31.5 m above sea level. Units A-J are:

a) A 2.3m bed of bioclastic limestone with *Lepidocyclina*, algal balls, shelly fragments; e.g. gastropods, pectin. The blocky limestone is weathering orange-pink and algal crusts are visible towards the top. There is a decrease upwards in *Lepidocyclina* content and an increase in carbonate cement. The top is almost completely algal. (Sample TNZ-09-107)
b) A *Lepdicyclinid* marl-limestone (Sample TNZ-09-106).
c) A 1m thick sparry white rubbly limestone with smaller benthic foraminifera, echinoid and pectin fragments. The top 30cm of this bed has been broken up and exposed. (Sample TNZ-09-105)
d) An almost 1m thick sandy marl with smaller thinner and flatter *Lepidocyclinas* than elsewhere in the sections. Large echinoid fragments and spines are also present.
e) A 1.7m weathered back dark green grey clay with no macrofossils and mixed with a very fine sand. It grades into the overlying unit for top 50cm. The sample (TNZ-09-104) yielded a 'Neogene' age based on the planktics although it was full of carbonate debris.

f) A 55cm thick bed of bioclastic limestone cuts down into the *Lepidocyclina* limestone with an erosive base. This limestone has no *Lepidocyclina* although it has one 'Kingfish boy ?' in an angular 3cm long intraclast. The top of this limestone bed has algal crusts and is burrowed indicating an exposure surface.

g) A remarkably well cemented *Lepidocyclina* limestone (Sample TNZ-09-103). The large benthic foramnifera reach up to 6cm in diameter and are principally aligned in the same plane. The matrix is a very fine marly sand and comprises ~40% of the bed. Occasional quartz, pecten and shell fragments occur. A minor disconformity occurs at the top.

h) A weathered back blue grey silty clay with a very powdery texture.

i) A 1m thick coarse grained poorly lithified calcarenite with numerous clay rip ups.

j) Sandy blue-grey clays (Sample TNZ-08-49/50) at the base. The top is a sharp contact.

MBUYUNI

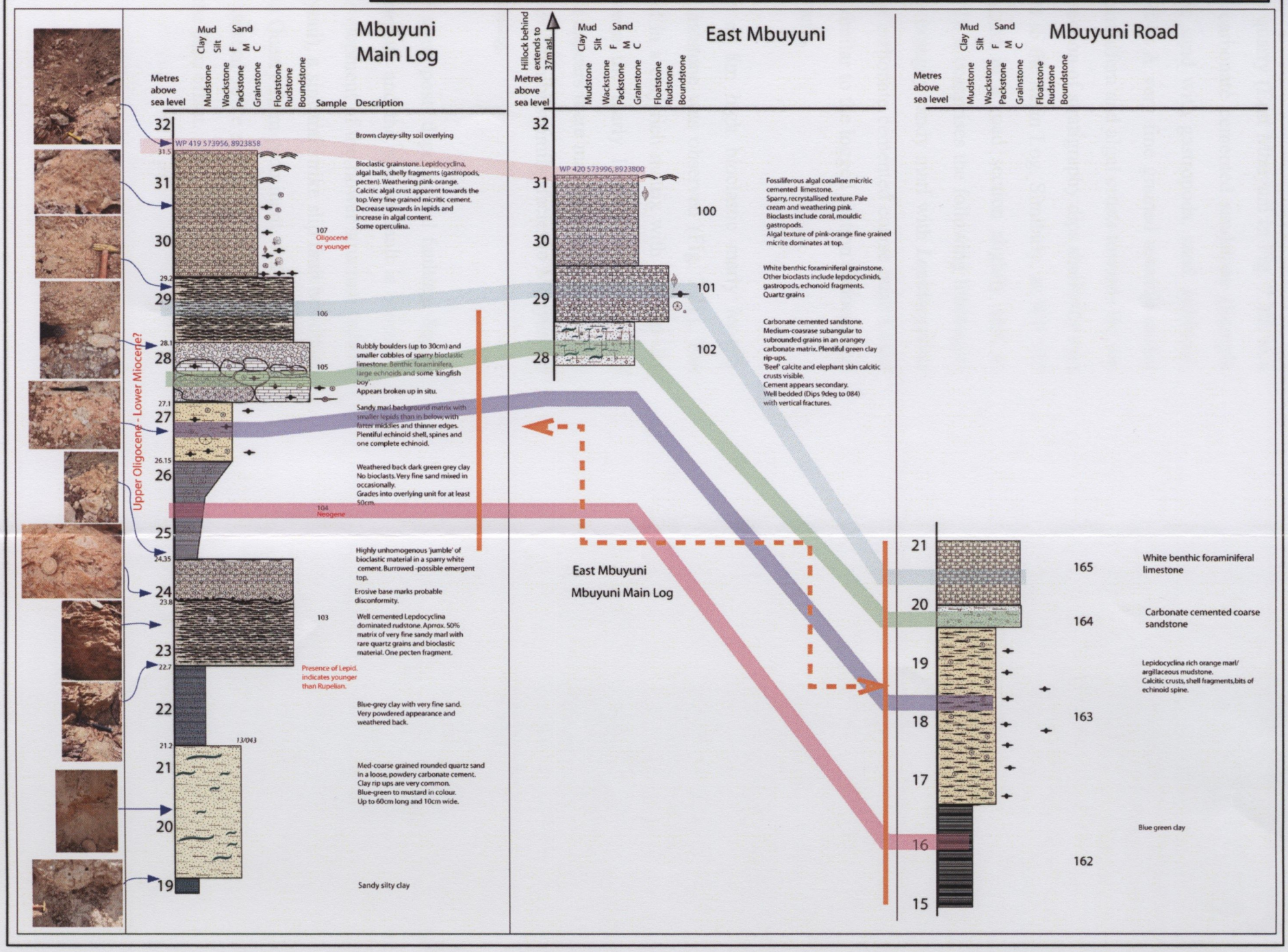

Figure 7.20 Compilation of Mbuyuni Logs and correlation based on their facies characteristics

Similar facies are observed to the east of the quarry (East Mbuyuni in Fig. 7.20) in a 3m high section of outcrop. At the base a carbonate cemented sandstone (Sample TNZ-09-102) is overlain by a white benthic sand with gastropods, sand, echinoid, *Lepidocyclina* fragments (Sample TNZ-09-101) A very fine grained micritic cream limestone with small amounts of benthic foraminifera and algal crusts towards the top cap the section (Sample TNZ-09-100). This section of stratigraphy dips shallowly east and appears to be stratigraphically equivalent to the Main Log. Similarly, at WP 575 there is a third section of stratigraphy logged in a road section slightly east of Mbuyuni Quarry (Mbuyuni Road in Fig. 7.20). It comprises the following lithologies from the base upwards; a blue-green clay, an orangey sandy marl with *Lepidocyclina* towards the top and coral, pectin fragments,a carbonate cemented coarse quartz sand and a benthic limestone. This stratigraphy is similar to the logged section although the clay (Sample TNZ-09-162) was barren of forams.

At 'Snake Quarry', WP381, an exposure of 8m high bioclastic marly loosely consolidated limestones capped by a reef limestone was observed (Fig. 7.21). The limestone has small benthic forams and sand in a clay-rich matrix with clay rip ups and echinoid fragments. The contact between the marly limestone and the reef limestone does not appear stratigraphic and it appears there may have been some clay between the facies at some point. As this quarry exhibits similar facies to Mbuyuni, it is considered part of the same depositional setting.

It appears that this outcrop has experienced some post- depositional faulting. Steep, reverse faults indicate a possible flower structure and the reverse fault is observed trending NE-SE (153). Subsequent to the development of the flower structure (which would also explain the variable dips at Mbuyuni), a sinistral strike slip fault has offset it. The outcrops at both Mbuyuni and Snake Quarry form prominent westerly facing ridges and as mentioned previously, a W-E dextral strike slip fault through Mchinga Bay is proposed as a mechanism to explain the 3km offset.

Figure 7.21: 'Snake Quarry' potential small scale reverse faults cross cutting the principal outcrop (a and b) and benthic foraminifera packstone facies (c).

7.4.4. Summary of interpreted depositional environments of the North Mchinga Area.

In order to accumulate such a thick succession of Early to Mid Miocene facies in this area while there was no contemporaneous deposition in Kiswere (to the north), a large fault in the Msungu Bay area is inferred, which created more accommodation space in North Mchinga and left Kiswere high. In order for this relatively thick uniform succession with little or no facies change to accumulate, the area was either (a) subsiding at the same rate as sedimentation or (b) experiencing a relative rise in sea level that kept pace with sedimentation. Eocene deep water patch reefs were recorded near Lake Mkoe and as a carbonate ramp environment was present a short distance away at Kiswere at this time, the Msungu Fault was likely initiated before the Eocene downthrowing the area south of Kiswere and creating a deeper water environment.

After the major regression during the Eocene-Oligocene transition, the relative sea level in this area began to rise again in the Upper Oligocene-Early Miocene. Based on the extensive benthic foraminiferal assemblage present, the basal Mid-Early Miocene clay was probably deposited on the mid-outer shelf and is recorded at Mchinga school and Mchinga turn. Due to its easterly dip and location east of Mchinga, the Mbuyuni section is considered older than the Early-Mid Miocene boundary. It is interpreted as being Early Miocene in age as the clay within the log (Sample TNZ-09-104) yielded a 'Neogene' age based on the planktics present. The age of the top of the Mbuyuni section is regarded as Oligocene or younger (Sample TNZ-09-30 based on the lbf ('large benthic foraminifera' assemblage), thereby concurring with the Miocene age attributed to the underlying assemblage.

The Mbuyuni Quarry succession may be interpreted as being located in a mid-outer shelf environment, where clay deposition with a high terrigenous input was the background lithology. The Lepidocyclina rich clay beds are interpreted as being in situ due to the unbroken nature of the fossils. The depositional environment is thus interpreted as the deepest part of the photic zone. The Lepido-rich beds pass up into a more mixed bioclastic limestone facies and as this sequence is repeated approximately three times it is interpreted as occurring as a result of sea-level variation or fault

movement. The top of the Mbuyuni section, an algal creamy micrite without the bioclastic debris indicates a quiet, deep environment.

The area around Mchinga was deep enough to accumulate a mid-outer shelf clay at the Early-Mid Miocene boundary (Mchinga Turn and Nondo/Mchinga school) Though varied, the facies above this clay usually include (1) an orange, sandy marl with benthic foraminifera, echinoid and bivalve fragments, (2) a benthic foraminiferal packstone/sparite and (3) a coral reef limestone. The top of the Miocene succession is a coral reef limestone which forms the dominant flat topography. This extends at least as far west as Kikopo and the edge of the platform may be inferred from the distinctive ledge it forms. Since this area was a coral reef platform in the Mid Miocene, it has been a relative high, with Quaternary reefs fringing the coast. This indicates a relative drop in sea level since the Mid Miocene, as a result of (a) uplift, (b) eustatic sea level fall or (c) both.

West of Kikopo a powdery white marl with high quartz content is seen. The area between Kikopo Kitomanga in inferred to be Kilwa Group clays over which the Miocene limestones have not transgressed. However, the marly facies were observed 22km inland at Ngomba Quarry and on the road near Kitomanga. These deposits may be interpreted as fossil mangrove swamps, dominated by the algal carbonate precipitation around pneumatophores. Mangrove swamps thrive in brackish water and are quite specific to a peritidal/tidal environment. They are commonly found along the coast today in sheltered, quiet bays. It is possible that these deposits represent the extent of the Early-Mid Miocene succession in this area, and are the shoreline lateral equivalents of the coral reef limestones of the plateau. The more resistant limestones have formed a platform, while these occurrences are remnants of the shoreline accumulations. The Ruawa Plateau is bounded by a N-S strike slip fault with an easterly facing dip component. This may have formed a buttress against which the Miocene facies could transgress no further.

There are potentially other localities with the marly facies exposed but they have not been observed as part of this study. There are three possible explanations for the isolated appearance of the Ngomba Quarry; (1) the Rivers Mariki and Mbwekuru existed during the Miocene times and had large river mouths/estuaries which were

intertidal as far inland as Ngomba; (2) Reactivation of the fault bounding the Ruawa plateau has recently had some reversal and the Miocene shoreline deposits have been squeezed up to 134m above sea level in a harpoon-like structure or indeed c) that the Ngomba Quarry deposits represent the most landward Miocene shoreline before subsequent regression.

7.5.Field Geology of the Lindi Area

The Mchinga area is laterally continuous south into the Lindi Area (Fig. 7.22). However, due to local tectonics and quality exposures around the coast it is discussed separately, although many of the same facies persist. The Lindi Area is here considered to be the area south of Mchinga Bay to the Kitunda Plateau. The following sections discuss the outcrop geology of North Lindi, Lindi Bay and the Kitunda Plateau.

7.5.1. North Lindi (Likonga-Mitonga-Mbanja)

The topography between Lindi and Mchinga is relatively flat-lying along the main road. Numerous rivers incise the surface however and it is generally at these locations or recent quarries, developed during recent road construction, that the stratigraphy is elucidated. The stratigraphy is exposed at the Mchinga Bay Turn, Likonga River, Mitonga River and Mbanja Quarry (Fig. 7.22).

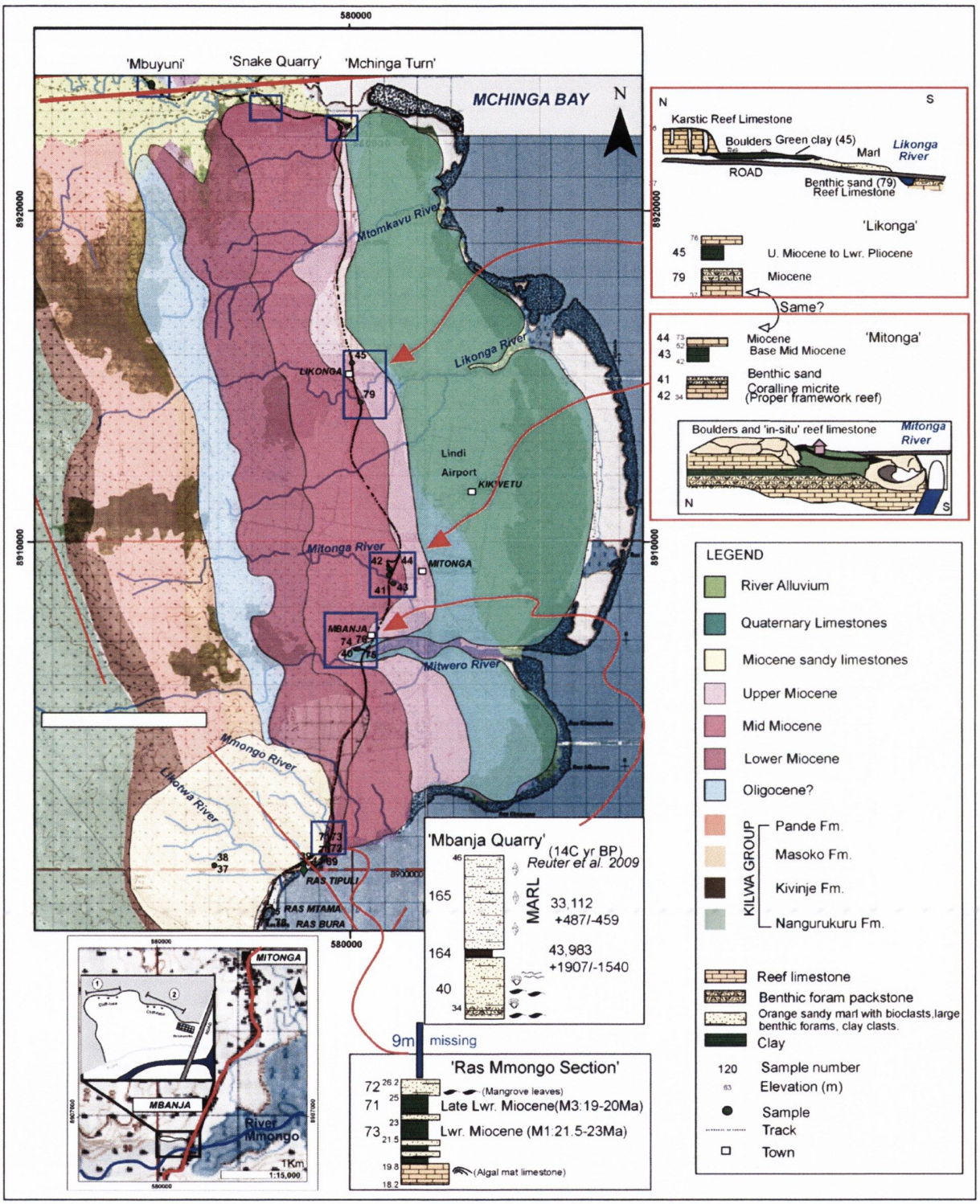

Figure 7.22: Geological map of North Lindi (Scale 1:100,000) and sketch logs of the key areas. Scale bar on main map is 5km.

Mchinga Turn (WP 80)

At the major bend in the road south of Mchinga Bay (WP 80) a road cutting of 16m is exposed above the road (Fig. 7.22, 7.23). A schematic log is drawn in Fig. 7.13. Although there are many slumps due to the recently excavated nature of the road cutting, the facies present include;

a) Reef limestone boulders
b) Green clay (Sample TNZ-09-81 is dated as Base Mid Miocene on the basis of the planktonic foraminiferal assemblage),
c) Yellow-orange, sandy bioclastic marl. Benthic foraminifera; *Lepidocyclina*. Clay rip ups. (Similar to Snake Quarry) (Sample TNZ-09-82)
d) Clay and poorly consolidated marl with occasional more cemented thin bands. (Clay sample TNZ-09-80 is Early – Mid Miocene (Praeorbulina glomerosa zone)).

Figure 7.23: Newly excavated Mid Miocene facies exposed at Mchinga Turn. Looking NW. Although slumped, coherent stratigraphy was logged (see text and Mchinga Turn log in Fig. 7.13)

Likonga River

Driving south towards Likonga River the elevation starts to drop. Approximately 40m of outcrop is exposed between WP 339 and the base of the Likonga Riverbed. At the top of the plateau (76m asl) reef limestone with a karstic weathering pattern (Fig. 7.24) overlies a green clay exposed in the road gullies (Sample TNZ-09-45) which is Upper Miocene-Lower Pliocene in age. A white marly carbonate is located in the roadside before dipping into the riverbed. On the southside of the riverbed there is approximately 5m of stratigraphy exposed, beneath the bridge (Fig. 7.24) at 37m asl. It is composed of;

a) Benthic foram packstone; mix of shell, carbonate and quartz grains in a carbonate cement. Planar beds with slightly weathered back tops.
b) Carbonate cemented sandstone
c) Rubbly, coral rich reef limestone

A Miocene age was assigned the benthic foram packstone in the Likonga Riverbed on the basis of the large benthic foraminifera assemblage. Thus it lies beneath the Upper Miocene-Pliocene green clay (See sketch cross section in 7.22) and above the Mid-Miocene Mchinga Turn section. Hence, the reef limestone at the top of Mchinga Turn and in the base of Likonga may be age equivalent. Thus the Likonga section is Mid-Upper Miocene in age.

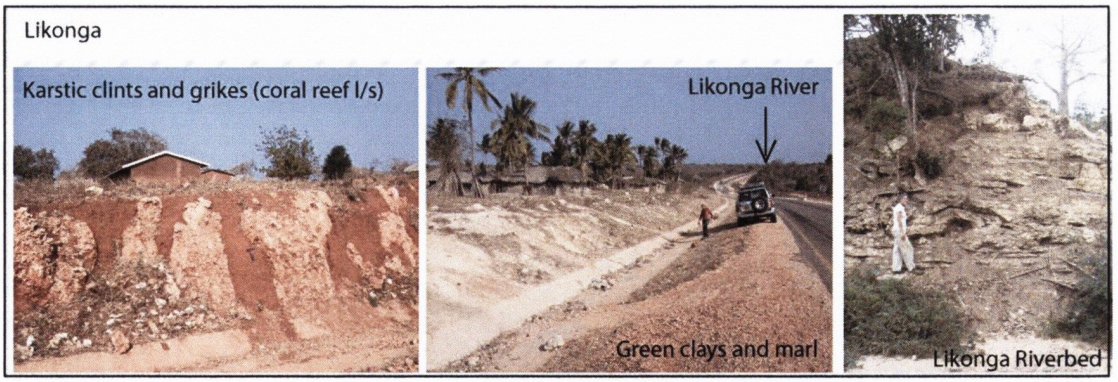

Figure 7.24: Photos of the exposures at Likonga, from L-R; Plio-Pleistocene coral reef limestone; Upper Miocene to Pliocene clays and powdery marls and underlying in the Likonga Riverbed, Miocene reef limestone, calcarenite and benthic foram packstone.

Mitonga River Quarry

Driving south towards Lindi the next exposures are in the Mitonga village/river area. Over 40m of stratigraphy is exposed and a sketch map of the outcrops is shown in Fig.7.22 and in photos of Fig. 7.25. The stratigraphy is described from the base upwards

a) Boulders of reef limestone and in-situ reef limestone occur between 52m and 73m above sea level. The scattered black stained boulders litter the landscape and are weathering out all around (Sample TNZ-09-44).This reef limestone forms the reddened coralline sand on the road surface from here northwards towards Likonga (Fig.7.25a).
b) A weathered back section is the road surface above the previous quarry. Green clays are evident in the gullies and Sample TNZ-09-43 yielded a base Mid-Miocene age. The clays occur between 42m and 52.(Fig. 7.25a)
c) A quarry of very white, proper framework reef (Sample TNZ-09-42) with large (almost m-scale) corals and pockets where they have fallen out, algal mats, micritic, calcite infilling vugs. Elsewhere a benthic foram sand with ~80% benthics (TNZ-09-41). The floor of the quarry is at 34m above sea level and the quarry is approximately 3.5m high. (Fig.7.25 c and d)

It seems likely that this stratigraphy at Mitonga lies stratigraphically below that at Likonga. The 'top reef' at Mitonga is the same reef at the base of the Likonga section. The quarry in Mitonga of framework reef is most likely Early Miocene in age though this may need further confirmation in the future.

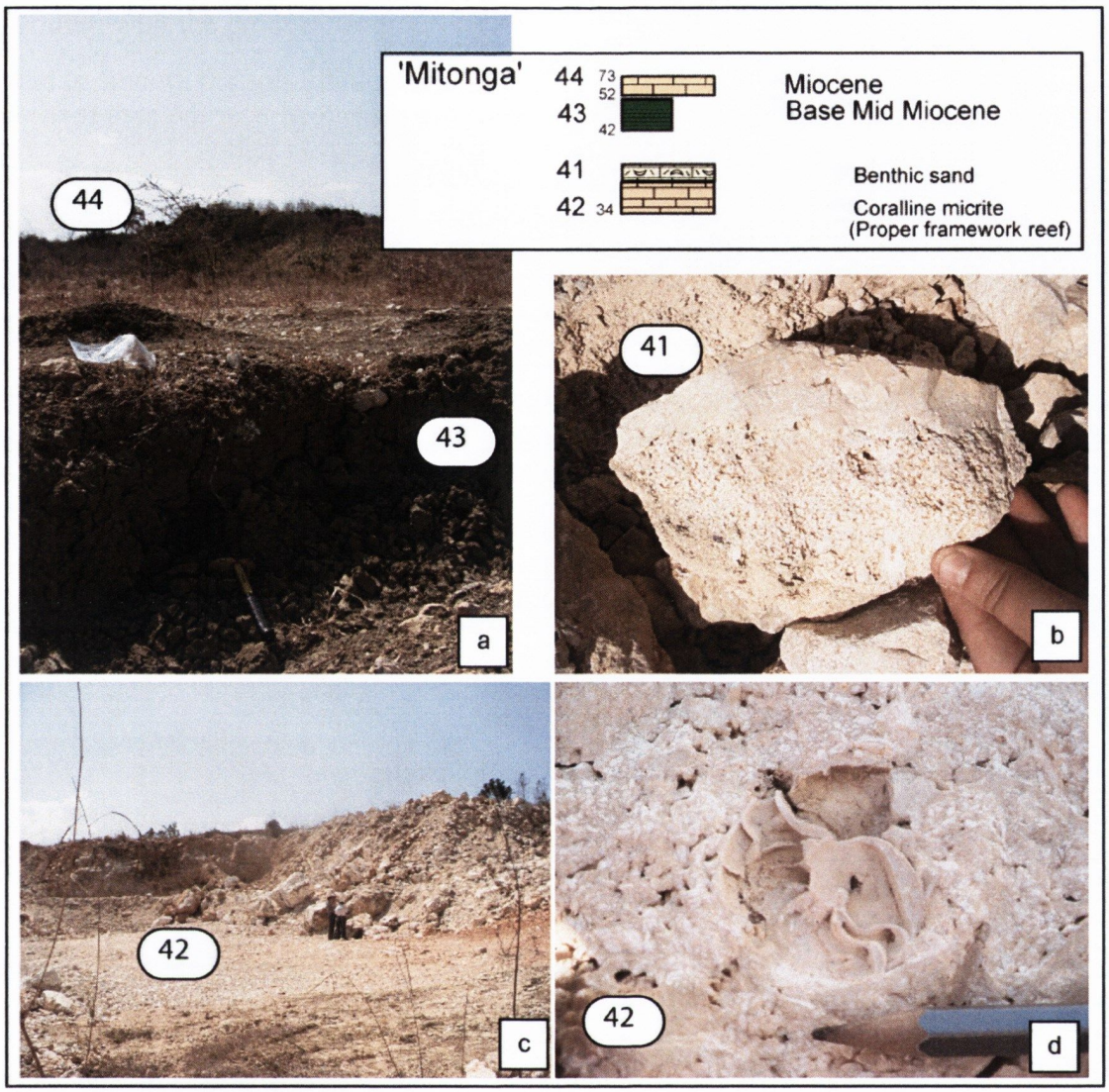

Figure 7.25: Mitonga Quarry sketch logs and field photos with sample numbers highlighted. Smaller text refers to height in metres above sea level. (a) Boulders of reef limestone overlying the green clay exposed in the roadside at the entrance to the quarry, (b) benthic foram packstone that dominates the quarry and (d) a fossilised nautilus exposed in the quarry.

Mbanja Quarry

A large quarry has been excavated to the west of the main road near the area marked Mbanja on the topographic map (See sketch map in Fig. 7.22). The Mmongo River enters the sea nearby and the quarry is quite visible when descending into the Mmongo River Valley from Lindi. The quarry is approximately 330m wide and 55m long. The outcrop exposed is approx 12m at its thickest. It was visited and described in some detail by Reuter *et al.* (2009). Reinvestigation of the quarry and its lithostratigraphic correlation to a section just below the main road towards Ras Mmongo indicate the interpretation as a 'regressive fenland' is erroneous.

The Mbanja Quarry is described in terms of three localities; Quarry Face 1, the quarry floor and the Back Quarry Area (Fig. 7.26).

On Mbanja Quarry face 1 approximately 12m of stratigraphy is exposed (Fig. 7.26) and can be subdivided into four sections (from the base upwards);

a) Fine white marl with gastropods that forms a ledge (possibly a karst).
b) Brown silty peaty clay with small gastropods which laterally pinches out and has a weathered back appearance. It one locality it has a slightly paler colour and lobate geometry which passes laterally into the dark clay. Pinches out after quarry face 1. Similar facies were observed in road section south of Mbanja.
c) Powdery white limestone with fossil encrusting oysters. (Often strewn across the quarry floor)
d) Chalky white marl with calcified moulds of tube moulds and leaves.(Weathering orangey-yellow). *
e) Chalky white marl with harder benthic foraminiferal packstone boulders *

* Units d and e are gradational and not strictly separate units *

To the east of the quarry the clay pinches out laterally and the quarry has been more extensively dug out and slopes gently back. The white marly limestones are dominant and are often stained reddish-orange. It can be difficult to pick out structures and

bedding with the grooves from the machinery the most obvious feature. The 'scrapes' tend to smooth the soft lithologies, obscuring obvious structural features.

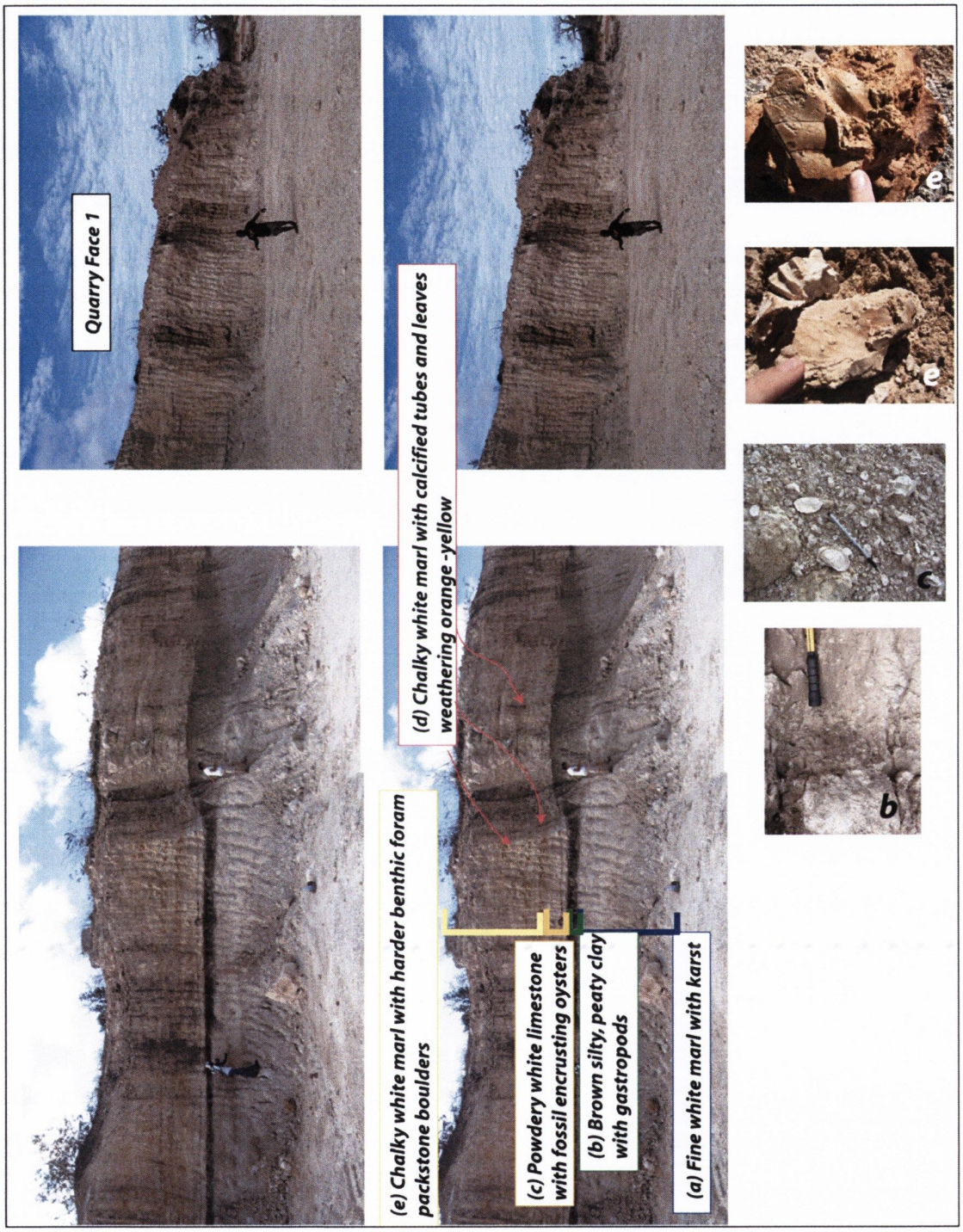

Figure 7.26: Mbanja Quarry; face 1 described with accompanying photos of the key lithologies/features.

Ras Mmongo Section

Approximately 5km south of the River Mbanja there is a small river, the River Mmongo. Between the main road and the beach there is approximately 8m of stratigraphy exposed, between 28m and 20m asl. It is most likely that this section lies beneath the Mbanja Quarry, with 10m of missing stratigraphy however as the Mbanja Quarry is at 41m asl. (See sketch map in Fig. 7.22).

The stratigraphy of the river cut may be described as below (Base at (g)):

a) Marl
b) Mangrove leaves in a grey sandy marl
c) Green clay (Sample TNZ-09-71; Late early Miocene 15-20Mya)
d) Interbedded blue grey fine sands and green clays with caliche
e) Green clay with well developed caliche
f) Marly loosely consolidated grey-blue fine sand with occasionally cemented beds
g) Algal mat limestone

At the base of the section it is approximately 300m to the next exposure on the seafront, located to the north of Ras Tipuli. At this section cliff section shows a benthic foram sand overlying a benthic marly sand with a clay at the base (Sample TNZ-09- 69; Mid Miocene). More recent clays with caliche development abut the marly sands. This clay appears to form the base for this shoreline section with the other boulders resting on it.

As the section above this is dated Early Miocene there is probably a fault between this locality and the Ras Mmongo section. The benthic sand at this locality is highly inclined and with the abutting clays, it is likely there is a fault adjacent at this point.

7.5.2. Lindi Bay Area

There is excellent exposure around the north and south of Lindi Bay and the area has also been extensively shallow cored by the TDP. Fig.7.27 shows a composite 1:120,000 scale map of the Lindi Town/Lukuledi River. During the field surveys, a number of localities were visited in the north Lindi Area and to the Kitunda Plateau. Three wells have also been drilled in the area; Lindi 1, Lindi 2 and Lukuledi.

The outcrops described below are at Ras Tipuli, Ras Mtama, Ras Bura, Lindi shoreline, Mkwaya Jetty and the Kitunda Plateau.

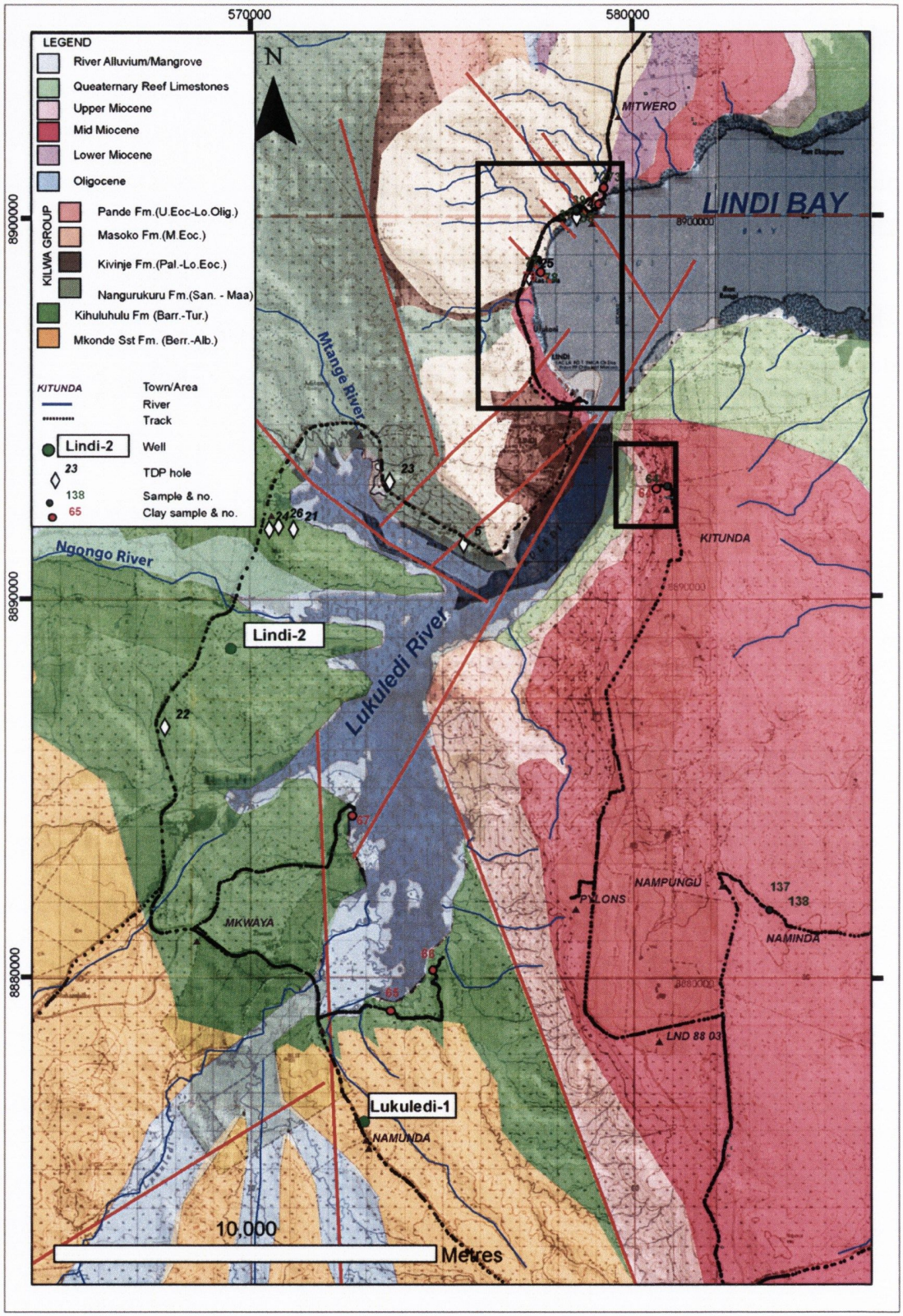

Figure 7.27: The Lindi Bay Area geological map. Boxed areas represent the locations of figure 28 and the location of the Kitunda Log in Fig. 7.30. Red lines refer to faults.

Figure 7.28: A schematic diagram of the Lindi bay coastal exposures with field photographs for illustration. The location of this figure within the overall geological map is shown in the box in Fig. 7.27.

Ras Tipuli Geobreccia

The enigmatic Ras Tipuli exposures are well described in Nicholas *et al.* (2007). They were revisited as part of this study to attempt to constrain the origin of the massive blocks that were first classified as a 'Geobreccia' after the unpublished report by Martin (1954) reported in Kent *et al.* (1971).

A compilation of field photos is shown in Fig.7.30. The dominant facies (the 'Tipuli facies') of the large blocks observed here, randomly oriented and with varied dips (Fig. 7.30a-d), is of a sandy orange-yellow calcarenite with varying amounts of bioclastic debris. A blue green sandy clay is often interspersed amongst the sandy marl. Larger benthic foraminifera including *Lepidocyclina*, Pecten, Coral, Echinoid are present (Fig. 7.29 i), often forming coquinas. In one locality, a large block abutted another with a 10-25cm seam of sandy clay running vertically between the two. (Fig. 7.30 d, h)

Walking north around the headland the facies change as the boulders are no longer present and underfoot are clean green clays overlain by planar bedded calcarenites (20cm). This clay (Sample TNZ-09-69) is dated as Mid Miocene (M6; 14.3-15.7 Ma). Further north, at WP376 an outcrop of mustard yellow, soft friable sandy marl with benthics is overlain by a white benthic sparite. Abutting this 1m section is a modern clay with caliche. A more marly section with benthic foram packstone is seen overlying a clay. Thus a fault is considered to be located between this locality and that of sample TNZ-09-69.

The Ras Tipuli area contains numerous massive boulders, some of which reach up to 10m in diameter, lying on what appears to be Early Miocene clay. Stewart (2004) analysed three samples from this locality and assigned ages of Early Miocene (M1) to a locality beside the bridge you enter the headland at; Base Mid Miocene (M6; 14.3-15.7 Ma.) and base Upper Miocene (M11-M12; 10.46-11.63) to clays north of the boulders, near this study's sample TNZ-09-69. At no locality are dated clays seen overlying the boulders of 'Tipuli' facies.

The 'Tipuli' facies is very similar to that seen at Mchinga turn and Mbuyuni. Both of these areas have been ascribed early-Mid Miocene ages. The nature of the outcrop is intriguing and it has been suggested that it formed as a result of movement of a nearby fault that shed debris from the hanging wall. The facies here have undoubtedly been mixed, rather turbulently and disturbed from their original depositional attitude on the Mid-Outer shelf. The pulses of bioclastic debris and sand as seen in Mbuyuni may be attributed to instability on the nearby shelf or storm pulses. Silty clay dominated in the quieter phases. This locality may have been located closer to the origin of the instability and thus there was more erosion and redeposition of the recently deposited beds.

If it is assumed that the cause of enough instability to accumulate at least 30m of stratigraphy was a fault, then the faulting is either syn-depositional or post-depositional, both of which will be examined below.

a) The syn-depositional faulting model

The presence of clays in the Ras Tipuli area from base Early to base Upper Miocene, with no in-situ interbedded lithologies, suggests the prinicipal sedimentation in this area during the Early-base Upper Miocene was mid-outer shelf, low energy, clay accumulation. Perhaps if there was intermittent movement of a nearby fault during the Early-Mid Miocene, creating accommodation space here sporadically, sediment from closer to the shelf (rich in Lepidocyclinids and other large benthic foraminifera) would be shed outwards to this locality in a mixed heap of boulders.

b) The post depostional faulting model.

A similar sediment column to that at Mbuyuni/Mchinga was located here, albeit with thicker accumulations of the same facies. The thicker beds may have been due to greater accommodation space or continued subsidence. Thus a sedimentary succession of clays, sandy bioclastic marls and benthic foraminiferal sands accumulated. At some stage post deposition of the youngest clay found in this area (Base Upper Miocene), there was significant movement on a nearby fault. This

sediment accumulation collapsed and became mixed in a mega-congomerate in deeper water with the clays largely washed out or redepositing in the sandy-marly mix, or between boulders.

The Ras Tipuli Area is condidered a NW-SE trending fault zone between the southside of the headland and the start of the succession at Mmongo. At the northern extent of the Tipuli outcrops the Sample TNZ-09-69 (M6, 14.3-15.7Ma) is located at the beach level. Thirty metres inland and at a height of ~20m asl, base Early Miocene clays occur in the Ras Mmongo section, indicating the presence of a fault between the two localities.

Evidence for relatively recent fault movement offshore may be found on the beach south of the Ras Tipuli headland, near the bridge. Located here over approximately 10m are at least 70cm accumulations of beach rock. Sedimentary structures include basal scouring, fining upwards, thinning landwards and an upward increase in sorting (Fig. 7.29). This deposit is tentatively identified as a beachrock type calcarenite tsunamite. In this area, there has been no previous examination of palaeotsunamites even though there is high seismic activity recorded along the Davie Ridge (Grimison & Chen 1988). Further examination is required of the samples obtained here.

Figure 7.29: Potential beachrock type calcarenite tsunamite (?) close to the road at Ras Tipuli. Outcropping over a 10m area it is 70cm thick. Basal scouring, fining upwards, thinning landwards and an upward increase in sorting are observed. Further work is required on this location to assess whether it might represent the sedimentary response of offshore fault movement.

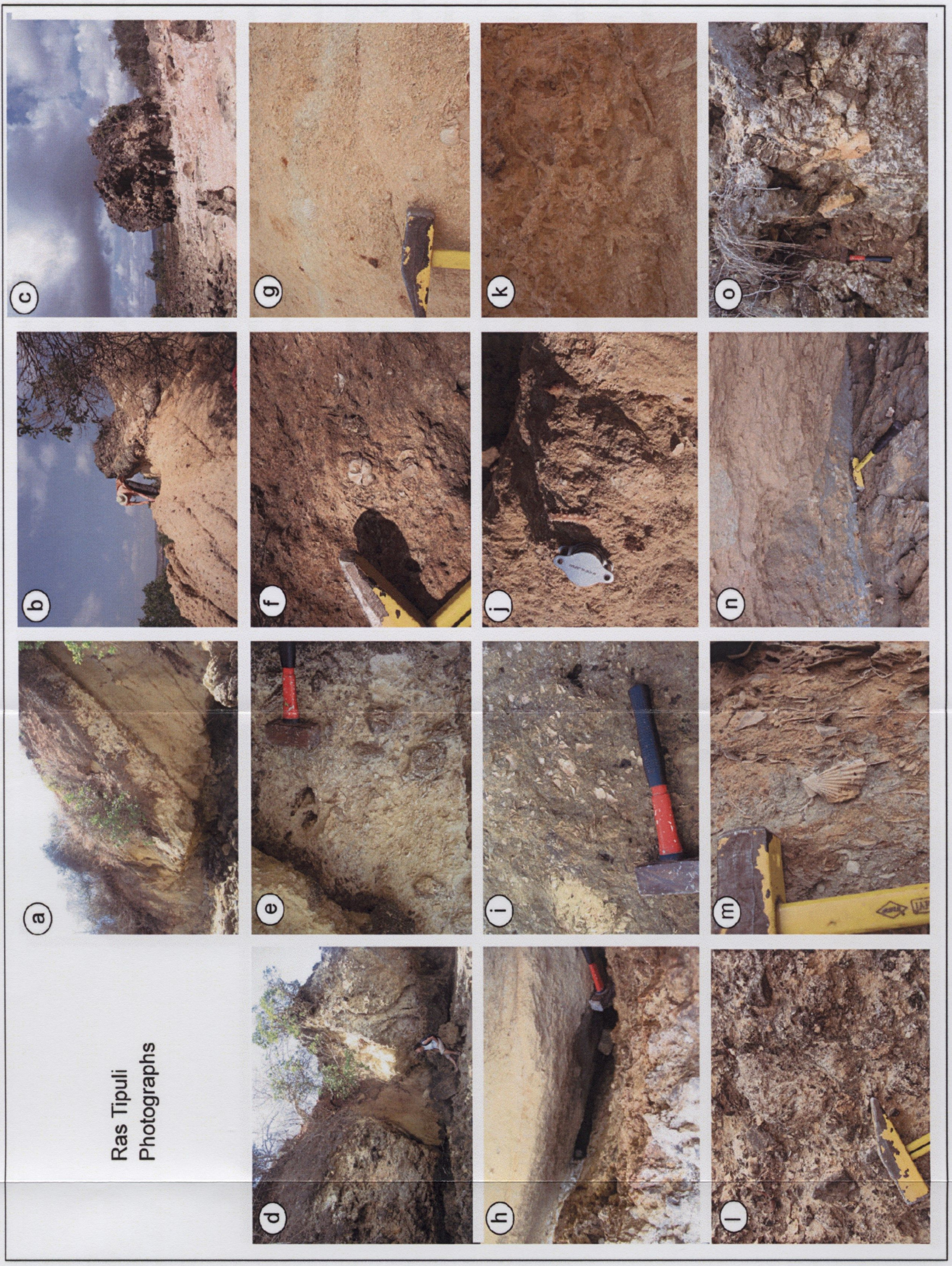

Figure 7.30: A compilation of field photos of the'Tipuli' facies from Ras Tpuli. a-d) Large scale rotated blocks with high angle dips; e-h) variable bioclastic calcarenite facies; i) Lepdicyclina rich clay; j-o) clay rich and blocky calcarenite facies.

Ras Mtama

In Ras Mtama, 'Pleistocene reefs' unconformably overly the Middle Eocene clays and limestones (Fig. 7.28). After the significant regressive event that led to no deposition in this area from the Middle Eocene to the Pleistocene, an overall transgressive Pleistocene package was noted.

Ras Bura

More excavations for road-building materials have taken place in the Ras Bura area in recent years, leading to an increase in exposure. Dark blue-green clays with carbonate stringers drape unconformably over sandy marl with numerous clay rip-up clasts. Blue clays this locality were previously dated as Upper Miocene. However, the exposures as photographed in Nicholas *et al.* (2007) have been removed by the recent excavations. At this new exposure surface, there is a disconformity between the underlying sandy marls and the draped clays with carbonate stringers (Fig.7.28). It is not clear whether this is an erosional contact with a hiatus and erosion or a thrust fault as previously suggested for this locality. However, these clays have been dated as Pleistocene from the planktonic foraminifera (sometime in the last 3Myr.) indicating this must have been a mid-lower slope environment and been elevated (or sea level dropped) in the last 3 Myr. The clays overlie the Miocene sandy marly limestones that have been seen elsewhere and are in turn overlain by pale orange stained reef limestones, most likely Plio-Pleistocene in age. The whole section dips gently towards the east.

There is probably a fault between the clays overlying the marls and the reddish calcarenites on the jutting headland. The Pleistocene section would need to have experienced significant uplift possibly from ~300m water depth to its present elevation (5m asl).TDP 25 was located on the other side of the main road and encountered Lower Miocene-Pleistocene limestones.

Between Lindi and Ras Mmtama, there are large cliffs of white sandy limestones often overlying Lower Miocene clays. They are stained red from above and have an

erosive base with angular quartz cobbles and pebbles jutting out. The quartz content decreases upwards.

The area around Lindi is intensely faulted and that is mainly due to the presence of the major SW-NE trending Lukuledi Fault. It appears likely that there has been an element of approximately North-South extension in order to create the accommodation space for the thick Upper Oligocene-Miocene-Pleistocene succession observed here in various slivers. This supports the flower structure hypothesised by Nicholas *et al.* (2007) as part of a transpressive regime in Lindi.

Kitunda Plateau

Kitunda is the name given to the area to the south of Lindi Creek (Fig. 7.27). A large scarp/cliff is present at the creekside and had been ascribed a 'Lower Miocene' age by various sources. At the base of the cliff, north of the landing jetty Pande Formation clays are reported by Nicholas *et al.* (2007) based on their lithofacies and planktonic foraminiferal assemblage. Thus the shallow slopes at the base of the cliff were assigned to the Pande formation. A section was logged on a footpath from the top of the Kitunda Plateau at WP362 downslope to a water-well at WP373, over 55m of almost-continuous section (Fig. 7.31).

At the base of the section the topography flattens out and gently dips towards the creek and the underlying Pande Formation clays. The clays collected at the base were quite sandy with relatively poor preservation. They yielded an Upper Oligocene to Lower Miocene age (and are being further examined to constrain that age). Thus the overlying section of 55m is probably younger than Upper Oligocene. From the base at 88m asl, to 130m asl, is an inhomogeneous mix of argillaceous powdery white marls with occasional planar bedded calcarenites, with burrowed tops. Up to 140m asl is a distinctive bench-like outcrop of benthic foraminifera packstone. The *Lepidocyclinids* are very large, flat with bulbous centres and are weathering proud of the surrounding rock. Other shelly debris includes gastropods, pecten and echinoids. It is perhaps a more cemented example of the bioclastic sandy marl facies observed at Ras Tipuli, Mchinga Turn and Mbuyuni. This passes up into a similar limestone with an almost

vuggy texture, quartz grains and oncoids. Sample TNZ-09-62 from this section (2m below the top of the section) has a Miocene assemblage of larger benthic foraminifera *Lepidocyclina, Miogypsina, Heterostegina, Alveolina?*. The section is capped by a white algal bioherm with pockets of sandy material and benthic foraminifera.

Thus there is at least 53m of Miocene limestone facies located here. Elsewhere, near Naminda, similar facies (Sample TNZ-09-137 & 138) also yield Miocene ages indicating that it is likely that this plateau comprises Miocene limestones entirely, extending as far south as the Mambu River and inland as far as Lake Kitere. A 64m section was logged in Navanja further inland within the Kitunda Plateau. Alternating (barren) silty clays, calcarenites, benthic foram packstone and quartz rich sparite dominate; a similar Miocene facies as that we've seen elsewhere. Due to the similarity of the facies observed with those at Tipuli, Mbuyuni and Mchinga, a mid Miocene age was assigned to the Kitunda Plateau, though this is inferred.

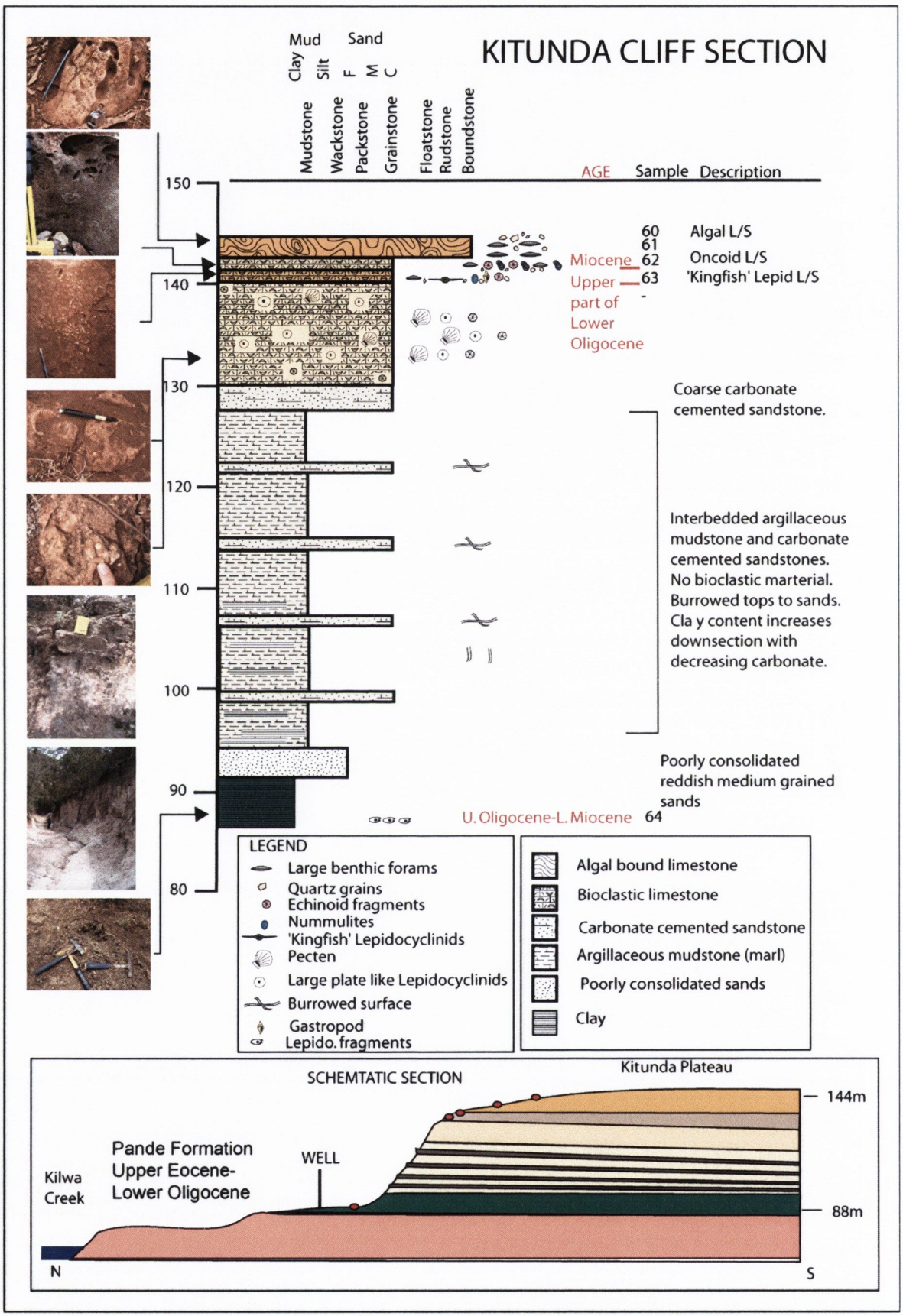

Figure 7.31: Schematic log and cross section of the Kitunda section. (Sample 63 needs to be re-examined as its age seems inconsistent with other ages obtained for this section).

7.6.The Coastal Ruvuma Area

The Tanzanian part of the Ruvuma basin is considered to cover much of the area between the River Lukuledi and the River Ruvuma. The present day surface is mainly blanketed with terrestrial sands, gravels and conglomerates of Lower Cretaceous age and younger Plio-Pleistocene Mikindani Sands. However, there are some marine Neogene exposures near Lake Kitere, in the Ntegu area and near Mikindani. The area was surveyed by Texaco in 1991 and the results of that map were incorporated into the geological map presented here in Fig. (7.32). Note that topographic sheets were not available for this area entirely and so are not included on the map, as they were for previously discussed areas.

7.6.1. Lake Kitere

Travelling inland towards Lake Kitere along the Mambi River Valley gives a good overview of the geology of the Ruvuma Area (Fig. 7.32). To the south of the road at WP 400, 65m asl. there is an approximately 12m high and 30m long outcrop of coarse unconsolidated quartz pebbles and grits, with more lithified beds standing out (Fig. 7.33a and c). Some cross bedding mostly to the northwest is apparent, although there is no overall direction, possibly indicating dune migration. Bedding is horizontal and it is overlain by a red soil.

Further inland the road travels over a very hard, bioclastic sparite (WP 401). The outcrop forms a roadcut of black-stained rubbly limestone (Fig. 7.33d). Some tube structures, small bivalve shell fragments and coralline texture indicate an age of Oligocene or younger (there are few corals in the Eocene). At WP402, a 20m long roadcut of *Lepidocyclina* coquina is present (Fig. 7.33b). It exhibits a very similar facies to Kitunda, Ras Tipuli , Mchinga and Mbuyuni. The presence of small nummulites indicates a Top Lower Oligocene age. South of Lake Kitere red –yellow coarse quartzose sands that are probably Lower Cretaceous in age and part of the Mkonde Sandstone Formation form a prominent plateau (Fig.7.33e and f).

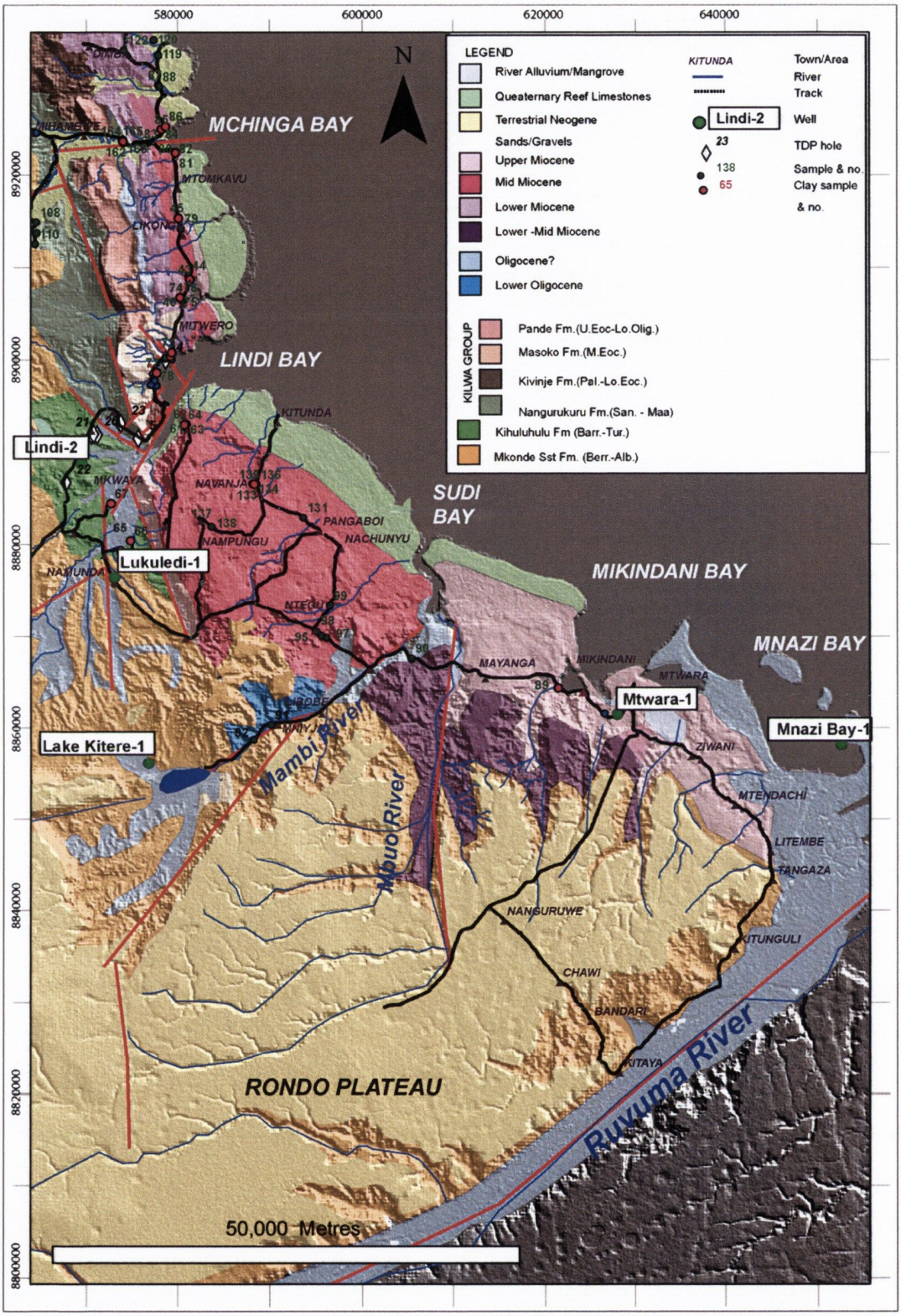

Figure 7.32: Geological map of the coastal Ruvuma Area, lain over a digital elevation model. Scale is 1:500,000. Red lines refer to faults.

7.6.2. Mtwara –Mikindani –Ntegu.

South of Mikindani Village (0623162, 88653454) is a quarry with a face approximately 15m high of buff yellow to reddish stained poorly sorted coarse sandstone, gravels and conglomerates (Fig. 7.34). As the only previously reported Plio-Pleistocene deposits have been named Mikindani Sands and the German geologists that first surveyed the area would have most likely stayed at the old German consulate in nearby Mikindani, it is likely this name was assigned to nearby exposures.

However, surveying mainly road tracks in the vicinity, these facies are not as widespread as initially expected, although the poorly consolidated sand and gravels in Mambi Valley (Fig. 7.33b) are probably the same lithofacies.

North of Mikindani an 8m succession is exposed beside the Mtwara Hygiene and Sanitation Plant (WP 396). At the base a 30cm blue-green clay is dated as Upper Miocene Overlying it are bioclastic argillaceous marls that are quite clay rich and occasionally more cemented beds stand out. The shelly material is largely bivalve fragments and rare solitary corals. It has a similar lithofacies to the Tipuli facies but there are no Lepidocyclinas or large benthic foraminifera This section is Upper Miocene or younger in age.

A framework reef limestone weathering red appears to lie above the previous section at 44m (WP 397). Similar Mikindani facies outcrop at (0621584, 8867480) and WP 397. At WP 398, thin 20-30cm beds of fine grained powdery marl sand within a background of softer marl reached approximately 15m thick and dips 15° to 232°. It appears there may be a fault between here and the last locality.

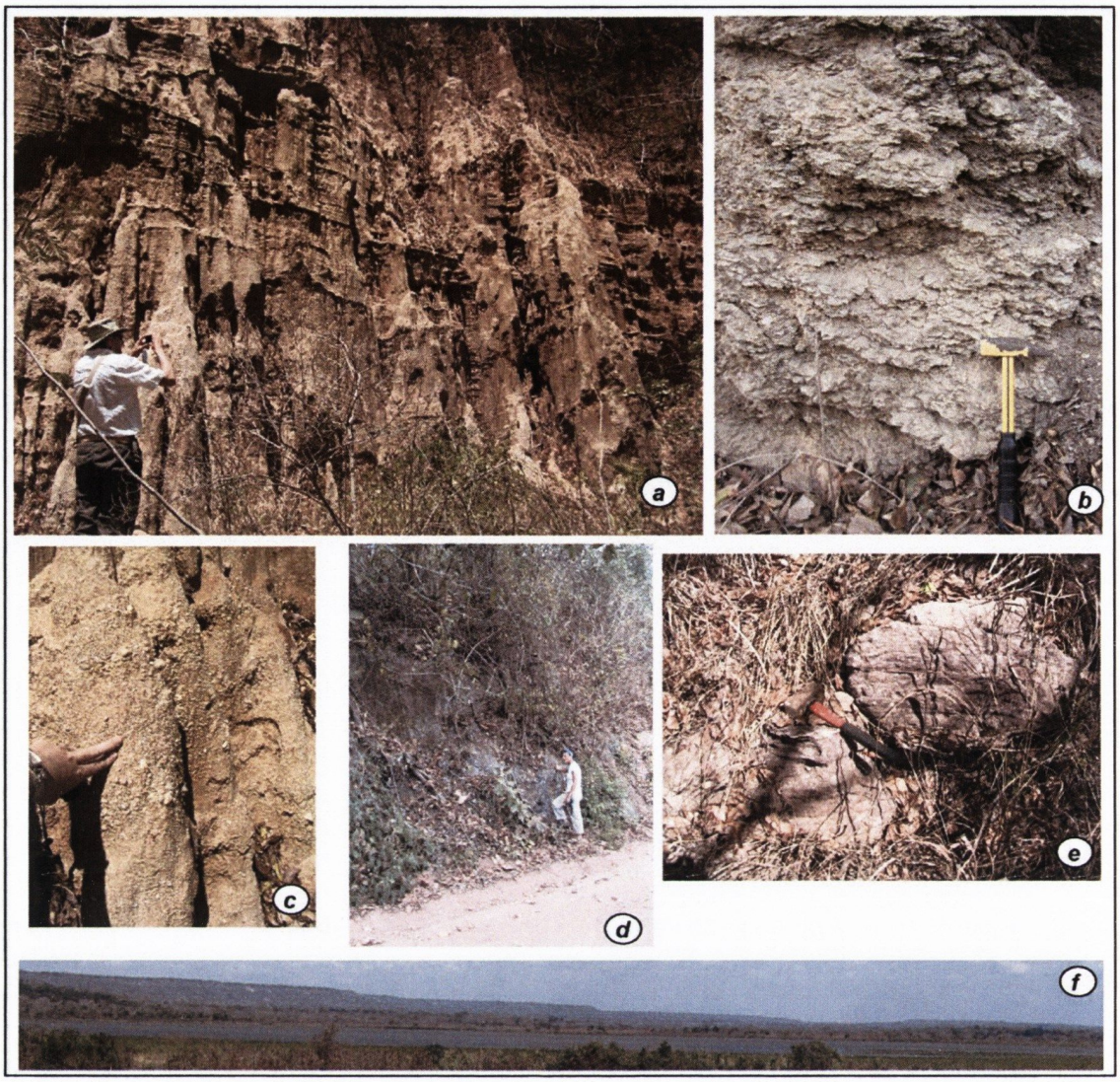

Figure 7.33: Outcrops from the Mambi River Valley and the Lake Kitere Area.a) Poorly condolidated red quartzose sands and gravels (also (c)); b) Lepidocyclina Packstone d) Bioclastic sparite, e) Planar reddish coarse arenite on road to Dihimba, e) Looking south across Lake Kitere towards the Rondo Plateau.

Figure 7.34: Mikindani Quarry; potential type section of the Mikindani Sands.

At Ntegu a running log was composed along the roadside outcrops in the Ntegu area (WP 403 to 405; 74m – 118m). At the base is an outcrop of facies similar to those at Mbanja and Ngomba at WP 403. Approximately 3m of powdery white marl occurs, with calcite crusts in a thin band in the middle and gastropods occurring in the top marly half. Overlying this (WP404, 102m) is a very weathered sandy calcarenite with a large gastropod, tube structures and possible oyster shells(?). This in turn is overlain by a thin coarse grained dark grey quartz sandstone with silicified benthic foraminifera. At WP 405, driving upslope (118m), there is a cream calcarenite (with no benthics). A rubbly grey outcrop off powdery white, angular, poorly sorted quartz bearing calcarenite occurs at 124m (WP 406) with minor amounts of benthic forams and gastropods. However located slightly below this at WP 407(120m) are boulders of an assortment of shell, calcified tubes, coral and quartz sand in a fine grained marl cement. This Sample 98 is Miocene in age due to the presence of *Miogypsinids (Miogypsina?), Lepidocyclina.* Finally, capping this section is a proper cream micritic framework reef coralline limestone at WP 408, which seems to form the surface of this plateau as it dips gently eastwards towards the sea. Similar facies were recorded at WP 513 near Pangaboi, which is located approximately halfway between this Ntegu road section and the Navanja sequence.

7.7.The Upper Oligocene-Pleistocene Tipuli unit (Tu) and the Pleistocene (?) Mbanja subunit (Msu)

The 'Tipuli unit' is proposed to incorporate the Upper Oligocene to Upper Miocene facies described in the previous sections and is extended to include the sporadic occurrences of Upper Miocene to Pleistocene that tend to occur locally around the Lindi Bay area. A compilation chronostratigraphic synthesis of the sections described in previous sections, previously published data and subsurface wells was constructed (Fig. 7.35). As a result, it is clear that a separate chronostratigraphic unit may be recognised separately from the Upper Cretaceous to Lower Oligocene Kilwa Group (Nicholas *et al.* 2006). As a consequence of contemporaneous and post-depositional tectonic control of sedimentation patterns, similar litho- and bio- facies developed in different localities at different times and may not be constrained to one particular stratigraphic period. Thus the 'Tipuli unit' is a heterogeneous unit which records fundamental Oligocene-Recent environmental and tectonic change in the southern coastal region of Tanzania. It is important to note that the facies of the 'Tipuli unit' are distinct from the underlying Kilwa Group, therefore enabling identification in the field and establishing it as a separate chronostratigraphic unit.

In Chapter 8, the key unconformable surfaces identified here are extended to resolve the stratigraphy of the seismic data recorded in the transition zone.

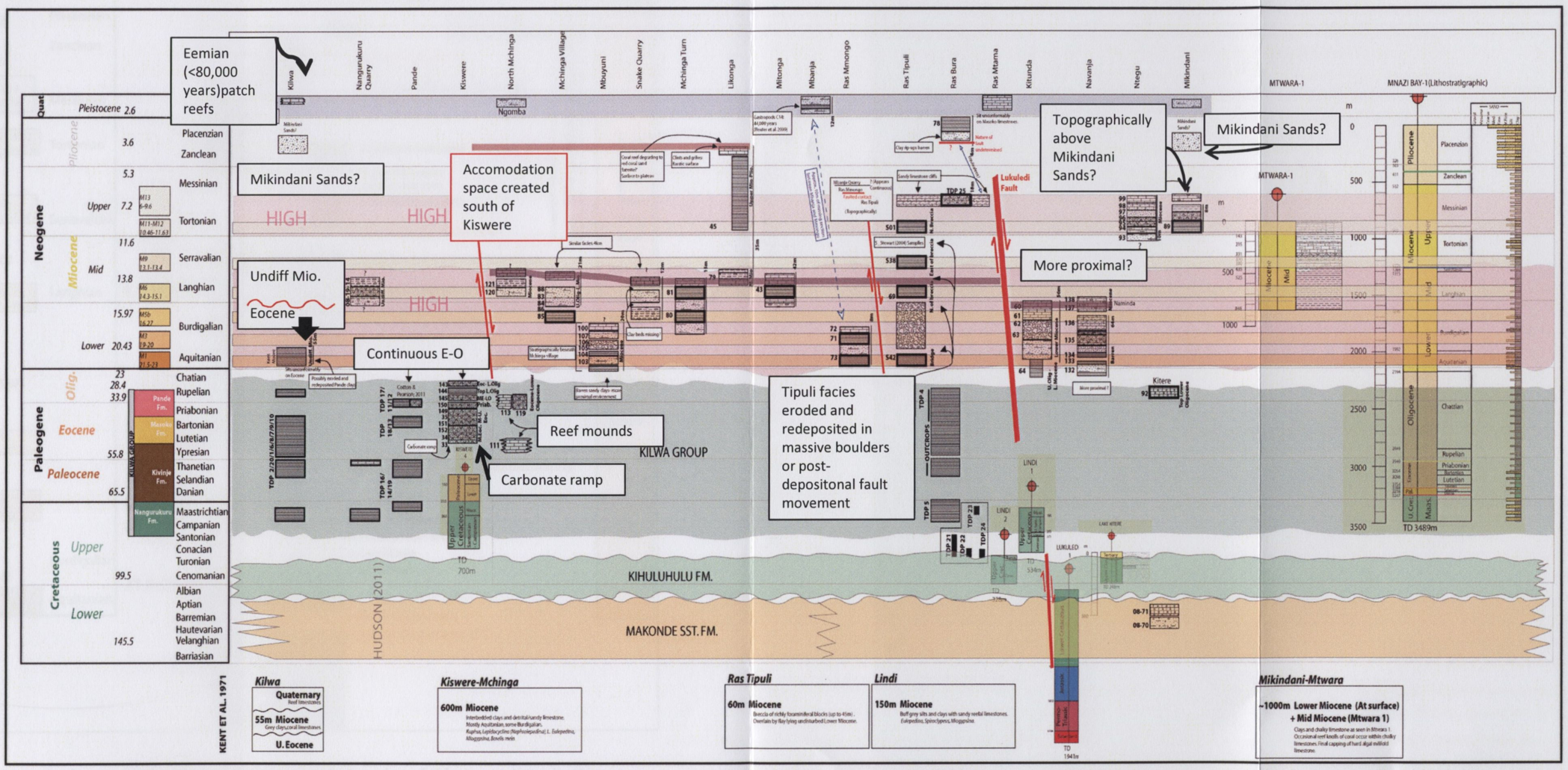

Figure 7.35: A synthesis stratigraphic framework of the onshore sections described in this chapter, onshore and coastal wells and previously published occurrences. Boxes in bold are field samples that have been accurately biostratigraphically dated. For a more detailed view in A0, please see Enclosure C.

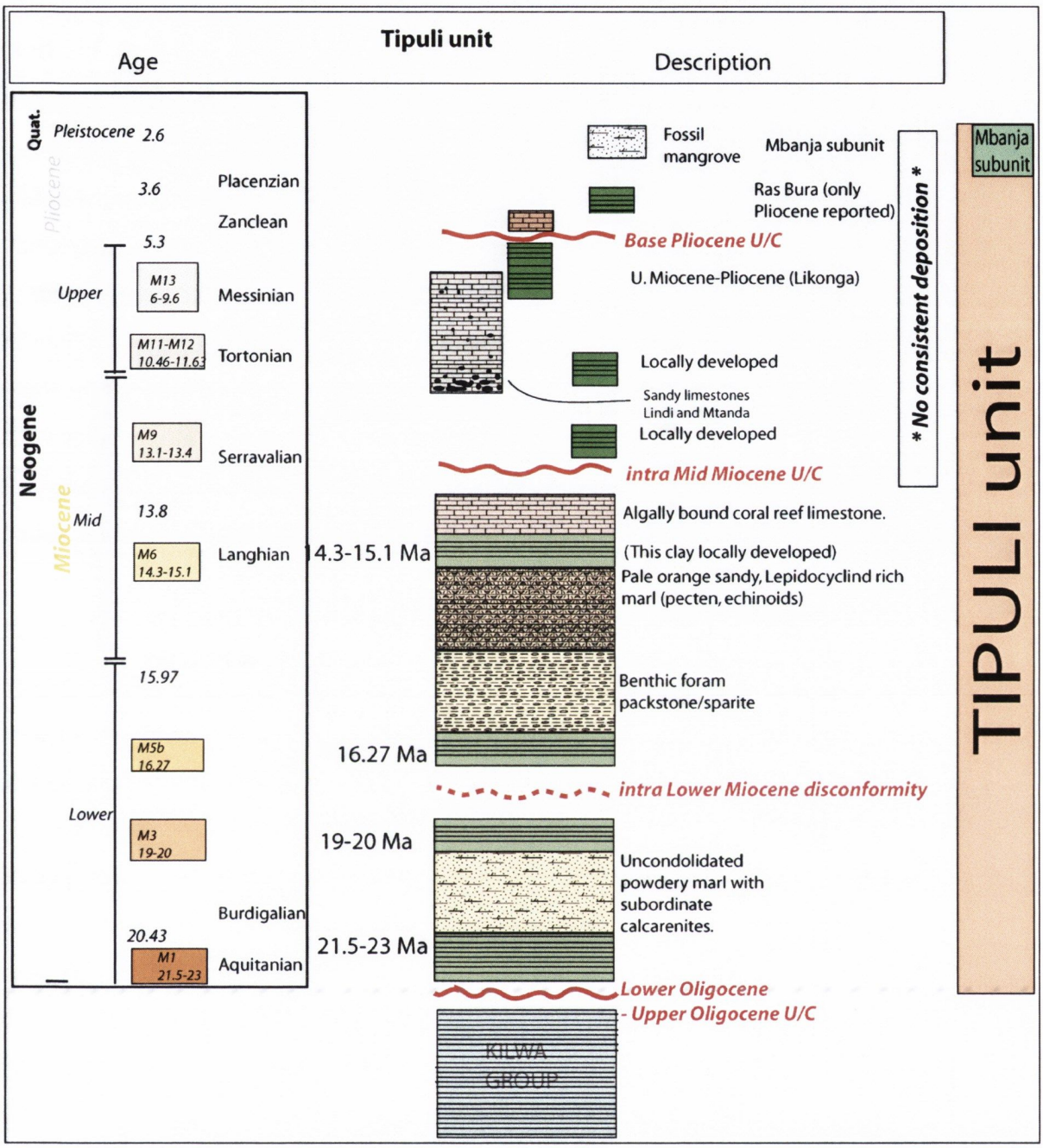

Figure 7.36: Schematic chronostratigraphy of the Tipuli unit, based on field observations in this study. Ages are based on planktonic foraminiferal assemblages in the clays and large benthic foraminiferal assemblages in the packstones. The basal surface is the Lower Oligocene-Upper Oligocene regional unconformity.

7.7.1. Upper Oligocene-Lower Miocene occurrences and facies

The base of the unit is defined by the Lower-Upper Oligocene unconformable surface (Fig. 7.36). Base early Miocene clays (21.5-23Ma) were observed in Ras Tipuli and Upper Oligocene-Lower Miocene clays are present in Kitunda cliffs. Immediately overlying this clay in both Kitunda and Ras Mmongo are poorly consolidated, sandy though often powdery marls with occasional harder calcarenites standing proud. A similar outcrop is observed near Mchinga School, beneath a Mid Miocene section. In Ras Mmongo, another clay was deposited at 19-20Ma, though this is the only occurrence of clay with this age. It is possible however, that similar slope facies were deposited elsewhere and were since eroded or deposited over. It certainly appears that the deposition of Miocene facies in the Ras Tipuli – Ras Mmongo area had a strong structural control.

7.7.2. Lower -Mid Miocene occurrences and facies

Across the Lower-Mid Miocene boundary, there is strong lateral agreement between facies deposited in the North Lindi-Mchinga area. The age of this section ranges from M5b-M9 (16.27 Ma-13.1 Ma). The stratigraphy is composed of clay, benthic foraminiferal packstone/sparite, clay, orange *Lepidocyclina* sandy marl with pecten and echinoid fragments and finally an algally bound coralline reef limestone. The basal clay is 16.27Ma (exposed at Mchinga School and Mchinga Turn). At both Mitonga and Mchinga Turn the top clay is dated as 14.3-15.1Ma. Clay in Ras Tipuli of ages 13.1-13.4Ma and 10.46-11.63Ma recorded by Stewart *et al.* (2004) is the only Serravalian and Tortonian age confirmed in this area. The north Mchinga area and the Kitunda Plateau appears capped by this coral reef limestone and the benthic foram packstone of Mid Miocene age. After the development of this reef limestone there was a significant hiatus, due either to relative sea level fall and/or significant tectonic activity.

7.7.3. Upper Miocene occurrences and facies

North of Ras Tipuli the only Upper Miocene recorded is in Likonga where a clay of Upper Miocene to Pliocene age is overlain by a karstic coral reef. The Upper Miocene is probably represented by the sandy, powdery limestones which cap Mtanda Hill in Lindi and the coastline along Lindi Bay. These limestones were cored by TDP 25 near Ras Bura. Thus the Upper Miocene appears localised to areas near the Lindi Bay area and Lukuledi Fault. A possible explanation for this is that there was contemporaneous movement on the Lukuledi Fault with continuous subsidence to the north creating the accommodation space to continually accumulate Mid-Upper Miocene clays, with shallower facies located closer to the shoreline, located further northwest of the fault.

7.7.4. Mid and Upper Miocene in the Ruvuma Basin

South of the Lukuledi Fault however the Mid Miocene and Upper Miocene is considerably thicker than to the north but of different litho and bio-facies. The diagnostic *Lepidocyclina* packstone is present only inland in Lake Kitere but the presence of small nummulites in this section indicates a Top Lower Oligocene age. There appears to have been significant accommodation space created in the Ruvuma Basin, probably by a series of normal faults extending roughly east-west that enabled significant Mid and Upper Miocene facies to be accumulated. Overall they may be considered similar argillaceous carbonate facies. However, the bioclastic debris as seen further north is missing here in significant quantities. This may be due to two factors; less dependence on storm events further upslope to carry bioclastic debris further downslope or a faster sedimentation rate.

7.7.5. The Mbanja subunit

The Mbanja subunit is here introduced for the first time to incorporate the enigmatic fossil mangrove deposits observed at both Mbanga/Mmongo, Ngomba and possibly at Ntegu which are completely distinct from the Tipuli unit and Kilwa Group and recognisable in the field. The Mbanja Quarry deposits, after which this unit is named have been recently described as a tidal flat/fen environment (Reuter *et al.* 2009) with a ^{14}C date of 44,000 ybp (years before present). However, as previously discussed, this facies is now interpreted as a fossil mangrove environment. Although this date applies to the Mbanja Quarry, it may be erroneous and applying a similar age to similar facies deposited elsewhere lacks supporting field evidence.

The entire mangrove plant assemblage is called a mangal and typically has the following ecological characteristics; a quiet, sheltered coastal environment protected from high energy wave action, accumulation of fine grained sediment with a high organic content and brackish, saline water with frequent inundation. The sediment accumulating around a mangrove settlement comprises, (from the base upwards): roots, dark peaty clay, pneumatophore network, leaf and wood litter, fine grained carbonate with gastropod and oyster associations.

The substrate beneath mangrove forests is predominantly clay composed mainly of mangrove roots (McKee, 2000). Leaves and wood account for <20% mass. This fine anoxic sediment acts as a trace metal sink forming a dark peaty anoxic substrate beneath the mangrove plants. In areas where the roots are continuously submerged they host algae, barnacles, oysters, sponges and bryozoa. Mangroves have specific associations with different gastropod taxa i.e. the specific ecology and environmental stresses associated with mangroves has also resulted in gastropod associations that almost always occur (Cooly *et al.* 1999). Mangrove forests typically provide a good habitat for oysters and slow water flow enhancing sediment deposition. The fine grained, powdery white marl with calcite precipitates, oyster shells and gastropods are typical of this sediment accumulation in or around the base of the mangals.

To be conclusive about the age of the fossilised mangrove section at Mbanja Quarry, the reliability of the fossil record must be established. The complex modern mangrove

ecosystem developed in the Paleogene. The species of mangrove are likely to be less than 30my and may be identified by a specialist using pollen, wood or root network. The age of 44,000 y.b.p. obtained by ^{14}C dating of the gastropod shells by Reuter *et al.* 2009 is almost at the limit of the range of ^{14}C dating and may therefore be erroneous.

There are a number of ways the geological history of the Mbanja subunit fossil mangrove facies may be interpreted reflecting both a C^{14} latest Pleistocene age and an inferred age based on the field relationships reported;

1. Reuter *et al.* (2009) Model

The C^{14} date of 44,000 ybp for the Mbanja deposits are correct and this locality has been significantly uplifted from a shoreline environment at a time when sea level was 60-90m below its present level to its present elevation of 110m above sea level (Reuter *et al.* 2009) suggesting an uplift rate of 1.6-2.5mm/yr.

2. Reuter *et al.* (2009) Model in a transpressional fault zone

As for the previous model, although the uplift suggested doesn't apply to the entire shelf but rather to a localised fault zone, probably a transpressional flower structure with various individual fault bound slivers, as proposed by Nicholas *et al.* (2007). The geology of the entire Lindi area is strongly influenced by structural control as evidenced by the field geology. Thus there might have been a significant depression formed due to adjacent fault movement creating the space here for the Pleistocene sea to form a small incursion along the River Mmongo and form a localised onshore Pleistocene mangrove deposit. Subsequent compression and reactivation on this fault uplifted this deposit to its current elevation.

3. A Lower-Mid Miocene age for the Mbanja deposits?

The Mbanja deposits are the youngest part of the Lower-Mid Miocene succession at Ras Mmongo as they appear to lie stratigraphically above it. Thus they may represent the late Lower-early Mid Miocene shoreline before the mid Mid Miocene regression. Although there is 9m of missing stratigraphy between the two sections, there are

fossilized mangrove leaves in a grey sandy marl at the top of the section at Mmongo, indicating a lithological similarity between this section and the potentially overlying Mbanja deposits.

4. A Lower-Mid Miocene age for the Ngomba Quarry deposits?

At Ngomba the Mbanja subunit may represent the lateral shoreline equivalents of the lower Mid Miocene shallow water facies reported in the North Mchinga area. It appears likely that a normal extensional fault created the scarp and NW-SE linear feature of the Ruawa plateau, creating a relatively deepwater environment for the Kilwa Group clays to accumulate. Following the Lower-Upper Oligocene regression, Miocene facies transgressed over the Kilwa Group. The Mchinga coastal platform forms a flat, relatively extensive platform of shallow water benthic foraminifera packstones and coral reef limestones which laterally grade into sandy marls to the west near Kikopo. It is possible the shoreline of this Lower-Mid Miocene environment is represented by the fossil mangrove deposits at Ngomba Quarry. Indeed the Ruawa Plateau scarp would have formed a significant barrier to the sea transgressing any further inland. Following the regional hiatus in the intra Mid Miocene, there is no evidence of subsequent transgression over the Lower-Mid Miocene facies. Thus, a Mid Miocene age may be applied and an age-correlation on the basis of lithological similarities with the Mbanja Quarry appears unlikely.

Further work needs to confirm whether the Ngomba Quarry mangrove facies are age-equivalent to the Mbanja Quarry deposits. Thus this is not strictly a chronostratigrapic unit, confined to one time period. A Lower-Mid Miocene age for the Mbanja subunit is plausible, based on the field evidence for Models 3 and 4. Further evidence to support Lower-Mid-Miocene age is provided when analysing the rates of uplift suggested by these models. A 44,000ybp age (Reuter *et al.* 2009) implies an uplift rate of 1.8-2.5mm/yr (Reuter *et al.* 2009) to the Mbanja Quarry section (currently 80-90m asl). This is greater than the 1.6mm/yr rate of uplift for the >5000m high Rwenzori Mountains in Uganda (Ring *et al.* 2008). As the Rwenzori Mountains form major topographic rift shoulder features on the well-developed western arm of the East African Rift, comparisons with this area need to be substantiated by more than a

single C^{14}date from one quarry. While there is other evidence of Recent compression and uplift, further discussed in Chapter 9, the rate of uplift proposed here is not supported by other field evidence and a Lower-Mid Miocene age yields a more appropriate uplift rate. However, it is clear that further work is needed on this issue.

7.8.The Tipuli unit and global climatic intervals.

The Upper Oligocene to Pleistocene Tipuli unit records fundamental critical climate intervals and regional unconformities observed onshore can be correlated to global falls / rises in sealevel.The relative timings of these episodes are explained in the following paragraphs. This indicates that the unconformities likely extended into the offshore realm and may be reflected in the seismic sequences observed.

Three major unconformities and one disconformity were observed and may be correlated to global climatic changes; Lower – Upper Oligocene U/C, an intra Lower Miocene disconformity, an intra Mid Miocene U/C and a base Pliocene U/C (Fig. 7.37).

The Lower - Upper Oligocene U/C coincides with the Mi-1 (Zachos *et al.* 2001). The transition from the Oligocene to the Miocene was marked by a very short episode characterised by intense continental erosion, c. 23.7Ma (Wright & Miller 1993). A cooling and increased ice accumulation in East Africa led to a sudden drop in sea level, exposing the coastal plateaux to erosion.

The early Miocene was a stable period punctuated by glaciation and from 17-15Ma, this warm phase peaked during the Mid-Miocene climatic optimum. This correlates with the intra-Lower Miocene disconformity observed onshore southern coastal Tanzania.

The Late Miocene was gradually cooling and was 6-7 degrees cooler (Shevenell 2004), due to the reestablishment of major Antarctic ice by 10Ma (Vincent *et al.* 1985; Flowers, 1995). A major cooling took place from 14.2-13.7Ma, associated with

the growth spurt of the East Antarctic ice sheet and increased production of cold Antarctic deep waters. This may be correlated to the intra mid Miocene unconformity. It appears likely that after his time the Tanzanian coast was never fully submerged again. The overall cooling trend continued and a further episode of aridity occurred between 8-4Ma (Upper Miocene). A short warming period occurred in the early Pliocene. This may be correlated with the Base Pliocene unconformity.

In summary there is excellent agreement between the Upper Cretaceous to Lower Oligocene Tipuli unit and global climatic intervals. Assessing the interplay between climatic and tectonic influence on sedimentation is more difficult. Unfortunately a thorough assessment of the onshore structural geology was beyond the scope of this project although it is broadly outlined in Hudson (2011). A series of palaeogeographic maps for the key time slices discussed throughout this chapter are provided in Fig. 7.38.

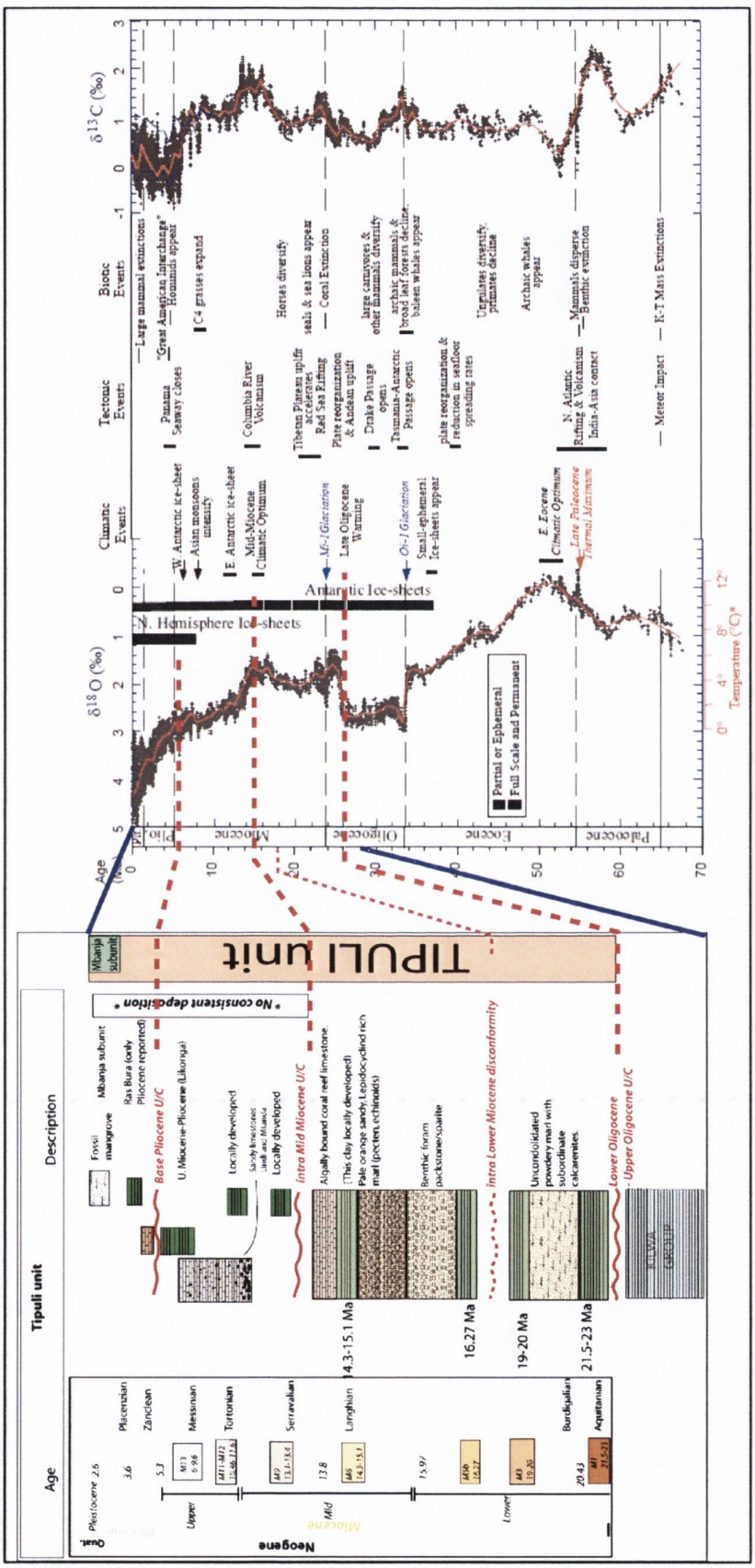

Figure 7.37: Correlation between the regional unconformities identified in the Tipuli Formation and the global Cenozoic deep sea oxygen and carbon isotope data (Zachos et al., 2001).

7.9. Palaeogeographic Maps

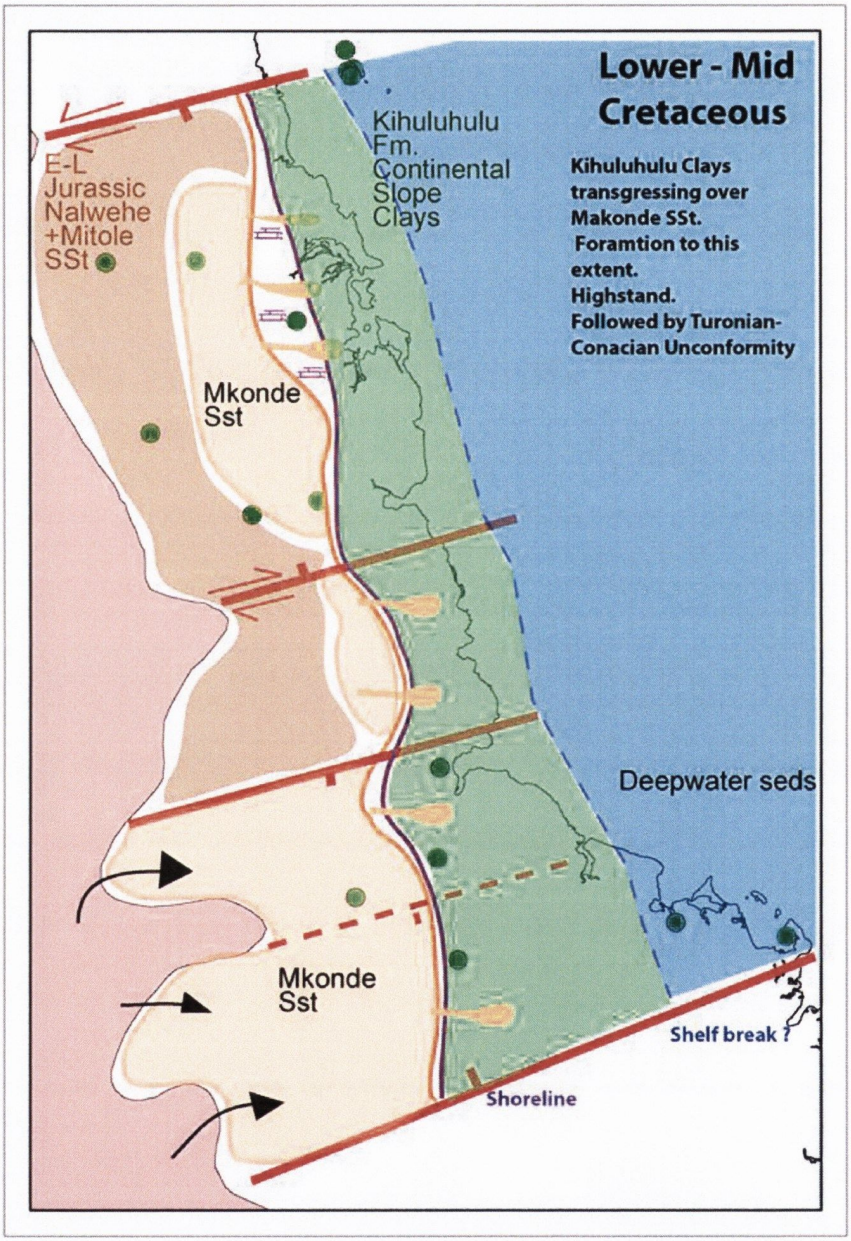

Figure 7.38: Palaeogeographic reconstructions of the Lower-Mid Cretaceous.

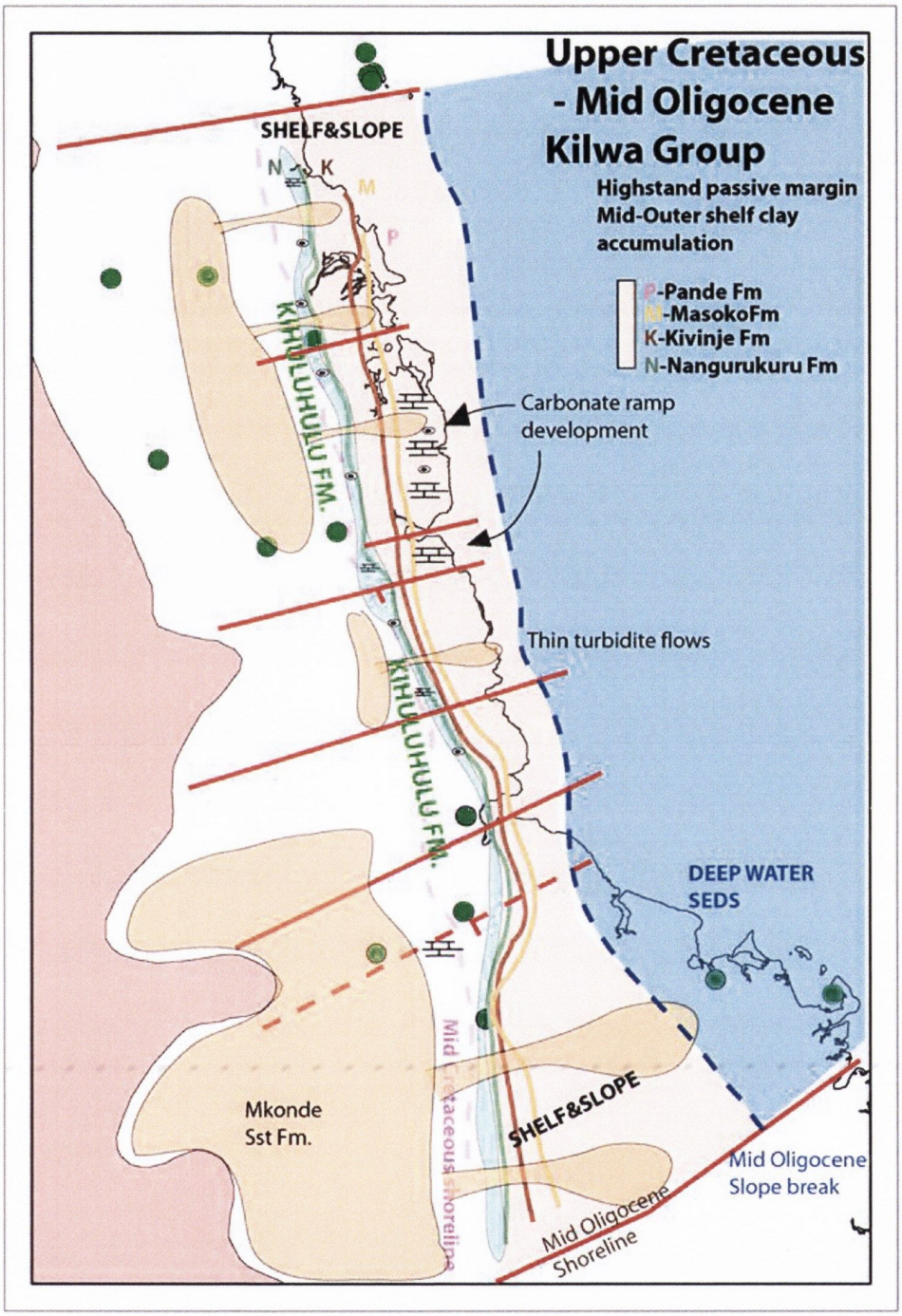

Figure7.39: Palaeogeographic reconstruction of the Upper Cretaceous – Mid Oligocene.

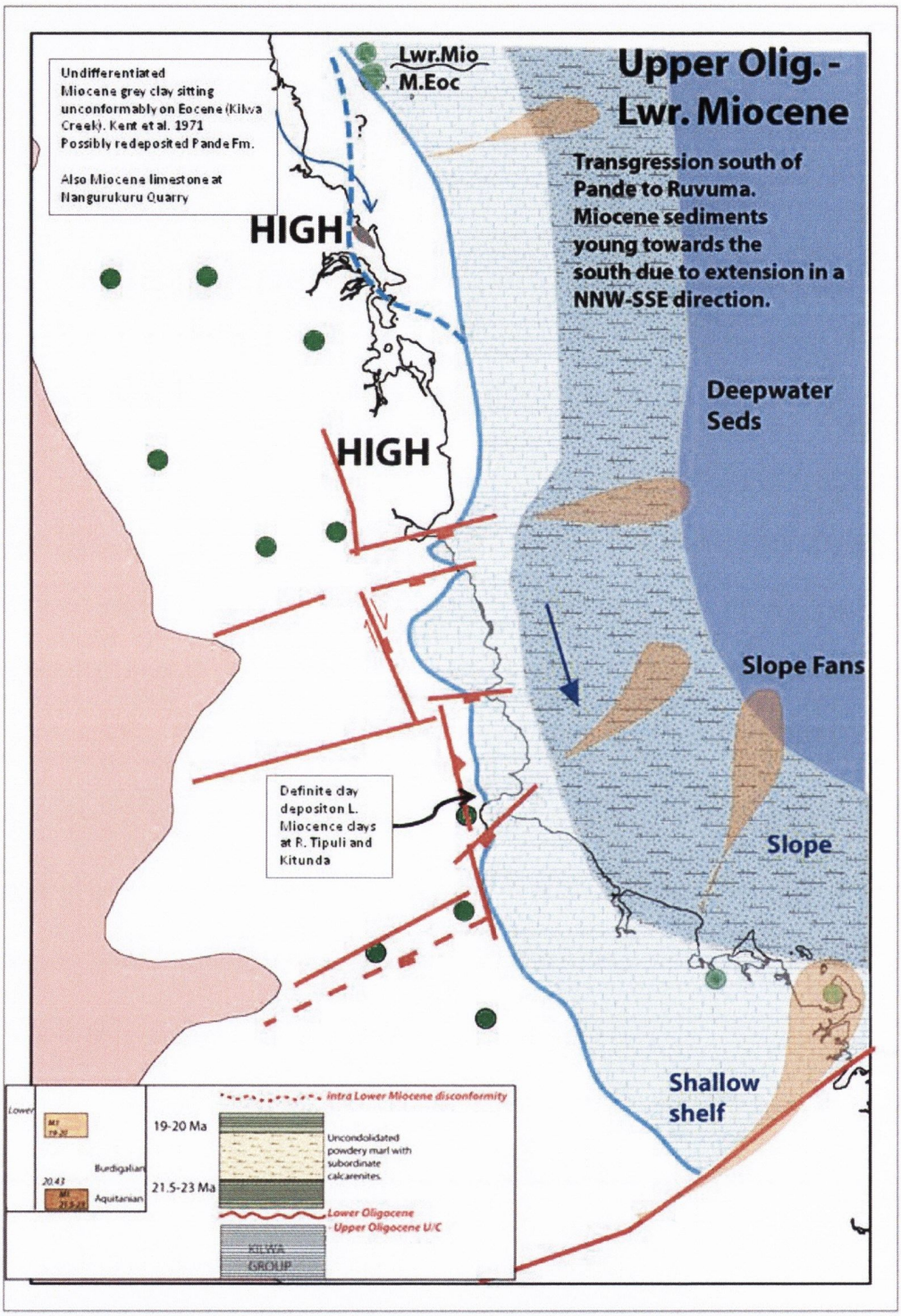

Figure7.40: Palaeogeographic reconstruction of the Upper Oligocene to Lower Miocene.

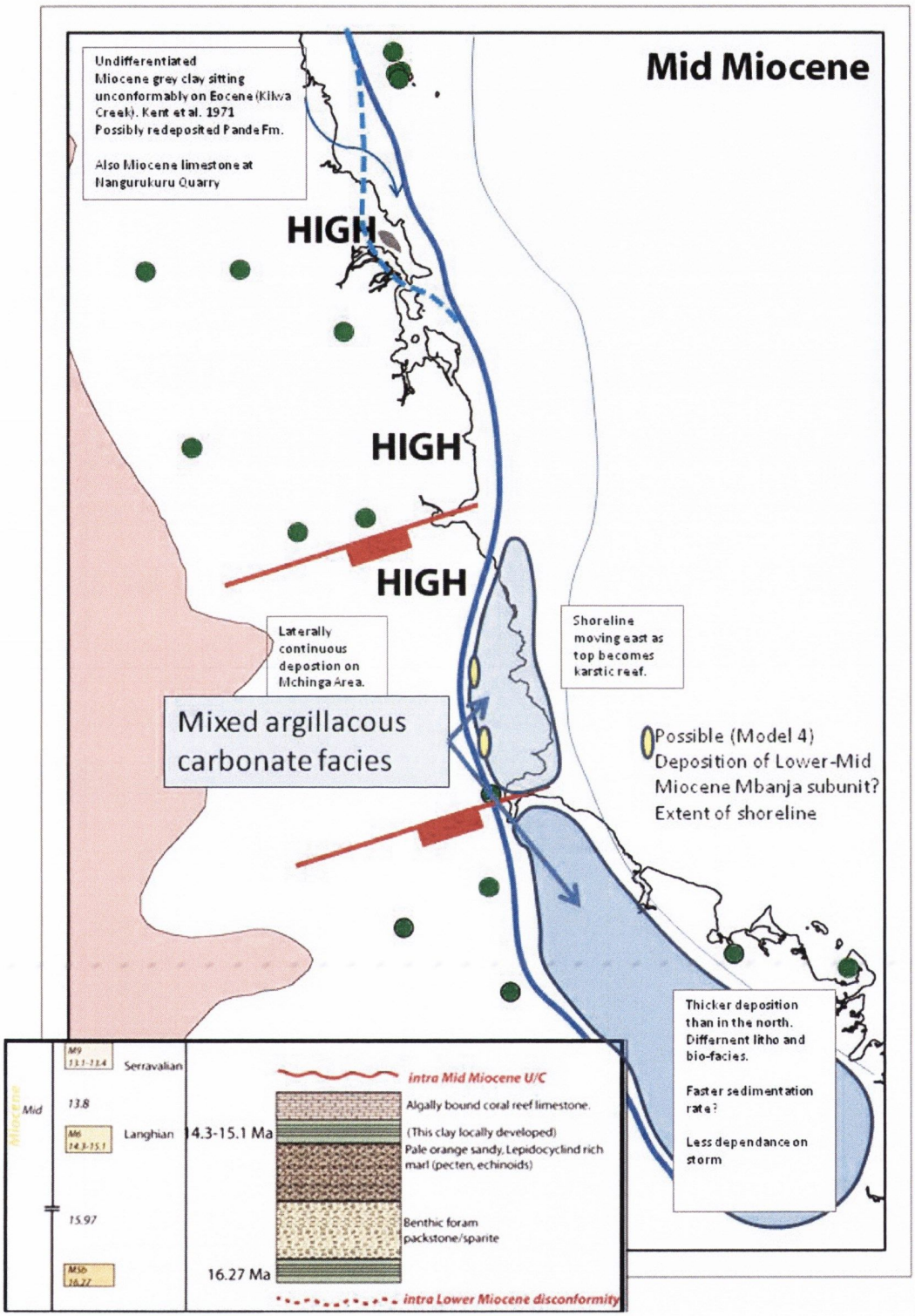

Figure7.41: Palaeogeographic reconstruction of the Mid Miocene.

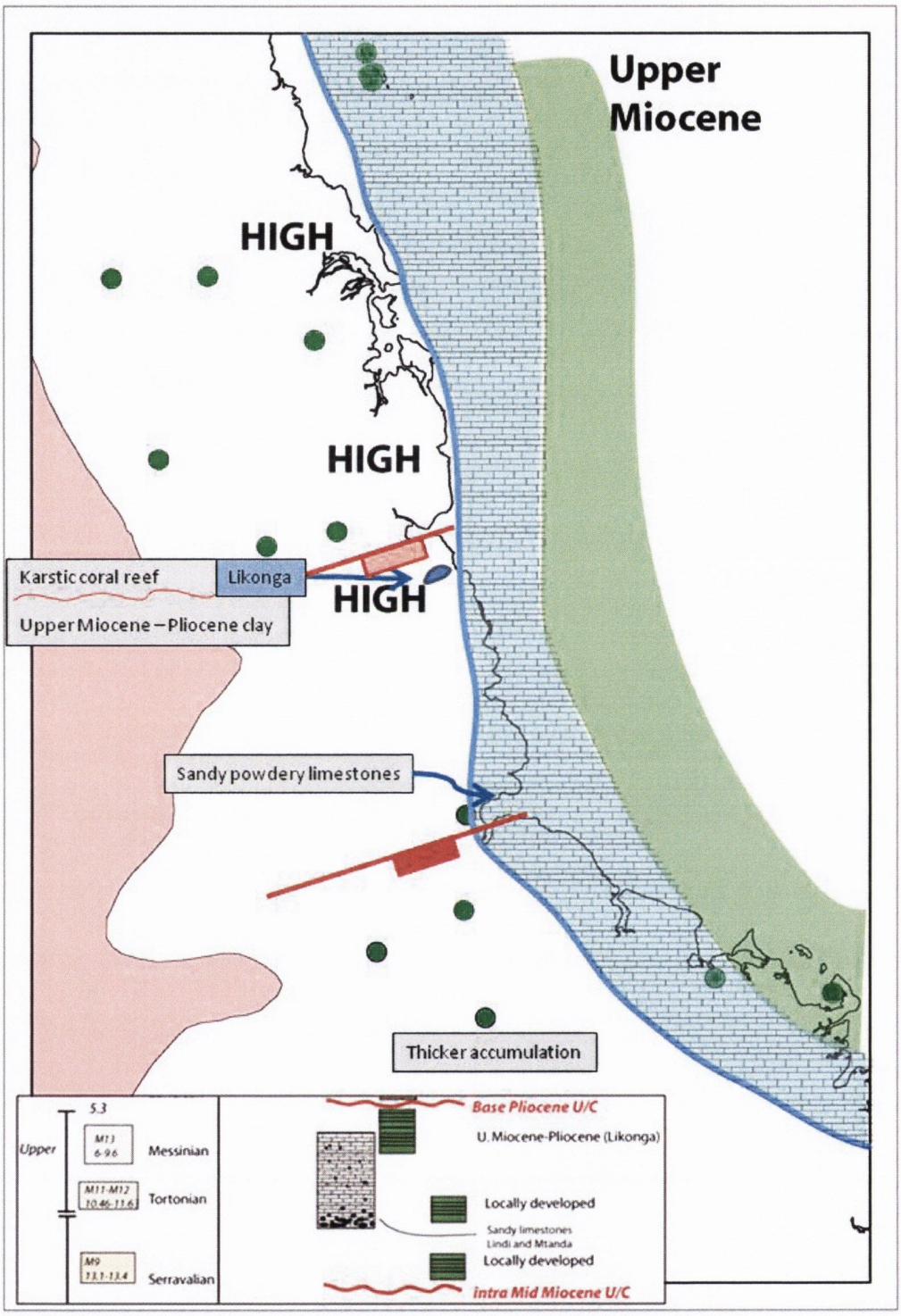

Figure 7.42: Palaeogeographic reconstruction of the Upper Miocene.

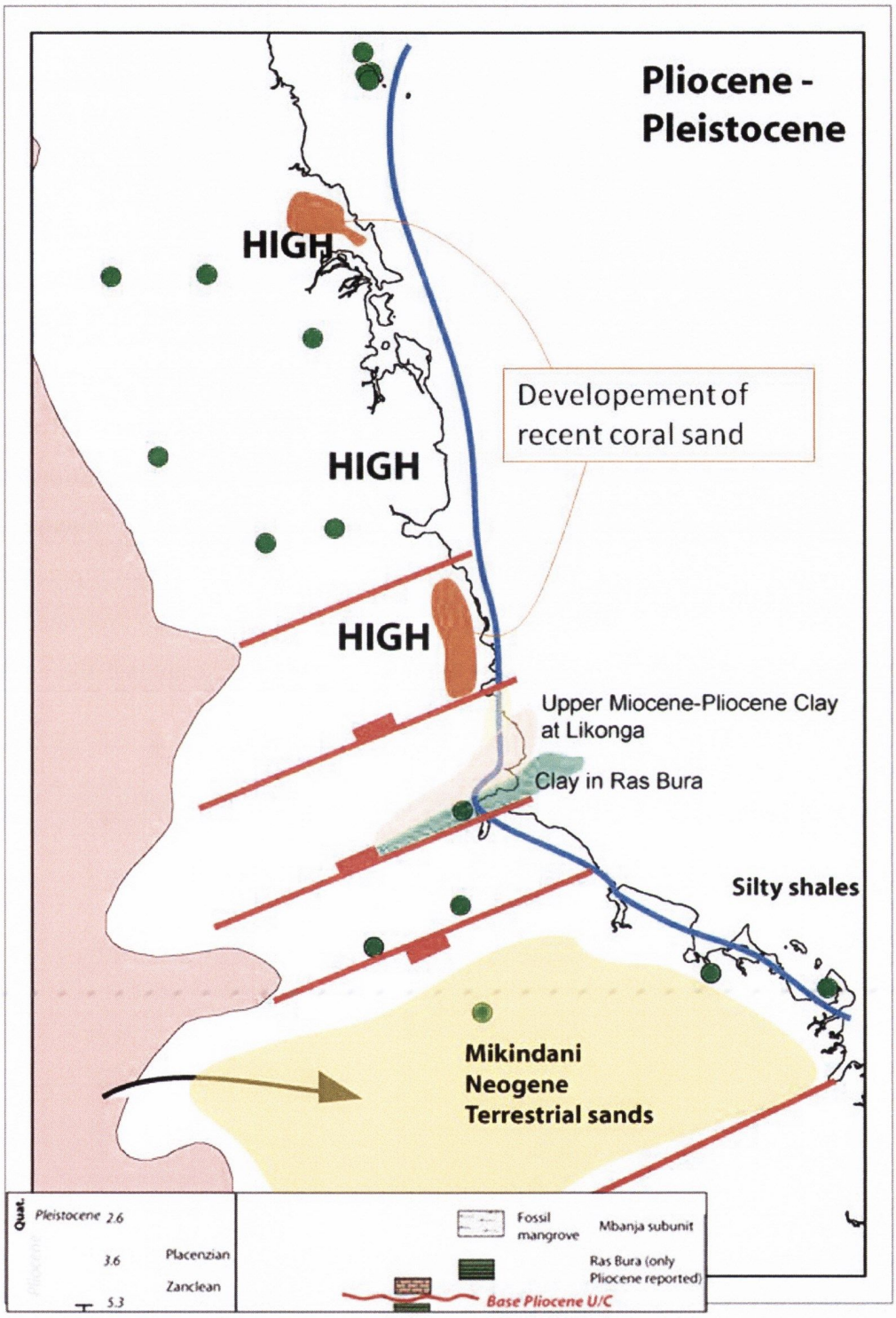

Figure 7.43: Palaeogeographic reconstruction of the Pliocene-Pleistocene.

7.10. Summary

As stated in Chapter 2, one of the thesis objectives was to describe and define the Upper Oligocene and younger stratigraphy onshore Tanzania. This chapter provides the first thorough description and interpretation of the Upper Oligocene to Pleistocene stratigraphy onshore coastal Tanzania since Kent *et al.* (1971). A number of objectives were achieved. The chronostratigraphic unit, the Tipuli unit (and Mbanja subunit) is formally recognised as a separate unit lying above the Upper Cretaceous – Lower Oligocene Kilwa Group. The occurrence of the mixed litho- and bio-facies for the Kiswere-Mtwara areas was presented with maps, logs and photos. A number of hypotheses were presented for the age of the Mbanja subunit. Regional unconformities were identified that may extend into the offshore and transition zone. Indeed the regional unconformities observed in the chronostratigraphic scheme may be tied to global climatic intervals. Palaeogeographic maps were drawn representing the study area at key time slices. The results of this chapter are incorporated into Chapter 8 where sequence stratigraphic methods are used to extrapolate the ages of key seismic markers into the transition zone.